

Quest for factors involved in the extraction of
transmembrane proteins from the PPM to the
PVM and the effect of jamming PTEX on
PfEMP1 export in *Plasmodium falciparum*

Dissertation with the aim of achieving a doctoral degree at the
Faculty of Mathematics, Informatics and Natural Sciences

Department of Biology
University of Hamburg

Submitted by
Isabel Cristina Naranjo Prado

2020
Hamburg

Day of oral defense: May 15th 2020

The following evaluators recommend the admission of the dissertation:

Prof. Dr. Tim Gilberger

Dr. Tobias Spielmann

Eidesstattliche Versicherung

Declaration of academic honesty

Hiermit erkläre ich an Eides statt, dass ich die vorliegende Dissertationsschrift selbst verfasst und keine anderen als die angegebenen Quellen und Hilfsmittel benutzt habe.

I hereby declare, on oath, that I have written the present dissertation by my own and have not used other than the acknowledged resources and aids.

Hamburg, the 16th of November 2019

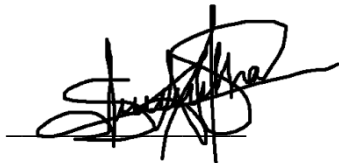


Isabel Cristina Naranjo Prado (MSc)

Language certificate

I am a native speaker, have read the present PhD thesis and hereby confirm that it complies with the rules of the English language.

Hamburg, the 16th of November 2019

A handwritten signature in black ink, appearing to read 'Samantha Gonzalez', written over a horizontal line.

Samantha Gonzalez

Summary

In 2017 an estimated 219 million cases of malaria occurred worldwide, resulting in 435,000 deaths. Those numbers place malaria as one of the world's leading causes of death due to infectious diseases. The most severe form of malaria is caused by the protozoan parasite *Plasmodium falciparum*. The symptoms of the disease are associated with the parasite's multiplication within red blood cells. In this life cycle phase, the parasite exports a large number of proteins beyond its own cellular boundaries into the host red blood cell. This leads to extensive remodelling of the host cell, a process that ensures parasite survival and is a direct mediator of parasite virulence. The transmembrane domain (TMD) protein PfEMP1 is of central importance for this virulence. PfEMP1 is exported from the parasite and displayed on the red blood cell surface, where it mediates the cytoadherence of infected red blood cells to the endothelium of blood vessels. While the transport step leading to the export of proteins across the PVM into the host cell is well characterized and appears to involve the *Plasmodium* translocon of exported proteins (PTEX) for all so far analyzed proteins, the transport of PfEMP1 is much less clear and in general the process of extraction of exported TMD proteins out of the parasite plasma membrane (PPM) to be further transported into the host cell, remains elusive.

The aim of this thesis was to identify translocation factors involved in the extraction of exported TMD proteins out of the PPM, enabling the delivery to PTEX to continue their way to the erythrocyte cytosol. The identification of these factors is an important gap in the understanding of how the parasites achieves protein export, and hence how it modifies the host cell that result in parasite virulence. Inactivation of this step could potentially prevent the export of PfEMP1, and thus abolish the parasite's virulence and adhesion properties, leading to a more efficient clearance of it by the host immune system. This export step was addressed by two approaches in this thesis, firstly by a general quest for proteins that aid the PPM extraction step and secondly, by a direct analysis of PfEMP1 trafficking.

For the first aim, two constructs containing an mDHFR-BirA* sequence were designed. One fused with SBP1 (construct SBP1-mDHFR-L-BirA*-3xHA) as a control arrested at the PVM and the other with REX2 (construct REX2-mDHFR-L-BirA*-3xHA) that is arrested at the PPM. This had the aim to biotinylate proteins that contribute to the extraction of proteins out of the PPM. By arresting constructs on both membranes, it was hoped that the transport factors at each membrane would be tagged to be able to distinguish the proteins specifically involved

in the extraction at the PPM. By this approach a total of 2000 different proteins were identified. From those identified proteins, the ones that were enriched in the interactome of the arrested constructs compared to the non-arrested, exported condition were analyzed. The fact that the SBP1-mDHFR-L-BirA*-3xHA detected mostly PTEX components confirmed that this construct was arrested deeply in the translocon in the PVM, whereas REX2-mDHFR-L-BirA*-3xHA detected a much wider range of proteins (including PTEX components), in agreement with previous data suggesting an arrest of at least part of the population of this molecule in the PPM, immediately before or in the process of being translocated through PTEX. Using the SLI methodology 10 proteins considered to be promising hits identified with the REX-mDHFR-L-BirA*-3xHA construct were cloned, revealing the location and function of previously unknown proteins in *P. falciparum*. As several of these proteins were located in the parasite periphery, this suggested that the approach was in principle successful. Additionally, proteins involved in the Endoplasmic-reticulum-associated protein degradation (ERAD) pathway were identified, suggesting that some of the PPM arrested REX2-mDHFR-L-BirA*-3xHA molecules were back extracted and degraded using the cells quality control system. However, a detailed characterization of the other analyzed hits revealed that none of the ten hits aided the extraction of TMD proteins out of the PPM towards the PV. This indicates that either the mechanism of removal out of the PPM depends entirely on PTEX which was detected and could provide force for the PPM extraction from the PVM and interacts with the protein only on the outer face of the PPM, or the proteins contributing to extraction were not available for BirA* mediated biotinylation because they were not in reach, for instance if buried deeply in the PPM.

In second part of this work PfEMP1 was directly analyzed. This was not possible in previous work as this protein is very large (which precludes episomal expression) and part of a gene family subject to mutually exclusive expression, leading to parasite cultures consisting of mix of parasites expressing a different PfEMP1 molecule. These problems were here solved for the first time by generating a SLI activated PfEMP1 that was tagged with a small HA epitope and expressed from its own genomic locus. All parasites expressed this PfEMP1, which was conveniently detectable using an anti-HA serum. These cells were used to assess the trafficking of PfEMP1 through the pathway other exported proteins are known to take through PTEX. For this it was assessed if blocking PTEX would inhibit PfEMP1 transport. Due to a number of confounding factors, this could not be fully resolved, but the data provided in this thesis indicates that PfEMP1 may not depend on PTEX, congruent with previously published ideas. The PfEMP1 SLI line could also serve as an excellent tool to study the proteins involved in

PfEMP1 transport. However, for this a second genomic integration would be needed which so far was difficult to achieve. Therefore, a new version of SLI was developed that can be used in parasites that already have a SLI genome modification. This system was termed SLI2 and permitted to disrupt genes in the PfEMP1 SLI line. Unexpectedly, this revealed that PfEMP1 transport to the Maurer's clefts (MCs) was not disturbed after disruption of PTP1, contradicting previous findings. Furthermore, the disruption of SBP1 consistently led to a reversion of the PfEMP1 SLI integration event, suggesting that disrupting SBP1 likely prevented PfEMP1 trafficking as previously reported and that its transport arrest had a dominant negative effect. While these findings do not with certainty reveal the exact pathway PfEMP1 takes to reach its final destination, it provides critical tools for the field to (i) identify factors in PfEMP1 transport, (ii) to monitor expression and trafficking of this protein and (iii) crucially, to test the binding properties of individual PfEMP1 molecules that can be activated using SLI as done for the first time in this thesis.

With the results of this thesis and the technical advances provided here it is hoped that the enigmatic and long-standing question how TMD proteins and in particular PfEMP1 are transported into the host cell can finally be resolved to understand this important and fascinating aspect of parasite biology.

Zusammenfassung

Im Jahr 2017 traten weltweit schätzungsweise 219 Millionen Fälle von Malaria auf, die 435.000 Todesopfer forderten. Diese Zahlen machen Malaria zu einer der weltweit führenden Todesursachen aufgrund von Infektionskrankheiten. Die schwerste Form der Malaria wird durch den Protozoenparasiten *Plasmodium falciparum* verursacht. Die Symptome der Krankheit sind mit der Vermehrung des Parasiten in den roten Blutkörperchen verbunden. In dieser Phase des Lebenszyklus exportiert der Parasit eine große Anzahl von verschiedenen Proteinen über seine eigenen Zellgrenzen hinaus in die Wirtszelle, was zu einer weitreichenden Umgestaltung dieser führt. Ein Prozess, der das Überleben des Parasiten sichert und ein direkter Verursacher der Parasitenvirulenz ist. Das Transmembrandomänen- (TMD-) Protein PfEMP1 ist für dessen Virulenz von zentraler Bedeutung. PfEMP1 wird aus dem Parasiten exportiert und auf der Oberfläche der roten Blutkörperchen präsentiert, wo es die Cytoadhärenz der infizierten roten Blutkörperchen an das Endothel von Blutgefäßen des Wirts vermittelt. Während der Transportschritt, der zum Export von Proteinen über das PVM in die Wirtszelle führt, gut charakterisiert ist und für alle bisher analysierten Proteine den Plasmodium-Translokon der exportierten Proteine (PTEX) zu beinhalten scheint, ist der Transport von PfEMP1 viel weniger klar. Generell bleibt der Prozess der Extraktion der exportierten TMD-Proteine aus der Plasmamembran des Parasiten (PPM) um weiter in die Wirtszelle transportiert zu werden, unklar.

Das Ziel dieser Arbeit war es, Translokationsfaktoren zu identifizieren, die an der Extraktion der exportierten TMD-Proteine aus der PPM beteiligt sind, um sie an PTEX weiter zu geben, damit sie ihren Weg zum Erythrozyten-Cytosol fortsetzen können. Die Identifizierung dieser Faktoren ist eine wichtige Lücke im Verständnis, wie der Parasit den Proteinexport bewerkstelligt und damit die Wirtszelle modifiziert und so die Parasitenvirulenz hervorruft. Die Inaktivierung dieses Schrittes könnte möglicherweise den Export von PfEMP1 verhindern und damit die Virulenz und die Adhäsion des Parasiten aufheben, was zu einer effizienteren Beseitigung durch das Immunsystem des Wirts führt. Dieser Exportschritt wurde in dieser Arbeit mit zwei Ansätzen angegangen. Zum einen durch eine allgemeine Suche nach Proteinen, die den PPM-Extraktionsschritt ermöglichen, und zum anderen durch eine direkte Analyse des PfEMP1-Transports.

Für das erste Ziel wurden zwei Konstrukte entworfen, die eine mDHFR-BirA*-Sequenz enthalten. Eines, die Kontrolle, wurde mit SBP1 fusioniert (Konstrukt SBP1-mDHFR-L-

BirA*-3xHA) , das konditional an der PVM im Transport blockiert werden kann, und das andere mit REX2 (Konstrukt REX2-mDHFR-L-BirA*-3xHA), das an der PPM blockiert werden kann. Dieser Ansatz hatte das Ziel, Proteine zu biotinylieren, die zur Extraktion von Proteinen aus dem PPM beitragen. Durch die Arretierung der Konstrukte an beiden Membranen wurde erwartet, dass die Transportfaktoren an jeder Membran markiert werden, um die Proteine, die spezifisch an der Extraktion am PPM beteiligt sind, spezifisch zu identifizieren. Durch diesen Ansatz wurde ein Total von 2000 verschiedenen Proteinen identifiziert. Von den identifizierten Proteinen wurden diejenigen analysiert, die im Interaktom der arretierten Konstrukte im Vergleich zum nicht arretierten, exportierten Zustand angereichert waren. Die Tatsache, dass SBP1-mDHFR-L-BirA*-3xHA hauptsächlich PTEX-Komponenten detektierte, bestätigt, dass dieses Konstrukt tief im Translokation in der PVM blockiert war, während REX2-mDHFR-L-BirA*-3xHA ein viel breiteres Spektrum von Proteinen (einschließlich PTEX-Komponenten) detektierte, was in Übereinstimmung mit früheren Daten auf eine Arretierung von zumindest eines Teils der Population dieses Moleküls in der PPM unmittelbar vor oder während der Translokation durch PTEX hindeutet. Mit Hilfe der SLI-Methodik wurden 10 Proteine, die als vielversprechende Treffer mit dem REX-mDHFR-L-BirA*-3xHA-Konstrukt identifiziert wurden, geklont, was die Lage und Funktion von bisher unbekannt Proteinen in *P. falciparum* aufdeckte. Da mehrere dieser Proteine in der Parasitenperipherie lokalisiert waren, deutete dies darauf hin, dass der Ansatz im Prinzip erfolgreich war. Außerdem wurden Proteine identifiziert, die am ERAD Prozess (Endoplasmic-reticulum-associated protein degradation) beteiligt sind, was darauf hindeutet, dass einige der PPM-arretierten REX2-mDHFR-L-BirA*-3xHA-Moleküle mit Hilfe des Qualitätskontrollsystems in die Zellen zurück extrahiert und degradiert wurden. Eine detaillierte Charakterisierung der anderen analysierten Proteine ergab jedoch, dass keiner der zehn in der BioID identifizierten Kandidaten die Extraktion von TMD-Proteinen aus der PPM in Richtung der PV begünstigte. Dies deutet darauf hin, dass der Mechanismus der Extraktion von exportierten Proteinen aus der PPM vollständig von PTEX abhängt (dessen Komponenten ebenfalls durch die Massenspektrometrie nachgewiesen wurden) und Kraft für die PPM-Extraktion von der PVM aus liefern könnte und so nur an der Außenseite des PPM mit dem exportierten Protein interagieren könnte,. Alternativ, könnten die zur PPM Extraktion beitragenden Proteine nicht für die BirA*-vermittelte Biotinylierung zur Verfügung gewesen sein, z.B. wenn sie tief im Lipid-bilayer der PPM lagen.

Im zweiten Teil dieser Arbeit wurde PfEMP1 direkt analysiert. Dies war in früheren Arbeiten nicht möglich, da dieses Protein sehr groß ist (was eine episodale Expression ausschließt) und

Teil einer Genfamilie ist, von welcher jeweils nur eine Kopie pro Parasit exprimiert ist, was zu Parasitenkulturen führt, die aus einer Mischung von Parasiten bestehen, die jeweils eines von den 60 unterschiedlichen PfEMP1-Moleküle exprimieren. Diese Probleme wurden hier zum ersten Mal durch die Erzeugung eines SLI-aktivierten PfEMP1 gelöst, das mit einem kleinen HA-Epitop markiert und von seinem eigenen genomischen Locus aus exprimiert wurde. Alle Parasiten exprimierten dieses PfEMP1, das mit einem Anti-HA-Serum bequem nachweisbar war. Diese Zellen wurden verwendet, um den Transport von PfEMP1 mit Fokus auf PTEX zu untersuchen, und mit dem Weg zu vergleichen, den andere exportierte Proteine bekanntermaßen nehmen. Dazu wurde untersucht, ob eine Blockierung von PTEX den Transport von PfEMP1 hemmt um die Passage durch diesen Komplex zu belegen. Aufgrund einer Reihe von Störungsfaktoren konnte dies nicht vollständig geklärt werden, aber die in dieser Arbeit vorgelegten Daten weisen darauf hin, dass PfEMP1 Transport möglicherweise nicht von PTEX abhängig ist, was mit bereits veröffentlichten Überlegungen kongruent ist. Die PfEMP1-SLI-Linie könnte auch als ein ausgezeichnetes Werkzeug zur Untersuchung der am PfEMP1-Transport beteiligten Proteine dienen. Dazu wäre jedoch eine zweite genomische Integration in den selben Parasiten erforderlich, etwas das bisher mit grossen technischen Hindernissen verbunden war. Daher wurde eine neue Version von SLI entwickelt, die bei Parasiten eingesetzt werden kann, welche bereits eine SLI-Genomveränderung aufweisen. Das System wurde als SLI2 bezeichnet und erlaubt es zum Beispiel, Gene in der PfEMP1-SLI-Linie zu disruptieren. Dabei zeigte sich unerwartet, dass der Transport von PfEMP1 zu den Maurer's Clefts (MCs) nach der Disruption von PTP1 nicht gestört war, was im Widerspruch zu früheren Erkenntnissen steht. Darüber hinaus führte die Disruption von SBP1 durchweg zu einer Revertierung der PfEMP1-SLI-Integration, was darauf hindeutet, dass die Unterbrechung von SBP1 wahrscheinlich den PfEMP1-Transport, wie zuvor publiziert, verhinderte und dass die Unterbrechung des Transports jedoch einen dominant negativen Effekt hatte. Diese Ergebnisse geben zwar nicht mit Sicherheit Aufschluss über den genauen Weg, den PfEMP1 nimmt, um seinen endgültigen Bestimmungsort zu erreichen, aber sie liefern entscheidende Instrumente für das Forschungsfeld, um (i) Faktoren zu identifizieren die den PfEMP1-Transport beeinflussen, (ii) die Expression und den Transport dieses Proteins zu verfolgen und (iii) - was entscheidend ist - die Bindungseigenschaften einzelner PfEMP1-Moleküle zu testen, da sie spezifisch mit SLI aktiviert werden können, wie dies in dieser Arbeit zum ersten Mal geschehen ist.

Mit den Ergebnissen dieser Arbeit und den hier vorgestellten technischen Fortschritten wird erhofft, dass die rätselhafte und seit langem bestehende Frage, wie TMD-Proteine und

insbesondere PfEMP1 in die Wirtszelle transportiert werden, endlich gelöst werden kann, um diesen wichtigen und faszinierenden Aspekt der Parasitenbiologie zu verstehen

Table of contents

Eidesstattliche Versicherung	ii
Declaration of academic honesty	ii
Language certificate	iii
Summary	iv
Zusammenfassung	vii
Table of contents	xi
List of figures	xv
List of tables	xvi
List of abbreviations	xvii
1 Introduction	1
1.1 Malaria.....	1
1.1.1 Epidemiology	1
1.1.2 Clinic	3
1.1.3 Malaria control	4
1.1.3.1 Antimalarials and drug resistance	4
1.1.4 Vaccine development	8
1.2 Plasmodium falciparum biology	9
1.2.1 Plasmodium falciparum lifecycle	9
1.2.2 Organelles specific for malaria parasites.....	11
1.2.3 Mosquito stages	13
1.2.4 Liver stages.....	13
1.2.5 Blood stages	14
1.2.6 Protein export in the erythrocytic cycle of <i>P. falciparum</i>	16
1.2.6.1 Mechanism for export soluble and non-soluble proteins	17
1.2.6.2 <i>Plasmodium</i> Translocon of Exported Proteins (PTEX).....	19
1.2.6.3 PfEMP1 export and its role in <i>P. falciparum</i> virulence	21
1.3 Approaches to study <i>Plasmodium</i> proteins	23
1.3.1 Selection markers	23
1.3.2 Prevent protein unfolding using mDHFR to study protein translocation.....	24

1.3.3	Selection-linked integration system (SLI).....	25
1.3.3.1	Knock Sideways (KS).....	26
1.4	Aim of the thesis.....	28
2	Materials and methods.....	29
2.1	Materials.....	29
2.1.1	Technical devices	29
2.1.2	Kits	30
2.1.3	Labware and disposables.....	30
2.1.4	Reagents	31
2.1.5	Primers.....	33
2.1.6	DNA and protein ladders.....	37
2.1.7	Antibodies	37
2.1.7.1	Primary antibodies	37
2.1.7.2	Secondary antibodies	37
2.1.8	Enzymes	38
2.1.8.1	Ligase and polymerase enzymes.....	38
2.1.8.2	Restriction enzymes	38
2.1.9	Buffer, media and solutions.....	38
2.1.9.1	<i>E. coli</i> culture	38
2.1.10	Buffers for production of Thermocompetent <i>E. coli</i>	39
2.1.11	Solutions and buffers for molecular biology analyses.....	39
2.1.11.1	<i>DNA precipitation</i>	39
2.1.11.2	DNA gel electrophoresis	39
2.1.12	Media and solutions for parasite culture and cell biology experiments	40
2.1.12.1	<i>P. falciparum in vitro</i> culture	40
2.1.13	Solutions for cell biology and biochemical assays	41
2.1.14	Buffers and solutions for protein analysis	42
2.1.14.1	SDS-Page and Western blot.....	42
2.1.15	Vectors.....	43
2.2	Methods.....	43
2.2.1	Microbiological methods.....	43
2.2.1.1	Production of thermo-competent <i>E. coli</i>	43
2.2.1.2	Thermo-competent <i>E. coli</i> transformation	43

2.2.1.3	Bacteria growth for Plasmid DNA preparation.....	44
2.2.1.4	Transformed bacteria storage.....	44
2.2.1.5	Immunofluorescence assay (IFA).....	44
2.2.2	Biomolecular methods.....	45
1.1.1.1	Polymerase chain reaction (PCR).....	45
2.2.2.1	PCR product purification.....	46
2.2.2.2	DNA restriction digest.....	46
2.2.2.3	DNA Ligation.....	46
2.2.2.4	Colony PCR-screen.....	46
2.2.2.5	PCR for integration diagnostic.....	46
2.2.2.6	Plasmid preparation.....	47
2.2.2.7	Agarose gel electrophoresis.....	47
2.2.2.8	Isolation of genomic DNA from <i>P. falciparum</i>	48
2.2.3	Biochemical methods.....	48
2.2.3.1	Western blotting.....	48
2.2.3.2	Immuno-detection of proteins.....	48
2.2.3.3	Pulldown of biotinylated proteins for mass spectrometry analysis (BioID)	48
2.2.4	Culture of <i>P. falciparum</i> and cell biological methods.....	49
2.2.4.1	<i>P. falciparum</i> cell culture.....	49
2.2.4.2	<i>P. falciparum</i> freezing and thawing.....	49
2.2.4.3	Blood smears and Giemsa staining.....	50
2.2.4.4	Parasite synchronization with sorbitol.....	50
2.2.4.5	<i>P. falciparum</i> Transfection using the BioRad system (ring transfection)..	50
2.2.4.6	Transfection using the Amaxa system (schizont transfection).....	50
2.2.4.7	Percoll gradient.....	51
2.2.4.8	Magnetic column separation of mature parasites.....	51
2.2.4.9	Biotin labelling of parasite proteins (BioID).....	52
2.2.4.10	Selection for transgenic parasites by SLI.....	52
2.2.4.11	Knock Sideways induction.....	53
3	Results.....	54
3.1	Screen for interaction partners involved in the extraction of Trans-membrane proteins out of the PPM.....	54

3.1.1	REX2 and SBP1 mDHFR fusion constructs are properly arrested in the PPM and PVM, respectively.....	54
3.1.2	Mass spectrometry identification of biotinylated proteins.....	56
3.1.3	Tagging and functional analysis of the candidates obtained from mass spectrometry.....	60
3.1.3.1	PF3D7_1418000. UFD1: ubiquitin fusion degradation protein 1.....	61
3.1.3.2	PF3D7_0934500: V-type proton ATPase subunit E.....	64
3.1.3.3	PF3D7_1226400: Conserved <i>Plasmodium</i> protein with unknown function 67	67
3.1.3.4	Pf3D7_0104500: Conserved protein with unknown function.....	69
3.1.3.5	PF3D7_0704300: Conserved <i>Plasmodium</i> membrane protein with unknown function	71
3.1.3.6	PF3D7_1410000. EMC2: ER membrane protein complex subunit 2.....	72
3.1.3.7	Pf3D7_0830400. CRA: CRA domain-containing protein.....	75
3.1.3.8	PF3D7_1105600-PTEX88: PTEX Translocon component; PF3D7_0928600 and PF3D7_1472100 (YIP1).....	77
3.2	Jamming PTEX and its implications in PfEMP1 export.....	77
3.2.1	Effect of exported protein disruption in PfEMP1 export.....	77
3.2.1.1	Double integrant: PTP1-TGD in a PfEMP1-3xHA ^{endo} cell line.....	80
3.2.1.2	Attempts to double integrate: SBP1-TGD in a PfEMP1-3xHA ^{endo} cell line 81	81
3.2.2	Implications of blocking PTEX in the PfEMP1 transport.....	82
3.2.2.1	Mal7-SBP1-mDHFR-GFP transfected in PfEMP1-3xHA ^{endo}	85
3.2.2.2	Double integrant: SBP1-mDHFR-GFP in a PfEMP1-3xHA ^{endo} cell line..	88
4	Discussion.....	92
4.1	Integration of mDHFR conditional folding and BioID systems for the analysis of protein export.....	95
4.1.1	Arresting of SBP1 and REX2 constructs in PTEX in order to identify possible PPM TM-proteins extractors.....	96
4.1.2	Analysis of potential PPM extractors of exported TM proteins.....	99
4.2	Jamming PTEX and its implications in PfEMP1 export.....	105
4.2.1	The effect of arresting SBP1 in PTEX on PfEMP1 export.....	107
4.2.1.1	The impossibility to disrupt SBP1 in a PfEMP1 expressing cell line.....	110
4.2.2	The effect of disrupting PTP1 on PfEMP1 export.....	110
5	Conclusions.....	112

Bibliography.....	114
Acknowledgements	143
Appendix A: Supplementary figures	144
Appendix B: supplementary tables.....	145

List of figures

Figure 1: Estimated malaria cases (millions) of <i>P. falciparum</i> and <i>P. vivax</i> by WHO region, 2017	2
Figure 2: Distribution map of <i>P. falciparum</i> cases where mutations in <i>Pfkelch13</i> is detected	7
Figure 3: Life cycle of <i>Plasmodium falciparum</i>	11
Figure 4: Intra-erythrocytic cycle of <i>P. falciparum</i>	15
Figure 5: Model of the PTEX translocon	20
Figure 6: PfEMP1 structure.	21
Figure 7: Selection-linked integration strategy	26
Figure 8: Schematic of Knock Sideways	27
Figure 9: Model of conditional arrest of REX2 and SBP1 constructs in the PPM and PVM.	54
Figure 10: Demonstration of arrest of SBP1 and REX2 constructs in the transition from the PPM to the erythrocyte cytosol	56
Figure 11: Biotinylated proteins enriched in arrested over non-arrested SBP1-mDHFR-L-BirA*-3xHA	58
Figure 12: Biotinylated proteins enriched in arrested over non-arrested REX2-mDHFR-L-BirA*-3xHA	59
Figure 13: PF3D7_1418000 (UFD1) ubiquitin fusion degradation protein 1	63
Figure 14: Pf3D7_0934500. V-ATPaseSE: V-type proton ATPase subunit E	66
Figure 15: Pf3D7_1226400. Conserved <i>Plasmodium</i> protein with unknown function	68
Figure 16: PF3D7_0104500. Conserved protein with unknown function	70
Figure 17: PF3D7_0704300. Conserved <i>Plasmodium</i> membrane protein	72

Figure 18: PF3D7_1410000 (EMC2) ER membrane protein complex subunit 2	74
Figure 19: PF3D7_0830400. CRA domain-containing protein	76
Figure 20: Pf3D7_0809100. PfEMP1 cell line endogenously tagged with 3xHA	78
Figure 21: Schematic of pSLI2a and pSLI2b vectors	79
Figure 22: Characterization of the double integrant cell line PfEMP1-3xHA ^{endo} + PTP1-TGD-GFP ^{endo}	81
Figure 23: Attempt to integrate SBP1-TGD-GFP in PfEMP1-3xHA ^{endo} cell line	82
Figure 24: Model of SBP1-mDHFR-GFP conditionally arrested in PTEX and its effect on PfEMP1 export	84
Figure 25: Characterization of the double transfectant cell line PfEMP1-3xHA ^{endo} +Mal7-SBP1-mDHFR-GFP ^{epi}	87
Figure 26: Characterization of the double integrant cell line PfEMP1-3xHA ^{endo} + SBP1-mDHFR-GFP ^{endo}	90
Figure 27: Model of protein translocation scenarios at the PPM and PVM.	94

List of tables

Table 1: First reported resistance to antimalarial drugs and molecular markers for drug resistance.	5
Table 2: Preparative and analytical PCR	45
Table 3: PCR temperature settings	45
Table 4: Candidates chosen to assess as potentially involved in TM-protein extraction.	60

List of abbreviations

α	alpha/anti
μ	micro
<i>crt</i>	gene of the CRT resistance transporter
<i>E. coli</i>	<i>Escherichia coli</i>
<i>P</i>	<i>Plasmodium</i>
<i>T</i>	Toxoplasma
aa	amino acids
ACT	artemisinin-based combination therapy
AMA-1	apical membrane antigen-1
APR	apical polar ring
ARL-V	Apicomplexan Related Lineage-5
ATP	adenosine triphosphate
BBB	blood-brain barrier
BioID	proximity-dependent biotin identification
BLASTp	Basic Local Alignment Tool (for proteins)
bp	Base pairs
C-	Carboxy-
CIDR	cysteine-rich interdomain region
CM	cerebral malaria
CoIP	co-immunoprecipitation
CRISPR	clustered regularly interspaced short palindromic repeat
CRT	chloroquine resistance transporter
CSA	chondroitin sulphate-A
CSP	circumsporozoite surface antigen
DAPI	4'6-Diamino-2-phenylindol
DBL	Duffy binding-like
DDT	dichlorodiphenyltrichlorethane
dH ₂ O	distilled water
DHFR	dihydrofolate reductase
DMSO	dimethylsulfoxide
DNA	deoxyribonucleic acid
DTT	dithiothreitol
DVS	dominant vector species
e. g	exempli gratia/ for example
EBA	erythrocyte binding antigen
ECL	enhanced chemoluminescence
EEF	exoerythrocytic form
EPCR	Endothelial Protein C Receptor
ER	endoplasmic reticulum
<i>et al</i>	et alii
EV	extracellular vesicle
EXP1/2	exported protein 1/2

FDR	false discovery rate
g	grams
GDP	gross domestic product
GFP	green fluorescent protein
GPI	glycosylphosphatidylinositol
h	hours
HBsAg	hepatitis B surface antigen
HIV	human immunodeficiency virus
hpi	hours post invasion
HRP	horseradish peroxidase
HSPG	Heparan sulphate proteoglycan
HT	host targeting
ICAM-1	Intercellular Adhesion Molecule 1
IE	infected erythrocyte
IFA	immunofluorescence analysis
IFA	immunofluorescence assay
IMC	inner membrane complex
IRS	indoor residual spraying
ITN	insecticide-treated bed net
KAHRP	Knob-associated histidine-rich protein
kDa	kilodalton
l	liter
LC-MS	liquid chromatography-mass spectrometry
LLIN	long-lasting insecticide-treated bed net
M	molar
m	milli
MAHRP	membrane associated histidine rich protein
MC	Maurer's cleft
min	minute
MSP-1	merozoite surface protein-1
MSRP	merozoite surface protein 7-related protein
MTOC	microtubule organizing center
mTRAP	merozoite thrombospondin related adhesion protein
n	nano
N-	Amino-
NANP	N-acetylneuraminic acid phosphatase
nm	nanometer
NPP	new permeation pathways
OD	optical density
PBS	phosphate buffered saline
PCR	polymerase chain reaction
PEXEL	<i>Plasmodium</i> export element
pH	potential hydrogen
PIESP2	parasite-infected erythrocyte surface protein 2
PNEP	PEXEL-negative exported protein

POI	protein of interest
PPM	parasite plasma membrane
PTEX	<i>Plasmodium falciparum</i> translocon of exported proteins
PV	parasitophorous vacuole
PVM	parasitophorous vacuole membrane
RBC	red blood cell
REX	ring exported protein
Rh	reticulocyte-binding like homolog
RON	rhoptry neck protein
RTS, S	purified recombinant circumsporozoite protein vaccine
s	seconds
SBP	skeleton binding protein
SERA	serine-repeat antigen
SP	signal peptide
SPC	signal peptidase complex
SPZ	sporozoites
SRP	signal recognition particle
STEVOR	sub telomeric variant open reading frame
TBV	transmission blocking vaccine
TGN	trans-Golgi network
TM	transmembrane
TMD	transmembrane domain
TNF-	tumour necrosis factor
TRAP	thrombospondin-related anonymous protein
TVN	Tubo-vesicular network
U	units
UV	ultraviolet
V	Volt
v	volume
<i>var</i>	<i>var</i> genes
WHO	World Health Organization

1 Introduction

1.1 Malaria

Malaria is a parasitic disease caused by organisms belonging to the genus *Plasmodium*, (order Haemosporidia). The genus *Plasmodium* comprises around 200 known species (Ajioka, 1997) that were categorized based on the morphology and appearance in blood smears. *Plasmodium* species were found to infect a wide variety of vertebrates like mammals, reptiles and birds (Boundenga *et al.*, 2017; Duval *et al.*, 2007; Witsenburg, Salamin and Christe, 2012). *Plasmodium* parasites are transmitted by several clades of blood feeding dipteran insects. Mosquitoes of the genera *Anopheles* are responsible for the transmission of human malaria.

Five species of *Plasmodium* are described as infecting humans: *Plasmodium malariae*, *P. knowlesi*, *P. ovale*, *P. vivax* and *P. falciparum*. Of these *P. falciparum* is responsible for almost all the human malaria fatalities (WHO, 2018; Rajahram *et al.*, 2019).

Even when there were 20 million fewer cases worldwide in 2017 than in 2010, there was only a minimal if slightly upward trend change in the 2015 to 2017 period, and malaria remains one of the world's leading killers, claiming the life of one child every two minutes (WHO, 2018).

1.1.1 Epidemiology

In 2017 an estimated 219 million cases of malaria occurred worldwide, resulting in 435.000 deaths (99.7 % due to *P. falciparum* infections). Children under 5 years are of the most vulnerable group affected by malaria, accounting for 61% of all malaria deaths worldwide (WHO, 2018).

Almost half of the world's population is at risk of being infected with malaria, with the African continent bearing 92% of all the reported cases, followed by the South East Asian region (10%), the Eastern Mediterranean Region (2%), the Western Pacific Region (0.86%) and the Americas, where the incidence of *P. vivax* is higher in comparison with the rest of the world (WHO, 2018).

While *P. falciparum* undoubtedly is the most important malaria parasite in terms of morbidity and mortality, the geographic distribution of *P. vivax* is more widespread (Howes *et al.*, 2016). This is due to this parasite's ability to reproduce at lower temperatures within the mosquito (Price *et al.*, 2007). Although in Africa the incidence of malaria caused by *P. vivax* is just

0,3%, this parasite is responsible for 74,1% of all malaria episodes in Latin America (WHO, 2018). The low prevalence of *P. vivax* infection in Africa is attributable to the fact that the majority of the human population does not express the Duffy binding receptor (Miller *et al.*, 1976) which is necessary for the invasion of this parasite into reticulocytes (Russo *et al.*, 2017). *P. vivax* infections have typically low blood-stage parasitemia with gametocytes (the transmitting stage taken up by mosquitoes) emerging before illness manifests. Furthermore, *P. vivax* generates dormant liver stages (hypnozoites), causing undetermined number of relapses that can occur even months or years after infection (Howes *et al.*, 2016; Battle *et al.*, 2015). These relapses result in a strong immune response that reflex in prostration and subsequently convalescence. During this time, the person is unable to work or assist to school, having significant negative socio-economic consequences beyond malaria.

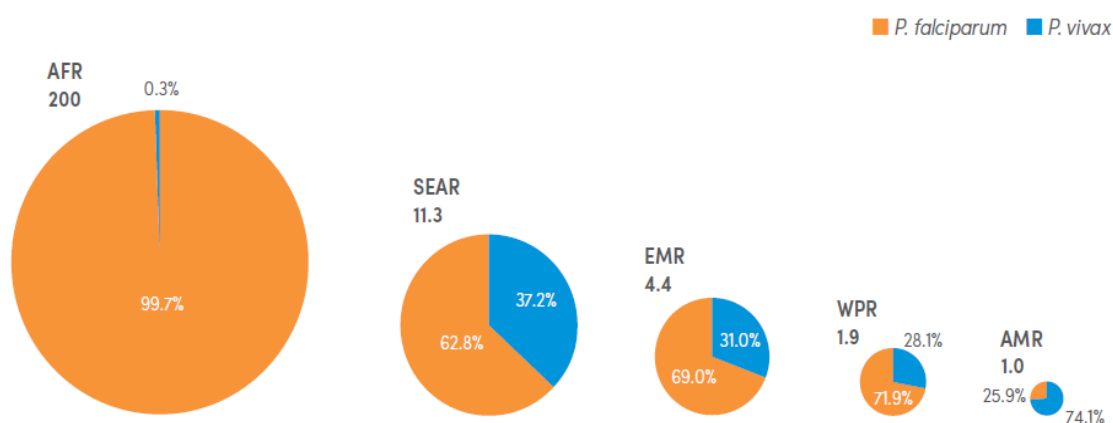


Figure 1: Estimated malaria cases (millions) of *P. falciparum* and *P. vivax* by WHO region, 2017
 The area of the circles is shown as a percentage of the estimated number of cases in each region. AFR: African Region; SEAR: South East Asia Region; EMR: Eastern Mediterranean.

In addition to *P. falciparum* and *P. vivax*, infections by other malaria species are also widespread. *P. malariae* is distributed similarly and often mix with *P. falciparum* infections (Collins and Jeffery, 2007) and *P. ovale* is present in Africa and the Western Pacific region (Collins and Jeffery, 2005). The simian parasite *P. knowlesi* has emerged as an important cause of human malaria, and despite being a zoonosis (transmitted only from apes to humans and not between humans), it is the most common cause of malaria in Malaysia, and cases have also been reported in nearly all countries of Southeast Asia (Barber *et al.*, 2017; WHO, 2018)

1.1.2 Clinic

Malaria illness results from the reproduction of the asexual, intraerythrocytic stage of *Plasmodium* parasites. The disease symptoms display a wide variety of pathologies that depend on the parasite species, the patient's age, immune status, general health, and nutritional constitution and time to initiate appropriate treatment (Gilles and Warrell, 2019). Uncomplicated Malaria symptoms are very diverse, including chills, sweating, headache, fatigue, myalgia, cough, and nausea; however fever is present in the majority of patients (Leder *et al.*, 2004).

The five human infecting species of *Plasmodium* are clinically distinguishable due to their blood stage cycle time and their clinical picture. *Plasmodium vivax*, *ovale* and *malariae* show a synchronous development cycle in the human blood. The newly formed parasites are released synchronously which lead to fever attacks of the patient. *P. vivax* and *P. ovale* preferentially infect young red blood cells, (reticulocytes) (McKenzie, Jeffery and Collins, 2001; McKenzie, Jeffery and Collins, 2002). The infection of reticulocytes is limited due to their low availability on the peripheral blood, what leads to a comparably low parasitemia when compared with other species. *P. vivax* and *P. ovale* cause the Malaria tertiana, which received its name because of the continuous fever attacks reoccurring on a 3rd day basis, coinciding with the 48 hour blood stage cycle of these species (McKenzie, Jeffery and Collins, 2002; Collins and Jeffery, 2005; Collins and Jeffery, 2007).

Since *P. falciparum* stages are not growing synchronously the fever attacks are irregular (Bartoloni and Zammarchi, 2012; Collins and Jeffery, 2005). It is remarkable that the clearly periodic fevers are often hidden due to mixed infections, resulting in fever-re-occurrence-patterns that are atypical for the infecting species and hence compromise diagnosis on this unique fact. The fever occurrences in all malaria infections coincide with the rupture of the infected red blood cell (iRBC) and posterior release of pyrogenic material into the blood stream. Malaria glycosylphosphatidylinositols' (GPIs) and hemozoin are recognized by toll-like receptors inducing the production of TNF- α , which is thought to be the major cytokine mediating malaria fever (Oakley *et al.*, 2011; Schofield *et al.*, 2002).

There are two main reasons for clinical outcomes of *P. falciparum* malaria: anaemia and cerebral malaria. Increased Splenic lysis and red blood cell (RBC) lysis by the parasite can result in haemolytic anaemia (Buffet *et al.*, 2011; Kai and Roberts, 2008). The ability of *P. falciparum* to bind to other infected RBCs (autoagglutination), to uninfected RBC (rosetting)

and to the endothelium of capillaries (cytoadherence) is believed to be a main reason for its increased pathology compared to the other malaria species (Dumbo *et al.*, 2009; Miller *et al.*, 2002). Rosetting and cytoadherence are thought to result in the sequestration of the infected red blood cells in small capillaries primarily in the brain and the placenta of pregnant women, but also in the kidneys, heart, lung, and liver (Spitz, 1946). This phenomenon can lead to a disrupted blood flow (Maier *et al.*, 2009), causing organ failure due to hypoxia and lactic acidosis (Miller *et al.*, 2013). A combination of obstruction of blood vessels and the blood-brain-barrier, reduced blood flow and inflammatory effects causing edema and axonal injury seem to play an important role in cerebral malaria (CM).

1.1.3 Malaria control

The WHO Global Malaria Program (GMP) is responsible for coordinating a global effort to control and eliminate malaria. The Global Technical Strategy provides a technical framework for all malaria-endemic countries working towards malaria control and elimination. It sets ambitious but presumably attainable global targets for 2030, including the reduction of malaria case incidence and mortality by at least 90%, the elimination of malaria in at least 35 countries and finally, preventing a resurgence of malaria in all countries that are already malaria-free (WHO, 2017).

All these achievements have been accomplished through vector control, proper use of antimalarial drugs and educational campaigns (WHO, 2018). Nevertheless, the emergence of insecticide resistant mosquitoes and drug resistant parasites paused the success of the program and today malaria rates remain high, especially in sub-Saharan Africa and South-East Asia (Greenwood *et al.*, 2008).

In 2007 the United Nations Millennium Declaration called for a 75% reduction in the global malaria burden by 2015. Through joint effort of different private and public organizations, and based on increased funding, the target was achieved, stopping the transmission and beginning to reverse the incidence of malaria and other major diseases such as HIV and Tuberculosis (Nations, 2015).

1.1.3.1 Antimalarials and drug resistance

Since 17th century when the first antimalarial compound was discovered and later on synthesized, several types of antimalarials are circulating on the market. Those drugs can be

classified in Quinine and derivatives (Chloroquine, mefloquine and lumefantrine); Atovaquone, Antifolates (proguanil, trimethoprim and pyrimethamine); and Artemisinin and its derivatives (dihydroartemisinin, artesunate and artemether).

The development of resistance to all previously mentioned drugs poses one of the greatest threats to malaria control and results in increased malaria morbidity and mortality. Resistance of malaria parasites to all the released drugs arises from several factors, including overuse of antimalarial drugs for prophylaxis, inadequate or incomplete therapeutic treatments of active infections, a high level of parasite adaptability at the genetic and metabolic levels, and a massive proliferation rate that permits selected populations to emerge relatively rapidly (Hyde, 2007). The molecular markers responsible for the resistance to most drugs have been identified and are summarized in Table 1

Table 1: First reported resistance to antimalarial drugs and molecular markers for drug resistance.

Antimalarial drug	Introduction date	1 st reported resistance*	Molecular marker
Quinine	1632	1910	<i>pf_nhe</i>
Proguanil	1948	1949	<i>dhfr</i>
Chloroquine	1945	1957	<i>crt</i> and <i>mdr1</i>
Sulfadoxine + Pyrimethamine	1967	1967	<i>dhps</i> and <i>dhfr</i>
Artemisinin	1971	2008	<i>pfmdr1</i> , <i>pfatpase6</i> , <i>pfubp1</i> and <i>pfk13</i> -propeller domain
Mefloquine	1977	1982	<i>pfmdr1</i>
Halofantrine	1988	1993	<i>pfmdr1</i>
Atovaquone	1996	1996	<i>cyt b</i>
Artesunate + Mefloquine	2000	2009	<i>pfmdr1</i>

* Taken and modified from (Sinha, Medhi and Sehgal, 2014)

In the 17th century, the first antimalarial compound, quinine, was discovered. Before 1820 quinine and the related cinchona alkaloids quinidine, cinchonine and cinchonine, were ingested as the pulverized bark of the cinchona tree mixed into a liquid. The compounds can be obtained from the bark since 1820 and were then used as the normal malaria therapy. New synthetic and more efficient drugs were available in the 1920s and finally in 1934 chloroquine (CQ) appeared in the panorama, becoming the primary antimalarial drug (Achan *et al.*, 2011).

The extensive use of CQ led to resistance emergence 3 decades after its introduction in the market, which spread across the world from two foci, one in South-East-Asia and the other in

South America, to become conjoint in the 1980s. Since then quinine became more relevant again and today is still used as a drug for malaria management (Achan *et al.*, 2011). With the exception of some areas in North Africa, Central America and the Caribbean, chloroquine resistance is spread through all the transmission areas (WHO, 2018)

Chloroquine and other quinine derivatives like amodiaquine, piperaquine, and mefloquine affect the haemoglobin degradation. The haemoglobin degradation leads to a formation of hemozoin, that is a *Plasmodium*-specific metabolite. Mutations in the Chloroquine Resistance Transporter (CRT) protein In *P. falciparum*, and specially the K76T are the responsible for CQ resistance (Fidock *et al.*, 2000). PfCRT mutations also mediate or promote resistance to other malaria drugs, such as amodiaquine and mefloquine (Muller and Hyde, 2010). Other drugs like Sulfadoxine-pyrimethamine and atovaquone-proguanil have been more used for malaria therapy since chloroquine resistance appeared, but for many of them resistance also has arisen.

Since 2006 the WHO recommends the use of artemisinin and its derivatives (e.g. artemether, artesunate, and dihydroartemisinin) in combination with longer acting antimalarials such as mefloquine or lumefantrine. The treatment is known as Artemisinin-based combination therapy (ACT) and adequate dose regimens of combinations of artemisinin and mefloquine or artemether and lumefantrine were very effective until the first parasitic clearance delay were reported in 2009 in Thailand-Cambodia border (Dondorp *et al.*, 2009). An artemisinin resistance mutation in the PfKelch13 protein (C580Y) is now recognized as a molecular sign of resistance (Ariey *et al.*, 2014). It is not known which is the target of the artemisinin and therefore, the mechanisms of how this drug acts are unknown. One study suggested that artemisinin is a potent inhibitor of the *P. falciparum* phosphatidylinositol-3-kinase (*Pf* PI3K) (Mbengue *et al.*, 2015), and another study showed that artemisinin activation at the early ring stage seems to rely on the parasite's haem biosynthesis, whereas drug activation depends on haemoglobin digestion as the main haem source at the latter parasite stages, which determines the high specificity of the drug towards the parasite (Wang *et al.*, 2015).

Drug resistance is probably the greatest challenge that malaria-control programs are facing. The useful lifespan of a new antimalarial may be lengthened if it is used in combination with other drugs, and therefore combination therapies have been the focus for the management of multidrug-resistant malaria. The past decade has brought progress in the understanding of the molecular basis of drug resistance in *P. falciparum*. Sets of mutations in *dhfr* and *dhps*, *pfprt*, *pfmdr1* and now *pfkelch13* genes are the center of studies on resistance. Overall, the right

combination of point mutations in specific *P. falciparum* genes may be necessary for a drug-resistant phenotype.

As more information on antimalarial resistance becomes available, design of new molecular-based tools for early detection may become possible. This together with interventions aiming to limit the extent of established multidrug resistance and prevent the emergence of new foci of drug resistance (Wongsrichanalai *et al.*, 2002).

Since 2006 the WHO recommends the use of artemisinin and its derivatives (e.g. artemether, artesunate, and dihydroartemisinin) in combination with longer acting antimalarials such as mefloquine or lumefantrine for *P. falciparum* malaria treatment. The treatment is known as Artemisinin-based combination therapy (ACT) and adequate dose regimens of combinations of artemisinin and mefloquine or artemether and lumefantrine were very effective until the first parasitic clearance delay were reported in 2009 in Thailand-Cambodia border (Dondorp *et al.*, 2009) Since then, more cases of delay in the parasite clearance has been reported in the South-East of Asia, Africa and South America. An artemisinin resistance mutation in the *PfKelch13* protein (C580Y) is now recognized as a molecular sign of resistance (Ariey *et al.*, 2014), also in 2015 was reported that K13-propeller mutations confer artemisinin resistance in *P. falciparum* clinical isolates (Straimer *et al.*, 2015). These mutations in *PfKelch13* have been recorded and are concentrated in Southeast Asia (Figure 2).



Figure 2: Distribution map of *P. falciparum* cases where mutations in *Pfkelch13* is detected

Map showing the worldwide distribution of cases where *Pfkelch13* mutations were detected, with darker colours represents higher number of cases reported vs lower number of cases being represented by lighter colours. Map with plotted cases from 2015 to 2019. Extracted from Interactive maps of parasite drug efficacy and resistance, (WHO, 2019).

Drug resistance is probably the greatest challenge that malaria-control programs are facing. The useful lifespan of a new antimalarial may be lengthened if it is used in combination with other drugs, and therefore combination therapies have been the focus for the management of

multidrug-resistant malaria. The past decade has brought progress in the understanding of the molecular basis of drug resistance in *P. falciparum*. Sets of mutations in *dhfr* and *dhps*, *pfprt*, *pfmdr1* and now *pfkelch13* genes are the center of studies on resistance.

As more information on antimalarial resistance becomes available, design of new molecular-based tools for early detection may become possible. This together with interventions aiming to limit the extent of established multidrug resistance and prevent the emergence of new foci of drug resistance (Wongsrichanalai *et al.*, 2002).

1.1.4 Vaccine development

The greatest challenge in the development of an antimalarial vaccine lies in the fact that even with constant and multiple exposures to the parasite, humans do not develop a sterile immune response and this is one of the reasons that, despite having conducted many studies and many clinical trials, there is no efficient vaccine for commercial use.

The WHO published strategic goals to license malaria vaccines targeting *P. falciparum* and *P. vivax* with at least 75% protective efficacy against clinical malaria and reducing transmission to enable elimination (WHO, 2013). The most advanced candidate vaccine to the date was the RTS,S/AS01, completed phase 3 testing in seven sub-Saharan African countries and demonstrated four-dose efficacy against clinical malaria of 27% over a median 38 months in children aged 6–12 weeks, and 39% efficacy over a median 48 months in those aged 5–17 months (The RTS, 2012). Based on the RTS, S phase 3 efficacy and safety data, the vaccine received a favourable opinion from the European Medicines Agency. At the recommendation of the WHO Strategic Advisory Group of Experts (SAGE) on immunization and the Malaria Policy Advisory Group (MPAC), the vaccine is currently being tested in children 5–17 months of age in three sub-Saharan African countries with moderate-to-high transmission. Efforts to improve on the low efficacy of RTS,S/AS01 include modified dosing regimens of RTS,S and over 20 other malaria vaccine strategies currently in clinical testing, using candidate antigens in monovalent and multivalent formulations either alone or with other agents, viral vectors, and/or vaccine adjuvants.

Another approach tried as a vaccine is the use of whole sporozoite vaccines (WSV) to induce a highly effective pre-erythrocytic immunity. WSV consist of either radiation attenuated sporozoites (RAS) (Clyde *et al.*, 1973; Nussenzweig *et al.*, 1967) or genetically attenuated parasites (GAP) (Matuschewski *et al.*, 2002). Protection induced by RAS appears to be based primarily on the induction of T cell responses, but antibodies responses were also detected.

The company SANARIA® developed an injectable product composed of radiation attenuated, aseptic, purified and cryopreserved sporozoites that can be safely administered intravenously (Seder *et al.*, 2013) and high-level protection can be achieved by four to six doses. Challenges regarding the manufacture, delivery, administration and long-term immunogenicity with such a vaccine are still debated (Richie *et al.*, 2015). GAP is made out of parasites that bear genetic deletions that arrest parasite development during hepatocyte infection (Mueller *et al.*, 2005; VanBuskirk *et al.*, 2009; Spring *et al.*, 2013). SANARIA® recently also generated the vaccine PfSPZ-GA1 which consists of purified, aseptic, cryopreserved *P. falciparum* sporozoites genetically attenuated by removal of the *b9* and *slarp* genes that are required for liver development (van Schaijk *et al.*, 2014). The phase 1 trial started in 2017 with 19 volunteers. The first stage of this trial is already finished and currently, the samples obtained from the stage B patients are being analyzed (SanariaInc, 2019).

1.2 Plasmodium falciparum biology

1.2.1 Plasmodium falciparum lifecycle

The lifecycle of the five species of Plasmodium that infect humans is similar in most of the aspects, differing only in the duration of the phases, the morphology of the intraerythrocytic forms and the production of hypnozoites in *P. vivax* and *P. malaria*.

The cycle can be divided in two phases, the sexual phase that occurs in the mosquito and the asexual phase, that occurs in the vertebrate host (Figure 3). The cycle starts when Anopheles mosquitos ingest gametocytes from an infected host. Gametocytes are the sexual stages of *Plasmodium spp* that develops in the human host. With the blood meal gametocytes enter the midgut of the mosquito and further develop to gametes, leading to the formation of female (macrogamete) and male (microgamete) stages that upon fertilization form a motile parasite stage known as ookinete. The ookinete penetrates the gut wall and under the basal lamina of the midgut epithelium develops to an oocyst. This oocyst then ruptures and releases up to 1.000 sporozoites which migrate to the mosquito's hemolymph to invade the salivary gland epithelium where they are accumulated waiting for being transmitted to the second intermediary host with the next blood meal (Greenwood *et al.*, 2008).

When the infected mosquito bites a human, several hundred sporozoites are injected with the saliva into the dermis of the human host. In the dermis sporozoites find blood vessels and enter the blood stream for migrate later to the liver. With the active invasion of the hepatocytes by the sporozoites, the hepatic phase starts. This so called 'exoerythrocytic schizogony' is the first

of two asexual multiplications that the parasite must complete in the human host. Within the liver cell the parasite develops to a liver schizont, reproduces asexually, and forms up to 30.000 merozoites. Under destruction of the host hepatocyte, these merozoites are released into the sinusoid lumen in parasite-filled vesicles called merozoites. Thus, the parasite bypasses the recognition through the immune system and ensures the release of merozoites into the bloodstream (Sturm *et al.*, 2006). The merozoites then rupture to release merozoites that now are ready to invade red blood cells (RBC) to initiate the second asexual reproduction phase. Within the RBC the parasites start the intraerythrocytic cycle or blood cycle (detailed later in section 1.2.5) that is the responsible for the characteristic symptoms of malaria. In the blood cycle merozoites are produced, most of those merozoites are released and re-invade RBCs to replicate the cycle. However, a few merozoites, upon entry into new RBCs, develop to gametocytes instead of continuing with the asexual multiplication. Those gametocytes are released on the human blood stream for being transmitted again to the mosquito, thus completing the cycle (Greenwood *et al.*, 2008).

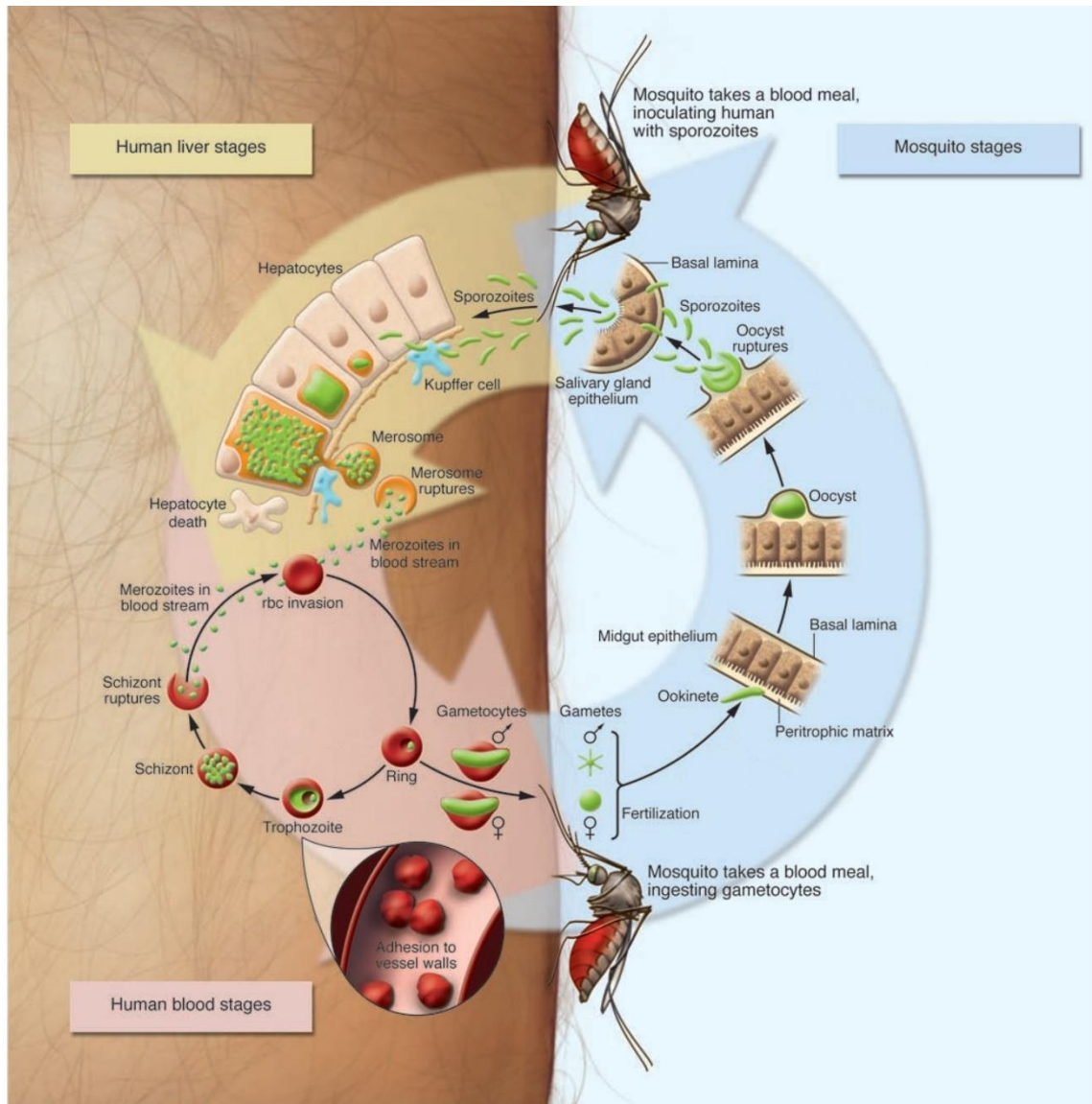


Figure 3: Life cycle of *Plasmodium falciparum*

The cycle of *P. falciparum* (green) starts when gametocytes are taken up by an Anopheles mosquito with its blood meal. Then, the parasite develops within the mosquito's midgut into sporozoites. Through another mosquito bite, these sporozoites are transferred to the human host, develop within the liver to merozoites and are released into the blood stream where they invade RBCs. Here new merozoites are formed and released. A few of the merozoites develop into gametocytes that can be ingested by the mosquito through another blood meal thus completing the cycle. Taken and modified from Greenwood *et al.*, 2008.

1.2.2 Organelles specific for malaria parasites

In addition to the basic organelles shared with other eukaryotic organisms *Plasmodium* parasites possess highly specialized organelles, including some that are critical for their intracellular lifestyle. This includes for instance the apical organelles, which are essential for the invasion into RBCs or other types of host cells such as hepatocytes the parasite resides in during liver stage development. The apical complex contains secretory organelles termed micronemes, rhoptries, exonemes and dense granules. In addition to these, the parasite contains

a secondary endosymbiont termed the apicoplast and a lysosome-like organelle termed the food vacuole (FV) where haemoglobin that was internalized from the host cell is digested.

Further structures critical for invasion of host cells, are the subpellicular microtubuli and the inner membrane complex. These structures act together during the invasion process mechanically induce the entrance of the parasite. The formation of these organelles (rhoptries, micronemes, dense granules) during merozoite and sporozoite biogenesis is just partly understood, but it seems that proteins typically involved in endocytosis in model organisms were repurposed to operate in this specialized secretory pathway in Apicomplexans (Kremer *et al.*, 2013; Pieperhoff *et al.*, 2013; Tomavo *et al.*, 2013). When inside the host cell, the parasite loses some of these defining organelles and forms distinct stages that are typical for each phase of the life cycle.

The apicoplast is originated from an algae through secondary endosymbiosis, therefore is surrounded by four membranes (Lim and McFadden, 2010). It might have served as a supplier of energy through photosynthesis but lost this ability during the course of evolution. It is maternally inherited (Okamoto *et al.*, 2009) and present throughout the entire life cycle of the parasite (Stanway *et al.*, 2009). The apicoplast carries important metabolic pathways like fatty acid synthesis, isoprenoid precursor synthesis and parts of the heme biosynthetic pathway (McFadden, 2019; Yeh, 2019). This organelle contains more than 500 proteins, but only about 50 are still encoded in the apicoplast itself (on the 35 kb plastid genome). Like for the mitochondrion, most parts of the apicoplast genome were transferred to the nucleus and the gene products are transported back to the apicoplast (Heiny *et al.*, 2014; Spork *et al.*, 2009).

Contrasting to the apicoplast, the FV may be formed *de novo* during each cycle in a new host cell, as it presumably is dissolved during merozoite egress from the RBC. Its formation may be driven by the fusion of several endocytic vesicles in the late ring stage (Abu Bakar *et al.*, 2010; Lazarus, Schneider and Taraschi, 2008). The FV contains a set of proteases e.g. falcipain, plasmepsin I and plasmepsin II, that drive haemoglobin digestion (Goldberg *et al.*, 1991; Goldberg *et al.*, 1990). A degradation product is α -hematin, which is toxic for the parasite due to its property to induce the production of free radicals in the FV. The parasite polymerizes α -hematin into the nontoxic hemozoin, but the enzymes catalyzing this polymerization are still not entirely clear.

1.2.3 Mosquito stages

The sexual cycle of the parasite initiates when the mature gametocytes are taken up by an Anopheles mosquito during a blood meal on an infected human. Due to the temperature changes and the presence of the mosquito metabolite xanthurenic acid (XA), the gametocytes can be differentiated on male (microgametocytes) or female (macrogametocytes) that will later fuse as a zygote (Kuamsab *et al.*, 2012). The zygote transforms into a motile ookinete, which undergoes one meiotic division, after 24 hours migrates through the mosquito's gut wall, and remains underneath the mosquito midgut basal lamina, where it is protected from the host immune system and transforms into an oocyst. Within the oocyst thousands of sporozoites are formed. The sporozoites egress from the oocyst and distribute through the hemolymph to reach the basal lamina of the mosquito's salivary glands, where they invade acinar cells to finally accumulate inside the salivary duct. Here the sporozoites reach full maturity and thus infectivity (Matuschewski, 2006). Finally, the sexual cycle in the primary host is completed with the next blood meal which leads to inoculation of sporozoites into the intermediate (vertebrate) host.

1.2.4 Liver stages

The asexual cycle in the intermediate host (humans) initiates with the injection of usually several dozens of sporozoites into skin during the bite of an infected mosquito. From there the sporozoites migrate to lymphatic and dermal blood vessels. Approximately 50% of the sporozoites remain in the skin, where they develop into exoerythrocytic forms (EEFs) and can contribute to the blood cycle infection (see section 1.2.5) (Gueirard *et al.*, 2010). The majority of the sporozoites invading lymphatic vessels are eliminated by phagocytosis, but some manage to reach the bloodstream and are transported towards the liver (Amino *et al.*, 2007; Amino *et al.*, 2006b; Amino *et al.*, 2006a). Once in the liver, sporozoites are sequestered in the sinusoids, probably through the interaction of highly sulphated heparin-sulphate proteoglycans (HSPGs) extending from stellate cells through fenestrations in endothelial cells and CSP on the surface of sporozoites (Coppi *et al.*, 2007; Rathore *et al.*, 2003). Activated sporozoites migrate through hepatocytes (transmigration) (Mota and Rodriguez, 2002; Prudencio and Mota, 2007) and initially traverse cells inside non-replicative transient vacuoles (Risco-Castillo *et al.*, 2015). Sporozoites use pH sensing and a perforin-like protein 1 (PLP1) to exit these vacuoles and finally invade a hepatocyte where they establish a replication competent parasitophorous vacuole (PV) to turn into EEFs (Risco-Castillo *et al.*, 2013).

Once in the hepatocyte the parasite develops into a schizont containing thousands of merozoites. In this process, the sporozoite changes its shape from a stretched into a round form, disassembles the machinery necessary for invasion and modifies the PV membrane (PVM). At the end of the liver stage, the PVM disintegrates, releasing the merozoites into the host cell cytoplasm. The release of merozoites into the blood stream occurs via merozoites (vesicles containing thousands of merozoites) (Sturm *et al.*, 2006), which were shown, for the rodent malaria parasite *P. yoelii*, to rupture in the pulmonary microvasculature (Vaughan *et al.*, 2012; Coquelin *et al.*, 1999).

During the merozoite release into the host cell hepatocyte, the parasite alter the central mechanisms of the infected cell, such as protein synthesis or the expression of genes involved in inflammation in order to survive (Singh *et al.*, 2007). Currently just the CSP protein (Singh *et al.*, 2007) and the Liver stage specific protein 2 (LISP2) (Orito *et al.*, 2013) have been shown to localize in the cytosol of the murine parasite *P. berghei*. However, a recent study in the same parasite suggested that protein export from the parasite into the host cell may differ between liver and RBC stages (see section 1.2.1). This idea was based on the fact that GFP-fusions of proteins exported to the RBC were not translocated into the hepatocyte, and essential components for protein export in the RBC phase were absent in the PV of liver stages (Kalanon *et al.*, 2016; Kalanon *et al.*, 2015) whereas others were however present (Kaiser *et al.*, 2004).

1.2.5 Blood stages

The intra-erythrocytic cycle or blood cycle starts with the merozoites released from the liver into the blood stream. This cycle takes 48 hours in *P. falciparum* infections and comprises morphologically distinct stages: termed rings, trophozoites and schizonts (Figure 4). During the ring stage, the parasite intensively modifies the host RBC by exporting parasite-derived proteins into the RBC cytosol. This process is necessary to establish a niche supporting its survival (Sleebs *et al.*, 2014; Spillman, Beck and Goldberg, 2015). As mature RBCs lack organelles that could be used by the parasite to transport its own proteins, the parasite must itself produce a machinery capable to mediate protein trafficking in the host cell (Marti and Spielmann, 2013).

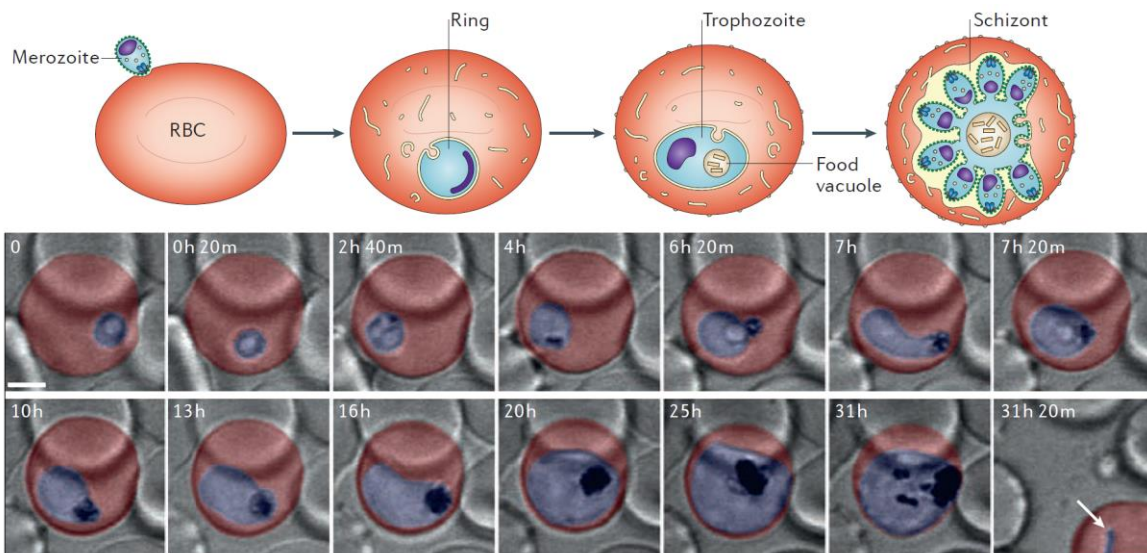


Figure 4: Intra-erythrocytic cycle of *P. falciparum*

Graphic representation of the four main blood stages of *Plasmodium* spp. development (upper panel), and 4D imaging of the developing *Plasmodium falciparum* parasite (blue) using confocal microscopy (lower panel), showing the complete erythrocytic stage of development in an individual infected red blood cell (RBC; red). Selected time points in differential interference contrast (DIC) microscopy are shown, from ring stages to schizont stages. The first time point corresponds to a late ring stage and is labelled (0) as imaging was started at this point (i.e. imaging time indications do not correspond to parasite age). The white arrow at 31h 20m shows a ring stage derived from reinvasion after rupture. Scale bar represents 2 μ m. (De Niz *et al.*, 2017) adapted from (Gruring *et al.*, 2011)

Ring stages are so named because of the ring-like appearance in Giemsa smears. However, when observed by differential interference contrast (DIC) microscopy living ring stages are motile in the host cell and show different shapes that range from amoeboid, starfish shaped to annular forms (Grüring *et al* 2011). This phase normally encompasses 0 to ~18 hours post invasion (hpi). During that time rings show only slight increase in size and it is believed that the main effort of the parasite concentrates on producing and exporting proteins to modify the host RBC. Ring stages (and to a usually much lower extent also gametocytes) are normally the only forms found in a patient's peripheral blood. This due to the fact that the late developmental stages (trophozoites and schizonts) sequester to the endothelium of capillaries and venules to bypass the clearing of RBCs infected with these stages in the spleen (David *et al.*, 1983; White, 2017).

The next stage, the trophozoite (Trophos= Greek for food) stage occurs between ~18 to ~36 hpi and is characterized by rapid parasite growth. During transition of rings to trophozoites, the position of the parasite in the RBC becomes fixed (Gruring *et al.*, 2011). *P. falciparum* trophozoites are roundish or oval in shape and with continued growth start to fill out most of the RBC cytosol. A key process during this growth phase is the continuous uptake of RBC

cytosol (Francis, 1997) which consist mostly of haemoglobin. However, the parasite is unable to digest the Haem group of the haemoglobin (Toh *et al.*, 2010), which it transforms to a polymerized form termed hemozoin (often called malaria pigment). The malaria pigment appears as a black crystal structure (Moore *et al.*, 2006), which is stored in the food vacuole (FV).

Finally, the trophozoite develops into a schizont, the stage in which the infective merozoites are formed. The parasites undergo multiple mitotic divisions in a manner called schizogony (Skhiz= Greek for divide). The schizogony starts around 36 hpi and depending on the condition (*in vivo*, *in vitro*, different species or strains etc.) could last until 42 to 47 hpi (Crutcher and Hoffman, 1996). During this phase, the merozoites are assembled in a process that includes the replication and segregation of the mitochondria and apicoplast (each merozoite obtaining one), formation of the IMC and the *de novo* generation of the apical complex (van Dooren *et al.*, 2005; Kono *et al.*, 2012; Francia and Striepen, 2014). At the end of the cycle the segmented schizont will contain from 10 to 36 merozoites that are released to the blood stream in a process termed egress that destroys the host RBC. Merozoites then re-invade into naïve RBCs to initiate another round of intra-erythrocytic replication.

1.2.6 Protein export in the erythrocytic cycle of *P. falciparum*.

Mature RBCs lack many basic features of eukaryotic cells, including mechanisms of protein transport. Nevertheless, malaria parasites are well adapted to this environment and they are able to induce extensive alteration to their host cell. These alterations require export of a large number of parasite proteins that are trafficked across multiple membranes to reach the host cells cytosol (Marti and Spielmann, 2013). Approximately 10% of all *P. falciparum* proteins are predicted to be exported (exportome) (Spielmann and Gilberger, 2015), showcasing the magnitude and importance of this process.

Protein export of the parasite is essential for phenomena like cytoadhesion of infected RBCs to the endothelium of blood vessels, which depends on the expression of PfEMP1, a primary virulence factor of *P. falciparum* parasites (Baruch *et al.*, 1995; Smith *et al.*, 1995; Su *et al.*, 1995). However, the function of most exported proteins is still unknown and their study is impeded by the fact that many of them may play a role that only *in vivo* is essential (Maier *et al.*, 2008). Multigene families such as *rifin*, *stevor* and *var*, encode for the surface proteins RIFIN, STEVOR and PfEMP1, which are involved in antigenic variation, cytoadhesion and rosetting: the interaction of infected RBCs with non-infected RBCs (David *et al.*, 1983).

Trafficking of exported proteins could be divided in two phases: Transport within the parasite and transport to the iRBC surface. The initial phase starts when the proteins leave the ER. Following the classical vesicular secretory pathway as evidenced by the sensitivity of this phase to brefeldin A or ER retention signals (Deponete *et al.*, 2012). It's here in the ER, where the PEXEL motif (further described in section 1.2.6.1) is processed, but how processing of the motif influences export is still not very clear. One possibility is that Plasmepsin V cleavage already directs the protein to a specific vesicular trafficking route designated for export ending in the parasite boundary (Spielmann and Gilberger, 2015).

In the second phase, the exported protein leaves the parasite and enters the host cell, a process that requires passage across PPM and PVM. The cross of proteins through those membranes is given by the PTEX (further described in section 1.2.6.2). PTEX is in the PVM and while soluble exported proteins will be directly released into the PV after fusion of transport vesicles with the PPM, membrane-embedded exported proteins will end up in the PPM and require extraction mechanism to reach the PTEX. So, it is intriguing that TM proteins are also substrates of PTEX. It is also interesting to note that exported proteins with more than two TM domains have not been described. This could indicate restrictions imposed by the membrane translocation/extraction steps during export (Spielmann and Gilberger, 2015). Finally, after passing the PPM, the proteins will reach the iRBC cytosol and exported TM proteins permanently or transiently appear at the Maurer's clefts, highlighting these structures as a sorting hub in the host cell. However, how TM proteins reach the clefts is unclear.

1.2.6.1 Mechanism for export soluble and non-soluble proteins

Exported proteins must cross two membranes: the PPM and the PVM in the parasite periphery. For the successful delivery to the parasite periphery, exported proteins must contain a special sorting signal termed the PEXEL (*Plasmodium* Export Element). The PEXEL is a motif (RxLxE/Q/D) was described to be preferably located 15–20 amino acids downstream of an N-terminal hydrophobic signal sequence (Hiller *et al.*, 2004; Marti *et al.*, 2004; Goldberg, 2012) and is cleaved after the conserved L amino acid by an ER protease called Plasmepsin V (PM5) (Russo *et al.*, 2010; Boddey *et al.*, 2010). The new N-terminus of the exported protein, now starting with xE/Q/D, is N-acetylated and the mature protein is exported into the host cell (Boddey *et al.*, 2009). The downstream region of the mature PEXEL N-terminus (~20 amino acids) was found to contain additional export information, which can compensate for a mutated xE/Q/D in reporter constructs (Tarr *et al.*, 2013; Gruring *et al.*, 2012). Non-canonical PEXEL-motifs in *Plasmodium* proteins (e.g. the RxLxxE sequence in the RESA protein family) were

also shown to be cleaved by PM5 and exported to the host cell (Boddey *et al.*, 2013). The major virulence factor of *P. falciparum*, PfEMP1, contains the non-canonical sequence KxLxD which cannot be processed by PM5, whereas processing of different non-canonical motifs can occur in other proteins, depending on the surrounding sequence environment (Schulze *et al.*, 2015).

Based on the number of proteins containing a predicted PEXEL motif it was estimated that the exportome of *P. falciparum* parasites comprises 300–400 different proteins (Marti *et al.*, 2004; Hiller *et al.*, 2004; Sargeant *et al.*, 2006; van Ooij *et al.*, 2008), and of these approximately 75% belong to protein families, leaving ~100 exported protein with no phylogenetical relation to any family (Heiber *et al.*, 2013; Sargeant *et al.*, 2006). On the other hand, the number of exported proteins without a PEXEL-motif to date comprises only ~20 proteins (not counting members of protein families) and are denoted as PNEPs (PEXEL-negative exported proteins) (Spielmann and Gilberger, 2010). 'Classical' PNEPs do not contain a SP and entry into the ER is mediated by a transmembrane domain (TMD). The export relevant information is located within the first 10-20 amino acids of the N-terminus. However, no consensus sequence could be identified yet, so that a prediction of PNEPS based on the amino acid sequence is not possible. Replacement of a PNEP N-terminus with a mature PEXEL N-terminus can restore the export of a PNEP reporter construct, showing that PNEPs and PEXEL-proteins share a common export domain and might be exported via the same export pathway (Gruring *et al.*, 2012). The first PNEPs were discovered by chance and included integral TM proteins without signal peptide that localized to the Maurer's clefts such as for instance SBP1 (Blisnick *et al.*, 2000), REX2 (Spielmann *et al.*, 2006), and MAHRP1 (Spycher *et al.*, 2008) along with peripheral Maurer's clefts proteins for instance MAHRP2 (Pachlatko *et al.*, 2010) and REX1 (Hawthorne *et al.*, 2004).

PNEPs may be more prevalent in the *Plasmodium* genome than initially thought and are now known to include also soluble and non-soluble proteins with a classical N-terminal signal peptide. (Heiber *et al.*, 2013). A study considering only proteins as PEXEL positive if they were processed by PM5 changed the initial exportome classification, excluding several proteins with a relaxed or non-canonical PEXEL motif, including PfEMP1, which was reclassified as a PNEP (Boddey *et al.*, 2013). However, some proteins with a non-canonical PEXEL motif were later found to be cleaved in a manner typical for PM5 (Schulze *et al.*, 2015), indicating that the motif alone is not a perfect indicator for this classification.

1.2.6.2 Plasmodium Translocon of Exported Proteins (PTEX)

In order to remodel the host cell and create a niche to survive, the parasite produces a large amount of proteins that need to be exported. To reach their final destination, those proteins have to cross through the PPM and the PVM. In 2009 the *Plasmodium* translocon of exported proteins (PTEX) was identified (de Koning-Ward *et al.*, 2009) and later on confirmed as responsible for the translocation of proteins across the PVM (Garten *et al.*, 2018; Beck *et al.*, 2014). More recently the structure of PTEX was described (Ho *et al.*, 2018).

The PTEX comprises five components in *P. falciparum* (de Koning-Ward *et al.*, 2009) and *P. berghei* (Matthews *et al.*, 2013; Matz *et al.*, 2015a). The three main components are the AAA+ ATPase heat shock protein 101 (HSP101), exported protein 2 (EXP2) and PTEX150. EXP2, PTEX150 and HSP101 were found to assemble in that order relative to the PVM, forming a complex of ~1,230 kDa. The other two proteins are accessory components of the complex and are thioredoxin 2 (TRX2) (Matthews *et al.*, 2013) and PTEX88 (Matz *et al.*, 2015b; Matz, Matuschewski and Kooij, 2013) (Figure 5). TRX2 is dispensable in blood stages of *P. falciparum* but due to its low weight and low expression levels, TRX2 is not often detected and not included in the total size of the complex.

PTEX88 is non-essential in *P. berghei*. Proteomic analysis of PTEX88 interactome showed that PTEX88 interacts closely with HSP101 but has a weaker affinity with the other core constituents of PTEX (Chisholm *et al.*, 2016). PTEX88 was also found to associate with other PV-resident proteins, including chaperones and members of the exported protein-interacting complex that interacts with the major virulence factor PfEMP1 in *P. falciparum*, contributing to cytoadherence and parasite virulence (Chisholm *et al.*, 2016). PTEX88 knockout parasites in *P. berghei* showed a striking growth defect (Matz, Matuschewski and Kooij, 2013). Remarkably, protein export to the host erythrocyte was not affected in PTEX88 knockout parasites but the protein seems to be necessary for tissue sequestration *in vivo* and for virulence (Matz *et al.*, 2015b).

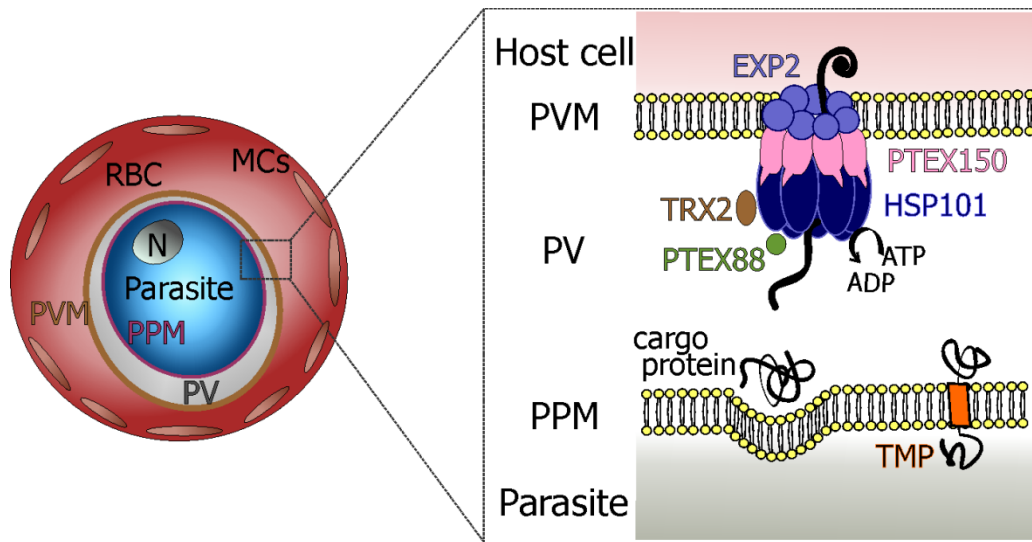


Figure 5: Model of the PTEX translocon

(Left) Schematic of a human RBC infected with a malaria parasite. **(Right)** Enlargement of a section of the PV region. Schematic showing a soluble protein (coiled black line) on the PV and non-soluble (orange block with coiled lines) embedded in the PPM. Proteins reach the translocon and are transported in an unfolded state from the PV into the host cell cytosol. The PTEX translocon is formed by 5 proteins: EXP2 is the protein-conducting channel in the PVM to which the other components are attached. HSP101 contains an AAA+ ATPase domain. It unfolds exported proteins in the PV coupled to ATP hydrolysis and feeds them through the complex. PTEX150 is essential for the structure of the complex. PTEX88 and TRX2 are accessory factors that may be transiently in contact with the complex. MCs: Maurer's Clefts; RBC: Red blood cell; PVM: parasitophorous vacuole membrane; PV: parasitophorous vacuole; PPM: parasite plasma membrane; PVM: parasitophorous vacuole membrane; TMP: Transmembrane protein. Designed based on (Ho *et al.*, 2018) and (Boddey and Cowman, 2013).

In the dense granules of invasive merozoites, the PTEX elements HSP101, PTEX150 and EXP2 are stored and secreted from these organelles into the newly formed PVM during invasion (Bullen *et al.*, 2012). The complex is concentrated in foci that dynamically alter their spatial position, which are proposed to be the areas for export (Riglar *et al.*, 2013). PTEX is present during the whole blood cycle and with little protein turnover of its components in the ring stages (Bullen *et al.*, 2012).

PTEX components such as PTEX150 are found throughout the *Plasmodium* genus and obvious orthologues are not present in any other organism (de Koning-Ward *et al.*, 2009). However, proteins with detectable homology to EXP2 are also found in other Apicomplexans and in *Toxoplasma gondii*. EXP2 was found to complement the solute pore function of GRA17 and GRA23 in *T. gondii* (Gold *et al.*, 2015). In 2016 Mesén-Ramírez *et al* provided evidence that EXP2 was part of a translocating entity and suggested that PTEX has translocation activity and provide a mechanistic framework for the transport of soluble as well as transmembrane proteins from the parasite boundary into the host cell (Mesén-Ramírez *et al.*, 2016). Later on it was demonstrated that the EXP2 has two functions: one as Protein-translocating pore in the

PTEX complex (Mesen-Ramirez *et al.*, 2016), and the other as the nutrient-permeable channel of the PVM (Garten *et al.*, 2018).

1.2.6.3 PfEMP1 export and its role in *P. falciparum* virulence

By the late 1970s it was discovered that the sequestration of iRBC involves high-molecular weight (200 – 450 kDa) and strain-specific parasite molecules displayed on electron-dense iRBC surface protrusions called Knobs (Langreth *et al.*, 1979; Langreth *et al.*, 1978; Leech *et al.*, 1984). Ten years later, the trypsin-sensitive *P. falciparum* erythrocyte membrane protein 1 (PfEMP1) was described (Howard *et al.*, 1988) and afterward demonstrated that PfEMP1 was in fact a family of proteins (~60 gene) encoded by a multigene family named *var* (Baruch *et al.*, 1995; Smith *et al.*, 1995; Su *et al.*, 1995).

PfEMP1 has 3 basic structural components, the extra cellular domain (ECD), a trans-membrane domain (TMD) and an intracellular acidic terminal segment (ATS). The extracellular domain is exposed on the cell surface and exposed to the host's immune system and is a highly variable region. It is composed by a variable number of subdomains starting at the N-terminus with a 60 amino acids long and partially conserved N-terminal segment (NTF). The NTF is followed by “the head structure”, that consist of a highly variable Duffy-binding-like (DBL) domain (it received that name because of its similarity with the Duffy binding proteins in *P. vivax*) with six variant types (DBL α , DBL β , DBL γ , DBL δ , DBL ϵ and DBL ζ) and one or two also variable cysteine-rich inter-domain region (CIDRs). The last CIDR region is followed by the TMD which connects the molecule to the intracellular part termed the acidic terminal sequence (ATS). Both the ATS and the TMD are highly conserved among different PfEMP1s (Figure 6).

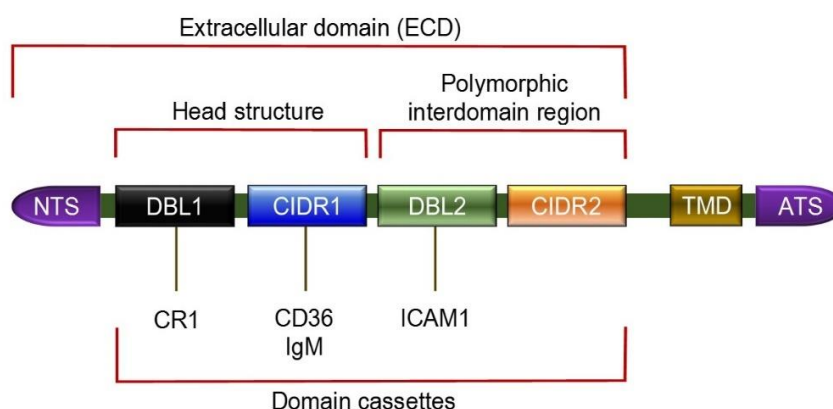


Figure 6: PfEMP1 structure.

Scheme illustrating one of the possible arrangements of PfEMP1. The extracellular domain contains the NTS: N-terminal segment; a variable number of Duffy Binding like protein domains, the DBL1

and 2; and one or two Cysteine-rich inter-domains, here the CIDR1 and 2. TMD: transmembrane domain and the intracellular region; ATS: acidic terminal segment. Designed by: K. Lalchandama. 2016.

The process of how PfEMP1 reaches the RBC membrane is only poorly understood. It probably involves the insertion of PfEMP1 into MCs as they form at the PV membrane, followed by cisternal maturation of the MCs and relocation closer to the RBC periphery (Maier *et al.*, 2009). Some studies suggest that PfEMP1 is transferred to the RBC membrane in transport vesicles (Taraschi *et al.*, 2003; Taraschi *et al.*, 2001), whereas other studies indicate a possible role for a chaperoned complex (Knuepfer *et al.*, 2005; Papakrivos, Newbold and Lingelbach, 2005). Those chaperones may be involved in several steps of the export process, including the transport through the endomembrane system of the parasite; the loading of exported proteins into the transporter in the PV membrane; the loading of integral membrane proteins (as MAHRP1 or SBP1) into nascent Maurer's clefts; the delivery of soluble proteins to the cytoplasmic surface of MCs (as PfEMP1 and KAHRP) and the insertion of PfEMP1 into the RBC membrane.

The disruption of the membrane skeleton in the region where PfEMP1 will be introduced may be necessary to allow the insertion of PfEMP1 into the RBC membrane, possibly at bilayer regions that are enriched in cholesterol (Frankland *et al.*, 2006). In the MCs the proteins are linked via ATS to the *Plasmodium* helical interspersed sub-telomeric proteins (PHIST) (Warncke, Vakonakis and Beck, 2016; Mayer *et al.*, 2012).

The main function of PfEMP1 is to bind and attach the iRBC to the epithelium and blood vessels wall to prevent the clearance of parasite-infected RBCs by the liver. The binding is mediated by the head structure (DBL and CIDR domains) of the PfEMP1 which can bind to many receptors, including Thrombospondin (TSP), Complement receptor 1 (CR1), Chondroitin sulfate A (CSA), P-selectin, Endothelial protein C receptor (EPCR), Heparan sulfate. Also the DBL domain next to the head structure binds to ICAM1 (Smith *et al.*, 2000). CIDRs primarily bind to a great variety of cluster determinant 36 (CD36) (Pasternak and Dzikowski, 2009; Howell *et al.*, 2008). All the previously described bindings produce the pathogenic characteristics of the parasite, such as sequestration of infected cells in different tissues (Howell *et al.*, 2008).

In a normal scenario, the host produces antibodies against the exposed regions of PfEMP1 and those antibodies inactivate the protein, avoiding the parasite binding. However, to circumvent the host immune response, the parasite developed a way to “switch on and off”

different *var* genes and each parasite dominantly expresses one type of PfEMP1 on the iRBC surface during each erythrocytic cycle (Chen *et al.*, 1998; Scherf *et al.*, 1998). Additionally, the *var* genes of *P. falciparum* undergo constant changes due to recombination or due to rearrangements that generate a great collection of *var* genes in nature. Recombination processes can occur within one parasite genome as well as between two parasite genomes during both mitosis and meiosis (Flick and Chen, 2004). This recombination process does not affect the adherence function of PfEMP1.

The adhesion of iRBC to endothelial cells is a response of the interaction of PfEMP1 with a wide range of host receptors (Kyes, Horrocks and Newbold, 2001). The preference of sequestration of infected parasites in different tissues is determined by the specific adhesion properties of each PfEMP1 variant and the restriction of host ligand expression on endothelial cells in those tissues. The adhesion to CD36 is a common adhesive phenotype for many PfEMP1 variants, adhesion to ligands such as intercellular adhesion molecule 1 (ICAM1, CD54) and chondroitin sulphate A (CSA) are properties of more restricted subsets of PfEMP1 variants (Newbold *et al.*, 1999; Newbold *et al.*, 1997). Adhesion to ICAM1 on endothelial cells in the brain is associated with cerebral malaria (Turner *et al.*, 1994) and adhesion to CSA expressed in the placenta is associated with malaria during pregnancy (Fried and Duffy, 1996). Thus, specific PfEMP1 adhesive properties play a significant role in determining the pathology of disease.

1.3 Approaches to study *Plasmodium* proteins

1.3.1 Selection markers

Selection markers have played a key role in the study of *Plasmodium* proteins. The transfection of parasites is currently restricted to few selection markers that allow us to purify parasites containing the plasmids.

In 1996 the first selection marker was described, the Dihydrofolate reductase-thymidylate synthase (*dhfr-ts*) that can be selected using pyrimethamine (Wu, Kirkman and Wellems, 1996). Later on the human dihydrofolate reductase (*hDHFR*) was introduced which confers resistance to WR99210 (Fidock and Wellems, 1997) and is currently the most used - and generally considered very robust - marker in *P. falciparum* research.

In 1999 two additional plasmid selection systems for *P. falciparum* were developed. They were based on the compounds blasticidin-S and geneticin (G418) that efficiently killed the parasites.

The genes *bsd*, encoding blasticidin S deaminase of *Aspergillus terreus*, and *neo*, encoding neomycin phosphotransferase II from transposon Tn 5, confer resistance to blasticidin or G418, respectively. One of the most used selection markers in the last years is the yeast Dihydroorotate dehydrogenase (yDHODH) that is selected by atovaquone or DSM1 (Phillips *et al.*, 2008; Ganesan *et al.*, 2011).

Negative selection markers are selectable markers that eliminate or inhibit growth of the host organism upon selection, also including prodrugs that become active just after being metabolized. That is the case of the thymidine kinase (TK) that is selected using the pro-drug ganciclovir and also the cytosine deaminase (CD), selected with the prodrug 5-fluorocytosine. These markers can be used for removal of episomes and selection of double-crossover recombination integrands, improving the ability to analyze protein functions in *Plasmodium* (Ghorbal *et al.*, 2014; Duraisingh, Triglia and Cowman, 2002).

1.3.2 Prevent protein unfolding using mDHFR to study protein translocation

The DHFR is a well described enzyme that converts dihydrofolate into tetrahydrofolate, a methyl group shuttle required for the de novo synthesis of pyrimidines, thymidylic acid, and certain amino acids (Chen *et al.*, 1984; Schnell, Dyson and Wright, 2004). One of the systems currently used to study protein transport in *Plasmodium* employs the murine DHFR (mDHFR) which was first used to study protein import into mitochondria (Eilers and Schatz, 1986) and is useful to distinguish vesicular from unfolding dependent protein translocation steps in protein trafficking. When mDHFR comes into contact with folate analogues, (e.g. methotrexate, aminopterin or also WR99210) the folate analogue binds to the enzyme's catalytic site and the protein is highly stabilized in its folded conformation. Therefore the chaperones or the membrane translocation machineries are incapable to relax the folding of the protein and the transport is interrupted (Backhaus *et al.*, 2004). As most translocon need to unfold the cargo protein to transport it from one compartment to other, the fusion of the mDHFR domain to cargo proteins therefore represents a valuable tool to conditionally modify the folding state of the cargo-mDHFR fusion to analyze the requirement for unfolding at specific transport steps.

This system is very useful to identify the necessity of unfolding for a given transport step. If a protein is transported in vesicles, there is no necessity for unfolding. Whereas if it is translocated by a translocon, the protein needs to be in an unfolded conformation and the mDHFR fused cargo will arrest, revealing the involvement of a translocon. This technique is

robust both *in vivo* (Wienhues *et al.*, 1991) and *in vitro* (Eilers, Hwang and Schatz, 1988; Mesen-Ramirez *et al.*, 2016; Boucher and Yeh, 2019) and it helped to identify how proteins are transported within a cell. In mitochondria (Wienhues *et al.*, 1991) and lysosomes (Salvador *et al.*, 2000) proteins are imported in an unfolded conformation, but in the glycosomes in trypanosomes (Häusler *et al.*, 1996) the protein transport is independent of the protein unfolding. These findings suggest that the trypanosome glycosomes proteins are transported using a vesicular pathway. The chloroplast and mitochondria proteins are transported via translocon. There is a machinery pumping the proteins through the membranes, and this machinery is also responsible for the protein unfolding. The mDHFR conditionally folding system also helped to identify components of the import machinery interacting with the arrested reporter in *P. falciparum*. The mDHFR system provided the first indication that exported proteins in *P. falciparum* required to be unfolded to be exported as an mDHFR fusion of an exported protein arrested in the parasite periphery in a folding dependent manner (Gehde *et al.*, 2009; Heiber *et al.*, 2013). This gave credit to the time only suspected translocation machine PTEX at the PVM. Afterward, it was shown that also exported integral transmembrane proteins require unfolding to be exported, indicating that they also are passed through a translocon (Grüning *et al.* 2012). Further studies demonstrated that transported cargo was in contact with EXP2, this protein was needed for export and the pore of PTEX was formed from oligomers of EXP2 (Mesen-Ramirez *et al.*, 2016; Elsworth *et al.*, 2014; Beck *et al.*, 2014; Ho *et al.*, 2018; Garten *et al.*, 2018).

1.3.3 Selection-linked integration system (SLI)

Regular systems to study essential genes in *P. falciparum* were often inefficient and time consuming because they depended on the genetic modification of the target locus, a process hindered by the low frequency of integration of episomal DNA into the genome. In 2017 the SLI system was introduced and this allowed the rapid selection of parasites with genomic integration of plasmids (Birnbaum *et al.*, 2017). This system permits to tag and disrupt proteins and can be harnessed for a method known as knock sideways (KS) that allows the conditional depletion of the target protein from its site of action into an unrelated cellular compartment. SLI is also effective for floxing to induce diCre-based excision of genes.

In the SLI system a targeting region is fused to a tag of choice and an additional selection marker that is expressed upon fusion to the target gene by single homologous recombination-based integrated into the genome. Thus, the gene fused to the tag is expressed under the endogenous promoter. The tag of choice and the additional selection marker are separated by

a skip peptide (Szymczak *et al.*, 2004; Straimer *et al.*, 2012), leading to the translation of two independent peptides from a single RNA. Hence, the resistance marker is not fused to the tagged gene product. Addition of the selection drug, corresponding to the additional resistance marker, only permits the survival of parasites carrying the integration (Figure 7).

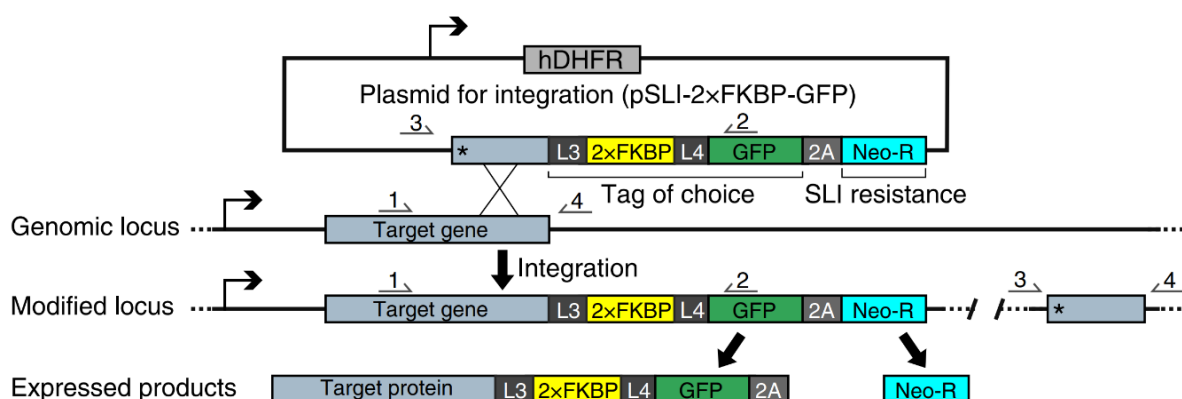


Figure 7: Selection-linked integration strategy

Schematic of SLI strategy. L3 and L4 are linkers; 2A is a T2A skip peptide; Neo-R represents neomycin-resistance gene; asterisks represent stop codons; arrows represent promoters; the arrows with numbers represent the regions where the primers for integration diagnostic PCRs bind. Extracted from (Birnbaum *et al.*, 2017)

1.3.3.1 Knock Sideways (KS)

Most strategies for functional evaluation of a gene or its product are primarily based on their elimination or a decrease in their expression. Controlled modifications of the localization of a target protein is an alternative approach that is particularly rapid and proved to be valuable for functional studies (Haruki *et al.*, 2008; Robinson *et al.*, 2010; Birnbaum *et al.*, 2017) This approach is based on the heterodimerization reaction of which the FRB-FKBP system has been most widely used (Putyrski and Schultz, 2012). The FRB-FKBP is classified as a chemically inducible dimerization (CID) system where the interaction of the components is controlled by a small molecule, (heterodimerizer). The heterodimerizer induces the dimerization of FRB and FKBP. The system is derived from the interaction of the immunosuppressant sirolimus (also known as rapamycin) with the cytosolic 12 kDa FK506 binding protein (FKBP, also FKBP12). The complex inhibits the mechanistic target of rapamycin, the mTOR kinase. The exact binding region of the kinase is termed FKBP rapamycin binding domain (FRB) (Belshaw *et al.*, 1996; Chen *et al.*, 1995; Choi *et al.*, 1996; Liang, Choi and Clardy, 1999).

Rapamycin alone binds FRB only with moderate affinity ($KD = 26 \mu M$), whereas the rapamycin-FKBP complex ($KD = 0.2 nM$) binds FRB with high affinity ($KD = 12 nM$), rendering the dimerization nearly irreversible, but with no interaction between FRB-FKBP in

the absence of rapamycin (Banaszynski *et al.*, 2006). To avoid the toxic effects of rapamycin, one of its derivatives called rapalog is used in combination with a modified FRB (termed FRB*) (Bayle *et al.*, 2006; Stankunas *et al.*, 2003).

The FRB-FKBP dimerization technique is called Anchor-away (AA) (Haruki, Nishikawa and Laemmli, 2008) or Knock-sideways (KS) (Robinson, Sahlender and Foster, 2010; Birnbaum *et al.*, 2017); and it has been used to remove the protein of interest (POI) from its side of action and thus, identify its function. In this system the POI should be fused with an FKBP and a tag. Separately the FRB* domain should be expressed as a second protein with a localization signal to a different cell compartment (e.g. nuclear, ribosomal, mitochondrial) (Choi *et al.*, 1996; Armstrong and Goldberg, 2007; Robinson, Sahlender and Foster, 2010; Xu *et al.*, 2010; Birnbaum *et al.*, 2017). After the addition of rapalog, the POI is dragged out of its original localization due to the dimerization of the FRB* with the FKBP, leading to different phenotypes, for example a lethal phenotype in the case of essential proteins (Figure 8) (Birnbaum *et al.*, 2017).

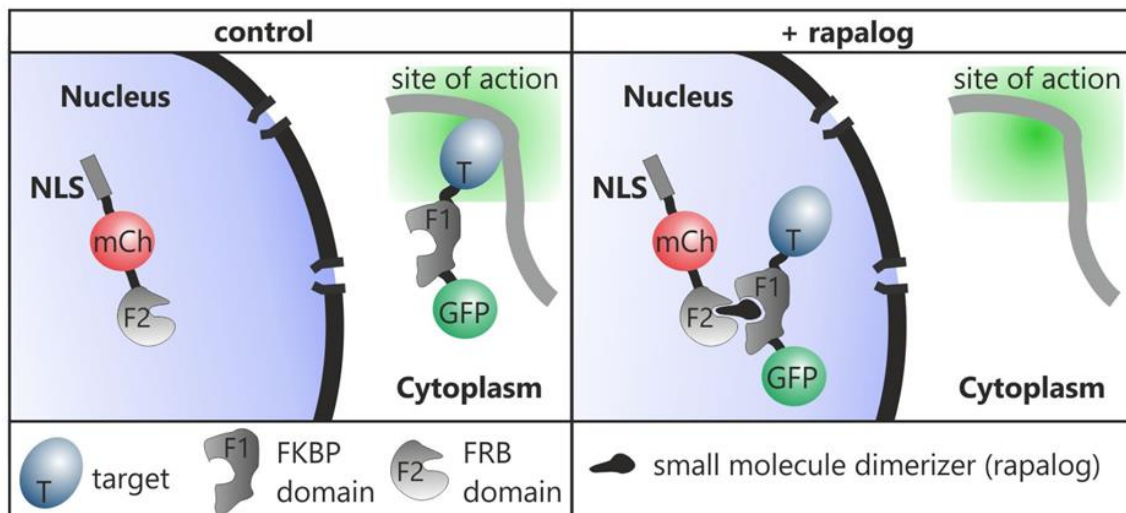


Figure 8: Schematic of Knock Sideways

The protein of interest is tagged with FKBP, and a flag (GFP) and it is expressed under its endogenous promoter. A second protein (mislocalizer) consisting of a localization signal, an FRB* domain and an mCherry is expressed episomally. Addition of rapalog leads to dimerization of FKBP and FRB* and subsequent the POI is relocalized to the nucleus. NLS, nuclear localization signal; mCh, mCherry; GFP, green fluorescence protein; F1, FKBP domain; F2, FRB domain; T, target protein. Extracted from (Birnbaum *et al.*, 2017)

1.4 Aim of the thesis

Although there is a significant amount of information on how *P. falciparum* exports proteins to its host cell, the process of how proteins with trans membrane (TM) domains are extracted from the parasite plasma membrane (PPM) remains elusive. One of these TM-proteins is *P. falciparum* erythrocyte membrane protein 1 (PfEMP1), the major virulence factor of this parasite that is responsible for the cytoadherence of infected red blood cells to the endothelium of the host.

The objective of this thesis is to identify the translocation factors involved in the extraction of TM-proteins out of the PPM and their subsequent delivery to PTEX. In order to identify these extractors, constructs will be designed that are differentially arrested in either the PVM or in the PPM. These constructs will contain a sequence for a protein, a mDHFR domain and a BirA domain. The mDHFR will allow for the conditional arrest of the construct at the respective translocation step, while the BirA will biotinylate the proteins that are interacting with the arrested construct to identify the PPM extractor.

As a specific exported TM protein, the transport of PfEMP1 will be analysed. This part of the project aims to determine if PfEMP1 uses a similar pathway than other exported proteins by testing if it is using PTEX to cross the PVM. In order to do this, a specific PfEMP1 will be tagged and activated using SLI to circumvent problems associated with previous studies attempting to study this protein. The transport of this PfEMP1 will then be analysed by conditionally blocking PTEX.

2 Materials and methods

2.1 Materials

2.1.1 Technical devices

Device	Specifications	Brand/ Distributor
Agarose gel chamber	Sub Cell GT basic	Bio-Rad, München
Analytical Balance	870	Kern
Blot device	Mini Protean Tetra Cell	Bio-Rad, München
Gel holder cassettes	System	
Foam pads		
Electrode assembly		
Cooling unit		
Centrifuge	Megafuge 1.0R J2- HS	Heraeus, Hannover
Ultracentrifuge	Rotor JA-12 Avanti J-26S XP Rotor JA- 14	Beckman Coulter, Krefeld
Table centrifuge	Eppendorf 5415 D	Eppendorf, Hamburg
Casting gel stuff	Mini Protean	Bio-Rad, München
Casting stand		
Casting plates		
Casting frames		
12 –wells combs		
Developer	Curix 60	AGFA-Gevaert, Mortsel/Belgium
Developer cassette	Cronex Quanta III	Dupont, Neu Isenburg
Electrophoresis chamber	Mini Protean 67s	Bio-Rad, München
Electroporator	Gene Pulser X- Cell	Bio-Rad, München
Electroporator	Nucleofector II	Amaxa Biosystems, Germany
	AAD-1001N	
Ice machine	EF 156 easy fit	Scotsmann, Vernon Hills/USA
<i>P. falciparum</i> cell culture incubator	Heratherm IGS400	Thermo Scientific, Langensfeld
Bacterial incubator	Thermo function line	Heraeus, Hannover
Shaking incubator	Max Q4000	Barnstead, Iowa/ USA
Light Microscope	Axio Lab A1	Zeiss, Jena
Fluorescence Microscope	Axioscope 1	Zeiss, Jena
Microscope digital camera	Orca C4742-95	Hamamatsu Phototonics K.K., Japan
Microwave	Micro 750W	Whirlpool, China
Laboratory scale	Atilon	Acculab Sartorius, Göttingen

PCR Mastercycler	eppgradient	Eppendorf, Hamburg
Photometer	BioPhotometer plus	Eppendorf, Hamburg
pH-meter	SevenEasy	Mettler-Toledo, Gießen
Pipettes	1-10/200/1000 µl	Gilson, Middleton, USA
Pipettor	Pipetboy acu	IBS,
Power supply	EV31	Consort, Belgium
	Power Source 300 V	VWR, Taiwan
Roller mixer	STR6	Stuart
Sterile laminar flow bench	Steril Gard III Advance	Baker, Stanford USA
Thermoblock	Thermomixer compact	Eppendorf, Hamburg
UV transilluminator	PHERolum289	Biotec Fischer, Reiskirchen
Vacuum pump	BVC Control	Vacuubrand, Deutschland
Vortexer	Genie 2	Scientific Industries, USA
Waterbath	1083	GFL, Burgwedel

2.1.2 Kits

Kits	Brand/ Distributor
NucleoSpin. Plasmid	Macherey-Nagel, Düren
NucleoSpin. Extract II	Macherey-Nagel, Düren
QIAamp DNA Mini Kit	Qiagen, Hilden
QIAGEN Plasmid Midi Kit	Qiagen, Hilden
Chemiluminescent Substrate Detection Kit	Thermo Scientific, Schwerte
Western Blot ECL-SuperSignal West Pico	Thermo Scientific, Schwerte

2.1.3 Labware and disposables

Labware and disposables	Specifications	Manufacturer
Conical Falcon tubes	50 / 15 ml Material	Sarstedt, Nümbrecht
Pasteur pipette		Brand, Wertheim
Sterile filter	0.22 µm	Sarstedt, Nümbrecht
Disposable pipette tips	1-10/20-200/100-1000 µl	Sarstedt, Nümbrecht
Filter tips	1-10/20-200/100-1000 µl	Sarstedt, Nümbrecht
PCR Reaction tubes	Multiply-µStrip Pro 8-Strip	Sarstedt, Nümbrecht
Eppendorf Reaction Tubes	1.5 ml / 2 ml	Sarstedt, Nümbrecht/ Eppendorf Hamburg
Glass slides		Engelbrecht, Edermünde
IFA glass slides	10 wells ER-208B-CE24 6.7 mm	Thermo Scientific, USA
Glass cover slips	24 X 65 mm Thickness 0.13-0.16	R. Langenbrinck, Emmendingen
Transfection cuvettes	0.2 cm	Bio-Rad, München
Cryotubes	1.6 ml	Sarstedt, Nümbrecht

Plastic pipettes	5/ 10/ 25 ml	Sarstedt, Nümbrecht
Chromatography paper		Whatman
Nitrocellulose blotting		GE Healthcare,
Membrane Protran	Amersham 0.45 µm	Deutschland
Parafilm		Bemis, USA
Petri dishes	5 mL/ 10 ml	Sarstedt, Nümbrecht

2.1.4 Reagents

Reagent	Brand/ Distributor
(4-(2-Hydroxyethyl)-1-piperazineethanesulfonic acid) (HEPES)	Roche, Mannheim
1,4,-dithiothreitol (DTT)	Biomol, Hamburg
3-(N-morpholino) propansulfonic acid (MOPS)	Sigma, Steinheim
4',6-diamidino-2-phenylindole (DAPI)	Roche, Mannheim
Acetic acid Roth	Roth, Karlsruhe
Acrylamide/Bisacrylamide solution (40 %)	Roth, Karlsruhe
Agar LB (Lennox)	Roth, Karlsruhe
Agarose	Invitrogen, USA
AlbumaxII	Gibco, Life Technologies, USA
Albumin bovine Fraction V (BSA)	Biomol, Hamburg
Ammonium persulfate (APS)	Applichem, Darmstadt
Ampicillin	Roche, Mannheim
Bacto™ Pepton	BD, USA
Bacto™ yeast extract BD	BD, USA
Biotin Sigma	Sigma Aldrich, Steinheim
Blasticidin S	Invitrogen, USA
Bromophenol blue	Merck, Darmstadt
Calcium chloride (CaCl ₂)	Sigma Aldrich, Steinheim
Concanavalin A G-250 Sigma	Sigma Aldrich, Steinheim
Deoxynucleotide's (dNTPs)	Thermo Scientific, Lithuania
D-Glucose	Merck, Darmstadt
Dihydroethidium (DHE)	Cayman, Ann Arbor, USA
Dimethyl sulfoxide (DMSO)	Sigma, USA
Dipotassium phosphate	Merck, Darmstadt
Disodium phosphate	Roth, Karlsruhe
Dulbecco's Phosphate Buffered Saline (DPBS)	PAN, Biotech, Aidenbach
Ethanol	Roth, Karlsruhe
Ethidium bromide	Sigma, Steinheim
Ethylenediaminetetraacetic acid (EDTA)	Biomol, Hamburg
Gentamycin	Ratiopharm, Ulm
Giemsa's azure, eosin, methylene blue solution	Merck, Darmstadt
Glutaraldehyde (25 %)	Roth, Karlsruhe
Glycerol	Merck, Darmstadt

Glycine	Biomol, Hamburg
Human red blood cells Sterile, concentrate	Blood bank, Universitätsklinikum, Eppendorf (UKE), Hamburg
Hydrochloric acid (HCl)	Merck, Darmstadt
Hypoxanthine	Sigma, Steinheim
Isopropanol	Roth, Karlsruhe
LB-Medium (Lennox)	Roth, Karlsruhe
Magnesium chloride (MgCl ₂)	Merck, Darmstadt
Methanol	Roth, Karlsruhe
Milk powder	Roth, Karlsruhe
N, N, N, N-Tetramethylethylenediamin (TEMED)	Merck, Darmstadt
Paraformaldehyde (PFA)	Polyscience, Warrington, USA
Percoll	GE Healthcare, Sweden
Phenyl methyl sulfonyl fluoride (PMSF)	Sigma, Steinheim
Potassium chloride	Merck, Darmstadt
Protease inhibitor cocktail ("Complete Mini")	Roche, Mannheim
Rapalog (A/C Heterodimerizer AP21967)	Clontech, Mountain View, USA
RPMI (Roswell Park Memorial Institute)-Medium	Applichem, Darmstadt
Rubidium chloride	Sigma, Steinheim
Saponin	Sigma, Steinheim
Sodium acetate	Merck, Darmstadt
Sodium bicarbonate	Sigma, Steinheim
Sodium chloride	Gerbu, Gaiberg
Sodium dihydrogen phosphate	Roth, Karlsruhe
Sodium dodecyl sulfate (SDS)	Applichem, Darmstadt
Sodium hydroxide	Merck, Darmstadt
Sorbitol	Sigma, Steinheim
β-Mercaptoethanol	Merck, Darmstadt
Tetanolysin	Sigma, Steinheim
Trichloroacetic acid	Roth, Karlsruhe
Tris base	Roth, Karlsruhe
Triton X-100	Biomol, Hamburg
Water for molecular biology (Ampuwa)	Fresenius Kabi, Bad Homburg

2.1.5 Primers

All oligonucleotides were synthesized by Sigma-Aldrich (Steinheim). Restriction sites and non-codifying regions are indicated in lowercase and codifying regions are indicated in uppercase letters.

Sequence	Name
CAGGTTAATAGCATGGTATATAAAG	0104500 3'int check
gctatttaggtgacactatagaataactcaagctgcggccgcTAAATATTTATA GAGAACTTTACAGAAGC	0104500 3xHA fw Gib
CTGGAACATCGTATGGGTACATGGTggtaccATTATCTAT TATTGATACGTGATGGCGCC	0104500 3xHA Rv Gib
GGGTACCTTTTTGAGGTAATAATTACATATGC	0104500 5'int check
gctatttaggtgacactatagaataactcgcggccgctaaATATTTATAGAGAA CTTTACAGAAGCAACAG	0104500 GFP fw Gib
GCAGCAGCAGATCTTGATCTCAATCCTGAcctaggATTAT CTATTATTGATACGTGATGGCGCC	0104500 GFP Rv Gib
gctatttaggtgacactatagaataactcgcggccgctaaGTTTCCATTTTTTC ATTATTAACATAC	0104500 TGD fw Gib
CCTCCAGCACCAGCAGCAGCACCTCTAGCacgcgtTTCCT TATCATACGGTATATACGAACATG	0104500 TGD Rv Gib
ggtgacactatagaataactcgcggccgctaaGATGGTGTAAATAAATGAT GGTGTAAATAAATGATGG	0704300 GFP Fw Gib
GCAGATCTTGATCTCAATCCTGAcctaggTTTTTTTTTATT TTTTTTTCTGTTATTTTTTTTTGTTGC	0704300 GFP Rv Gib
CCTTAAGATACCCTTTAACGATAC	0704300 int check GFP Rv
GACGGTGAAAATATATCTTTTCATG	0704300 int check GFP fw
GTTTTATATTACATTTAGATACTTACTCTTGAAC	0704300 int check TGD fw
CATGTTGTAATTCTGTGGTATTCATTTTGTTTC	0704300 int check TGD rv
ggtgacactatagaataactcgcggccgctaaGAAAAGAATAAATACGA TATAGAGG	0704300 TGD Fw Gib
GCAGCAGCACCTCTAGCacgcgtTTTTTTTTCTATGCATA TATATTTTTTATTTTATAATGAG	0704300 TGD Rv Gib
ggtgacactatagaataactcgcggccgctaaAATAGAAACACTTATAAA TGTA AAAACG	0829500 GFP Fw Gib
GCAGATCTTGATCTCAATCCTGAcctaggAGATAAACTA AAAAAGTTTCGATATATC	0829500 GFP Rv Gib
GCACTTATTTTTATTTGCACTTATTTTTATTTGC	0829500 int check GFP Rv
CCAACGGAAAACCTTAATAAATACACATTCGGG	0829500 int check GFP fw
GAATATATGACATAACGTTTTGAATAC	0829500 int check TGD fw
GGTTCGTTATGATTAGAATCTTTGTCTTTAC	0829500 int check TGD rv
ggtgacactatagaataactcgcggccgctaaAATAGAAACACTTATAAA TGTA AAAACG	0829500 TGD Fw Gib
GCACCAGCAGCAGCACCTCTAGCacgcgtCTCTTCATTAA CATATTCATTTTTATTAG	0829500 TGD Rv Gib
CTTTACATAATGCATATTAATAACATCAC	0830400 3'int check
gctatttaggtgacactatagaataactcaagctgcggccgcTAAcagtatgaatttatt attatgag	0830400 3xHA fw Gib
GCGTAATCTGGAACATCGTATGGGTACATGGTggtaccA AGCATCCATACGCGGTTACTTTTTTGATTTAATCTGG	0830400 3xHA Rv Gib
CGATTATTATTATTTAAAAAAGTACATTGAAGTTC	0830400 5'int check
gctatttaggtgacactatagaataactcgcggccgctaacagtatatgaattattattatgag	0830400 GFP fw Gib

CCAGCAGCAGCAGATCTTGATCTCAATCCTGAcctaggA	0830400 GFP Rv Gib
AGCATCCATACGCGGTTACTTTTTTTG	
ggtgacactatagaataactcgggccgctaaAGAATAAACTTTCTACAT	0830400 TGD fw Gib
TATTTTTTATTAC	
GCACCTCCAGCACCAGCAGCAGCACCTCTAGCacgcgtcat	0830400 TGD Rv Gib
atactgataaaatataatc	
CCAATTGTAATAACAAAAAGTATTAGTTC	0913400 3'Int Check
CGATTTATTAATAAAGAATGAAAAGTTTG	0913400 5'Int Check
ggtgacactatagaataactcgggccgctaaAGAAAAGTATAATAA	0928600 GFP for
ATTTAAAG	
GCAGCAGATCTTGATCTCAATCCTGAcctaggTATAGATT	0928600 GFP rev
TTGCAATATTTGGTAAAGC	
ggtgacactatagaataactcgggccgctaaTTGGTACCTCCAGAATTT	0928600 TGD Fw
TATAATGG	
CCAGCACCAGCAGCAGCACCTCTAGCacgcgtATCGAAT	0928600 TGD rv
AAATCATTTAATATATTC	
cactatagaataactcaagtcgggccgTAAGCTAGATCATCAGCTAT	0934500 3xHA Gibs for
AAATAAAG	
GCGTAATCTGGAACATCGTATGGGTACATGGTggtaccT	0934500 3xHA Gibs Rev
GCGTTTTCAAAAAACATTCTTTTAATTTCC	
gctatttaggtgacactatagaataactcgggccgctaaGCTAGATCATCAGC	0934500 GFP Gibs For
TATAAATAAAGCTAG	
gctatttaggtgacactatagaataactcgggccgctaaGCTAGATCATCAGC	0934500 GFP Gibs For
TATAAATAAAGCTAG	
CAGCAGCAGATCTTGATCTCAATCCTGAcctaggTGCGTT	0934500 GFP Gibs Rev
TTCAAAAAACATTCTTTTAATTTCC	
CAGCAGCAGATCTTGATCTCAATCCTGAcctaggTGCGTT	0934500 GFP Gibs Rev
TTCAAAAAACATTCTTTTAATTTCC	
gccaaagctatttaggtgacactatagaataactcgggccgctaaGCATTAgtaagat	0934500 TGD Gibs For
gaaagaag	
gccaaagctatttaggtgacactatagaataactcgggccgctaaGCATTAgtaagat	0934500 TGD Gibs For
gaaagaag	
CCTCCAGCACCAGCAGCAGCACCTCTAGCacgcgtCCAT	0934500 TGD Gibs Rev
TTGTTTAGCTTTTTTCTGAAATTC	
CCTCCAGCACCAGCAGCAGCACCTCTAGCacgcgtCCAT	0934500 TGD Gibs Rev
TTGTTTAGCTTTTTTCTGAAATTC	
CGTTGGTACAACAATCTTGTTACTACTC	1226400 3'int check
GGTTATTTAATATATCAGATATTTCC	1226400 3'TGD int check
ggtgacactatagaataactcaagtcgggccgTAAGATGCTGAGGAAT	1226400 3xHA Fw Gib
ATATGTTAAAATATAAAATTAATAAAG	
CTGGAACATCGTATGGGTACATGGTggtaccTATATCTTC	1226400 3xHA Rv Gib
AACAAGTGTAACCC	
GATATCGTGTTAGATGTATTTTCATCC	1226400 5' TAG int check
CGAATTTTTTATTATCCATAAATAATAGC	1226400 5'int check
gctatttaggtgacactatagaataactcgggccgctaaGATGCTGAGGAAT	1226400 GFP Fw Gib
ATATG	
GCAGCAGATCTTGATCTCAATCCTGAcctaggTATATCTT	1226400 GFP Rv Gib
CAACAAGTGTAACCC	
gctatttaggtgacactatagaataactcgggccgctaaAATAGTAATTATTT	1226400 TGD Fw Gib
AATTGAAAAAG	
CACCAGCAGCAGCACCTCTAGCacgcgtAAAACATATAT	1226400 TGD Rv Gib
GCTCACATATATCC	
CTTCTTGAGACAAAGGCTTGGCCATTGGTCCTGGATTT	2A + BSD Gibson RV C
TCTTCTACATCTCC	

tcctcctaggTGCGTTTTCAAAAAACATTC	RV GFP Avr2 PFI1670C
tcctcctaggATTTTTTCGTTCTGTGAATTTTCCAAC	RV GFP Avr2 UFD1
CCAGTGAAAAGTTCTTCTCCTTTACTCATCGTACGAAA	SBP1 + GFP RV
AAATTGTAAGTCTAAGAATAGGGGAC	
CTATTTCAAATTCTCATTATTGTTGGCACAATTG	SBP1 Int Check
GGATATAATTAAGATAAAAATCTATTAGAATC	SBP1 Int Check
GCTATTTAGGTGACACTATAGAATACTCGCGGCCGctaa	SBP1 mDHFR*rec Gib F
TGTAGCGCAGCTCGAGCATTGATTTTTTTACTG	
CTGCAACTATACAATTCAAAGGCCTTACCATCCTAGG	SBP1 mDHFR*rec Gib Rv
GGTTTCTCTAGCAACTGTTTTTGTGTGG	
AAGCTATTTAGGTGACACTATAGAATACTCGCGGCCG	SLI + PIESP2 TGD Not1
CTAATTACTCTTTTTTGCAAAACTTG	Gibson Fw
GCTATTTAGGTGACACTATAGAATACTCGCGGCCGCT	SLI + SBP1 Not1 Gibson Fw
AATGTAGCGCAGCTCGAGC	
CGAACATTAAGCTGCCATATCCCTCGACCCGGGTAA	SLI + yDHODH Gibson Rv
ATGCTGTTCAACTTCCCACGGAAC	
tcctacgctCATTTGTTTAGCTTTTTTCTGAAATTC	TGD Fw Not1 PFI1670C
tcggcgccgctaaGCATTAgaagaatgaagaag	TGD Fw Not1 PFI1670C
ctcgcgccgctaacatacatgaatcattgtcttaattac	TGD Fw Not1 UFD1
tcctacgctCAAACCCCACTATGTGTTCTTTTATC	TGD RV Moloi UFD1
CAGATCTTGATCTCAATCCTGAcctaggATTTTTTCGTTCT	UFD1 L-GFP Gib RV
GTGAATTTTCCAACAATACCAGGAATAC	
CTGGAACATCGTATGGGTACATGGTggtaccATTTTTTCG	UFD1- 3xHA Gib RV
TTCTGTGAATTTTCCAACAATACC	
gacactatagaataactcaagctcgcgccgctaaataatgtatattttttcttattag	UFD1 3xHA Gibs For
CGTAATCTGGAACATCGTATGGGTACATGGTggtaccATT	UFD1 3xHA Gibs Rev
TTTTTCGTTCTGTGAATTTTCCAACAATACC	
gctatttaggtgacactatagaataactcgcgccgctaaataatgtatattttttcttatta	UFD1 GFP Gibs For
gG	
CAGCAGCAGCAGATCTTGATCTCAATCCTGAcctaggATT	UFD1 GFP Gibs Rev
TTTTTCGTTCTGTGAATTTTCCAACAATACC	
gctatttaggtgacactatagaataactcgcgccgctaaagtaataaaaaattgtttttg	UFD1 TGD Gibs For
tcttttg	
CCTCCAGCACCAGCAGCAGCACCTCTAGCacgcttattttaac	UFD1 TGD Gibs Rev
aaattcattgtacCGTG	
ATGACAGCCAGTTTAACTACCAAGTTCTTG	yDHODH Gibson Fw
GTTATTGTGATGAAGCAAATGAACATC	YIP1 3'Rv
GTACGTATTTATTTATTTATTTAAATATATTATAAG	YIP1 5'for
ggtgacactatagaataactcgcgccgctaaGTTATATTTATTTGATTGG	YIP1 GFP for
TATTGTAAGTAGCC	
GCAGCAGATCTTGATCTCAATCCTGAcctaggAAAAATT	YIP1 GFP RV
ATAATTAAGGCAAAACATG	
ggtgacactatagaataactcgcgccgctaaAGTTACTACAATCAAAAA	YIP1 TGD for
ATAATGAATCGTATGAACCG	
GCACCAGCAGCAGCACCTCTAGCacgctAGATATAAGA	YIP1 TGD RV
TCAAAATTAATTCCCAATTCTTCC	

Specific primers for SLI vectors:

ggaattgtgagcggataacaatttcacacagg	pARL Fw (int check)
ccaattgattgtattataactg	pARL Rv (int check)
CGAATAGCCTCTCCACCCAAG	Neo 40 Rv (int check)
ACCTTCACCCTCTCCACTGAC	GFP 85 Rv (int check)

CCTTCGGGCATGGCACTC	GFP 272 Rv
CCCAGGGCGTCCTCTCTGAGGTCCAGGAGG	mDHFR 495 Fw
GGGACACGGCGACGATGCAGTTCAATGGTCGAAC	mDHFR 9 Rv
C	

2.1.6 DNA and protein ladders

Reagent	Brand/ Distributor
GeneRuler™1000 bp ladder	Thermo Scientific, Schwerte
PageRuler™ prestained protein ladder	Thermo Scientific, Schwerte
PageRuler™ unstained protein ladder	Thermo Scientific, Schwerte

2.1.7 Antibodies

2.1.7.1 Primary antibodies

Antigen	Organism	Dilution		Source
		WB	IFA	
Aldolase	Rabbit	1:4000	-	Nyalwidhe & Lingelbach, 2006 Newly raised
GFP	Mouse	1:1000	1:500	Roche, Mannheim
GFP	Rabbit	1:2000	1:500	Thermo Scientific
REX2	Mouse	-	1:250	Haase et al., 2009
SERP	Rabbit	1:2000	-	Mesén-Ramirez et al, 2016
SBP1 C Terminal	mouse	1:2500	1:1000	Mesén-Ramirez et al, 2016
SBP1 C Terminal	rabbit	1:10000	1:1000	Mesén-Ramirez et al, 2016
SBP1 N Terminal	mouse	1:2500	1:1000	Mesén-Ramirez et al, 2016
SBP1 N Terminal	rabbit	1:10000	1:1000	Mesén-Ramirez et al, 2016
Triple hemagglutinin (HA)	Rat	1:1000	1:500	Roche, Mannheim

2.1.7.2 Secondary antibodies

Antigen	Conjugate	Organism	Dilution	Application	Source
Mouse	HRP	Goat	1:3000	Western blot	Dianova, Hamburg
Mouse	Alexa 488	Goat	1:2000	IFA	Thermo Fisher Scientific, USA
Mouse	Alexa 594	Goat	1:2000	IFA	Thermo Fisher Scientific, USA
Rabbit	HRP	Donkey	1:3000	Western blot	Dianova, Hamburg
Rabbit	Alexa 488	Donkey	1:2000	IFA	Thermo Fisher Scientific, USA
Rabbit	Alexa 594	Donkey	1:2000	IFA	Thermo Fisher Scientific, USA
Rat	HRP	Goat	1:3000	Western blot	Dianova, Hamburg
Rat	Alexa 594	Goat	1:2000	IFA	Thermo Fisher Scientific, USA
Streptavidin	Sepharose		1:2000	Pulldown	GE. Healthcare life sciences

2.1.8 Enzymes

2.1.8.1 Ligase and polymerase enzymes

Name	Manufacturer
T4 DNA-ligase [3 U/μl]	NEB, Ipswich, USA
Taq DNA-ligase [40 U/μl]	NEB, Ipswich, USA
FIREPol® [5 U/μl]	Solis Biodyne, Taipei, Taiwan
Phusion® High-Fidelity [2 U/μl]	NEB, Ipswich, USA

2.1.8.2 Restriction enzymes

Name	Recognition site	Buffer
AvrII	5'-CCTAGG-3'	Cutsmart
BamHI	5'-GGATCC-3'	Cutsmart
BsiWI	5'-CGTACG-3'	NEB 3.1
DpnI	Methylated 5'-GATC-3'	Cutsmart
KpnI	5'-GGTACC-3'	Cutsmart
MluI	5'-ACGCGT-3'	Cutsmart
NheI	5'-GCTACG-3'	Cutsmart
NotI	5'-GCGGCCGC-3'	Cutsmart
SalI	5'-CTCGAG-3'	Cutsmart
SpeI	5'-ACTAGT-3'	Cutsmart
XhoI	5'-CTCGAG-3'	Cutsmart
XmaI	5'-CCCGGG-3'	Cutsmart

2.1.9 Buffer, media and solutions

2.1.9.1 E. coli culture

Solution/media	Components
10x Luria-Bertani (LB) medium stock solution	10% NaCl 5% peptone 10% yeast extract in dH2O, autoclaved
Ampicillin stock solution	100mg/ml in H2O
LB medium working solution (1X LB Amp)	1% (w/v) NaCl 0.5% (w/v) peptone 1% (w/v) yeast extract 1% Ampicillin in dH2O
LB Agar plate solution	1.5% Agar-Agar 1x LB Amp

2.1.12 Media and solutions for parasite culture and cell biology experiments

2.1.12.1 *P. falciparum* in vitro culture

Solutions	Components
RPMI complete medium	1.587% (w/v) RPMI 1640 12 mM NaHCO ₃ 6 mM D-Glucose 0.5% (v/v) AlbuMAX II 0.2 mM Hypoxanthine 0.4 mM Gentamycin pH 7.2 in dH ₂ O sterile filtered
10% Giemsa solution	10 ml Giemsa's azure, eosin, methylene blue solution 90 ml dH ₂ O
Synchronization solution	5% (w/v) D-Sorbitol in dH ₂ O sterile filtered
Transfection buffer (Cytomix)	120 mM 150 μM CaCl ₂ 2 mM EGTA 5 mM MgCl ₂ 10 mM K ₂ HPO ₄ /KH ₂ PO ₄ 25 mM HEPES pH 7.6 in dH ₂ O sterile filtered
Amaxa transfection buffer	90 mM NaPO ₄ 5 mM KCl 0.15 mM CaCl ₂ 50 mM HEPES pH 7.3 in dH ₂ O sterile filtered
Malaria freezing solution (MFS)	4.2% D-sorbitol 0.9% NaCl 28% Glycerol in dH ₂ O sterile filtered
Malaria thawing solution (MTS)	3.5% NaCl in dH ₂ O sterile filtered
WR99210 stock solution	20 mM WR99210

	in DMSO
WR99210 working solution	1:1000 dilution of stock solution in RPMI complete medium sterile filtered
Blasticidin S (BSD) working solution	5 mg/ml BSD in RPMI complete medium sterile filtered
G418 working solution	50 mg/mL in RPMI complete medium sterile filtered
Human red blood cells sterile concentrate	Blood group O+ Blood bank Eppendorf (UKE), Hamburg

2.1.13 Solutions for cell biology and biochemical assays

Solutions	Components
Parasite lysis buffer	4% SDS 0.5% Triton X-100 0.5x PBS in dH2O
Percoll stock solution	90% (v/v) Percoll 10% (v/v) 10x PBS
80% Percoll solution	8.9 ml 90% Percoll stock solution 1.1 ml RPMI compl. medium 0.8 g Sorbitol sterile filtered
60% Percoll solution	6.7 ml Percoll stock solution 3.3 ml RPMI compl. medium 0.8 g Sorbitol sterile filtered
40% Percoll solution	4.4 ml Percoll stock solution 5.6 ml RPMI compl. medium 0.8 g Sorbitol sterile filtered
Saponin solution	Saponin 0.03% (w/v) in DPBS
Diluting buffer	10 mM Tris/HCl pH 7.5 150 mM NaCl 1 mM PMSF 2x Protease inhibitor cocktail

in dH2O

DSP (Stock solution)

20 mM in DMSO

2.1.14 Buffers and solutions for protein analysis

2.1.14.1 SDS-Page and Western blot

Solutions	Components
10x Running buffer	250 mM Tris base 1.92M Glycine 1% (w/v) SDS in dH2O
Ammonium persulfate (APS)	10% (w/v) in dH2O
Separating gel buffer	1.5M Tris-HCl, pH 8.8 in dH2O
Stacking gel buffer	1M Tris-HCl, pH 6.8 in dH2O
Stacking gel (for two gels, 5%)	0.75 ml stacking gel buffer 4.35 ml dH2O 750 µl Acrylamide (40%) 60 µl SDS (10%) 60 µl APS (10%) 6 µl TEMED
Separating gel (for two gels, 12%)	2.5ml running gel buffer 4.2 ml dH2O 3 ml Acrylamide (40%) 100 µl SDS (10%) 100 µl APS (10%) 4 µl TEMED
6x SDS sample buffer	375 mM Tris-HCl pH 6.8 12% (w/v) SDS 60% (v/v) Glycerol 0.6M DTT 0.06% (w/v) Bromophenol blue
10x Western blot transfer buffer	250 mM Tris-Base 1.92M glycerol 0.1% (w/v) SDS in dH2O
1 x Western transfer buffer 10%	10x Western transfer buffer 20% Methanol in dH2O
Blocking solution	5% (w/v) milk powder in 1xPBS

2.1.15 Vectors

The pARL1-vector (Crabb *et al.*, 2004) containing 2xFKBP-GFP (Birnbaum *et al.*, 2017) or 3xHA (Mesen-Ramirez *et al.*, 2016) were used for cloning the possible hits related with the membrane protein extraction. The parasites containing the episomal plasmid were selected using WR99210 and posterior selection for genomic integration and were attained using G418 (neomycin). The sequences encoding for the proteins to be disrupted were cloned using the SLI TGD vector (Birnbaum *et al.*, 2017). For the double integrants, the pSLI2a-GFP vector was used (Naranjo, non-published), carrying a Blasticidin marker for the episomal selection and a DSM1 marker for the genomic integration. For the arresting constructs and posterior BioID assays, the sequences encoding for the proteins SBP1 and Rex2 were fused to a modified pARL2 plasmid containing mDHFR-L-BirA*-3xHA.

2.2 Methods

2.2.1 Microbiological methods

2.2.1.1 Production of thermo-competent *E. coli*

To improve plasmid uptake of *Escherichia coli* the rubidium chloride method was applied to interfere with the bacterial cell wall stability (Hanahan, 1983). 20 ml of LB medium was inoculated with the *E. coli* XL-10 Gold strain from a glycerol stock and incubated overnight at 37°C with vigorous shaking; posteriorly 10 mL of the mentioned culture was transferred to a 1 L Erlenmeyer flask with 200 mL LB-medium and incubated at 37°C with vigorous shaking until it reached a OD600 of 0.5-0.6 nM. The bacteria were centrifuged (2400 x g at 4°C), posteriorly re-suspended in 60 ml TFBII buffer and incubated on ice for 10 min and centrifuged again. Finally, the pellet was suspended in 8 ml TFBII, aliquoted (100 µL) into 1.5 mL reaction tubes and stored at -80°C.

2.2.1.2 Thermo-competent *E. coli* transformation

A 100 µl aliquot of the thermo-competent *E. coli* was thawed on ice. Plasmid DNA (10 µL of a ligation or 0.5 µl of a sequenced construct) was added and incubated on ice for 20min. Suspension was heat shocked at 42 °C for 30 sec and put back into ice for 1 min. 30 µl of the suspension were plated on LB agar plates containing ampicillin as a selection marker and the rest of the suspension was kept overnight at 4°C. The plate was incubated over night at 37 °C and in case of having low number of colonies the rest of the bacteria were plated

The transformation with Gibson ligation produces fewer colonies compared with a T4 ligation. To yield a higher number of colonies the bacteria were incubated at 37 °C during 15 min in LB medium without ampicillin and later on plated and incubated overnight at 37 °C.

2.2.1.3 Bacteria growth for Plasmid DNA preparation

For plasmid mini and midi preparations, 1,5 ml in a 2 ml reaction tube or 150 ml in an Erlenmeyer flask were inoculated with bacteria respectively, posteriorly incubated overnight at 37°C with vigorous shaking.

2.2.1.4 Transformed bacteria storage

For long term storage of transformed *E. coli*, an aliquot of 500 µl was taken from the midi preparation, centrifuged, and re-suspended in a solution of 50-50% Glycerol and 1X LB medium with ampicillin. The aliquot was stored at -80°C.

2.2.1.5 Immunofluorescence assay (IFA)

500 µl of parasite culture was transferred to a 1.5 ml reaction tube and pelleted by centrifugation for ~10-20 seconds at 9000 x g. The pellet was washed with DPBS once and then re-suspended in 1ml DPBS. Approximately 10µl of parasite suspension was transferred to each well of a 10-well glass slide and air-dried. The parasites were fixed in acetone for 30 minutes, after which the slides could be stored until further usage. All subsequent steps were performed in a humid chamber. For antibody labelling of parasite proteins, first the cells were re-hydrated with 20 µl of DPBS per well for 5 minutes. Then unspecific binding sites were blocked with 3% BSA in PBS for 30-60 minutes. The primary antibodies were diluted in 3% BSA in PBS and incubated 20µl per well during 1 hour at RT or overnight at 4°C. After 5 washing steps with DPBS, the cells were incubated with the secondary antibodies. This one was diluted in 3% BSA in PBS and contained 1 ug/ml DAPI, the incubation lasted 1 hour at RT. After 5 washing steps with DPBS, a few drops of DAKO fluorescent mounting medium were added to the glass slide and covered with a cover slip. The cover slip was fixated using nail polish. After a few hours, the IFAs could be imaged with fluorescence microscopy.

2.2.2 Biomolecular methods

1.1.1.1 Polymerase chain reaction (PCR)

Genes of interest (GOI) were amplified from the genomic DNA (gDNA) of *P. falciparum* strain 3D7 and that tags and linkers (e.g. GFP, mDHFR, skip peptides) were amplified from pre-existent plasmids.

Two type of PCR were performed: Analytical PCR (integration checks and colony PCR) and Preparative PCR (gene amplifications). In general, for the Preparative PCR, Phusion High Fidelity DNA Polymerase was used. This polymerase has proofreading activity, which avoids undesired mutations. The Analytical PCR was performed with FIREPol polymerase (Solis Biodyne) (Table 2).

Table 2: Preparative and analytical PCR

Preparative PCR		Analytical PCR	
5x Phusion buffer	10 uL	10x FIREPol buffer	1 uL
dNTP's	5 uL	dNTP's	1 uL
Primer Fw	1 uL	Primer Fw	0,5 uL
Primer Rv	1 uL	Primer Rv	0,5 uL
Phusion DNA polymerase	0,3 uL	FIREPol DNA polymerase	0,05 uL
Template	0,3 uL*	Template	0,3 uL*
dH2O	Up to 50 uL	MgCl2	0,8 uL
		dH2O	Up to 10 uL

*from 1 to 200 ng/uL

The temperature settings were standardized for an A-T rich genome as the one of *Plasmodium* (Table 3). In those cases where no product was obtained or unspecific products were detected, the annealing temperature was optimized using a temperature gradient. Extension time was dependent on the product length and complexity. The PCR products were detected using an agarose gel with EtBr.

Table 3: PCR temperature settings

Phase	Temperature	Time
Initial denaturation (optional)	95 °C	4'
25-32 cycles	Denaturation	95 °C
	Annealing	48-70 °C
	Elongation	64-72 °C
Storage	4 °C	∞

*(X') depends on the length of the PCR-product. Usually 1 minute per 1000 bp

2.2.2.1 PCR product purification

The NucleoSpin Gel and PCR Clean-up kit was used to purify PCR-products and digested vector DNA for subsequent ligation. PCR products and vector DNA were eluted depending of the initial concentration in 15-to 30- μ l elution buffers.

2.2.2.2 DNA restriction digest

PCR-products and vectors were digested to generate "sticky ends" for posterior ligation. Depending on the vector that was used, specific restriction enzymes were incubated with the vector and PCR-product, respectively. DpnI was used in most preparative digests of PCR products to deplete methylated template DNA. Analytical restriction digests of minis were done to test the correct size of the insert and to exclude recombination events during ligation or bacterial passage. Analytical restriction digests were usually performed in a 10 μ l volume, using 1.5 μ l plasmid DNA and 0.3 μ l of each enzyme. Preparative digests were incubated at 37°C for 2-3 hours, analytical digests for 30-90 minutes

2.2.2.3 DNA Ligation

The previously digested fragments were ligated to be posteriorly transformed into *E. coli*. A typical ligation reaction is shown in table 2.21. Ligation reactions were incubated for 30-60 minutes at room temperature (RT)

2.2.2.4 Colony PCR-screen

The DNA ligation protocol used in this work results in a mix of plasmids containing the original insert and the new insert. To identify bacterial colonies containing the plasmid with the correct (new) insert, the colonies were screened using PCR. For this purpose, primers binding the new insert and the vector DNA were used, so that a PCR product was only generated when the plasmid containing the new insert was present within a colony. The PCR reaction resembled that of an analytical PCR (see section 2.2.2.1). A small amount of bacteria from 10-50 colonies was separately transferred to each PCR-reaction using sterile pipet tips. PCR products were analyzed using agarose gel electrophoresis.

2.2.2.5 PCR for integration diagnostic

PCR verification of genome integration in *P. falciparum* was performed with FIREpol polymerase on gDNA of integrant cell lines and 3D7 in a final volume of 40 μ l according to mix composition detailed below. Three different primer combinations were set up to confirm 5' and 3' integration and disruption of endogenous locus using 3D7 gDNA as control.

5' integration was checked using a primer specific for the region upstream of the modified locus (pARL55 Fw) and a vector specific reverse primer (see section 0). 3' integration was verified using a reverse primer specific for the downstream 3' region (pARL RV for pARL2 and GFP 85Rv for pARL2a) and a vector specific forward primer (see section 0).

Reagent	Volume(μ l)	Final concentration
dH ₂ O	25.5	-
10X FIREPol Buffer	4	1X
dNTP's (10 mM)	4	1 mM
Magnesium chloride (25 mM)	2.4	1.5 mM
Primer forward (10 μ M)	1.6	0.4 μ M
Primer reverse (10 μ M)	1.6	0.4 μ M
FIRE Polymerase (2U/ μ L)	0.4	0.02 U/ μ L
Template (gDNA)	0.5	-

PCR-step	Temperature ($^{\circ}$ C)	Time	Cycles
Initial denaturation	90	1 min	
Denaturation	90	20 s	30 X
Annealing	41	20 s	
Elongation	61-65*	1-4 min**	
Final hold	4	~	

* Optimized by temperature gradient

**variable depending on amplicon size and template concentration

2.2.2.6 Plasmid preparation

Plasmids were either purified with the Nucleo Spin Plasmid Kit for small scale purification (1.5 ml of overnight culture), or with the QIAfilter Plasmid Midi Kit for medium scale purification (200 ml of overnight culture) according to the manufacturer's protocols.

2.2.2.7 Agarose gel electrophoresis

DNA molecules are negatively charged due to their phosphate backbone and can thus be separated in an electric field as they move towards the anode according to their size. For this purpose, agarose (1%) was dissolved in 1x TAE buffer by boiling. After cooling down, ethidium bromide was added to a final concentration of 1 μ g/ml, the solution transferred to a gel tray and a comb inserted to generate pockets for DNA loading. Once the gel was polymerized it was transferred to the electrophoresis chamber containing 1x TAE buffer. The DNA was loaded 5:1 DNA – Loading dye. The samples run 160V for 20 minutes and DNA bands were analyzed under UV light in comparison to a DNA ladder.

2.2.2.8 Isolation of genomic DNA from *P. falciparum*

Genomic DNA from transgenic and wildtype *P. falciparum* was isolated to confirm the correct integration of knock-in constructs into the parasite genome. For this purpose, 5 ml of parasite culture was harvested and centrifuged at 1800-x g for 3 minutes. Genomic DNA from the pellet was purified using the QIAamp DNA Mini Kit according to the manufacturer's protocol. DNA was eluted with 50-to 150- μ l dH₂O.

2.2.3 Biochemical methods

2.2.3.1 Western blotting

For the identification and analysis of specific proteins, the proteins were separated by SDS-PAGE were transferred to nitrocellulose membranes by the wet transfer method. For this purpose, the polyacrylamide gel was layered on a nitrocellulose membrane and sandwiched between 6 Whatman filter papers and 2 sponges. The sandwich was transferred to a tank-blotting chamber filled with blotting buffer, with the nitrocellulose facing the anode and the polyacrylamide gel facing the cathode. A voltage of 100V was applied for 1 hour, or 12V overnight, at 4°C

2.2.3.2 Immuno-detection of proteins

After the protein transfer to a nitrocellulose membrane, proteins were visualized by immune detection. First, the membrane was blocked with 5% milk-PBS for 30 min at RT to block unspecific antibody binding. Then, the membrane was incubated with the primary antibody, diluted in 5% 1xPBS-milk (or 1% 1xPBS-milk for streptavidin) for minimum 2 hours at RT or overnight at 4°C. After 3 washing steps with 1x PBS the secondary antibody diluted in 5% 1xPBS-milk (or 1% 1xPBS-milk for streptavidin) was applied for 1 hour at RT. After 3 washing steps with 1x PBS the membrane was transferred to a transparent film and the enhanced chemo-luminescence (ECL) substrate pipetted onto the membrane. The membrane was covered with another transparent film and chemo-luminescence detected using a blue sensitive medical x-ray screen with exposure times ranging from 1 second to 45 minutes.

2.2.3.3 Pulldown of biotinylated proteins for mass spectrometry analysis (BioID)

Due to its quality, for the protein pulldown were only used reaction tubes from the company Eppendorf. All buffers were prepared using Ampuwa dH₂O and all steps were performed on ice. The described experiments were performed as duplicates. Harvested trophozoites and schizonts stage parasites from 100-200 ml of parasite culture were washed with DBPS twice

and lysed in 1 ml lysis buffer (50 mM Tris-HCl pH7.5, 500 mM NaCl, 1% TritonX-100, + freshly added 1 mM DTT, 2x protease inhibitor cocktail, 1 mM PMSF). The lysates were frozen at -80°C to further use.

After 10 minutes of centrifugation at 20000-x g the supernatants were transferred to 2 ml reaction tubes and diluted in 1 ml 50 mM Tris-HCl pH 7.5. 50µl of Streptavidin-Sepharose, equilibrated with 50 mM Tris-HCl pH 7.5, were transferred to the diluted supernatants and incubated overnight at 4°C with. The Sepharose was pelleted by centrifugation at 1600 x g for 1 minute at 4°C. The Sepharose pellet was washed 2 times with lysis buffer, 1 time with dH₂O (Ampuwa), 2 times with 50mM Tris-HCl pH 7.5 and three times with 100mM TEAB. After the last washing step, the Sepharose was re-suspended in 50µl of 100mM TEAB and shipped on ice for mass spectrometry analysis. The mass spectrometry analyses were performed by Wieteke Hoeijmakers (Radboud Institute, Nijmegen, Netherlands) using dimethyl labelling for quantification (Boersema *et al.*, 2009).

2.2.4 Culture of *P. falciparum* and cell biological methods

2.2.4.1 *P. falciparum* cell culture

P. falciparum blood stages were cultured in 15x60mm and 14x90mm petri dishes at 37°C in a low oxygen atmosphere (5% CO₂, 1% O₂, 94% N₂). 15x60mm petri dishes usually contained 5 ml and 14x90mm petri dishes 10 ml of RPMI complete medium and human erythrocytes (type O+) to a haematocrit of 5%. Transgenic parasites were selected by the addition of 10 nM WR, 1.5 g/ml blasticidin or 0.3 mg/ml G418 (for knock-in cell lines). The parasites were usually cultured with a parasitemia of 0.2-5% and RPMI complete medium was changed every 24-48 hours, depending on the parasitemia. Parasites were diluted to a parasitemia of 2-10%.

2.2.4.2 *P. falciparum* freezing and thawing

For long term storage of parasites cryo-stabilates were produced and stored in liquid nitrogen. 5-10 ml of parasite culture, containing 1-5% ring stages, were pelleted by 3 minutes centrifugation at 1800-x g. The pellets were re-suspended in 1 ml parasite freezing solution and transferred to cryo tubes and immediately frozen at -80°C for posterior transfer to liquid nitrogen. For thawing of parasites, the frozen cryo tubes were thawed at 37°C. The parasite suspension was transferred to a sterile 1.5 ml reaction tube and centrifuged for 1 minute at 2000 x g. The supernatant was discarded and the parasites were carefully re-suspended in 1 ml parasite thawing solution, centrifuged for 1 minute at 2000 x g, re-suspended in 1 ml RPMI complete medium, centrifuged again and the was pellet transferred to a 15x60mm petri dish

containing 6 ml RPMI complete medium and 200 μ l red blood cells. The selection drug was added after 16-24 hours and the medium was changed every 24 hours for 3 days.

2.2.4.3 Blood smears and Giemsa staining

To count the parasitemia it was necessary to smear 0.3 μ l of infected blood in a glass slide. The cells were smeared using another glass slide to obtain a single layer of red blood cells. After drying, the parasites were fixed in methanol for 10-20 seconds and then stained with Giemsa staining solution for 10-60 minutes (Ménard, 2013). After washing off the staining solution with water and drying the glass slides, the smears were analyzed using an optical light microscope at 100X.

2.2.4.4 Parasite synchronization with sorbitol

In order to obtain parasite cultures with synchronized parasite stages, 5-10 ml of parasite culture was pelleted by centrifugation for 3 minutes at 1800-x g. The pellet was re-suspended in 5 to 10 ml 5% D-sorbitol in dH₂O and incubated for 15 minutes at 37°C. After 3 minutes centrifugation at 1800 x g, the parasites were washed with 6 ml RPMI complete medium and then transferred to a petri dish containing RPMI complete medium.

2.2.4.5 *P. falciparum* Transfection using the BioRad system (ring transfection)

100 μ g plasmids were precipitated using 1/10 volume of 3M-sodium acetate and 3 volumes of ethanol 100%. The precipitated plasmid was pelleted by centrifugation for 5 minutes at 20000-x g. The plasmid pellet was washed with 70% ethanol, centrifuged again and the pellet air-dried. The pellet was dissolved in 15 μ l TE-buffer and added 385 μ l of cytomix. In the meantime, 5-10 ml of parasite culture containing 5-10% ring stage parasites was pelleted by 3 minutes centrifugation. The pellet was mixed with the cytomix/DNA solution and transferred to an electroporation cuvette (2 mm, BioRad). The electroporation was performed using the Gene Pulser Xcell (350 V, 950 F, 1). After electroporation, the parasites were immediately transferred to a 15x60mm or 14x90mm petri dish containing RPMI complete medium and 5% hematocrit. After 6 hours the medium was changed, and the selection drug added. During the following 5 days the medium was changed every 24 hours.

2.2.4.6 Transfection using the Amaxa system (schizont transfection)

50 μ g of plasmid DNA were precipitated using 1/10 volume of 3M sodium acetate and 3 volumes of ethanol. The precipitated DNA was pelleted by centrifugation for 5 minutes at 20000-x g. The DNA pellet was washed with 70% ethanol, centrifuged again and the pellet

air-dried. The pellet was dissolved in 10 µl TE-buffer and 90 µl of Amaxa transfection solution were added. In the meantime, late schizont stage parasites were harvested by overlaying 4 ml of 60% Percoll solution with 8 ml of parasite suspension and subsequent centrifugation for 6 minutes at 2500 x g. The schizont layer was transferred to a new 15 ml tube and washed with RPMI complete medium. Then, the schizont pellet was transferred to a 1.5 ml reaction tube and re-suspended in the DNA solution. The suspension was transferred to an electroporation cuvette (2 mm, BioRad). The electroporation was performed using the Nucleofector II AAD-1001N (programU-033). Immediately after electroporation the parasites were transferred to a 1.5 ml reaction tube containing 250 µl red blood cells and an equal amount of RPMI complete medium. The tube was incubated at 37°C with vigorous shaking for 30-60 minutes. Then, the parasites were transferred to a 15x60mm petri dish containing 6 ml RPMI complete medium. After 12-16 hours the medium was changed, and the selection drug added. During the following 5 days the medium was changed every 24 hours

2.2.4.7 Percoll gradient

In this work the Percoll gradient was used to separate trophozoites and schizonts from non-infected red blood cells and ring stage parasites. In a 2 ml reaction tube, 500 µl of 40% Percoll solution was overlaid by 500 µl of 60% Percoll solution and 500 µl of 80% Percoll solution. 10-20 ml of parasite culture were pelleted by centrifugation at 1800-x g for 3 minutes. The pellet was laid on the Percoll gradient and the reaction tube centrifuged for 5 minutes at 20000 x g. The layer containing the trophozoites and schizonts was transferred into a 1.5 ml reaction tube and washed with DPBS twice. The resulting pellet containing trophozoites and schizonts was used for further analysis.

2.2.4.8 Magnetic column separation of mature parasites

MACS separation columns were placed into the vario MACS[®] magnetic support and equilibrated by adding 60 ml of pre-warmed (37°C) RPMI medium without supplementation (incomplete medium). Magnetic separation of mature parasite forms from iRBCs was conducted 48 hours after sorbitol treatment. 60 ml of parasite cultures at 5% hematocrit were centrifuged at 600 g for 5 min with no break, and then re-suspended with 20 ml of incomplete medium. The suspension loaded on the top of the column. A low flow rate was used to pass the culture through the column. The effluent containing the rings, young trophozoites and non-infected RBCs was discarded. Columns were washed using 30 ml of DPBS at medium flow. Column was removed from the magnetic field and 20 ml of pre-warmed (37°C) complete medium was added to elute the mature forms. The eluted was pelleted by centrifugation at

1600 rpm during 5 min and the cells were lysed in 1 ml lysis buffer (50mM Tris-HCl pH7.5, 500mM NaCl, 1% TritonX-100, + freshly added 1mM DTT, 2x protease inhibitor cocktail, 1mM PMSF). The lysates were frozen at -80°C for further use in mass spectrometry.

2.2.4.9 Biotin labelling of parasite proteins (BioID)

Biotin labelling of proteins was achieved using parasite cell lines expressing BirA* fusion proteins (Roux et al., 2012). For subsequent mass spectrometry analysis large amounts of parasite culture had to be harvested. For this purpose, parasites were grown in 50 ml cell culture flasks (Sarstedt). Before harvesting the parasites were cultured in the presence of 20mM biotin for 24-48 hours. The cells were harvested at a parasitemia of 5-10%, preferably mostly trophozoites and schizonts. The medium was changed every 24 hours. For Western blot analysis of parasite lysates, the parasites were cultured in 14x90mm petri dishes.

2.2.4.10 Selection for transgenic parasites by SLI

For the integrant selection using SLI, cultures containing an episomal plasmid previously selected with 10 nM WR were adjusted to 2-5% parasitemia and G418 was added to a final concentration of 400 µg/ml (Birnbaum *et al.*, 2017). For *yDHODH* as SLI resistance marker a concentration of 1.5 µM DSM1 and for Blasticidin S as resistance marker 2 µg/ml were used. WR selection pressure was removed upon the addition of G418. The cultures were fed daily until day 7 after start of G418 selection pressure and from then on fed every 48h. On day 16 of selection parasites were taken off drug. The cultures were maintained for a maximum of 8 weeks, if no parasites were obtained until then the culture was discarded.

Giemsa smears were made on day 2 of selection pressure to inspect the status of the culture (parasitemia and dead process). If parasitemia was above 10% 10 ml RPMI medium were added into the 15x60 mm petri dish. In case of parasite reappearing, gDNA was isolated with the QIAamp DNA Mini Kit to perform PCRs across the integration junctions and to test for leftover unmodified locus (in order to exclude the presence of wild type or incorrect integrants). If wild type locus was detected the parasite cultures were treated with 10 nM WR for 2 cycles and DNA isolation with subsequent integration diagnostic PCR was performed again. To identify the essentiality of the gene using SLI-TGD, six parallel 5-ml cultures containing the episomal plasmid were placed under G418 selection (400 µg/ml). If no correct integration occurred on two occasions (with a total of six cultures), the target was assumed to be essential and the cultures were discarded.

2.2.4.11 Knock Sideways induction

For the knock sideways induction, parasites with an integrant FKBP were transfected with a plasmid leading to the episomal expression of a nuclear mislocalizer (NLS-FRB-mCherry). The plasmids were selected with 2 µg/ml Blasticidin S. In case of low expression of the mislocalizer the concentration of blasticidin S was increased to 9-18 µM (Epp, Raskolnikov and Deitsch, 2008). For the KS (see section 1.3.3.1), the culture was split into two dishes. To one of these dishes, rapalog (AP21967, Clontech) was added to a final concentration of 250 nM and the other dish served as a control. Mislocalization, as compared with the control culture, was verified microscopically after 6h and documented (Birnbaum *et al.*, 2017). Rapalog was stored at -20 °C as a 500 mM stock in ethanol, and working stocks were kept as 1:20 dilutions in RPMI at 4 °C for a maximum of 3 week

3 Results

3.1 Screen for interaction partners involved in the extraction of Transmembrane proteins out of the PPM

3.1.1 REX2 and SBP1 mDHFR fusion constructs are properly arrested in the PPM and PVM, respectively.

In order to identify interactors involved in the extraction of TM proteins out of the PPM, two constructs containing BirA* and that can be conditionally arrested in different transport steps were designed. The rationale behind the construct design was based on the fact that a fusion of mDHFR-GFP with the protein REX2 were shown to be arrested in the PPM (Gruring *et al.*, 2012), whereas the same construct fused to SBP1 is arrested in the PVM (Mesen-Ramirez *et al.*, 2016). The differential arresting phenotypes are attributed to the length of the region (termed spacer) between the blocking domain and the TM domain. With a longer spacer the construct is presumed to be able to reach and engage with the translocon at the PVM where it is arrested in transport due to the folded mDHFR domain (Mesen-Ramirez *et al.*, 2016).

Due to the specificity of the arrest of the constructs in different steps of the export process, it is expected that REX2-mDHFR-L-BirA*-3xHA construct biotinylates proteins from the cytosol and the PPM, including the proteins involved in its extraction out of the PPM (Figure 9 A), whereas the SBP1-mDHFR-L-BirA*-3xHA construct should be arrested in the translocon at the PVM and will biotinylate translocon components and potentially also proteins within the PV and at the PVM, serving as a control for the PPM arrested REX2-mDHFR-L-BirA*-3xHA (Figure 9 B).

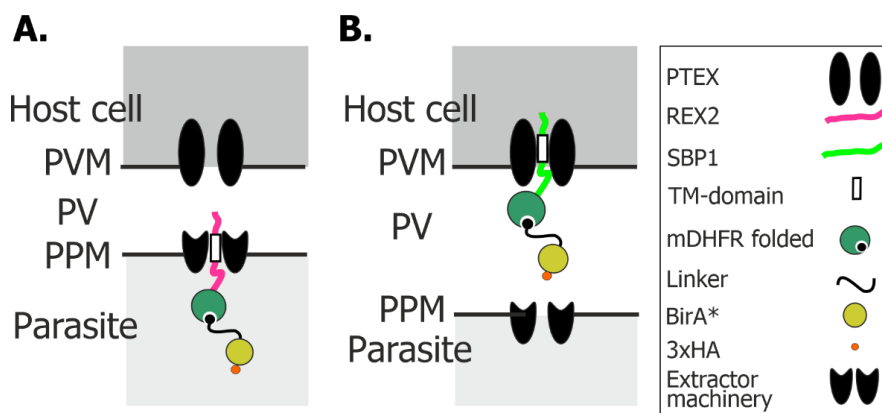


Figure 9: Model of conditional arrest of REX2 and SBP1 constructs in the PPM and PVM.

Upon the addition of 10 nM WR the mDHFR domain is stabilized, impeding the trafficking of the fused proteins to the RBC cytosol. **A.** Scheme showing the REX2-mDHFR-L-BirA*-3xHA construct arrested at the PPM. **B.** Scheme showing the SBP1-mDHFR-L-BirA*-3xHA, arrested at the PVM.

PVM: parasitophorous vacuole membrane; PV: parasitophorous vacuole; PPM: Parasite plasma membrane. Modified from (Mesen-Ramirez *et al.*, 2016).

The addition of WR avoids the unfolding of the mDHFR domain, thus causing the arrest of the construct on its way to the iRBC cytosol. To confirm the arrest of the constructs when WR is added, the SBP1-mDHFR-L-BirA*-3xHA and REX2-mDHFR-L-BirA*-3xHA cell lines were incubated in presence or absence of 10 mM WR and IFAs were performed to detect the constructs using α -HA antibodies. The REX2-mDHFR-L-BirA*-3xHA expressed construct (Figure 10 A) was strongly arrested in the periphery (Figure 10 B) when incubated with 10 nM WR for 24 h. The cell line expressing the SBP1-mDHFR-L-BirA*-3xHA construct (Figure 10 D) showed the construct arrested in the parasite periphery upon the addition of 10 nM WR, but some leakage was observed as evident by partial export to the Maurer's clefts (Figure 10 E).

Subsequently, 15 ml of culture of REX2-mDHFR-L-BirA*-3xHA and SBP1-mDHFR-L-BirA*-3xHA were cultivated in presence of 20 mM biotin and in absence or presence of 10 nM of WR. After 24 h a protein pellet was extracted from the cultures and isolated for performing Western blots. On the samples using α -HA antibodies, it was possible to detect REX2-mDHFR-L-BirA*-3xHA migrating at the predicted size of 76 kDa (Figure 10 C left) and SBP1-mDHFR-L-BirA*-3xHA migrating at the predicted size of 126 kDa (Figure 10 F left). In order to detect the biotinylated protein of each culture, Western blots were performed using streptavidin. The blot of proteins from the arrested construct was expected to show a differential pattern with stronger or additional bands when compared with the non-arrested control that would reflect the possible extractor that is in contact with the arrested construct. In the REX2-mDHFR-L-BirA*-3xHA is possible to observe an extra band that migrates at ~150 kDa in the sample obtained from the treated parasites (+WR) when compared with the non-arrested parasites (-WR) (Figure 10 C right). When analyzed, the blot of the proteins isolated from the SBP1-mDHFR-L-BirA*-3xHA parasites showed two extra bands, one migrating at ~150 kDa and another at ~90 kDa in the arrested construct (+WR) when compared with the non-arrested control culture (-WR) (Figure 10 F right).

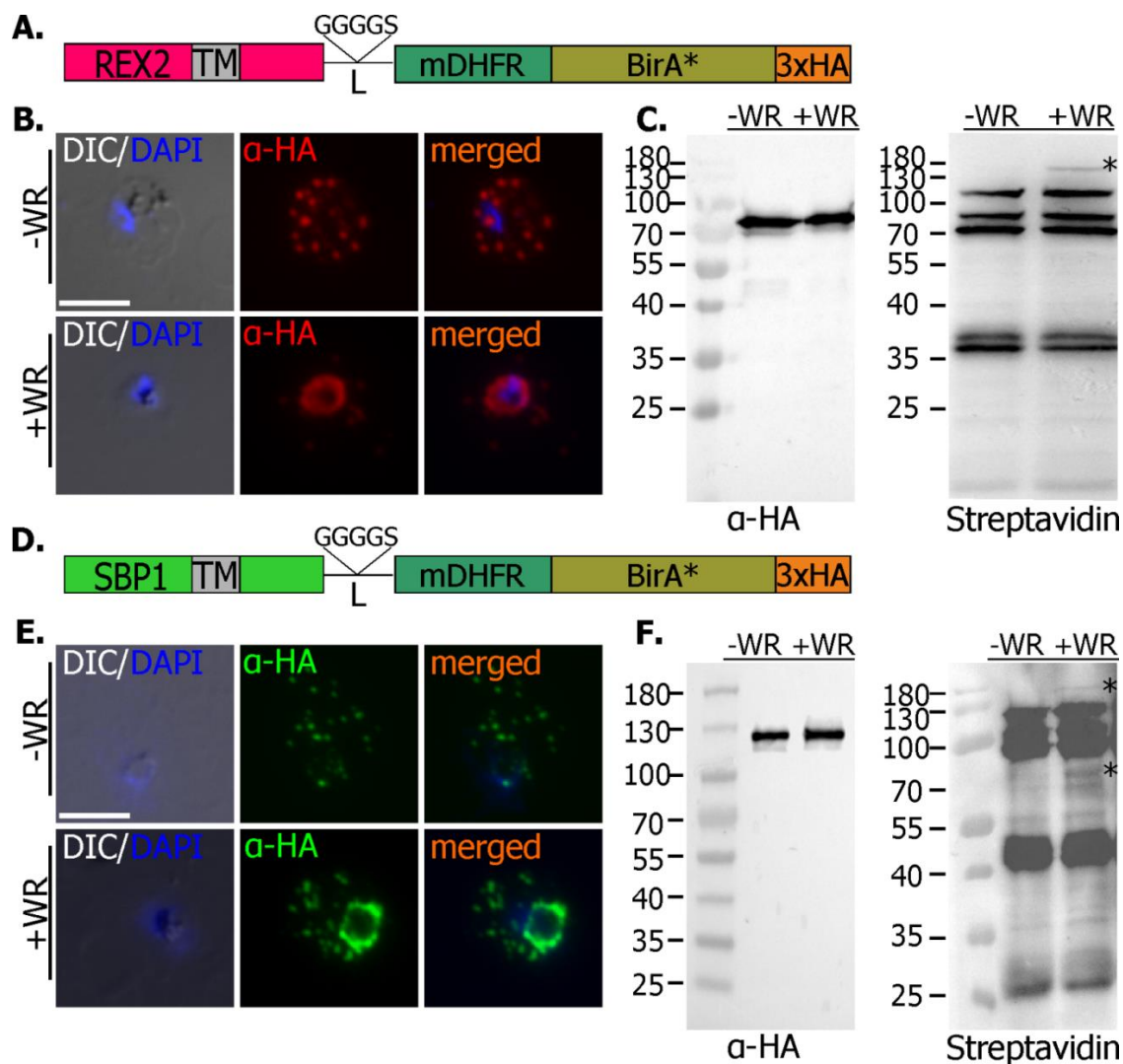


Figure 10: Demonstration of arrest of SBP1 and REX2 constructs in the transition from the PPM to the erythrocyte cytosol

A. Schematic of the construct containing REX2 fused to mDHFR, BirA* and a 3xHA tag. **B.** Fluorescence microscopy images of *P. falciparum* parasites episomally expressing REX2-mDHFR-L-BirA*-3xHA construct grown -WR (exported) or +WR (arrested). Detected with α -HA (red). **C.** Western blot probed with α -HA (left) and streptavidin (right) of protein extracts from REX2-mDHFR-L-BirA*-3xHA parasites generated after 24h post incubation with biotin and -WR or +WR. Construct size: 76 kDa. **D.** Schematic of the construct containing SBP1 fused to mDHFR, BirA* and a 3xHA tag. **E.** Fluorescence microscopy images of *P. falciparum* parasites episomally expressing SBP1-mDHFR-L-BirA*-3xHA construct grown -WR (exported) or +WR (arrested). Detected with α -HA (green). **F.** Western blot probed with α -HA (left) and streptavidin (right) of protein extracts from SBP1-mDHFR-L-BirA*-3xHA parasites generated after 24 h post incubation with biotin and -WR or +WR. Construct size: 123 kDa. TM: trans membrane domain; L: linker; BirA*: Biotin ligase A protein; 3xHA: 3 copies of hemagglutinin tag; NeoR: neomycin resistance cassette; -WR: no WR; +WR: 10 nM WR. Asterisk represent bands presents in +WR and absent in -WR. Schematic of the constructs are not-to-scale.

3.1.2 Mass spectrometry identification of biotinylated proteins

To identify the proteins interacting with the arrested constructs, it was necessary to do a comparative analysis of the biotinylated proteins when arrested compared to the control. For

this purpose, the biotinylated proteins from these cell lines were purified using streptavidin beads and analyzed via quantitative liquid chromatography-mass spectrometry (LC-MS) (performed by Dr. Wieteke Hoeijmakers, Bartfai lab, Netherlands). Two independent experiments were performed (biological replicas), each in a duplicate (technical replicas). The results are represented as plots, with enrichment of biotinylated proteins when the construct is arrested over the exported control and plotted as the respective log₂-ratios in each duplicate. Plots are shown for both biological replicas. The coloured dots in the figure represent proteins that were enriched in both biological replicas while grey dots represent proteins enriched in just one of them (Figure 11 and Figure 12).

The enrichment of biotinylated proteins in SBP1-mDHFR-L-BirA*-3xHA expressing parasites incubated with 10 nM WR compared to the control without WR is shown in Figure 11. The enriched proteins in this sample are either part of the PTEX translocon (EXP2 and PTEX150) or are reported to be at the PPM facing the PV lumen (Pf113). Due to the length of the construct SBP1-mDHFR-L-BirA*-3xHA and the flexibility conferred by the linker, the BirA* biotinylates the construct itself, being reflected on the detection of SBP1 in the mass spectrometry. The SBP1 fusion construct was also biotinylated itself which is expected as the BirA* part self-biotinylates. The fact that the proteins significantly enriched in SBP1-mDHFR-L-BirA*-3xHA +WR over -WR are known or suspected translocon components is evidence for the specificity of this experiment and suggests that the SBP1 construct is indeed arrested in the PVM translocon serving as control.

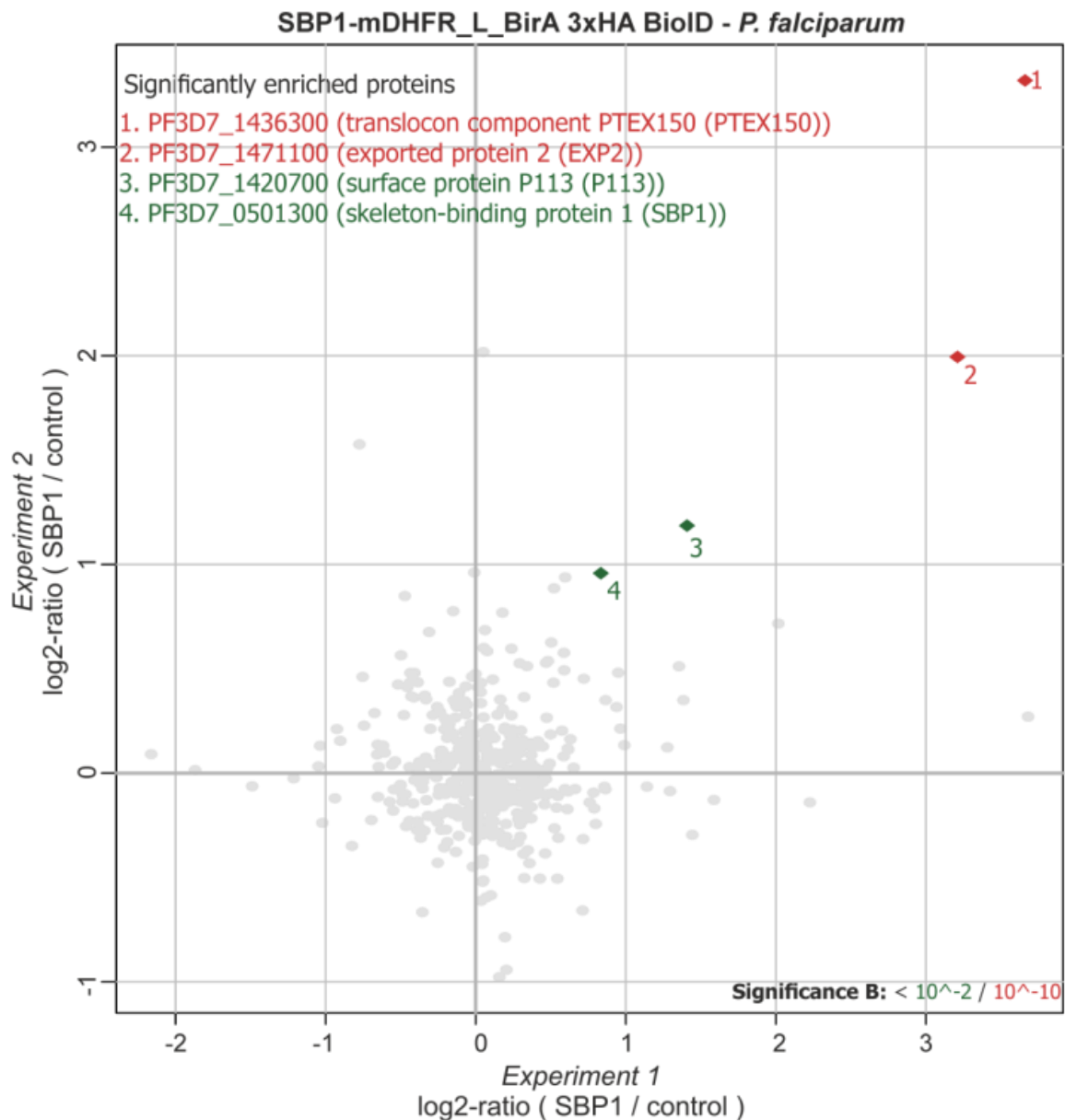


Figure 11: Biotinylated proteins enriched in arrested over non-arrested SBP1-mDHFR-L-BirA*-3xHA

Plotted are the log₂ ratio obtained from duplicates representing the enrichment of biotinylated proteins in SBP1 mDHFR-L-BirA* expressing cell line when arrested compared to control (no WR added). Significant proteins are marked with coloured dots (colour indicates significance of enrichment indicated as significance B).

Figure 12 shows the enrichment of the biotinylated proteins of the REX2-mDHFR-L-BirA*-3xHA expressing parasites when incubated in absence or presence of 10 nM WR. The enriched proteins are mostly, exported proteins, translocon related proteins, proteins located in the PV region or proteins belonging to the ER. This finding is consequent with the classical secretory pathway of exported proteins.

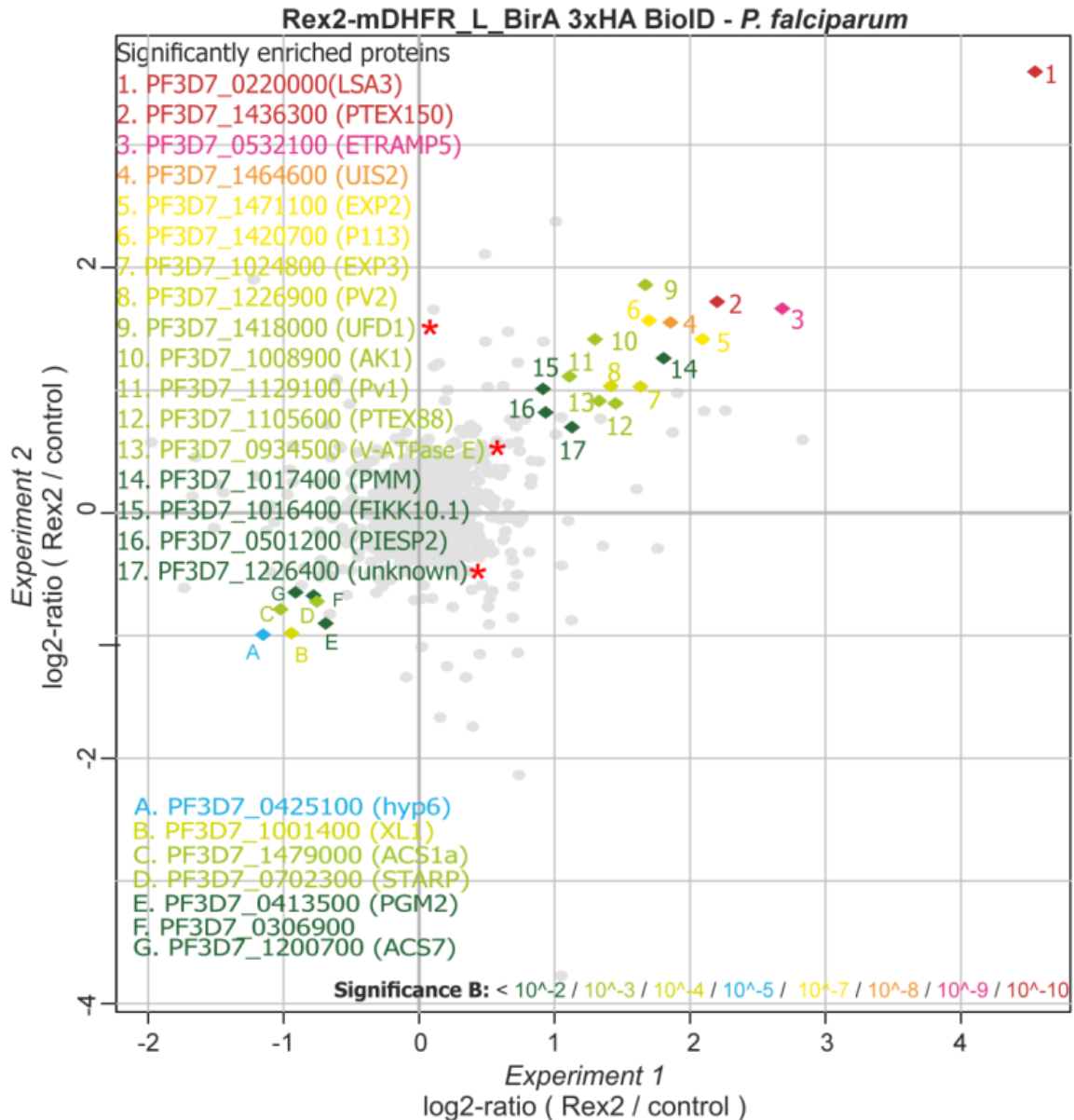


Figure 12: Biotinylated proteins enriched in arrested over non-arrested REX2-mDHFR-L-BirA*-3xHA

Plotted are the log₂-ratios obtained from duplicates representing the enrichment of biotinylated proteins in SBP1 mDHFR-L-BirA* expressing cell line when arrested compared to control (no WR added). Significant proteins are marked with coloured dots (colour indicates significance of enrichment indicated as significance B). 1 to 17: enriched proteins; A to G: non-enriched proteins. Red asterisk marks the candidates chosen for further analysis.

From a list of around 2000 proteins that were detected by mass spectrometry, the proteins with an unknown function and with a high level of enrichment over control (based on the respective log₂-ratios of each duplicate) were selected for further analysis. In addition proteins with homologues in other organisms and that based on this homology had potential functions in

protein-protein interactions or with membrane-transport or translocation were also selected as potential PPM protein extractors (Table 4).

Table 4: Candidates chosen to assess as potentially involved in TM-protein extraction.

List of the 10 cloned proteins. A list with additional information of the highest 200 hits is provided in Table S1. NaN: not a number, F and R: replicas

Protein ID in PlasmoDB	Name/Function	Log2 normalized			
		Ratio H/L Rex2 F	Ratio L/H Rex2 R	Ratio L/H SBP1 F	Ratio L/H SBP1 R
PF3D7_1418000	Ubiquitin fusion degradation protein 1, UFD1 (Figure 13)	1.67	1.86	NaN	0.21
PF3D7_1105600	Translocon component PTEX88 (Section 3.1.3.8)	1.45	0.89	0.40	0.41
PF3D7_0934500	V-type proton ATPase subunit E, V-ATPaseSE (Figure 14)	1.33	0.91	0,50	0,63
PF3D7_0928600	Conserved <i>Plasmodium</i> protein, unknown function (section 3.1.3.8)	2.01	1.80	NaN	NaN
PF3D7_1226400	Conserved <i>Plasmodium</i> protein, unknown function (Figure 15)	1.13	0.70	0.84	0.35
PF3D7_1472100	Protein transport protein YIP1, putative (section3.1.3.8)	1.77	1.26	NaN	NaN
PF3D7_0104500	Conserved protein, unknown function (Figure 16)	0.70	1.50	NaN	NaN
PF3D7_0704300	Conserved <i>Plasmodium</i> membrane protein, unknown function (Figure 17)	0.36	0.08	0,39	-0,10
PF3D7_1410000	ER membrane protein complex subunit 2, EMC2 (Figure 18)	-1.71	1.48	NaN	2.23
PF3D7_0830400	CRA domain-containing protein, putative (Figure 19)	1.01	2.38	-0.81	0.34

3.1.3 Tagging and functional analysis of the candidates obtained from mass spectrometry

For the analysis of the candidates selected based on the mass spectrometry results (Table 4 and Table S2), three different constructs were generated for each candidate. Firstly, a targeting region in the N-terminal region of the corresponding gene was cloned into, the pARL1-GFP-2A-NeoR plasmid (SLI-TGD). This had the goal to determine the essentiality of the protein for parasite survival in asexual blood stages (successful SLI-based selection of parasites with integration of this plasmid indicates non-essentiality, whereas a failure of selection is an indicator for essentiality (Birnbaum *et al.*, 2017)). For the SLI-TGD vector, targeting regions

were chosen so that integration resulted in a disrupted gene resulting in a protein encoding only the N-terminal 10 to 30% of the original sequence. The other two constructs used for each candidate were made using the SLI-2xFKBP-GFP and SLI-3xHA plasmids. Integration of these constructs with C-terminal targeting regions results in endogenous tagging of the proteins with 3xHA or 2xFKBP-GFP (the 2xFKBP would be used for KS). Two different tags were used due to their differing properties. The GFP tag is ideal for fast live detection of the protein by microscopy, but due to its size it can interfere with function or transport of some proteins (Dave *et al.*, 2016; Weill *et al.*, 2019). Triple HA (3xHA) is a small tag that is less likely to interfere with protein function or transport, but detection of the tagged protein in the cell is more time consuming because an immunofluorescence assay must be carried out.

3.1.3.1 PF3D7_1418000. UFD1: ubiquitin fusion degradation protein 1

UFD1 is a protein of 282 aa and a calculated molecular weight of 32.5 kDa. It contains neither a signal peptide nor predicted transmembrane domains. It is homologous to the well-described human UFD1, which is an essential component of the ubiquitin-dependent proteolytic pathway that degrades ubiquitinated proteins in the ER and contributes to retro-translocation of TM proteins out of the ER membrane (Spork *et al.*, 2009; Chung *et al.*, 2012). In the piggyBac transposon mutagenesis screen PfUFD1 appeared as likely essential for parasite growth (Zhang *et al.*, 2018). The essentiality of the orthologous gene in the murine parasite *P. berghei* ANKA (PBANKA_1024700) was not tested (Bushell *et al.*, 2017).

Using the SLI system the endogenous protein was tagged with 2xFKBP-GFP (Figure 13 A) and separately also with the epitope tag 3xHA (Figure 13 D) (see section 2.1.15). Parasites containing the episomal plasmid were selected with WR and after obtaining the parasites containing the episomal plasmid, integrants were selected using G418. The gDNA of the integrants was isolated and used for integration diagnostic PCR (see section 2.2.2.5). The plasmid was integrated correctly in the genome of both cell lines with no original locus detected as judged by a diagnostic PCR (Figure 13 B and E).

According to the GFP signal of the UFD1-2xFKBP-GFP cell line, the protein is dispersed in the cytosol of the parasite and is expressed during the entire asexual blood cycle (Figure 13 C). An IFA performed with the UFD1-3xHA cell line confirmed the cytosolic localization of the tagged protein (Figure 13 F). A Western blot performed with the same cell line showed a band migrating at ~67 kDa (Figure 13 G) corresponding to the expected molecular weight of the protein plus the 3xHA tag.

To identify the essentiality of the protein for parasite survival, 3D7 parasites were transfected with a SLI-TGD plasmid. Integration of this vector into the genome would result in a disrupted *ufd1* gene which only would be possible if the gene is dispensable for growth of asexual blood stage parasites. However, no correct integrants were obtained after 6 attempts (Table S1). This failure to select for parasites with a disrupted *ufd1* indicates that this gene is indispensable for parasite growth. To be able to conditionally inactivate UFD1, the UFD1-2xFKBP-GFP cell line was transfected with an episomally expressed nuclear mislocalizer (NLS-FRB-mCherry) to be able to inducibly remove the protein from its site of action using KS (see section 1.3.3.1) (Figure 13 H). Upon addition of 250 nM rapalog to induce the KS, UFD1 was completely re-located to the nucleus whereas in the control without rapalog, the protein remained in the cytosol (Figure 13 J). A growth assay over 5 days showed no difference in parasite growth between the rapalog treated and the untreated parasites (Figure 13 I and S1A). In contrast to the SLI-TGD attempt this indicated that UFD1 is dispensable for the growth of asexual blood stage parasites. Acetone fixed IFAs were performed in order to detect if the mislocalization of the protein led to dysfunctions on the export process. According to the localization of REX2 in the rapalog treated cells, the export is not affected by UFD1 mislocalization (Figure 13 K).

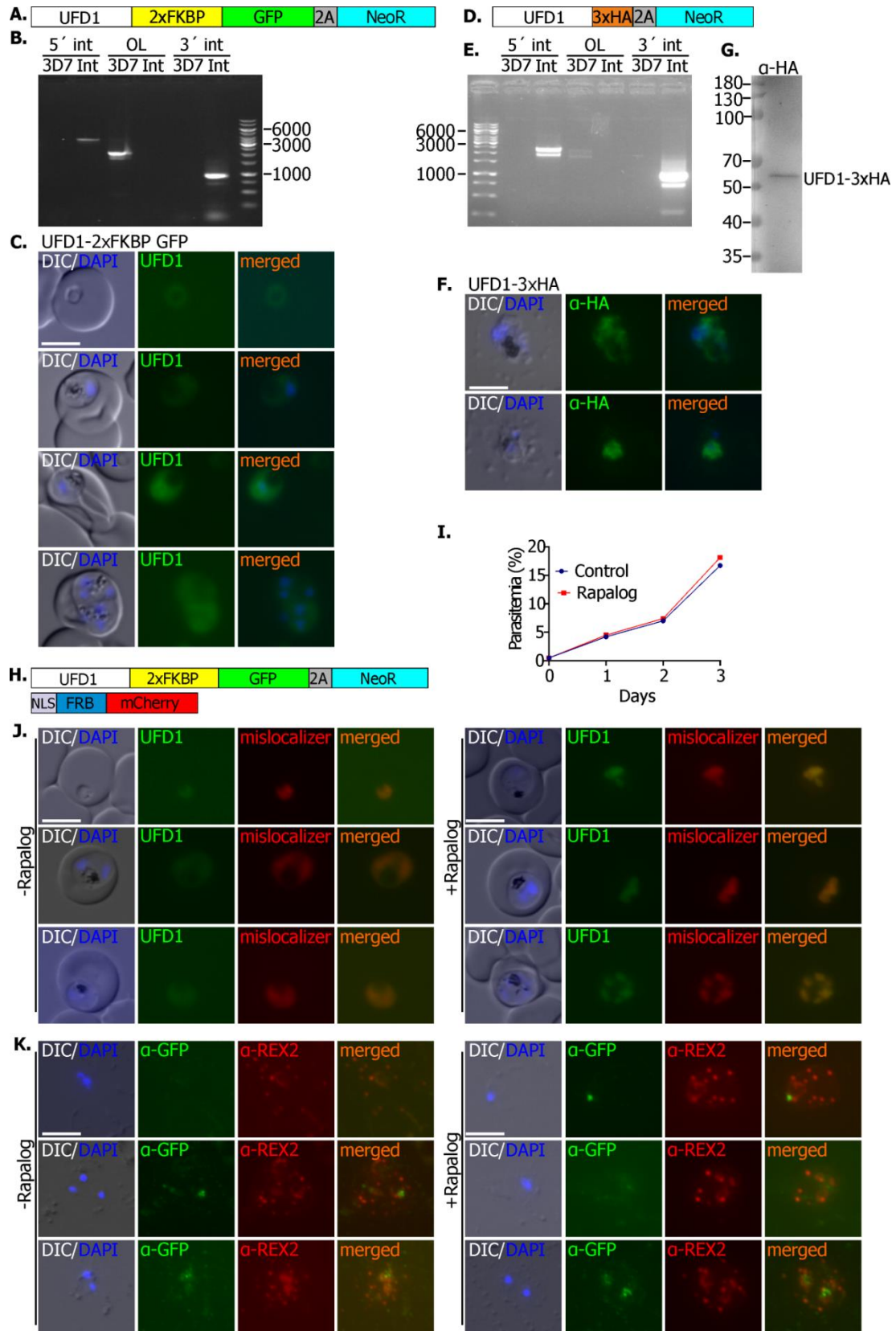


Figure 13: PF3D7_1418000 (UFD1) ubiquitin fusion degradation protein 1

A. Schematic of the transfected construct containing UFD1, 2xFKBP-GFP, a skip peptide (2A) and the Neo resistance cassette (NeoR). **B.** Agarose gel with PCR products from gDNA of the UFD1-2xFKBP-GFP expressing cell line confirming the correct integration of the plasmid into the genome. Absence of original locus (OL) shows that no parasite with wild type locus remained (int, integration parasite line; 3D7, untransfected parental cell line; 5' int, PCR product crossing the 5' integration

junction; 3' int, PCR product crossing the 3' integration junction; the marker is indicated in kbp). **C.** Live cell fluorescence microscopy images of UFD1-2xFKBP-GFP expressing parasites. Different development stages of the parasite from rings (top) to schizont (bottom) stages are shown. **D.** Schematic of the transfected construct containing UFD1 with a 3xHA tag, a skip peptide (2A) and the Neo resistance cassette (NeoR). **E.** Agarose gel with PCR products from gDNA of UFD1-3xHA expressing cell line (Features as in B). **F.** Fluorescence images of IFAs of acetone fixed UFD1-3xHA parasites. **G.** Western blot with protein extracts derived from UFD1-3xHA parasites, probed with α -HA, showing a band migrating at the expected size of 64 kDa. The marker is indicated in kDa. **H.** Scheme representing the integrated UFD1-2xFKBP-GFP construct together with the episomally expressed NLS-FRB-mCherry mislocalizer. NLS: nuclear mislocalizer. For FRB-FKBP see section 2.2.4.11 and 1.3.3.1. **I.** representative growth curve of 3 independent experiments analyzed by flow cytometry (replicates in Figure S1A), showing the development of the UFD1-2xFKBP-GFP + NLS-FRB-mCherry expressing cell line in presence (KS) or absence (control) of 250 nM rapalog. **J.** Live cell fluorescence microscopy images of the UFD1-2xFKBPGFP + NLS-FRB-mCherry expressing cell line after 10 h incubation with or without 250 nM rapalog. **K.** Fluorescence images of IFAs of acetone fixed parasites of cell lines expressing UFD1-2xFKBPGFP + NLS-FRB-mCherry probed with α -REX2 and α -GFP antibodies when incubated overnight with or without 250 nM rapalog, showing no interference with protein export. DIC: Differential interference contrast. The nuclei were stained with DAPI. Scale bars: 5 μ M. GFP, green fluorescent protein; mCherry: red fluorescent protein. Schematic of the constructs are not-to-scale.

3.1.3.2 PF3D7_0934500: V-type proton ATPase subunit E

The V-type proton ATPase (V-ATPase) is a highly conserved complex that acidifies intracellular organelles and pumps protons across membranes in eukaryotes (Maxson and Grinstein, 2014; Pamarthy *et al.*, 2018). It was reported to be situated in lysosomes and endosomes of eukaryotic cells (Nelson *et al.*, 2000) and in *Plasmodium* was detected surrounding the food vacuole (Lamarque *et al.*, 2008). V-ATPase has been implicated in a bewildering variety of additional roles that seem independent of its ability to translocate protons. Due these non-canonical functions, which include fusogenicity, cytoskeletal tethering, metabolic sensing (Weisz, 2003) and due to its function in lysosomes, endosomes and food vacuole membranes, the V-ATPase could potentially play a role in the transport of protons or aiding the transport of proteins in other membranes as for example the PPM. The complex is composed by two domains, the V₀ (non-soluble) and the V₁ (soluble) domain and the subunit E is part of the V₁ region. The Subunit E of the V-ATPase (V-ATPaseSE) is composed of 235 aa and a calculated molecular weight of 27.2 kDa. It contains neither a signal peptide nor predicted transmembrane domains. In the piggyBac transposon mutagenesis screen it was predicted to be likely essential (Zhang *et al.*, 2018) and the orthologous gene in the murine parasite *P. berghei* ANKA (PBANKA_0835300) is essential for parasite survival in blood stages (Gomes *et al.*, 2015).

Using the SLI system the endogenous protein was tagged with a fluorescent tag 2XFKP-GFP (Figure 14 A) and separately also with 3xHA (Figure 14 D) (see section 2.1.15). Parasites

containing the episomal plasmid were selected with WR and after obtaining the parasites containing the episomal plasmid, integrants were selected using G418. The gDNA of the integrants was isolated and used for a diagnostic PCR to ascertain correct integration of the plasmid into the genome (see section 2.2.2.5). For the V-ATPaseSE-2xFKBP-GFP some parasites with original locus remained in the culture after 8 weeks under G418 pressure (Figure 14 B). For the V-ATPaseSE-3xHA cell line only traces of the original locus remained (Figure 14 E).

The GFP signal of the V-ATPaseSE-2xFKBP-GFP cell line indicated that the protein is located around the food vacuole but also around the parasite, suggesting a PPM location (Figure 14 C). Those results were corroborated with the V-ATPaseSE-3xHA cell line, which also showed signal around the food vacuole and the parasite when an IFA was performed using α -HA antibodies (Figure 14 F).

In order to determine the essentiality of V-ATPaseSE for parasite survival, 3D7 parasites were transfected with a SLI-TGD plasmid (Figure 14 G) that upon integration would disrupt the gene *PF3D7_0934500*, encoding the subunit E of the V-ATPase. After the selection of parasites carrying the corresponding episomal SLI-TGD plasmid, the parasites were selected with G418 and after 3 weeks correct integrants were observed in the culture (Figure 14 H). The GFP signal of the cell line with the disrupted V-ATPaseSE showed a similar phenotype to the one observed in the cell line tagged with 2xFKBP-GFP (Figure 14 I). The fact that parasites with a disrupted V-ATPaseSE were obtained indicates that this protein is dispensable for the survival of asexual blood stage parasites. Finally, to test if the disruption of V-ATPaseSE affected the export of proteins to the erythrocyte, an IFA was performed with antibodies recognizing the exported protein REX2 (Figure 14 J) but no abnormalities were observed in the location of this protein indicating that V-ATPaseSE is not involved in protein export.

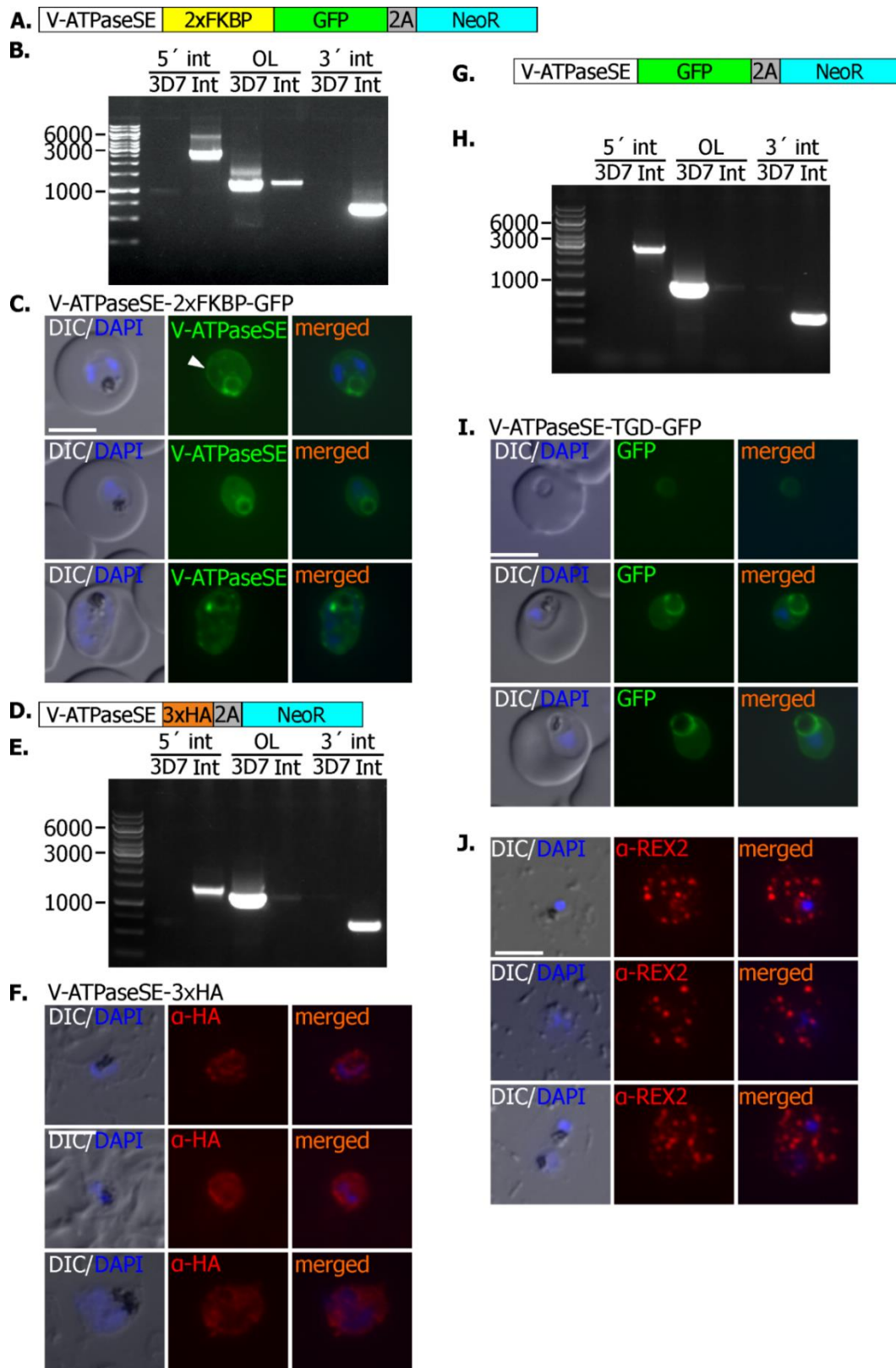


Figure 14: Pf3D7_0934500. V-ATPaseSE: V-type proton ATPase subunit E

A. Schematic of the transfected construct containing a subunit E of the V-ATPase with a 2xFKBP-GFP, a skip peptide (2A) and the Neo resistance cassette (NeoR). **B.** Agarose gel with PCR products from gDNA of the V-ATPaseSE-2xFKBP-GFP expressing cell line confirming the correct integration of the plasmid into the genome. There were remnants of cells with original locus (OL) in the integrated cell line. (int, integration parasite line; 3D7, untransfected parent cell line; 5' int, PCR product crossing the 5' integration junction; 3' int, PCR product crossing the 3' integration junction; the marker is

indicated in kbp). **C.** Live cell fluorescence microscopy images of V-ATPaseSE-2xFKBP-GFP expressing parasites. Different development stages of the parasite from rings (top) to schizont (bottom) are shown. Arrow indicates signal in the PV. **D.** Schematic of the transfected construct containing a subunit E of the V-ATPase fused to a 3xHA tag, a skip peptide (2A) and the Neo resistance cassette (NeoR). **E.** Agarose gel with PCR products from gDNA from the V-ATPaseSE-3xHA expressing cell line confirming the correct integration of the plasmid into the genome (features as in B). **F.** Fluorescence images of IFAs of acetone fixed V-ATPaseSE-3xHA expressing cell line showing signal surrounding the FV and the PV. **G.** Schematic of the transfected construct containing a fraction of the Subunit E of V-ATPase in a TGD-GFP vector with a skip peptide (2A) and the Neo resistance cassette (NeoR). **H.** Agarose gel with PCR products from gDNA of the V-ATPaseSE-TGD-GFP cell line showing the correct integration of the plasmid and successful disruption of the protein (features as in B). **I.** Live cell fluorescence microscopy images of V-ATPaseSE-TGD-GFP cell line showing a similar phenotype to the GFP tagged cell line. **J.** Fluorescence images of IFAs of acetone fixed V-ATPaseSE-TGD-GFP cell line probed with α -REX2 antibodies showing no interference with protein export. The nuclei were stained with DAPI. Scale bars: 5 μ M. Schematic of the constructs are not-to-scale.

3.1.3.3 Pf3D7_1226400: Conserved *Plasmodium* protein with unknown function

Pf3D7_1226400 is a protein of 856 aa and calculated molecular weight of 102 kDa. It contains neither a predicted signal peptide nor transmembrane domains. It is a conserved protein of *Plasmodium* species with no homology outside apicomplexans and to the date there is no data describing its function. In the piggyBac transposon mutagenesis screen *Pf3D7_1226400* appeared as likely essential for parasite growth (Zhang *et al.*, 2018). The essentiality of the orthologous gene in the murine parasite *P. berghei* ANKA (PBANKA_1441200) was not tested (Bushell *et al.*, 2017).

Using the SLI system the endogenous protein was tagged with 2xFKBP-GFP (Figure 15 A) (see section 1.3.3). Parasites containing the episomal plasmid were selected with WR and after obtaining the parasites containing the episomal plasmid, integrants were selected using G418. The gDNA of the integrants was isolated and used for integration diagnostic PCR. The plasmid was integrated correctly in the genome of both cell lines with no original locus detected as judged by a diagnostic PCR (Figure 15 B). According to the GFP signal (Figure 15 C) the protein is expressed during the entire cycle. In rings it was found dispersed in the parasite cytosol. In later stages it accumulated in foci.

To identify the essentiality of the protein for parasite survival, 3D7 parasites were transfected with a SLI-TGD plasmid (Figure 15 D). Integration of this vector into the genome would result in a disrupted *Pf3D7_1226400* which only would be possible if the gene is dispensable for growth of asexual blood stage parasites. Parasites with a disrupted *Pf3D7_1226400* appeared after 3 weeks in culture. Correct integration of the plasmid was confirmed by diagnostic PCR with gDNA from the TGD-GFP cell line (Figure 15 E). After 2 cycles with intermittent WR and neomycin passes it was not possible to completely remove the original locus of the TGD

cell line. The parasite survival after the disruption of *Pf3D7_1226400* indicates that this gene is dispensable for parasite growth of asexual blood stage parasites. The GFP signal of the disrupted *PF3D7_1226400* was barely detectable by fluorescence microscopy and remained cytosolic in the parasite during the entire cycle with no foci detectable (Figure 15 F). To identify if the capacity to export proteins was disturbed due to the *PF3D7_1226400* disruption, the TGD cell line was used for an IFA where the exported protein REX2 was detected. However, REX2 was normally exported to the MC (Figure 15 G), indicating that *PF3D7_1226400* has no role in protein export.

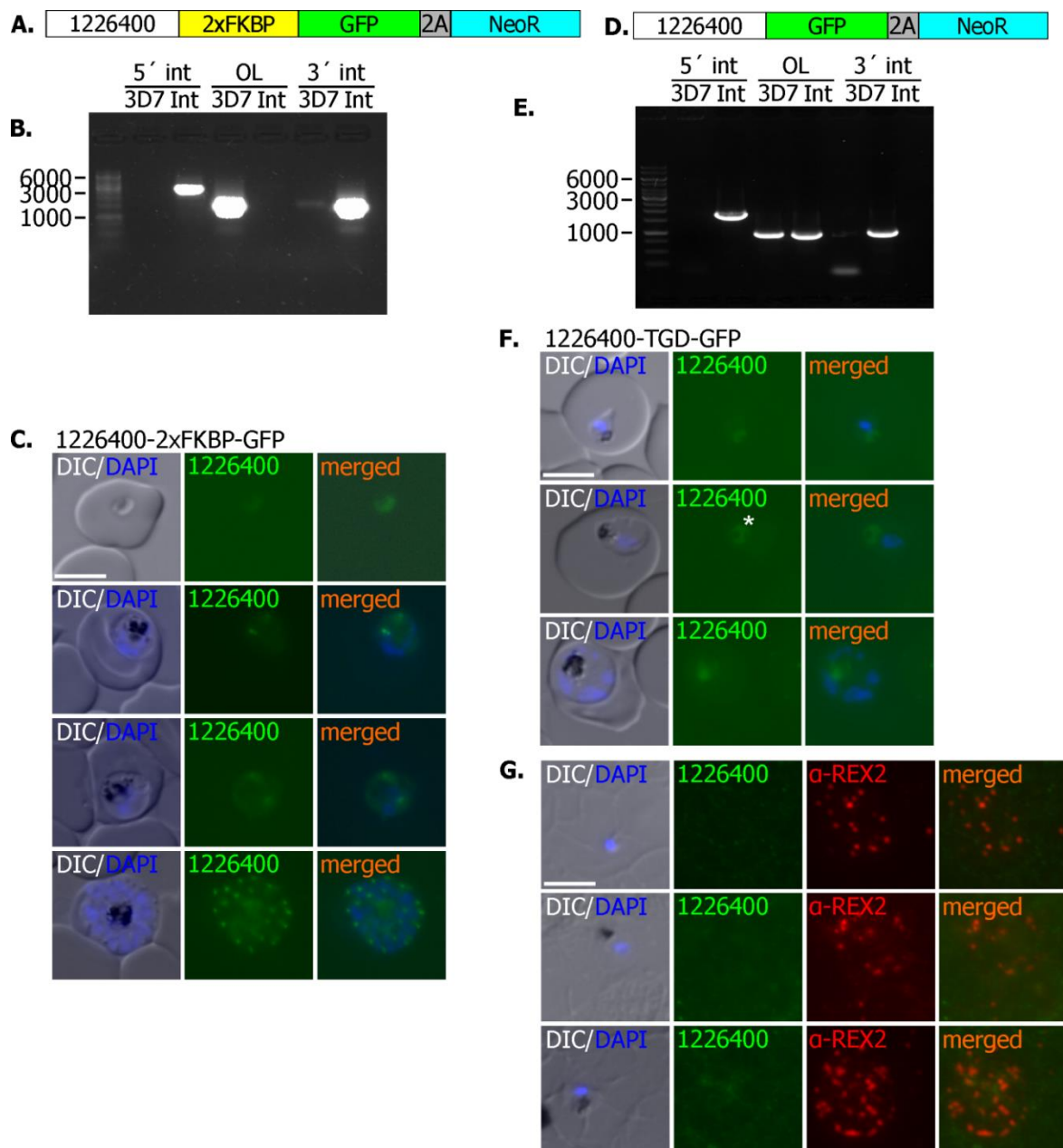


Figure 15: Pf3D7_1226400. Conserved *Plasmodium* protein with unknown function

A. Schematic of the transfected construct containing a sequence for 1226400, fused to 2xFKBP-GFP, a skip peptide (2A) and the Neo resistance cassette (NeoR). **B.** Agarose gel with PCR products from gDNA of 1226400-2xFKBP-GFP expressing cell line confirming the correct integration of the

plasmid into the genome. Absence of original locus (OL) shows that no parasite with wild type locus remained (int, integration parasite line; 3D7, untransfected parent cell line; 5' int, PCR product crossing the 5' integration junction; 3' int, PCR product crossing the 3' integration junction; the marker is indicated in kbp). **C.** Live cell fluorescence microscopy images of 1226400-2xFKBP-GFP, showing a weak cytosolic signal in rings and two foci in trophozoite stages. Different development stages of the parasite are shown from rings (top) to schizont (bottom). **D.** Schematic of the transfected construct containing a sequence for 1226400 disruption fused with a GFP flag, a skip peptide (2A) and the Neo resistance cassette (NeoR). 1226400-TGD-GFP. **E.** Agarose gel with PCR products from gDNA of the 1226400-TGD-GFP expressing cell line confirming correct integration of the plasmid into the genome and successful disruption of the protein. Parasites with OL remained on the culture. (Features as in B). **F.** Fluorescence live cell images of 1226400-TGD-GFP parasites, showing a faint cytosolic signal. Asterisk: food vacuole autofluorescence. **G.** IFA of the 1226400-TGD-GFP cell line with α -REX2 antibody showing no interference with the protein export of REX2. The nuclei were stained with DAPI. Scale bars: 5 μ M. Schematic of the constructs are not-to-scale.

3.1.3.4 Pf3D7_0104500: Conserved protein with unknown function

Pf3D7_0104500 is a protein of 277 aa and a calculated molecular weight of 33.2 kDa, it contains a signal peptide and no predicted transmembrane domains. It is a conserved protein of *Plasmodium* species with no homology outside apicomplexans and to the date there is no data describing its function. In the piggyBac transposon mutagenesis screen it was predicted to be dispensable (Zhang *et al.*, 2018). The essentiality of the orthologous gene in the murine parasite *P. berghei* ANKA (PBANKA_0208600) was not tested (Bushell *et al.*, 2017).

To determine its localization, the endogenous protein was tagged with 2xFKBP-GFP using the SLI system (Figure 16 A). Parasites containing the episomal plasmid were selected with WR and after obtaining the parasites containing the episomal plasmid, integrants were selected using G418. The gDNA of the integrants was isolated and used for integration diagnostic PCR (see section 2.2.2.5) (Figure 16 B). According to the faint GFP signal (Figure 16 C) the protein was detected dispersed on the parasite cytosol, is expressed at low levels based on the faint GFP signal and is present during the entire asexual blood cycle.

To identify the essentiality of the protein for parasite survival, 3D7 parasites were transfected with a SLI-TGD vector (Figure 16 D). Parasites with a disrupted *Pf3D7_0104500* appeared after 3 weeks in culture and the correct integration of the plasmid was confirmed by integration diagnostic PCR with gDNA from the corresponding TGD-GFP cell line (Figure 16 E). The GFP signal observed in the disrupted cell line was identical to the one observed in the GFP tagged cell line (Figure 16 F). The possibility to obtain disrupted parasites confirmed the dispensability of *Pf3D7_0104500* gene. Finally, to test if the disruption of *Pf3D7_0104500* affected the export of proteins to the erythrocyte, an IFA was performed with α -REX2 antibodies (Figure 16 G) but there was no noticeable abnormality in the protein export process.

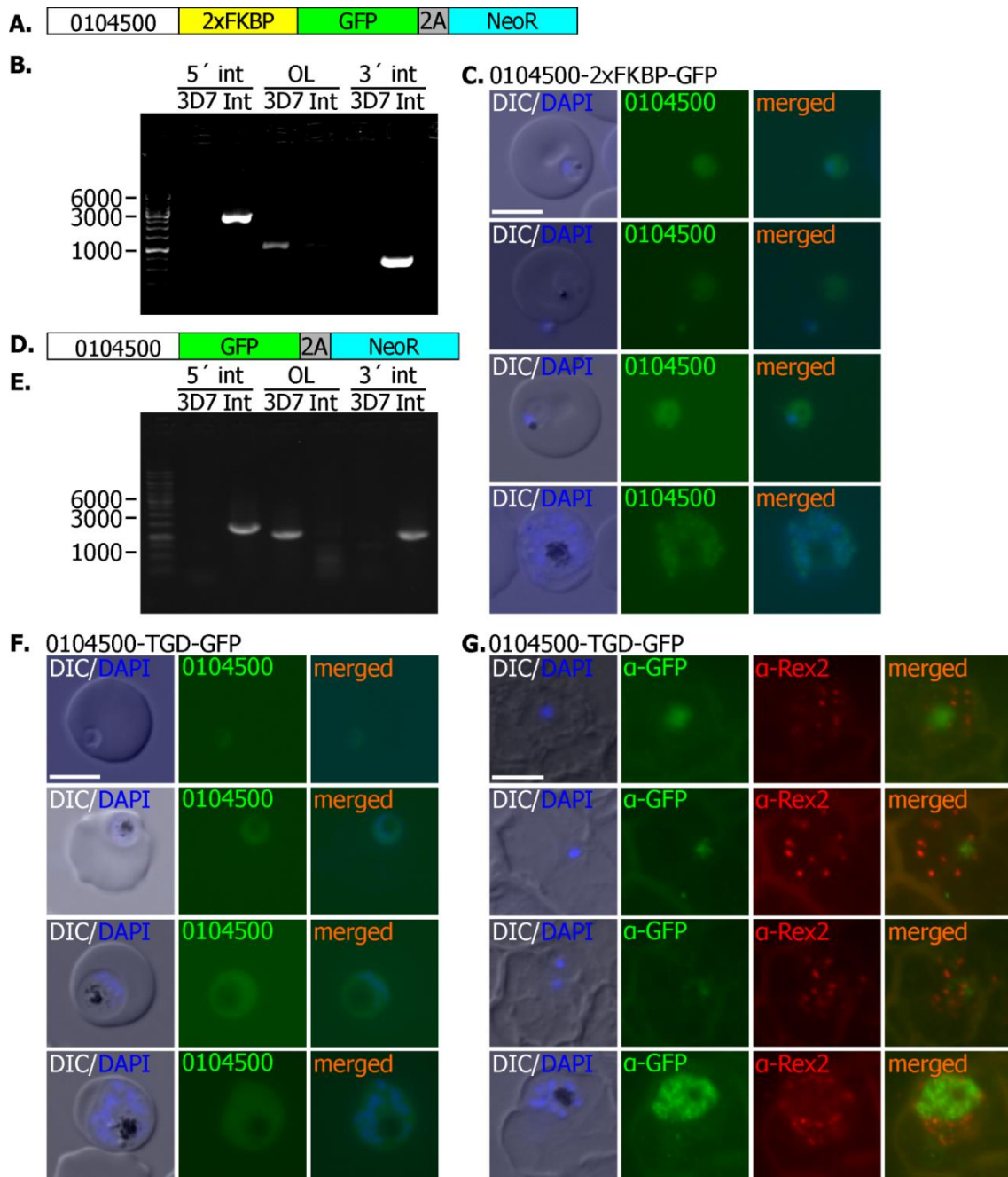


Figure 16: PF3D7_0104500. Conserved protein with unknown function

A. Schematic of the transfected construct containing a sequence for 0104500, fused to 2xFKBP-GFP, a skip peptide (2A) and the Neo resistance cassette (NeoR). **B.** Agarose gel with PCR products from gDNA of 0104500-2xFKBP-GFP expressing cell line confirming the correct integration of the plasmid into the genome. Absence of original locus (OL) shows that no parasite with wild type locus remained (int, integration parasite line; 3D7, untransfected parent cell line; 5' int, PCR product crossing the 5' integration junction; 3' int, PCR product crossing the 3' integration junction; the marker is indicated in kbp). **C.** Live cell fluorescence microscopy images of 0104500-2xFKBP-GFP, showing a weak cytosolic signal observable during the whole intraerythrocytic cycle. Different development stages of the parasite are shown from rings (top) to schizont (bottom). **D.** Schematic of the transfected construct containing a sequence for 0104500 disruptions fused with a GFP flag, a skip peptide (2A) and the Neo resistance cassette (NeoR). **E.** Agarose gel with PCR products from gDNA of the 0104500-TGD-GFP expressing cell line confirming correct integration of the plasmid into the genome and successful disruption of the protein. Parasites with OL remained on the culture (features as in B). **F.** Fluorescence live cell images of 0104500-TGD-GFP parasites, showing a faint

cytosolic signal. The nuclei were stained with DAPI. Scale bars: 5 μ M. **G.** IFA of the 0104500-TGD-GFP cell line with an α -REX2 antibody showing no interference with the protein export. The nuclei were stained with DAPI. Scale bars: 5 μ M. Schematic of the constructs are not-to-scale.

3.1.3.5 PF3D7_0704300: Conserved *Plasmodium* membrane protein with unknown function

Pf3D7_0704300 is a protein of 1852 aa and calculated molecular weight of 217.5 kDa, with a signal peptide and 3 transmembrane domains encoded within the first 134 aa. It is a conserved protein of the genus *Plasmodium* and to date there is no data describing its function. The piggyBac transposon mutagenesis screen indicated that it is dispensable (Zhang *et al.*, 2018). The essentiality of the orthologous gene in the murine parasite *P. berghei* ANKA (PBANKA_0802000) was not tested (Bushell *et al.*, 2017).

In order to identify the essentiality of the protein for parasite survival, 3D7 parasites were transfected with a SLI-TGD vector (Figure 17 A). Parasites containing the episomal plasmid were selected with WR and after obtaining the parasites containing the episomal plasmid, integrants were selected using G418. Genomic DNA from these parasites was isolated and used for an integration diagnostic PCR (Figure 17 B). Live imaging of the TGD cell line showed a localization in the parasite periphery with a faint cytosolic signal (Figure 17 C). The possibility to obtain disrupted parasites confirmed the dispensability of *PF3D7_0704300* for the survival of asexual blood stage parasites. It was not possible to properly describe the protein localization due to the impossibility to obtain 2xFKBP-GFP tagged parasites despite several attempts (Table S1). However, due to the localization of the disrupted protein, it could be speculated that the native protein would be also located at the PPM. To test this possibility, an IFA with α -REX2 antibodies was performed in order to determine whether the disruption of *PF3D7_0704300* interferes with the correct transport of REX2 (Figure 17 D). However, no abnormalities in the export of REX2 were detected.

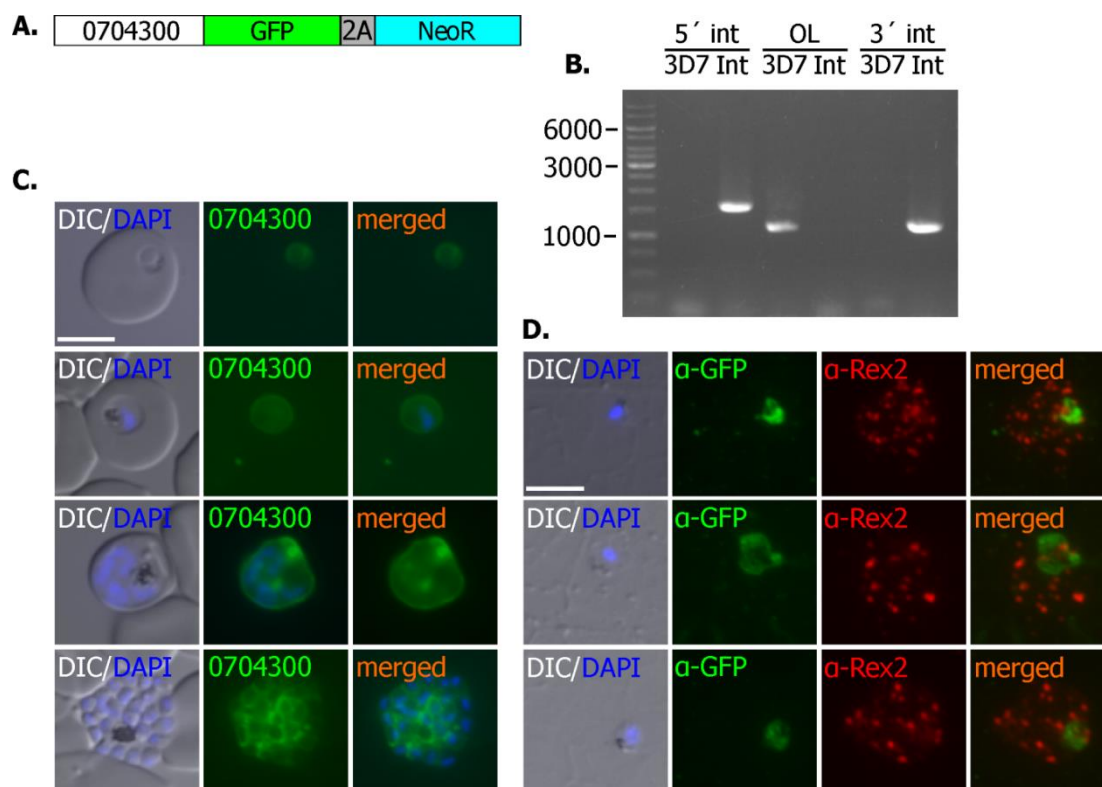


Figure 17: PF3D7_0704300. Conserved *Plasmodium* membrane protein

A. Schematic of the transfected construct containing sequence for 0704300 protein disruption in a TGD-GFP vector with a skip peptide (2A) and the Neo resistance cassette (NeoR). **B.** Agarose gel with PCR products from gDNA of the 0704300-TGD-GFP expressing cell line confirming the correct integration of the plasmid into the genome and successful disruption of the protein. (int, integration parasite line; 3D7, untransfected parent cell line; 5' int, PCR product crossing the 5' integration junction; 3' int, PCR product crossing the 3' integration junction; the marker is indicated in kbp). **C.** Fluorescence live cell images of 0704300-TGD-GFP parasites, showing a faint cytosolic signal. With a stronger signal around the PV. **D.** Fluorescence images of IFAs of acetone fixed 0704300-TGD-GFP expressing cell line probed with α -REX2 antibodies showing no interference with the protein export. DIC: Differential interference contrast. The nuclei were stained with DAPI. Scale bars: 5 μ M. Schematic of the constructs are not-to-scale.

3.1.3.6 PF3D7_1410000. EMC2: ER membrane protein complex subunit 2

The EMC2 is a protein of 292 aa with a calculated molecular weight of 35 kDa. It contains neither a signal peptide nor predicted transmembrane domains. EMC2 is part of the ER membrane protein complex (EMC) and it harbors three tetratricopeptide repeats (TPR1/2/3). The EMC has been shown a role on the post-translational insertion of tail-anchored membrane proteins into the ER (Guna *et al.*, 2018) and on the facilitation of TMD transfer from the cytosol into lipid bilayers (Chitwood *et al.*, 2018). In the piggyBac transposon mutagenesis screen it showed to be likely essential (Zhang *et al.*, 2018). The essentiality of the orthologous gene in the murine parasite *P. berghei* ANKA (PBANKA_1032500) was not tested (Bushell *et al.*, 2017).

To determine its localization, the endogenous protein was tagged with 2xFKBP-GFP using the SLI system (Figure 18 A). Parasites containing the episomal plasmid were selected with WR and after obtaining the parasites containing the episomal plasmid, integrants were selected using G418. The gDNA of the integrants was isolated and used for integration diagnostic PCR (see section 2.2.2.5) (Figure 18 B) showing a correct integration of the plasmid with no original locus detectable. According to previous reports of localization in mammalian cells, EMC2 should be found at the ER membrane (Guna *et al.*, 2018; Volkmar *et al.*, 2019; Wideman, 2015). Most of the GFP signal was found on the nuclear envelope, typical for an ER localization. However in some cells a halo surrounding the parasite was observed, suggesting that a fraction of the protein population was also at the PPM (Figure 18 C). To verify the localization of the protein, the GFP cell line was transfected with an episomal plasmid encoding SDEL-STEVAR mCherry as an ER marker (Figure 18 D). In this cell line, a total co-localization of the ER marker with the GFP signal of EMC2-GFP cell line indicates that the PPM signal observed was unspecific, as the ER marker also showed the same distribution (Figure 18 E).

To determine the essentiality of the protein for parasite survival and to elucidate if the disruption of the protein has an effect on protein export, 3D7 parasites were transfected with a SLI-TGD vector. Integration of this vector into the genome would result in a disrupted *emc2* gene which only would be possible if the gene is dispensable for growth of asexual blood stage parasites. However, no correct integrants were obtained after 6 attempts (Table S1). This failure to select for parasites with a disrupted *emc2* indicates that this gene could be necessary for parasite growth. To further confirm this theory, the EMC2-2xFKBP-GFP cell line was transfected with an episomally expressed nuclear mislocalizer (NLS-FRB-mCherry) to be able to inducibly remove the protein from its site of action using KS (see section 1.3.3.1) (Figure 18 F). The idea behind the mislocalization of EMC2 was to avoid that the protein detected in the parasite periphery reaches its site of action. In this case, if EMC2 has a role in protein export on the PPM, the mislocalization of the protein would show a deficient exporting phenotype. Upon the addition of 250 nM rapalog the protein was just partially mislocalized to the nucleus and no evident growth defect or aberrant morphology was observed when compared with the control without Rapalog (Figure 18 H). A growth assay over 5 days showed no difference in parasite development between the rapalog treated and the untreated parasites (Figure 18 G). Acetone fixed IFAs were performed in order to detect if the partial mislocalization of the protein led to dysfunctions of the protein export process. According to

the localization of SBP1, export of exported TM proteins was not affected by EMC2 mislocalization (Figure 18 I).

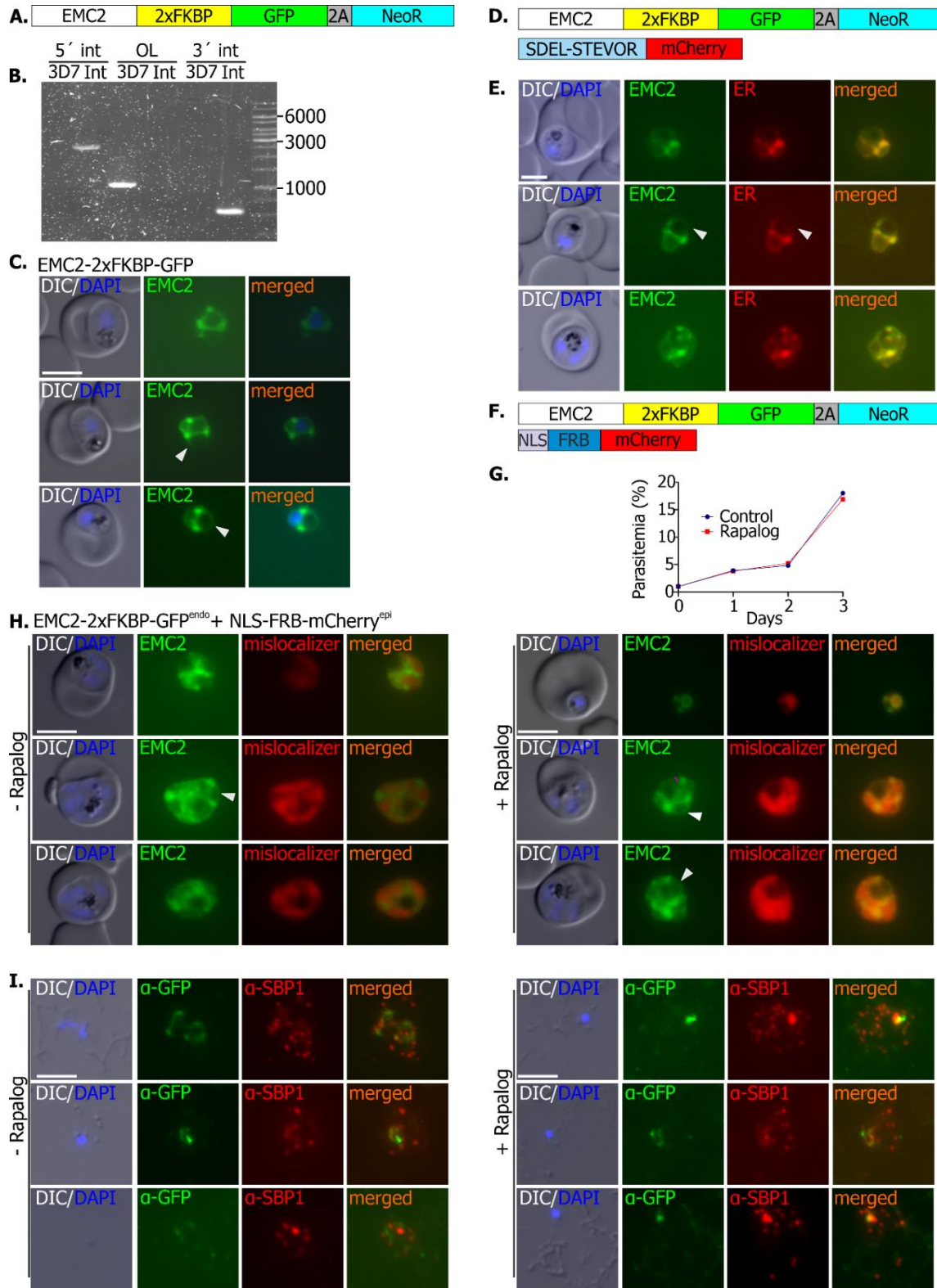


Figure 18: PF3D7_1410000 (EMC2) ER membrane protein complex subunit 2

A. Schematic of the transfected construct containing a sequence for EMC2 protein tagged with 2xFKBP-GFP, a skip peptide (2A) and the Neo resistance cassette (NeoR). **B.** Agarose gel with PCR products from gDNA of the EMC2-2xFKBP-GFP expressing cell line confirming the correct

integration of the plasmid into the genome. Absence of original locus (OL) shows that no parasite with wild type locus remained (int, integration parasite line; 3D7, untransfected parent cell line; 5' int, PCR product crossing the 5' integration junction; 3' int, PCR product crossing the 3' integration junction; the marker is indicated in kbp). **C.** Live cell fluorescence microscopy images of EMC2-2xFKBP-GFP expressing parasites. Arrow: light signal at the PPM. **D.** Schematic of the transfected construct containing an episomal ER marker SDEL-STEVEOR-mCherry in the episomally expressing Live cell fluorescence microscopy images of EMC2-2xFKBP-GFP cell line. **E.** Live cell fluorescence microscopy images of EMC2-2xFKBP-GFP + SDEL-STEVEOR-mCherry showing colocalization of both signals on ER. **F.** Scheme representing the integrated EMC2-2xFKBP-GFP construct together with the episomally expressed NLS-FRB-mCherry mislocalizer. NLS: Nuclear localization signal (see section 1.3.3.1). **G.** representative growth curve of 3 independent experiments analyzed by flow cytometry (replicates in Figure S1B), showing the development of the EMC2-2xFKBP-GFP + NLS-FRB-mCherry cell line in presence (KS) or absence (control) of 250 nM rapalog. **H.** Live cell fluorescence microscopy images of the EMC2-2xFKBP-GFP + NLS-FRB-mCherry cell line after 10 h incubation with or without 250 nM rapalog. **I.** Fluorescence images of IFAs of acetone fixed of cell lines expressing EMC2-2xFKBP-GFP + NLS-FRB-mCherry probed with α -SBP1 and α -GFP antibodies when incubated with or without 250 nM rapalog, showing no interference with protein export. DIC: Differential interference contrast. The nuclei were stained with DAPI. Scale bars: 5 μ M. GFP: green fluorescent protein. mCherry: Schematic of the constructs are not-to-scale.

3.1.3.7 Pf3D7_0830400. CRA: CRA domain-containing protein

The CRA domain-containing protein (from now on called CRA) consists of 137 aa and it has a molecular weight of 16 kDa. It contains a signal peptide and one transmembrane domain. The CRA domain is a protein-protein interaction domain presented in crown eukaryotes, and acts as an adapter protein to couple membrane receptors to intracellular signalling pathways (Menon, Gibson and Pastore, 2004). The piggyBac transposon mutagenesis screen indicated that it is dispensable (Zhang *et al.*, 2018). The essentiality of the orthologous gene in the murine parasite *P. berghei* ANKA (PBANKA_0701100) was not tested (Bushell *et al.*, 2017).

To determine its localization, the endogenous protein was tagged with 2xFKBP-GFP and with using the SLI system (Figure 19 A). Parasites containing the episomal plasmid were selected with WR and after obtaining the parasites containing the episomal plasmid, integrants were selected using G418. The gDNA of the integrants was isolated and used for integration diagnostic PCR (see section 2.2.2.5) (Figure 19 B) showing a correct integration of the plasmid with no original locus detectable. The protein was present in foci in the parasite periphery or within the parasite cytosol, as well as signals accumulating in the food vacuole (Figure 19 C). All stages showed a GFP signal, indicating that the protein was expressed throughout asexual development.

To identify the essentiality of the protein for parasite survival, 3D7 parasites were transfected with a SLI-TGD plasmid. The integration of this vector into the genome would result in a disrupted *Pf3D7_0830400* gene which only would be possible if the gene is dispensable for growth of asexual blood stage parasites. However, no correct integrants were obtained after 6

attempts (Table S1). This failure to select for parasites with a disrupted *Pf3D7_0830400* precluded an analysis of this protein's function in export. To be able to conditionally inactivate CRA, the integrant CRA-2xFKBP-GFP cell line was transfected with an episomally expressed nuclear mislocalizer (NLS-FRB-mCherry) to be able to inducibly remove the protein from its site of action using KS (see section 1.3.3.1) (Figure 19 D). Upon addition of 250 nM rapalog to induce the KS a growth assay over 5 days was carried out, showing no difference in parasite growth between the rapalog treated and the untreated parasites (Figure 19 E and S1C). the CRA protein contains a TMD which is known to prevent mislocalization. As a consequence, no mislocalization was achieved (Figure 19 F).

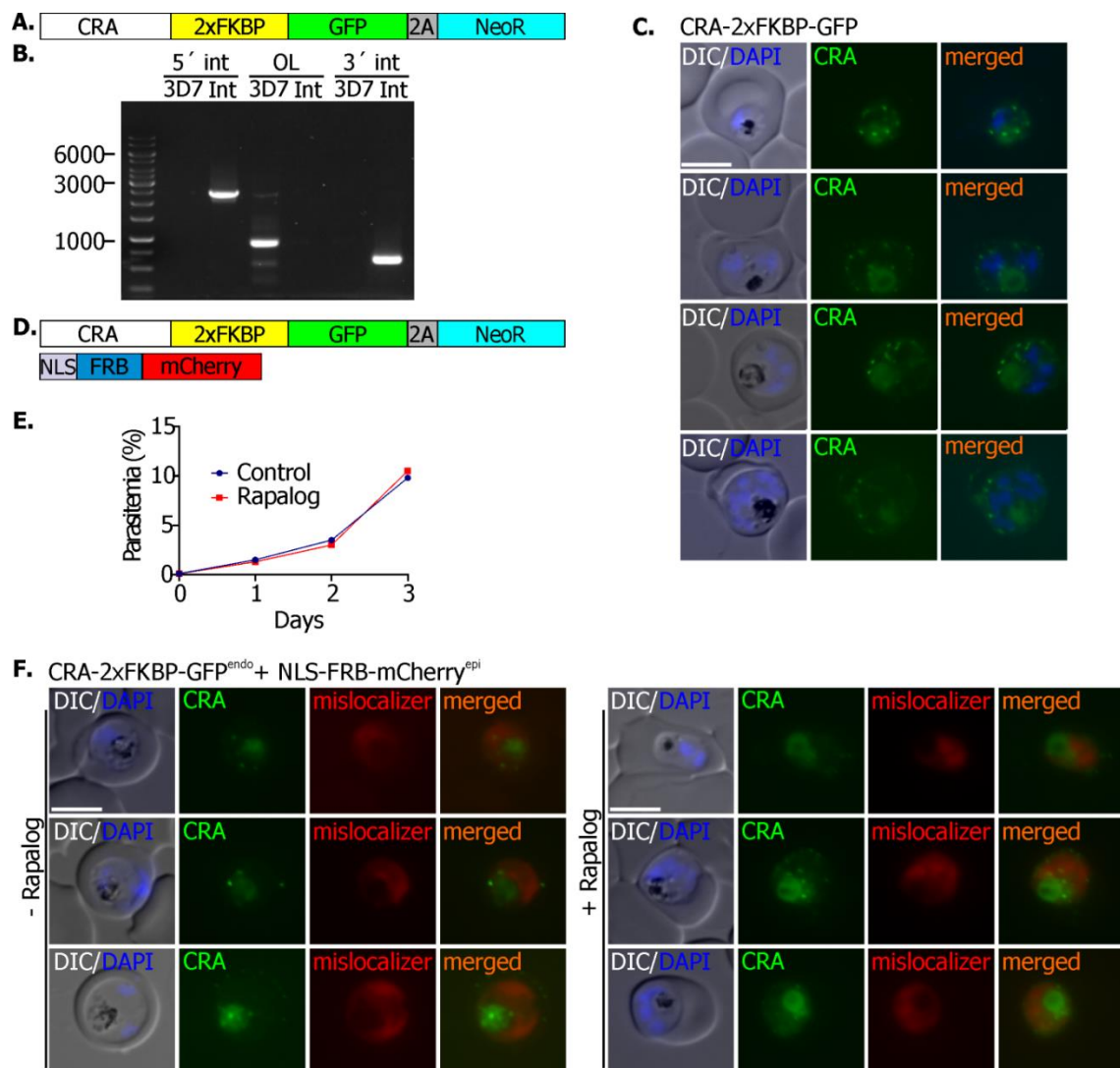


Figure 19: PF3D7_0830400. CRA domain-containing protein

A. Schematic of the transfected construct containing a sequence for CRA protein tagged with 2xFKBP-GFP, a skip peptide (2A) and the Neo resistance cassette (NeoR). **B.** Agarose gel with PCR products from gDNA of the CRA-2xFKBP-GFP expressing cell line confirming the correct integration of the plasmid into the genome. Absence of original locus (OL) shows that no parasite

with wild type locus remained (int, integration parasite line; 3D7, untransfected parent cell line; 5' int, PCR product crossing the 5' integration junction; 3' int, PCR product crossing the 3' integration junction; the marker is indicated in kbp). **C.** Live cell fluorescence microscopy images of *P. falciparum* parasites expressing CRA-2xFKBP-GFP, showing foci during the whole asexual intraerythrocytic cycle. Different development stages of the parasite from rings (top) to schizont (bottom) stages are shown. **D.** Scheme representing the integrated CRA-2xFKBP-GFP construct together with the episomally expressed NLS-FRB-mCherry mislocalizer (NLS, nuclear localization signal) (see section 1.3.3.1). **E.** representative growth curve of 3 independent experiments analyzed by flow cytometry (replicates in Figure S1C), showing the development of the CRA-2xFKBP-GFP + NLS-FRB-mCherry cell line in presence (KS) or absence (control) of 250 nM rapalog. **F.** Live cell fluorescence microscopy images of the CRA-2xFKBP-GFP + NLS-FRB-mCherry cell line after 10 h incubation with or without 250 nM rapalog. DIC: Differential interference contrast. The nuclei were stained with DAPI. Scale bars: 5 μ M. Schematic of the constructs are not-to-scale.

3.1.3.8 PF3D7_1105600-PTEX88: PTEX Translocon component; PF3D7_0928600 and PF3D7_1472100 (YIP1)

PTEX88, YIP1 and PF3D7_0928600 were also investigated because in the mass spectrometry, those 3 proteins were highly biotinylated. After several attempts to obtain integrants, it was not possible to tag or disrupt any of these proteins (Table S1), therefore they were not further analysed.

3.2 Jamming PTEX and its implications in PfEMP1 export

3.2.1 Effect of exported protein disruption in PfEMP1 export

Previously in our laboratory, using the SLI system, it was possible to generate a cell line where the *var* gene *Pf3D7_0809100* was endogenously tagged with a 3xHA tag, resulting in the expression of the corresponding PfEMP1 in all parasites by virtue of the G418 selection (Mesén-Ramírez, unpublished) (Figure 20 A and B). This is the first cell line expressing a tagged, full length PfEMP1 which is especially useful for studying the effect on PfEMP1 of disrupting or arresting proteins involved in PfEMP1 trafficking and assembling.

An IFA with α -HA antibodies was performed to detect PfEMP1-3xHA, the PfEMP1 (red) signal colocalized with the MCs resident protein SBP1 (green) (Figure 20 C). Finally, a trypsin protection assay was performed in order to confirm if PfEMP1 is expressed in the iRBC surface (Figure 20 D) (Trypsin assay kindly performed by Paolo Mesén-Ramírez). In the non-treated culture, the PfEMP1 is intact running around its calculated molecular weight of 201 KDa (Figure 20 D). When trypsin is added at a concentration of 0,02 μ M, the N terminal region of the protein is digested and the C-terminal fragment containing the TMD, the ATS and the 3xHA tag remain protected. The Protected fragment is observed as a band migrating around 80 KDa, in the sample treated with trypsin (Figure 20 D), sized in accordance with the

protected fragments previously described for PfEMP1 trypsin digestion (Cooke *et al.*, 2006; Maier *et al.*, 2007; Waterkeyn *et al.*, 2000).

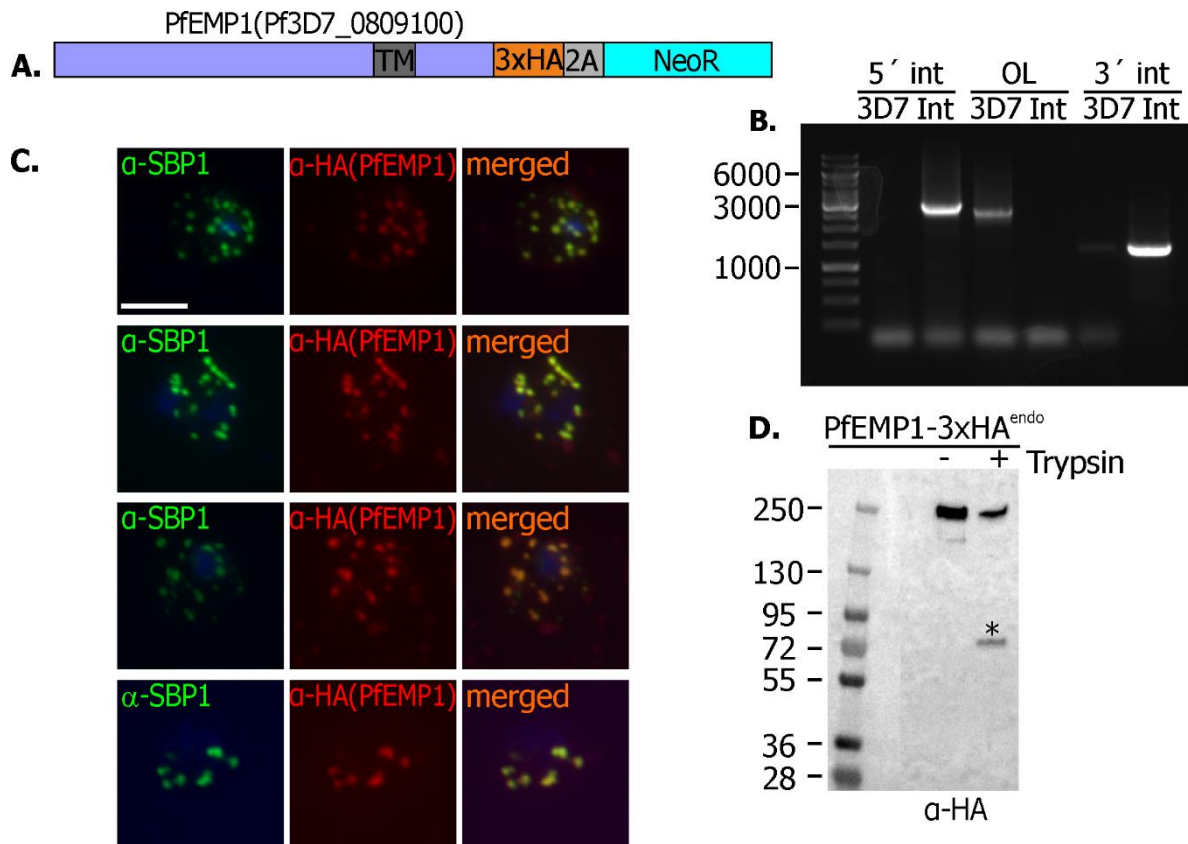


Figure 20: Pf3D7_0809100. PfEMP1 cell line endogenously tagged with 3xHA

A. Schematic of the resulting expression cassette containing the PfEMP1 *Pf3D7_0809100* tagged with 3xHA. Transmembrane domain (TM), skip peptide (2A) G418 resistance cassette (NeoR). Not to scale. **B.** Agarose gel with PCR products from gDNA of the PfEMP1-3xHA expressing cell line confirming the correct integration of the plasmid into the genome. Absence of original locus (OL) shows that no parasite with wild type locus remained (int, integration parasite line; 3D7, untransfected parent cell line; 5' int, PCR product crossing the 5' integration junction; 3' int, PCR product crossing the 3' integration junction; the marker is indicated in kbp). **C.** Fluorescence images of IFAs of acetone fixed PfEMP1-3xHA^{endo} parasites. PfEMP1 was detected using α -HA antibodies (red). SBP1 was used as a MCs marker and was detected using α -SBP1 antibodies (green). The nuclei were stained with DAPI. **D.** Western blot of trypsin protection assay probed with α -HA antibodies of the PfEMP1-3xHA^{endo} cell line. The control (-trypsin) shows the intact full-length PfEMP1-3xHA^{endo} migrating around the calculate MW of 250 kDa and the treated culture (+0,02 μ M trypsin) shows a protected fragment migrating around 80 kDa (asterisk). The marker is shown in kDa; scale bar: 5 μ M.

Exported proteins such as SBP1 are implicated in the correct transport (Maier *et al.*, 2007) and exposure of PfEMP1 on the iRBC surface (Cooke *et al.*, 2006). The disruption of the exported protein PTP1 causes severe alterations in the architecture of MC's and this affects the display of PfEMP1 on the RBC surface (Rug *et al.*, 2014). However, none of the previous studies were performed in cells where PfEMP1 were endogenously tagged and the antigenic variation of PfEMP1 makes it uncertain whether the gene being expressed is always the same.

The PfEMP1-3xHA cell line described in this work and developed using SLI, manages to overcome these problems, by retaining the expression of the same *var* gene through the pressure of the G418 drug selection. Furthermore, it avoids antibody specificity problems, as the full length PfEMP1 is tagged with an epitope tag, which to our knowledge has not previously been achieved.

In order to analyze the effect of disrupting proteins potentially involved on PfEMP1-3xHA, a new type of SLI vector (SLI2) was created to be able to disrupt such proteins (e.g. SBP1 and PTP1) by TGD in the PfEMP1-3xHA cell line that was established using the previous SLI plasmid configuration (Birnbaum et al., 2017), (henceforth termed SLI1 to distinguish from SLI2). The original SLI vector contains a WR episomal selection marker and a NeoR cassette for the selection of integrant cell lines. Those markers were replaced by BSD and *yDHODH* that provide resistance to Blasticidin-S and DSM1, respectively. Two strategies were employed, one uses BSD for episomal and DSM1 for integrant selection (pSLI2a), and one that uses DSM1 for episomal and BSD for integrant selection (pSLI2b) (Figure 21).

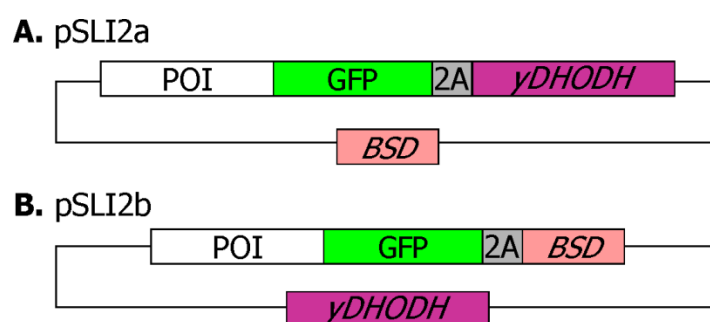


Figure 21: Schematic of pSLI2a and pSLI2b vectors

Schematic of the pSLI2 plasmids generated producing double integrant cell lines. **A.** pSLI2a with *BSD* (episomal) and *yDHODH* (integration) selection markers **B.** pSLI2b with *yDHODH* (episomal) and *BSD* (integration) selection markers. POI: protein of interest; GFP: green fluorescent protein; 2A: skip peptide. *yDHODH*: gene conferring resistance to DSM1; *BSD*: gene conferring resistance to BSD.

Both designed vectors were tested. In order to do this, a sequence to mediate disruption of *ptp1* was inserted into the new vectors and both were transfected into the PfEMP1-3XHA^{endo} cell line. Parasites containing the episomal plasmid appeared after 2 weeks in culture under pressure of both BSD and G418. After having the parasites growing with the episomal plasmid, drug pressure was applied using DSM1 to select parasites containing (PTP1-TGD-GFP and PfEMP1-3xHA) integrated into the genome. Parasites containing the pSLI2a plasmid appeared in the culture 5 weeks after the transfection and the parasites containing the pSLI2b appeared 6 weeks after the transfection. Both cell lines were phenotypically identical, but as the

transfectants containing the pSLI2a appeared first, this plasmid was chosen for further experiments.

3.2.1.1 Double integrant: PTP1-TGD in a PfEMP1-3xHA^{endo} cell line

The construct PTP1-TGD-GFP (Figure 22 A) was transfected in the PfEMP1-3xHA cell line and parasites containing the episomal plasmid were selected using BSD. After the episomal selection, the parasites containing the episomal plasmid, DSM1 pressure was applied to select for the parasites containing the endogenously 3xHA tagged PfEMP1 (Figure 22 B). This double integrant cell line was named PfEMP1-3xHA^{endo}+PTP1-TGD-GFP^{endo} and the integration process took 10 weeks since the transfection until the confirmation of the correct integration on the genome of both plasmids (PfEMP1-3xHA and PTP1-TGD-GFP).

Live images of the PfEMP1-3xHA^{endo}+PTP1-TGD-GFP^{endo} cell line showed a faint cytosolic GFP signal (Figure 22 C) as observed often when proteins are disrupted. This indicated complete inactivation of PTP1. To further evaluate if the inactivation of PTP1 had an effect on PfEMP1 exposure on the iRBC surface, a protection trypsin assay was performed. In the non-treated culture, PfEMP1 is intact, migrating at its expected size of 201 kDa, whereas in the trypsin treated culture the protected fragment of PfEMP1 containing the ATM, the TMD and the 3xHA appears as band migrating around 80 KDa (Figure 22 D), corresponding with the previously reported size for the protected fragment of PfEMP1 after trypsinization (See section 3.2.1).

Western blots were performed in order to identify the constructs in the parental cell line (PfEMP1-3xHA^{endo}) and in the PfEMP1-3xHA^{endo}+PTP1-TGD-GFP^{endo}. The HA tag was detected in both corresponding to PfEMP1, and in the double integrant just GFP was detected confirming the expression of both tagged proteins in the PfEMP1-3xHA^{endo}+PTP1-TGD-GFP^{endo} parasites. Aldolase was used as a loading control (Figure 22 E). Finally, an IFA to detect PfEMP1 and PTP1 in the PfEMP1-3xHA^{endo}+PTP1-TGD-GFP^{endo} cell line was performed. As observed in live images, PTP1 is dispersed around the parasite cytosol with no foci apparent, PfEMP1 was detected using α -HA antibodies being normally exported to MCs (Figure 22 F).

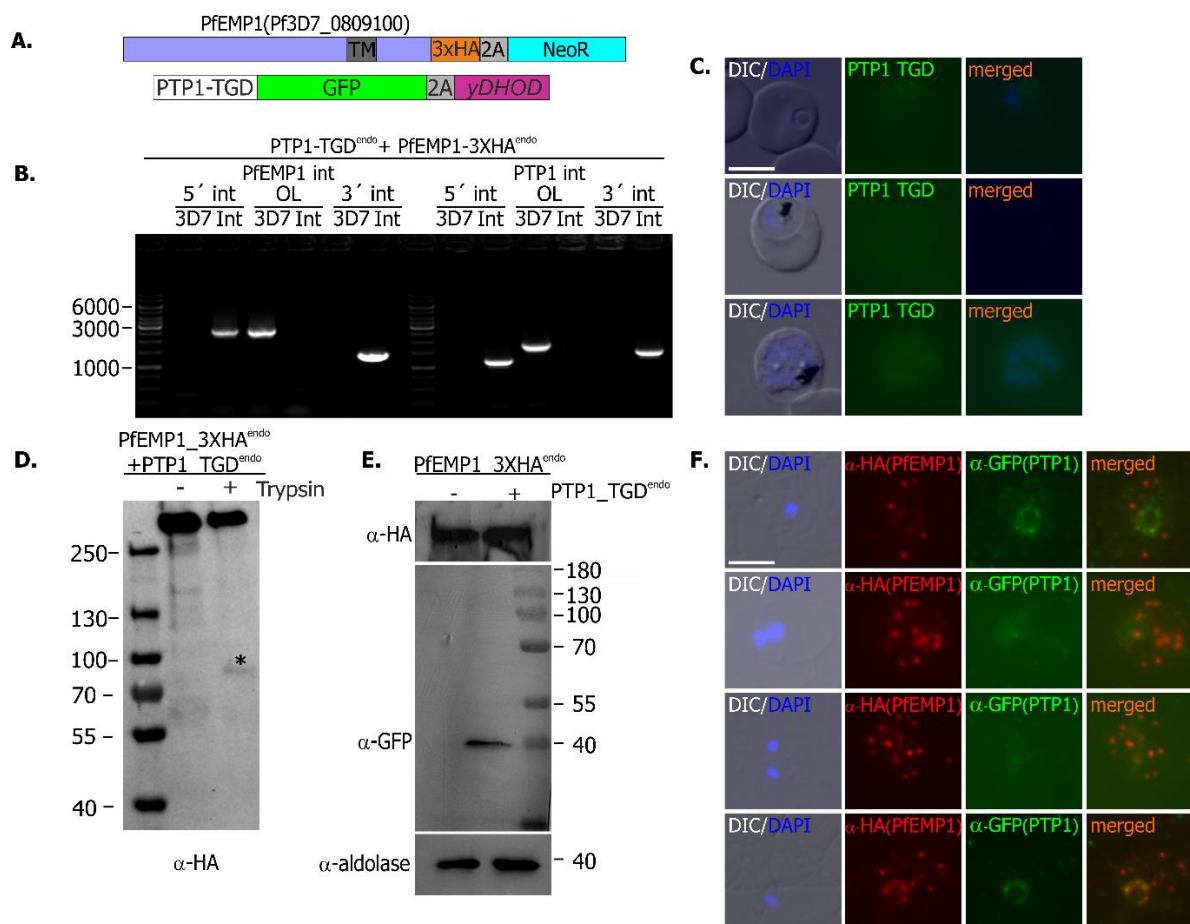


Figure 22: Characterization of the double integrant cell line PfEMP1-3xHA^{endo} + PTP1-TGD-GFP^{endo}

A. Schematic of the expressed construct in the parental cell line (PfEMP1-3xHA^{endo}) and the transfected construct containing a sequence for disruption of PTP1 and a GFP tag, a skip peptide (2A) and a DSM1 resistance cassette (*γDHODH*). **B.** Agarose gels with PCR products from gDNA of the double integrant cell line expressing PfEMP1-3xHA^{endo}+PTP1-TGD-GFP^{endo} confirming the correct integration of PfEMP1-3xHA (left) and PTP-TGD-GFP (right) into the genome. (int, integration parasite line; 3D7, untransfected parent cell line; 5' int, PCR product crossing the 5' integration junction; 3' int, PCR product crossing the 3' integration junction; the marker is indicated in kbp). **C.** Live cell fluorescence microscopy images of the PfEMP1-3xHA^{endo}+PTP1-TGD-GFP^{endo} cell line. Different development stages of the parasite from rings (top) to schizont (bottom). **D.** Western Blot of protection trypsin assay probed with α -HA antibodies of the PfEMP1-3xHA^{endo}+PTP1-TGD-GFP^{endo} cell line. The untreated cell line shows a non-digested fragment corresponding to PfEMP1-3xHA migrating at 201 kDa. The trypsin treated culture shows a protected fragment around 80 kDa (asterisk). **E.** Western Blot performed with proteins extracted from the parental PfEMP1-3xHA^{endo} and from PfEMP1-3xHA^{endo}+PTP1-TGD-GFP^{endo} cell lines, showing a band migrating at 201 kDa representing the PfEMP1-3xHA^{endo} tagged in both samples (α -HA), a band at 42,3 kDa corresponding to the size of the disrupted PTP1 plus GFP tag (α -GFP). Aldolase was used as a loading marker (α -aldolase) (39,33 kDa). The markers are shown in kDa. **F.** IFA of PfEMP1-3xHA^{endo}+PTP1-TGD-GFP^{endo} parasites detecting PfEMP1-3xHA^{endo} with α -HA antibodies (red) and PTP1-TGD-GFP^{endo} with α -GFP (green). DIC: Differential interference contrast. The nuclei were stained with DAPI. Scale bars: 5 μ M.

3.2.1.2 Attempts to double integrate: SBP1-TGD in a PfEMP1-3xHA^{endo} cell line

Several attempts to integrate SBP1-TGD into PfEMP1-3xHA cell line were made (PfEMP1-3xHA^{endo}+SBP1-TGD-GFP^{endo}) (Figure 23 A, Table S1). However, there is apparently

incompatibility between the disruption of SBP1 and the correct expression of the PfEMP1 encoded by the *var* gene PF3D7_0809100. The parental cell line containing the episomal plasmid SBP1-TGD-GFP to disrupt *sbp1* using SLI2 showed a correct integration of the original PfEMP1-3xHA (Figure 23 B). Nevertheless, when the parasites were brought under DSM1 pressure to select for integration of the SBP1-TGD-GFP plasmid, the integrants did not appear in culture or when they did, the PfEMP1-3xHA integration was reverted, with only original locus remaining in 5 out of 5 attempts (Figure 23 C).

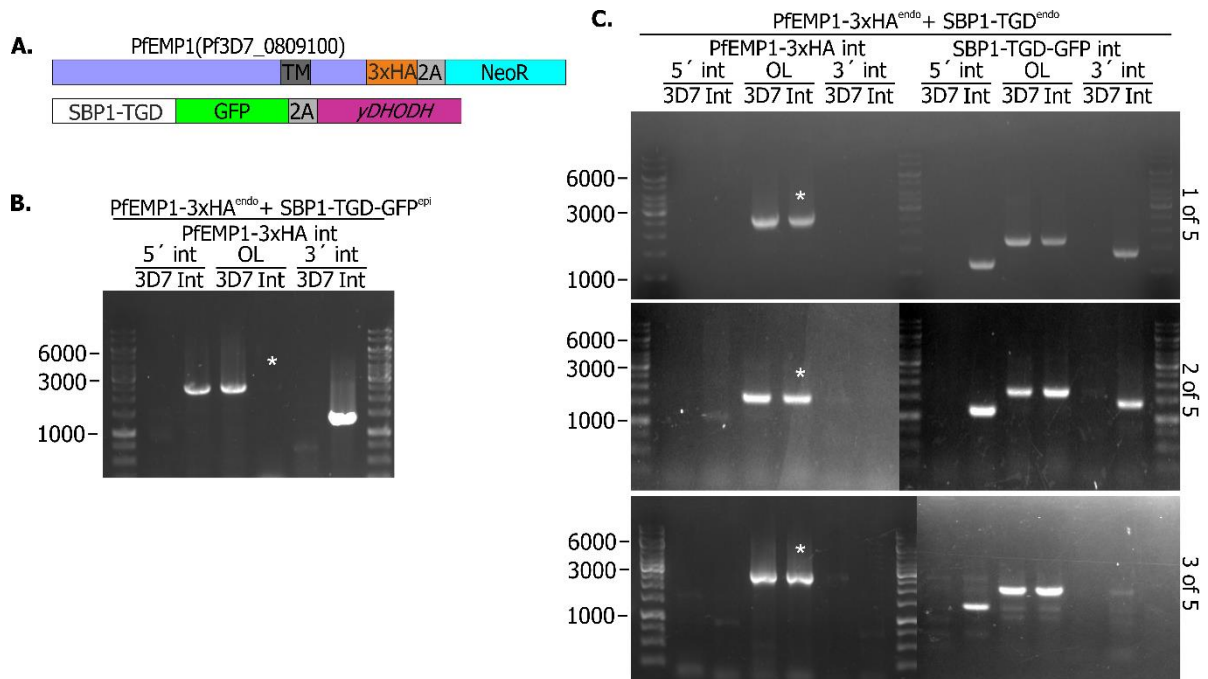


Figure 23: Attempt to integrate SBP1-TGD-GFP in PfEMP1-3xHA^{endo} cell line

A. Schematic of the expressed construct in the parental cell line (PfEMP1-3xHA^{endo}) and the transfected construct containing a sequence for disruption of SBP1 and a GFP tag, a skip peptide (2A) and a DSM1 resistance cassette (*yDHODH*). **B.** Agarose gels with PCR products from gDNA of the double transfectant cell line PfEMP1-3xHA^{endo}+SBP1-TGD-GFP^{epi} confirming the correct integration of PfEMP1-3xHA before the integration attempts. (Int, integration of PfEMP1-3xHA^{endo}; 3D7, untransfected parent cell line; 5' int, PCR product crossing the 5' integration junction; 3' int, PCR product crossing the 3' integration junction; the marker is indicated in kbp). **C.** Agarose gels with PCR products from gDNA of the PfEMP1-3xHA^{endo}+SBP1-TGD-GFP^{epi} cell lines after integration attempt. Left, PfEMP1-3xHA integration diagnostic PCR with no bands detected in the 5' int or 3' int and a band detected in the OL showing that the integration was reverted. Right, SBP1-TGD-GFP integration diagnostic PCR with cells containing remnant of OL. Asterisk: OL of PfEMP1 absent in the parental episomal cell line, present in the parasites after SBP1-TGD-GFP integration attempts. Representative pictures of agarose gels of five reverted PfEMP1-3xHA^{endo}+SBP1-TGD-GFP^{epi} cell lines. The markers are shown in kbp.

3.2.2 Implications of blocking PTEX in the PfEMP1 transport

The export of SBP1 starts early after merozoite invasion, and after 4 to 6 hpi is already detectable in the iRBC (Gruing *et al.*, 2011). In contrast PfEMP1 is first observed at the parasite surface from 8 to 11 hpi and reaches the MCs around 16 hpi (McMillan *et al.*, 2013;

Kriek *et al.*, 2003). SBP1 has been shown to be essential for PfEMP1 export as deletion of SBP1 prevented export of PfEMP1 to the erythrocyte membrane (Cooke *et al.*, 2006; Maier *et al.*, 2007). To the date, the PfEMP1 was not endogenously tagged before, and there is no record of both proteins being endogenously tagged in the same cell line. The attempts to arrest the PfEMP1-mDHFR fusion on its way to the MCs has been unsuccessful (Mesén-Ramírez personal communication). It was not possible to arrest PfEMP1 probably because this protein contains a very large C-terminus after the TM, and it was shown that the arrest of an exported protein depends on the length of the region between the mDHFR and the TM domain. This region is called the “spacer” (Mesén-Ramírez *et al.*, 2016) and in cases where the spacer is large the translocation occur by transient interaction of the PPM and PVM translocon which might be a reason for the reduced susceptibility to the mDHFR-mediated arrest (Mesén-Ramírez *et al.*, 2016).

Contrasting to what happens with the PfEMP1-mDHFR construct, in section 3.1.1 it was demonstrated that a SBP1-mDHFR-L-BirA*-3xHA construct can be conditionally arrested in the PTEX when WR is present. It is necessary to analyze this arrest from different perspectives: first SBP1 is directly responsible for the correct trafficking of PfEMP1, therefore its malfunctioning leads to failures in the export of PfEMP1 (Cooke *et al.*, 2006; Maier *et al.*, 2007). Second, in the event that PTEX is also used by PfEMP1 as a carrier, its clogging (caused by the SBP1-mDHFR construct) will cause PfEMP1 to remain co-blocked in the PV region and third, the blocking of PTEX also causes all exported proteins to co-block (Mesén-Ramírez *et al.*, 2016). Therefore the transport of PfEMP1 and also of proteins such as PTP1, REX1, MAHRP and KAHRP that are necessary for the correct formation of MCs and knobs will not be able to fulfill their function and the transport and exposure of PfEMP1 will also be affected.

Consequently, an experiment was designed to discern the variables described above. The export times of SBP1 (2 to 6 hpi) and PfEMP1 (appears on parasite surface from 8 to 11 hpi) were considered. The translocon was blocked at 0 hpi and at 18 hpi (Figure 24). In the control (-WR) the mDHFR domain is unfolded, permitting the normal transport of SBP1 to the MCs, also with no impediment for the normal export of PfEMP1. In this case SBP1 and PfEMP1 should co-localize at the MCs. When WR is added at the moment of the invasion (0 hpi), the folding of the mDHFR domain impedes the cross of the construct SBP1-mDHFR-GFP through the PTEX since the beginning of the cycle, hampering the export of PfEMP1, in this case the signal of both proteins should localize in the PV and PVM region. In contrast, when WR is added later on the cycle (18 hpi) the majority of exported proteins including the construct

SBP1-mDHFR-GFP and PfEMP1 would be already distributed on the MCs. The GFP signal corresponding to SBP1-mDHFR-GFP will present a mix phenotype with the SBP1 protein produced earlier on the cycle being normally exported to the MCs and a smaller amount of protein produced later being arrested in PVM. Here however, PfEMP1 should be detected on the MCs because there was enough time for the exported proteins to reach the MCs, thus confirming that the arresting of PfEMP1 was due to the SBP1-mDHFR-GFP jammed in the PTEX and not due to external factors.

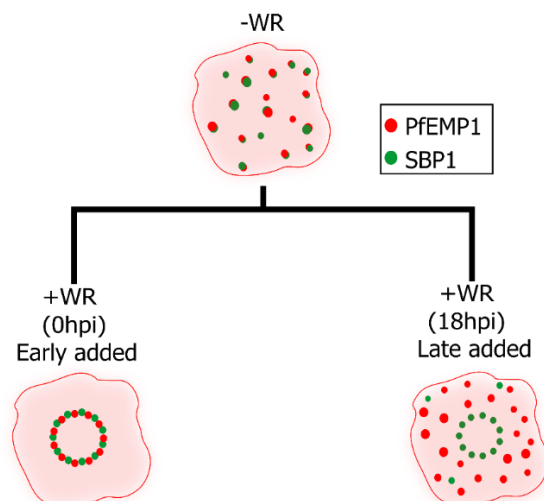


Figure 24: Model of SBP1-mDHFR-GFP conditionally arrested in PTEX and its effect on PfEMP1 export

Scheme showing the phenotypes of the PfEMP1-3xHA+SBP1-TGD-GFP expressing parasites. After 24 hpi, parasites in absence of WR should export both proteins PfEMP1 (red) and SBP1 (green) to the MCs. When WR is added early in the cycle (0 hpi) SBP1 is arrested in PTEX causing the retention of PfEMP1 in the PV region and showing colocalization of both signals. When WR is added later in the cycle (18 hpi), PfEMP1 is exported and SBP1 shows a mix phenotype with protein exported and protein arrested in the PTEX.

For the previously described schema (Figure 24), two cell lines were designed. In one, PfEMP1-3xHA^{endo} was transfected with a construct containing an early promoter (mal7, Grüring *et al.*, 2011) controlling expression of SBP1-mDHFR-GFP, and this construct was expressed episomally (see Section 3.2.2.1). For the other cell line, the parasites containing the genomic PfEMP1-3xHA were transfected with the SLI2 vector (Figure 21) for expressing endogenously the construct SBP1-mDHFR-GFP-2A-yDHODH (see Section 3.2.2.2). The cell line episomally expressing SBP-mDHFR-GFP is also expressing the native SBP1. In this case, when the parasite is incubated with WR, the SBP1-mDHFR-GFP construct would get arrested in the translocon while the endogenous SBP1 could eventually be exported. In the case of the integrant cell line, all the SBP1 produced will contain the mDHFR-GFP domains attached to it.

3.2.2.1 Mal7-SBP1-mDHFR-GFP transfected in PfEMP1-3xHA^{endo}

The sequence encoding SBP1-mDHFR-GFP was cloned into the pARL1 vector and expressed under the early Mal7 promoter (Gruring *et al.*, 2011). This plasmid was transfected into the PfEMP1-3xHA^{endo} cell line (Figure 25 A). After the appearance of fluorescent parasites carrying the episomal plasmid Mal7-SBP1-mDHFR-GFP, gDNA was extracted and a diagnostic PCR to assess correct integration of the plasmid into the genome was performed in order to exclude reversion of the plasmid to endogenously tag PfEMP1 with 3xHA (Figure 25 B). When observed with the fluorescence microscope, the cells showed a punctuated signal at the MCs corresponding with the expected phenotype for SBP1 in young rings stages (from 4 hpi GFP signal was detectable) (Figure 25 C top). When 10 nM WR was added to the culture, the parasite showed around the parasite, suggesting that Mal7-SBP1-mDHFR-GFP was arrested in the PTEX (Figure 25 C bottom).

To identify the effect on PfEMP1 due to arresting SBP1 in PTEX, parasites were cultured with or without 10 nM WR at the moment of merozoite invasion (0 hpi) or at the end of the ring stage (18 hpi) after which most of the endogenous SBP1 is presumed to have already been exported, but also including the unfolded construct SBP1-mDHFR-GFP. IFAs were performed after 20 to 24 hpi and the Mal7-SBP1-mDHFR-GFP construct was detected with α -SBP1 (green) and PfEMP1-3xHA was detected with α -HA (red). The control cells showed the expected phenotype with both proteins localizing at MCs (Figure 25 D top). When WR was added at 0 hpi, Mal7-SBP1-mDHFR-GFP remained arrested in PTEX, causing a block of PfEMP1-3xHA^{endo} export and evidenced as an overlapping signal in the PV region (Figure 25 D middle).

To confirm that the arrest of PfEMP1 in the PV region was indeed due to the clogging of PTEX by the Mal7-SBP1-mDHFR-GFP construct (i.e. a co-block as defined previously Mesén-Ramirez *et al.*, 2016), 10 nM WR was added late in the cycle (18 hpi) when most exported proteins were already in the iRBC cytosol. In that case PfEMP1-3xHA^{endo} was exported normally to the MCs, contrasting with the Mal7-SBP1-mDHFR-GFP^{epi} construct that remained arrested in PTEX (Figure 25 D bottom). The IFAs phenotypes were scored using the fluorescence microscope to calculate the percentage of cells that showed a PfEMP1 export phenotype when SBP1 was exported, early arrested or late arrested (Figure 25 E).

Episomally expressed SBP1-mDFR-GFP is expressed from multiple plasmid copies, leading to high expression levels whereas the endogenous SBP1 is produced normally and it can be transported without any interference to the MCs before the translocon is conditionally blocked.

Arresting SBP1-mDHFR-GFP early in the cycle (Figure 25 C middle) led to a jam in the translocon and a co-block of all the transported proteins (including PfEMP1-3xHA and the endogenous SBP1) and this is observable as a co-localizing signal of both red and green signals corresponding to PfEMP1 and SBP1-mDHFR-GFP, respectively. Yet, when WR was added later, the PfEMP1 signal localizes at the MCs whereas the SBP1 signal shows a mix phenotype with arrested and exported protein. The signal of SBP1 in the host cell corresponds not just to the SBP1-mDHFR-GFP construct that was exported before the jamming of the translocon, but it also reflects the endogenous SBP1 produced by the cell. The SBP1 signal around the PVM represents the arrested construct in PTEX. The signal of PfEMP1 at the MCs could indicate that PfEMP1 is not passing through the PTEX translocon or that the endogenous SBP1 exported during the first 18 hpi was sufficient to transport some PfEMP1 to the MCs (Figure 25 C bottom).

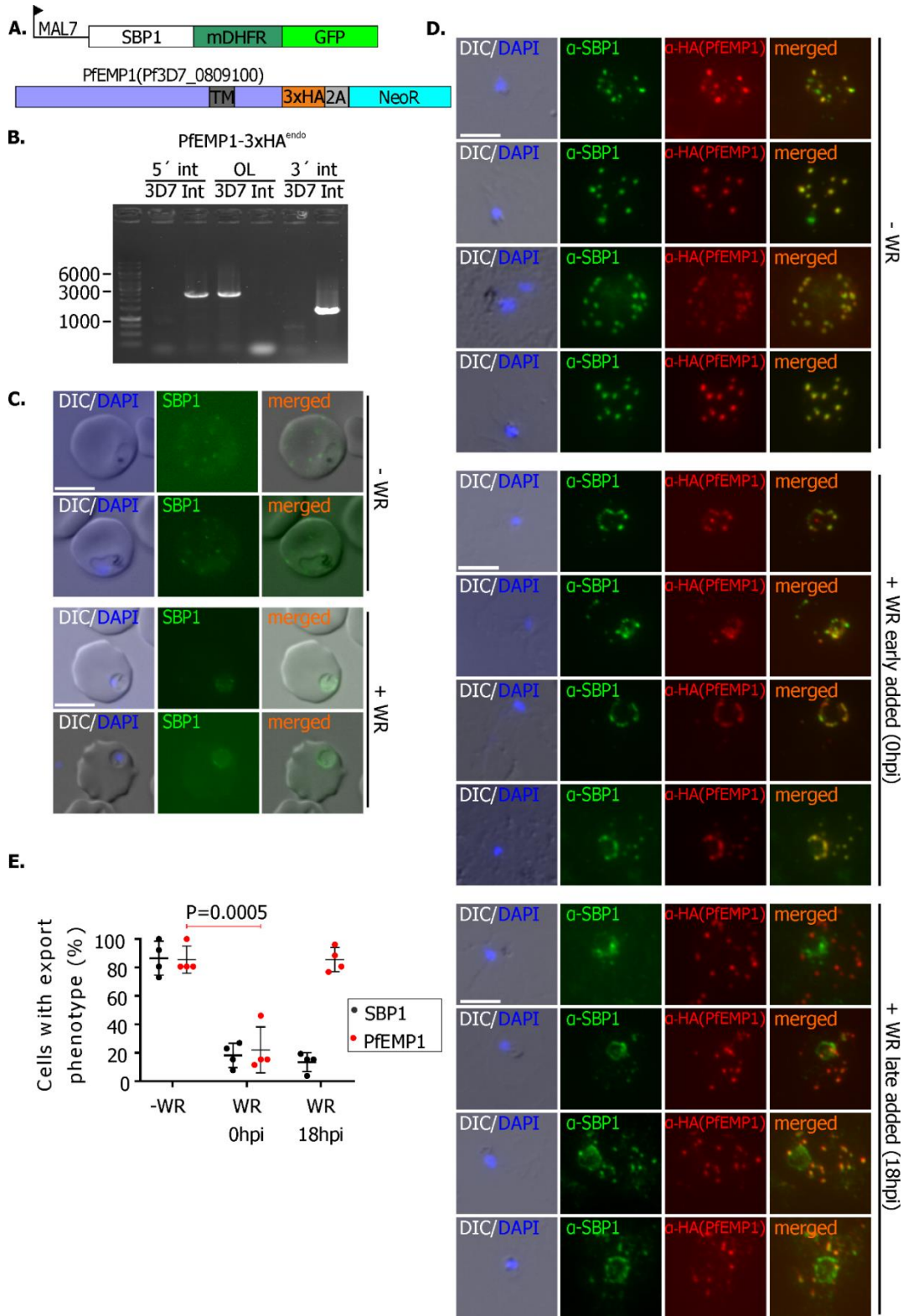


Figure 25: Characterization of the double transfectant cell line PfEMP1-3xHA^{endo} +Mal7-SBP1-mDHFR-GFP^{epi}

A. Schematic of a construct containing a sequence to episomally express Mal7-SBP1-mDHFR-GFP transfected in the parental cell line PfEMP1-3xHA^{endo}. **B.** Agarose gels with PCR products from gDNA of the cell line expressing PfEMP1-3xHA^{endo}+Mal7-SBP1-mDHFR-GFP^{epi}, confirming the maintained correct integration of PfEMP1-3xHA^{endo} into the genome. (int, integration parasite line; 3D7, untransfected parent cell line; 5' int, PCR product crossing the 5' integration junction; 3' int, PCR product crossing the 3' integration junction; the marker is indicated in kbp). **C.** Live cell fluorescence microscopy images of PfEMP1-3xHA^{endo}+Mal7-SBP1-mDHFR-GFP^{epi} parasites non-

treated (top) or treated with 10 nM WR (bottom). **D.** Fluorescence images of IFAs of acetone fixed PfEMP1-3xHA^{endo}+SBP1-mDHFR-GFP^{endo} parasites when incubated without (top) or with 10 nM WR at 0 hpi (middle) or at 18 hpi (bottom). Mal7-SBP1-mDHFR-GFP^{epi} was detected with α -SBP1 (green) and PfEMP1-3xHA^{endo} was detected with α -HA (red). **E.** Quantification of protein export of PfEMP1 when Mal7-SBP1-mDHFR-GFP^{epi} is arrested or exported. Data obtained by scoring the export phenotype of cells in IFAs under the fluorescence microscope when the culture was incubated without WR or with 10 nM WR at 0 hpi or 18 hpi. Four biological replicas were performed (n=26 cells per condition), dots represent the mean of each replica. (Unpaired T-test). Means of the replicas are represented as the central horizontal lines. DIC: Differential interference contrast. The nuclei were stained with DAPI. Scale bars: 5 μ M.

3.2.2.2 Double integrant: SBP1-mDHFR-GFP in a PfEMP1-3xHA^{endo} cell line

A sequence of SBP1-mDHFR was inserted into a pSLI2a vector that contained a GFP tag, a skip peptide and a yDHODH resistance cassette (Figure 26 A). This plasmid was transfected into the PfEMP1-3xHA^{endo} cell line and after 3 weeks of BSD pressure, double transfectants appeared in culture. Those transfectants were selected for parasites where the plasmid was integrated into the genome using DSM1. Finally, 5 weeks after the transfection, the SBP1-mDHFR-GFP^{endo}+PfEMP1-3xHA^{endo} parasites appeared in culture. gDNA was extracted and the correct integration of both constructs was verified through integration diagnostic PCR (Figure 26 B). Differently from the cell line described above, where SBP1 was expressed episomally (Section 3.2.2.2), all SBP1 expressed in this double-integrated cell line would contain an attached mDHFR-GFP domain.

When observed with the fluorescence microscope the cells showed a punctuated signal in the MCs corresponding to the expected phenotype for SBP1 (Figure 26 C top). When 10 nM WR was added to the culture, the parasites showed signal around the PV area corresponding to the SBP1-mDHFR-GFP arrested in PTEX (Figure 26 C bottom).

Western blots were performed in order to identify the constructs in the parental PfEMP1-3xHA^{endo} and in the PfEMP1-3xHA^{endo}+SBP1-mDHFR-GFP^{endo} expressing cell lines. PfEMP1 was detected using α -HA in both the parental and the double integrant cell lines. Using α -GFP, SBP1-mDHFR-GFP^{endo} (86 kDa) was detected migrating around 100 kDa. As previously reported for plasmodium proteins (Cowman *et al.*, 1984), SBP1 migrates considerably higher than its actual molecular weight. Aldolase was used as a loading control and detected with α -aldolase, which migrates at 39 kDa (Figure 26 D)

The rationale for creating the SBP1-mDHFR-GFP cell line was that SBP1 itself influences PfEMP1 export, but depending on the publication, this is either at the MCs (Cooke *et al.*, 2006) or in the parasite periphery (Maier *et al.*, 2007). If the latter is correct, ablation of SBP1 would result in the same phenotype as a co-block of PfEMP1. However, in the episomal SBP1 co-

blocking parasite line, this should not be less the case, as a functional copy of SBP1 still exists in the parasite, although arresting this protein in PTEX should lead to a co-block of all exported proteins and hence the different times for induction of the co-block. To assess if the function of SBP1 itself influenced this result, the experiment was here repeated using endogenously mDHFR tagged SBP1 to induce the co-block. Parasites were incubated without and with 10 nM WR at the moment of the invasion (0 hpi) or later in the cycle (18 hpi) when the majority of exported proteins were already exported. IFAs were performed with parasites from the three conditions. In absence of WR, both SBP1 (green) and PfEMP1 (red) were normally exported to the iRBC, showing a punctuated phenotype on the MCs (Figure 26 E top and F). When 10 nM WR was added at the moment of invasion, SBP1 was arrested in PTEX, producing also an arrest of PfEMP1, and showing a phenotype where both antibodies α -SBP1 (green) and α -HA (red) signals colocalize at the PV (Figure 26 E center and F). Finally, to identify if the arrest of PfEMP1 was indeed produced by the jamming of PTEX, the SBP1-mDHFR-GFP construct was arrested 18 hpi, when most exported proteins were already at the iRBC surface (including SBP1-mDFR-GFP). It is important to stress that in this cell line, all the SBP1 produced contains the mDHFR-GFP domains, so compared to the episomal cell line, there is no native SBP1 to aid with the PfEMP1 trafficking. After adding WR late on the cycle, the PfEMP1 signal was detected in the MCs (red) with no observable arrest in export, showing that on the other hand, SBP1 (green) showed a mixed phenotype, with signal both arrested and exported (Figure 26 E bottom and F).

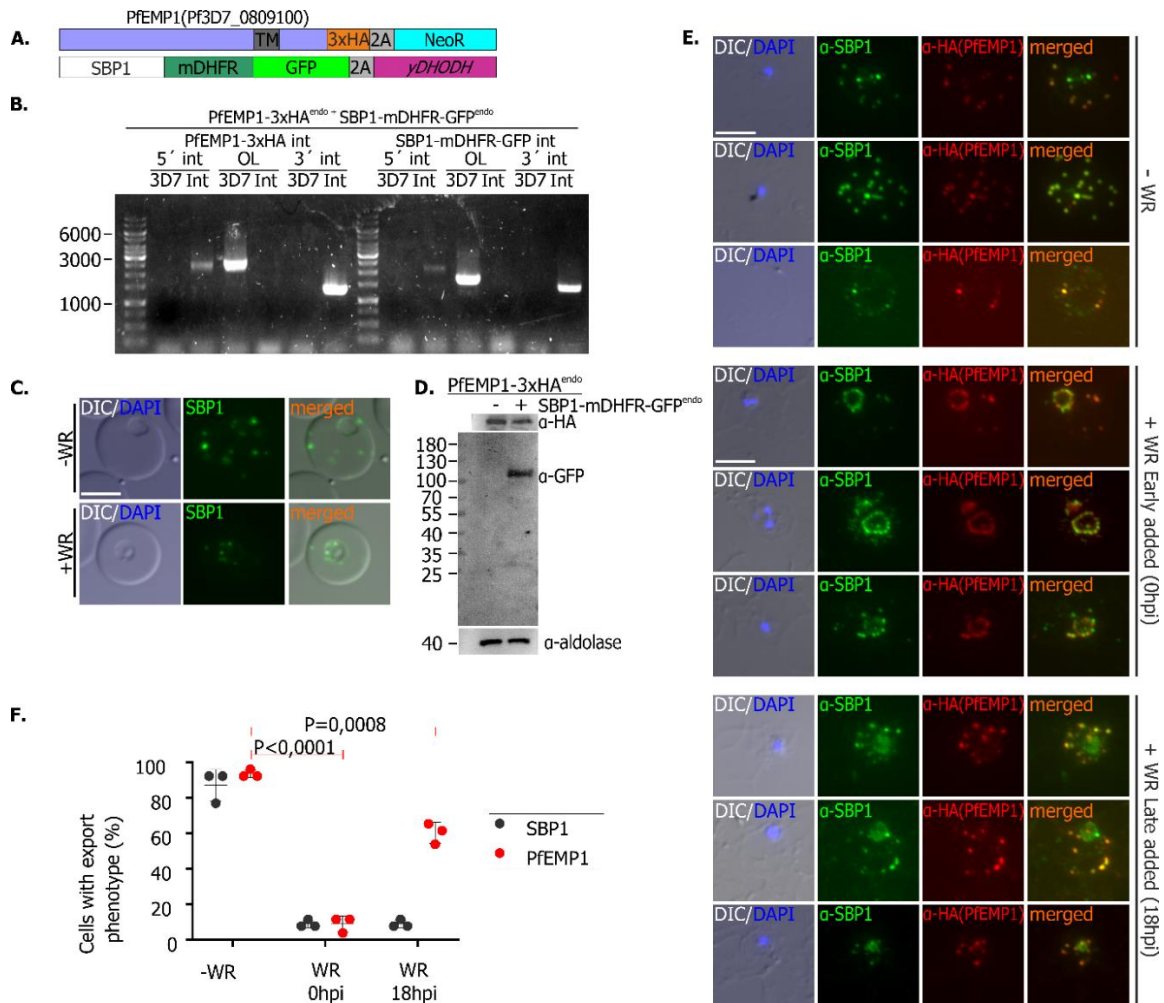


Figure 26: Characterization of the double integrant cell line PfEMP1-3xHA^{endo}+ SBP1-mDHFR-GFP^{endo}

A. Schematic of the parental cell line (PfEMP1-3xHA^{endo}) and the transfected construct with a plasmid containing a sequence to endogenously tag SBP1 with an mDHFR-GFP tag. A skip peptide (2A) and a DSM1 resistance cassette (*yDHODH*). **B.** Agarose gels with PCR products from gDNA of the double integrant cell line expressing PfEMP1-3xHA^{endo}+SBP1-mDHFR-GFP^{endo} confirming the correct integration of PfEMP1-3xHA (left) and SBP1-mDHFR-GFP (right) into the genome. (int, integration parasite line; 3D7, untransfected parent cell line; 5' int, PCR product crossing the 5' integration junction; 3' int, PCR product crossing the 3' integration junction; the marker is indicated in kbp). **C.** Live cell fluorescence microscopy images of PfEMP1-3xHA^{endo}+SBP1-mDHFR-GFP^{endo} expressing parasites not treated (top) or treated with 10 nM WR (bottom). **D.** Western Blot performed with protein extracts derived from the parental PfEMP1-3xHA^{endo} and from PfEMP1-3xHA^{endo}+SBP1-mDHFR-GFP^{endo} cell lines, showing a band migrating around the calculated size of 201 kDa that represents the endogenously 3xHA tagged PfEMP1 (α -HA), and a band around 86 kDa corresponding to the size of SBP1-mDHFR-GFP (α -GFP). As previously reported for plasmodium proteins (Cowman *et al.*, 1984) SBP1 ran higher than its actual molecular weight. Aldolase was used as a loading control (calculated MW of 39.3 kDa). The markers are shown in kDa. **E.** Fluorescence images of IFAs of acetone fixed PfEMP1-3xHA^{endo}+SBP1-mDHFR-GFP^{endo} parasites when incubated without (top) or with 10 nM WR at 0 hpi (middle) or at 18 hpi (bottom). SBP1-mDHFR-GFP^{endo} was detected with α -SBP1 (green) and PfEMP1-3xHA^{endo} was detected with α -HA (red). **F.** Quantification of PfEMP1 export when SBP1-mDHFR-GFP^{endo} is arrested or exported. Acetone fixed IFAs were observed under the fluorescence microscope when the culture was incubated without WR or with 10 nM WR at 0 hpi or 18 hpi. Four independent experiments were performed (Unpaired T-test). Dots represents the mean of each experiment (n=26 cells per condition). Means of the replicas are represented as the central horizontal lines. Data obtained by counting cells where PfEMP1 (red

dots) and SBP1 (black dots) were arrested or exported. “Arrested” were cells where clearly the protein localizes in the PV region and “Exported” were counted as cells where the protein localizes in the iRBC surface or with a mix between PV and iRBC surface regions. DIC: Differential interference contrast. The nuclei were stained with DAPI. Scale bars: 5 μ M.

4 Discussion

For proliferation within the erythrocytes, the malaria parasite *P. falciparum* needs to extensively modify its surrounding host cell. To achieve this, the parasite is predicted to export around 550 different kinds of proteins into the host cell (Maier *et al.*, 2009). These exported proteins are known as the exportome and are classified into two groups. The larger group comprises proteins with a five-amino-acid motif (RxLxE/Q/D) named the 'Plasmodium export element' (PEXEL). The second, smaller group of exported proteins are the PEXEL-negative exported proteins (PNEPs) (Spielmann and Gilberger, 2015).

The exportome of *P. falciparum* is predicted to be 5 to 10 times larger than other *Plasmodium* exportomes (Miller *et al.*, 2002). This great difference has been explained with two hypotheses. One is that, this difference comes in response of the necessity of *P. falciparum* for export an unique protein responsible for the adhesion to the epithelial cells (Su *et al.*, 1995) and virulence of the parasite: The *Plasmodium falciparum* erythrocyte membrane protein 1 (PfEMP1). However, it was also demonstrated that despite the absence of PfEMP1 in other *Plasmodium* species, the machinery for transport and assembling proteins in the parasite surface is conserved within human and rodent malaria (De Niz *et al.*, 2016). Another possible explanation to the great difference in exportomes sizes is that PEXEL and PNEPs proteins in other *Plasmodium* species are less well recognized (Haase and de Koning-Ward, 2010), rendering it more difficult to accurately determine the size of their exportomes.

Protein export is a well described process in *Plasmodium*, it starts with the entry of the protein into the parasite's ER, after which it follows a vesicular pathway towards the parasite boundary involving classical secretory components. At the parasite boundary, the exported protein needs to pass across two membranes, the PPM and the PVM. The PVM contains the PTEX, a translocon that is the responsible for the passage of all known types of exported proteins into the host cell, including both soluble and TM proteins as well as PEXEL and PNEPs (Spielmann and Gilberger, 2015). In the case of soluble proteins, the protein is transported within a vesicle and these vesicles coming from the ER-Golgi route fuse with the PPM, releasing its content directly into the PV. However, for proteins containing a TMD, the protein travels integral to the vesicle membrane (Deponte *et al.*, 2012) and after the vesicle fuses with the PPM, the protein remains embedded in this membrane.

The mechanism of how proteins with TMDs are extracted from the PPM to become substrates of PTEX is still unclear. It was shown that TM proteins are embedded in the membrane of the

ER, and later are integral in the PPM after the vesicle fusion. In principle the TM proteins could continue their way in vesicles from the PPM to the PVM for later becoming substrates of the PTEX (Spielmann and Gilberger, 2015). Nevertheless, this seems not very likely since it was shown that TM proteins containing an mDHFR domain, resulted in an arrest of these proteins in the PPM, not the PVM, when mDHFR unfolding was prevented (Gruring *et al.*, 2012). These findings suggested that these proteins have their N-terminus facing the PV lumen. The constructs containing a TM protein and an mDHFR domain are inserted into the membrane at the ER but also were found to be partially soluble once they reached the host cell cytosol (Gruring *et al.*, 2012). This solubility shift led to the hypothesis of membrane extractors being involved during the export process.

Based on these findings, three scenarios explaining how the TM proteins are extracted out of the PPM were proposed (Figure 27) (Spielmann and Gilberger, 2015). The first option is that there is an active extractor that contributes to the extraction from the PPM (Figure 27-1). The second option could be the contribution of factors like chaperons that assist the pulling out of proteins from the PPM by other proteins (Figure 27-2). The third option is that PPM located proteins do not contribute to the extraction at all (Figure 27-3). At the PVM the role of PTEX as a translocon has been demonstrated (Mesén-Ramírez *et al.*, 2016; Elsworth *et al.*, 2014; Beck *et al.*, 2014) and here three scenarios were also postulated. The first of them is that PTEX receives the TM proteins that are already present in the PV (Figure 27-A), the second scenario is that the dissociation of PTEX (e.g. HPS101) helps with the extraction, binding to the protein in the PPM and carrying it back when reassignment with PTEX (Figure 27-B) and finally that the entire PTEX connects with the PPM or with factors in the PPM, contributing to pull the TM protein out of the membrane (Figure 27-C). Those descriptions of how the proteins are extracted from the PPM and recruited to PTEX at the PVM are not mutually exclusive and could be combined (e.g. no extractor in PPM (3) and the dissociation of PTEX (b) could happen simultaneously).

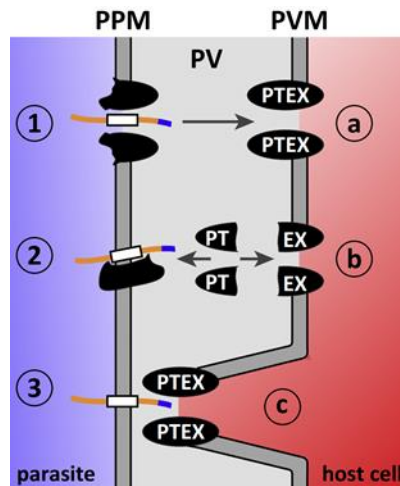


Figure 27: Model of protein translocation scenarios at the PPM and PVM.
 Extracted from (Spielmann and Gilberger, 2015).

Understanding how TM proteins are extracted is of great importance since blocking this pathway could be a therapeutic target. Especially because the major virulence factor of *P. falciparum* is PfEMP1, a TM protein with great importance in the pathogenesis of malaria infections. Despite its great importance and despite the large amount of information accumulated about its function and transport, the molecular basis of PfEMP1 export from the parasitophorous vacuole to the host cell surface is still poorly understood (Charpian and Przyborski, 2008). An mDHFR-3xHA domain was successfully fused to the PfEMP1, yet it was not possible to arrest the PfEMP1-mDHFR-3xHA construct on its way to the MCs (cloning and experiments performed by Mesén-Ramirez). The impossibility to arrest the PfEMP1-mDHFR-3xHA construct in the PTEX could be explained by the length of the spacer. The long spacer of the PfEMP1-mDHFR-3xHA construct allows the TMD of the protein to reach the PVM translocon during extraction out of the PPM and exported without PV intermediate and not causing any co-block (Mesén-Ramirez *et al.*, 2016). The failure to arrest the PfEMP1 construct may be also an indicator that this protein is not being transported via translocon.

Using two constructs described as arresting in PPM (REX2-mDHFR) and PVM (SBP1-mDHFR) fused with a BirA* we tried to identify the possible extractor(s) of TM proteins out of the PPM. We tried to elucidate if the blocking of PTEX causes a co-blocking of PfEMP1, which would show if PfEMP1 passes through PTEX on its way to the MC.

4.1 Integration of mDHFR conditional folding and BioID systems for the analysis of protein export

In this thesis two systems for protein analysis were implemented with the aim to arrest a protein at the transport step at the PPM (by using the mDHFR system) and tag the interactors of the arrested protein (using BirA*) to identify the proteins involved in PPM translocation of exported proteins. The mDHFR folding system has been a useful tool for the dissection of translocation mechanisms across membranes (Eilers, Hwang and Schatz, 1988; Mesen-Ramirez *et al.*, 2016; Boucher and Yeh, 2019). The folding of this domain can be stabilized with antifolate ligands (Wienhues *et al.*, 1991; Salvador *et al.*, 2000), in *P. falciparum* WR99210 (WR) (Gehde *et al.*, 2009). If a protein fused to mDHFR is transported through a translocon that requires unfolding for cargo to pass, trafficking of this protein will be blocked at this step due to ligand-induced stabilization of the mDHFR moiety. In *P. falciparum*, the export of several exported proteins such as REX2 (Gruring *et al.*, 2012), MSRP6 (Heiber *et al.*, 2013), and SBP1 (Mesen-Ramirez *et al.*, 2016) have been analyzed by fusing them with mDHFR.

The BioID system was first described as a method to identify protein-protein interaction partners and neighbouring proteins (Roux *et al.*, 2012). The BioID method requires constructing a translational fusion between a protein of interest and the promiscuous biotin ligase BirA* (a mutant of the *E. coli* protein BirA), bringing BirA* close to the target's association partners. Proximity labelling occurs upon addition of biotin to the media. The biotinylated proteins, presumably the interactors of the target, are then purified using stringent conditions via streptavidin chromatography (Bradley *et al.*, 2020). The BioID system has been used in *Plasmodium* parasites to identify proteins related with the gametocyte egress (Kehrer, Frischknecht and Mair, 2016), PV proteins (Schnider *et al.*, 2018; Khosh-Naucke *et al.*, 2018) and to identify apicoplast proteins (Boucher *et al.*, 2018). These findings demonstrate that the system is applicable in malaria parasites and that it is useful to identify proteins of specific parasite compartments.

In the current work both mDHFR and BirA* were fused to the exported proteins REX2 and SBP1. The resulting constructs REX2-mDHFR-L-BirA*-3xHA and SBP1-mDHFR-L-BirA*-3xHA were arrested in the PPM and PTEX translocon, respectively. Even if it is not possible to assume the exact location (PPM or PVM) of the construct based on the IFA, the biotinylated proteins obtained from each construct were consistent with the expected locations. These results were also consistent with what was previously reported when using mDHFR in similar

constructs. REX2-mDHFR-GFP was reported to arrest in PPM in Grüning *et al* 2012 and SBP1-mDHFR-GFP in Mesén-Ramirez, *et al* 2015 was co-immunoprecipitated with EXP2 confirming its arrest in PTEX translocon. The fact that both constructs were arrested at PTEX or the PPM is a an indicator that the construct would be able to serve the intended purpose to biotinylate proteins that are involved in the extraction of exported TM proteins at the PPM and compare them with the protein environment of proteins being translocated through PTEX.

4.1.1 Arresting of SBP1 and REX2 constructs in PTEX in order to identify possible PPM TM-proteins extractors

SBP1-mDHFR-L-BirA*-3XHA was used as a control, expecting to biotinylate PTEX components. Indeed, the most relevant hits were PTEX150 and EXP2, components of the PTEX translocon (de Koning-Ward *et al.*, 2009). The protein P113 was also pulled down, and this finding is consistent with the reports of Pf113 being a PTEX-associating protein (Elsworth *et al.*, 2016; Batinovic *et al.*, 2017). In several studies this protein was also co-pulled down when proteins from the PV (Khosh-Naucke *et al.*, 2018) or EXP2 (Mesén-Ramírez *et al.*, 2016) were immunoprecipitated. It was also detected in detergent resistant membranes (Sanders *et al.*, 2005; Sanders *et al.*, 2007) as the PVM and the merozoite membrane of *Plasmodium*. Additionally, Pf113 has been reported to be a merozoite surface protein (Galaway *et al.*, 2017) and it was shown to be a marker of protective immunity being therefore a protein of interest for vaccine design (Osier *et al.*, 2014). The fact that all the biotinylated proteins detected by the mass spectrometry assay are known PTEX components or PV residents, is a clear evidence of the correct localization of the arrested construct in the translocon.

The detection of SBP1 as a relevant hit is explained by the fact that the SBP1-mDHFR-L-BirA*-3XHA construct is able to biotinylates itself, and that this is sufficient for the fusion construct to be purified. The detection of proteins as PTEX150, EXP2, Pf113 is an indicator that the arrest of SBP1-mDHFR-L-BirA*-3XHA is indeed in the PTEX translocon, and not somewhere else. It also indicates that the construct is deeply buried in the translocon, as few other proteins were significantly enriched, consistent with the fact that this construct obstructs the passage of other substrates through PTEX (Mesen-Ramirez *et al.*, 2016).

REX2-mDHFR-L-BirA*-3XHA was expected to be arrested at the PPM extraction step, preceding transport through PTEX. According to the IFA images, the construct is arrested in the parasite periphery, congruent with a location in the step before transport through PTEX (Figure 10), although it was not formerly proven not to represent a location in the PV or the

PVM. However, previous data using proteinase protection assays with selectively permeabilized iRBCs indicated that a similar construct (REX2-mDHFR-GFP) was arrested in the PPM (Grüiring *et al* 2012). Yet, the results of the mass spectrometry showed many proteins known to be located in the PV region such as ETRAMP5, UIS2, EXP3, PV1, PV2 and PTEX components such as PTEX150, EXP2, PTEX88. There are 2 possible explanations for this:

(i) the previous data based on protease protection assays is incorrect (Grüiring *et al* 2012, Mesén-Ramírez *et al.*, 2016) and the protein is not in the PPM. However, clearly the constructs with a short spacer behave differently (no leakiness of the phenotype and no co-blocking activity) and have a different GFP-staining pattern than those with a long spacer (Mesén-Ramírez *et al.*, 2016). This might also be explained by failure of this construct to fully enter PTEX which would be in line with its differing properties (i.e. the lack of co-blocking activity).

(ii) that not all of the construct remained in the PPM, but that the REX2-mDHFR-L-BirA*-3XHA construct could be arrested in different locations. The protease protection assay used to determine the location of this construct (Grüiring *et al* 2012) would not have been able to detect this as long as a part of the protein indeed was in the PPM.

The latter possibility seems more likely, as EMC2 (located in the outer face of the ER and apparently at the PPM) and UFD1 (cytosolic), were highly biotinylated which clearly indicates that some of the REX2-mDHFR-L-BirA*-3xHA molecule population was indeed arrested in the PPM.

Some of the most relevant hits are proteins related with the Endoplasmic-reticulum-associated protein degradation (ERAD) pathway. The ERAD pathway targets misfolded proteins of the endoplasmic reticulum for ubiquitination and subsequent degradation by proteasomes (Smith, Ploegh and Weissman, 2011). Remarkably, proteins triaged as terminally misfolded are retro-translocated from the ER to the cytosol (Claessen, Kundrat and Ploegh, 2012) and escorted to the proteasome for degradation (Smith, Ploegh and Weissman, 2011). One of the proteins found on the mass spectrometry is the UFD1 and the UFD1-ubiquitin interaction is essential for the transfer of those misfolded proteins to the proteasome (Park *et al.*, 2005).

A jam in one of the steps of the export pathway is definitely a disturbance event for the cell and the blocked REX2-mDHFR-L-BirA*-3xHA may be removed from the PPM. The ERAD pathway could do this if the protein is still located in the ER membrane, however it is not clear if it is possible that a similar system involving ERAD components such as UFD1 remove and degrade PPM proteins in the parasite. In other organism, integral TM proteins in the plasma

membrane are degraded using ubiquitination (Hein *et al.*, 1995; Wang *et al.*, 1999; Belgareh-Touzé *et al.*, 2008). The ubiquitinated transmembrane cargo is recognized by factors of the endocytosis machinery, such as Ede1, and clathrin-mediated endocytosis delivers the ubiquitinated protein to an early endosome (Haglund and Dikic, 2012). At the endosome, the cargo (proteins sorted through the endosomal system) has two options: recycling to the cell surface either directly or indirectly via the trans-Golgi or continuing to the vacuole for degradation (Babst, 2014). This might explain the prominent detection of biotinylated UFD1 (see also Table 4). It is also noteworthy that V-ATPaseSE and EMC2 both showed a PPM pool (Figure 14 C and Figure 18 C). It is therefore possible that these proteins are involved in such a quality control (QC) system, explaining their presence at the arresting site of the constructs. As these proteins reside on the cytosolic side of the PPM, they also further confirm that some of the REX2-mDFHR-L-BirA molecules were located in the PPM with their C-terminus facing the parasite cytoplasm.

Finding proteins described as PV or PVM residents (e.g. ETRAMP5, UIS2, EXP3, PV1, PV2) and PTEX components (PTEX150 and PTEX88) is an indicator that the construct could also be in close contact with both membranes, as was hypothesized in the third case of Figure 27-C (Spielmann and Gilberger, 2015). In this case, the momentaneous fusion of both membranes, the PPM and PVM, would allow BirA* to reach the proteins from the PV and the components of the PTEX that are in the PV lumen. Another explanation could be an inverted topology of the REX2-mDHFR-L-BirA*-3xHA construct in the PPM. In this case the C-terminus would be facing the PV lumen. However, finding proteins as EMC2 and UFD1 is a clear indicator that the C-terminal part of the construct was facing the parasite cytosol.

Among the proteins biotinylated by the REX2-mDHFR-L-BirA*-3XHA construct the Liver-stage antigen 3 protein (LSA3) was the most highly enriched protein (in 2 of 2 samples with 2 replicas) with a significance of 10^{-10} (this refers to the enrichment of the arrested protein vs the control in both samples)(Figure 12). LSA3 is a protein that contains 2 hydrophobic regions that are both predicted to be TMDs although the N-terminal TMD region likely represents a SP. LSA3 has been reported to have a PEXEL motif at position (89-93 of the amino acid sequence) and is therefore predicted to be an exported protein (Maier *et al.*, 2008; Morita *et al.*, 2017). However, no export has been experimentally demonstrated for this protein yet. Solubility assays detected the protein in the pellet fraction after saponin treatment, as expected for a transmembrane protein (Khosh-Naucke, 2018).

LSA3 is expressed in liver stages (from where it received its name) and sporozoites. Attempts to disrupt LSA3 using SLI-TGD failed, suggesting an essential function of this protein (Khosh-Naucke, 2018), although it was previously reported not to be essential (Maier *et al.*, 2008).

LSA3 has recently been localized to dense granules in schizont blood stage parasites via immune fluorescence assays and electron microscopy (Morita *et al.*, 2017) and to the PV of ring stages (Khosh-Naucke, 2018). The fact that LSA3 localizes in dense granules in schizonts can be co-related with the described localization of PV1 (Parasitophorous Vacuolar protein 1), and the PTEX components such as HSP101 and EXP2 that are also found in the dense granules in merozoites (Morita *et al.*, 2018). This suggest that LSA3, PV1 and PTEX is likely carried into the newly forming parasite and released into the developing PVM of ring stages (Bullen *et al.*). Due to its location, LSA3 may be in contact with our constructs, however this protein was not analyzed. A conditional KO needs to be established to make possible the consequences of loss of LSA3 immediately after the merozoite invasion to identify the role of this protein in protein export

In addition to the proteins plotted in Figure 12, a list of around 2000 proteins was obtained from the mass spectrometry experiment of both SBP1-mDHFR-L-BirA*-3XHA and REX2-mDHFR-L-BirA*-3XHA. From those, 10 proteins were chosen for further analysis based on their level of enrichment, and their possible function as a extractors judged by their function in other cell pathways. Within the biotinylated proteins purified by mass spectrometry, it was expected to find a protein in the parasite periphery (most probably in the PPM or PV) that aids in the extraction of TM proteins out of the PPM. It is expected that the disruption of this hypothetical protein, would disturb the transport of exported proteins to the erythrocyte. Ten of the proteins obtained from the mass spectrometry were tagged with GFP and/or 3xHA to localize them. To test if any of these proteins had a role in mediating protein export, it was attempted to disrupt them (in 3 of 10 successful) or to conditionally inactivate them using KS (3 attempted, 3 successful).

4.1.2 Analysis of potential PPM extractors of exported TM proteins

One of the criteria for identifying whether biotinylated proteins were a possible extractor was their location. To determine whether the proteins were located in the PV region the candidates were fused either with GFP or with a 3xHA epitope tag. Both tags have advantages and disadvantages. The fluorescent tags are useful because the protein can be observed live with a fluorescence microscope. However, it was also demonstrated that for some proteins tagging

with a bulky tag (more than 20 kDa) can interfere with their native function or location (Dave *et al.*, 2016; Weill *et al.*, 2019). Small tags such as 3xHA (~4 kDa) are better tolerated and less likely to interfere with the function or location of the candidate tested. However, for the 3xHA detection it is necessary to perform immunofluorescence assays which is more time consuming and, due to the need for fixation and permeabilization of the sample, can lead to difficulties in obtaining a clear location of the target analyzed.

In order to accurately identify the location of the proteins, the proteins identified by the proximity biotinylation approach were tagged with GFP or 3xHA. To assess the essentiality or dispensability of the selected proteins in the asexual blood cycle, the POIs were also disrupted with SLI-TGD or removed from its site of action using KS.

Three of the ten chosen proteins (UFD1, V-ATPaseSE and EMC2) were in other systems connected with proton or protein translocation. While they can be assumed to perform the same canonical function in the parasite, the special situation could have repurposed this function for protein export. UFD1 is an essential component of the ubiquitin-dependent proteolytic pathway which degrades ubiquitin fusion proteins (Johnson *et al.*, 1995). It forms a ternary complex containing UFD1, VCP and NPLOC4. This complex is well described in mammalian cells as binding ubiquitinated proteins and being necessary for retro-translocation of misfolded proteins from the ER to the cytoplasm, where they are later degraded by the proteasome (Meyer *et al.*, 2000; Nowis, McConnell and Wojcik, 2006). Hence, the protein complex where UFD1 belongs, is attached to the ER membrane by the receptor protein Ubx2, however, the signal of UFD1-2xFKBP-GFP and UFD1-3xHA was cytosolic, which is the wrong side of the PPM if it were to aid membrane extraction of exported proteins in a similar way to the ERAD system. Unless some of the UFD1 was also located in the PV, which would not be distinguishable if its concentration in the PV is not higher than in the cytoplasm (which would lead to the appearance of a rim around the parasite). This is nevertheless very unlikely, as UFD1 does not contain any features (such as a SP) that could bring it to the PV. Such features would also need to be present in the form of alternative spliced exons, as otherwise the likely essential canonical function would be abolished. Essentiality of UFD1 for the parasite was indicated by the impossibility to obtain parasites where *ufd1* is disrupted. In contrast it was possible to, mislocalize it which would indicate that it is dispensable for parasite growth *in vitro*. Either this means that the TGD was not obtained for technical reasons or that the KS was incomplete and small amounts of UFD1 are enough to carry out its functions. However, the export of the trans membrane protein REX2 was not impaired after the mislocalization of UFD1. Overall, these

findings indicate that UFD1 likely is not involved in the extraction of exported TM proteins at the PPM for export. However, there is the possibility that the parasite possesses a quality control system at the PPM that acts in a similar manner to ERAD that retrieves proteins out of the membrane and this might have been the reason why the blocked REX2-mDHFR-L-BirA-3xHA tagged UFD1 if this was involved in removing proteins arrested in the PPM, such as achieved by using folded mDHFR.

Another ER protein analyzed was EMC2. This protein belongs to a protein complex of 10 subunits (in mammals) that is embedded in the ER membrane (Jonikas *et al.*, 2009). This protein was chosen due to its function of aiding the extraction of proteins from the ER (Wideman, 2015; Guna *et al.*, 2018) and because it contains three tetratricopeptide repeats (TPR1/2/3) (Christianson *et al.*, 2011) that are described with a function of inserting TM proteins into membranes (Lamb, Tugendreich and Hieter, 1995; Goebel and Yanagida, 1991; Das, Cohen and Barford, 1998). EMC2 contains no predicted transmembrane domain and is likely to interact with the other EMC components on the cytosolic side of the ER. Most recently, the EMC has been implicated in the proper assembly of multi-pass TM proteins in the ER membrane (Satoh *et al.*, 2015). These findings suggest that EMC may be involved in dealing with misfolded membrane proteins (Shurtleff *et al.*, 2018). Yet, the primary function of the EMC is still open for debate.

The GFP signal of the EMC2-2xFKBP-GFP expressing cell line surrounded the nucleus, indicating an ER localization. However, a faint signal was also detected in the parasite periphery, suggesting a possible PPM localization. The EMC2-2xFKBP-GFP parasites that were transfected with an ER marker, showed total colocalization of both signals, thus confirming EMC2 to be an ER resident protein in *P. falciparum*. Given the function of EMC in the ER membrane of mammalian cells (Jonikas *et al.*, 2009), EMC2 may be involved in the retro-translocation of misfolded proteins at the PPM and may therefore have been detected by our arrested construct.

Finally, the protein was attempted to mislocalize using a nuclear mislocalizer (NLS-FRB-mCherry). The general approach of the KS system is to mislocalize proteins of interest to a distinct cellular compartment. However, this approach could present some problems with ER proteins, as the ER is directly connected to the nuclear envelope. Hence, the mislocalization might not be sufficient using a nuclear mislocalizer. In the case of the EMC2 mislocalization, the rationale behind using a nuclear mislocalizer was to avoid that the protein that appeared as a faint signal on the PPM (Figure 18 C), reached the parasite periphery, by holding it down

with the nuclear mislocalizer attached to it. This was done based on the rationale that the lack of protein at the parasite periphery could influence protein extraction from the PPM which would manifest as an export defect. Nevertheless, it was not possible to mislocalize much of the protein and no effect on protein export was observed. Even though this altogether indicates that EMC2 has no role extraction of exported TM proteins at the PPM, it can not be fully excluded that technical issues were responsible for the lack of effect on protein export and that in principle, EMC2 could still have a role in protein export.

UFD1 and EMC2 are implicated in the ERAD pathway (Christianson *et al.*, 2011; Wideman, 2015; Johnson *et al.*, 1995). Even though UFD1 and EMC2 were prominently enriched proteins in the proximity biotinylation experiments, the results here indicate that most likely these proteins are not involved in protein export. This indicates that those proteins were in contact with the arrested constructs, not because they were helping to extract them out of the PPM for further transport but because they were degrading the “misfolded” proteins on the membrane, i.e. that they have a role in the retro-translocation. The function of UFD1 was probably to ubiquitinate the arrested construct whereas EMC2 could be other means help to retro-translocate the jammed proteins back into the cytoplasm for degradation in the proteasomes.

Another protein analyzed was the subunit E of the Vacuolar type ATP synthase (V-ATPaseSE). Functional V-ATPases are composed of two parts: a cytoplasmic V₁- and a transmembrane V₀ regions (Pamarthy *et al.*, 2018), which may dissociate from each other in response to some stimuli. Each of the two regions are composed of multiple different subunits. In mammalian cells eight different proteins are combined in the following stoichiometry A₃B₃C₁D₁E₃F₁G₃H₁ to form a V₁-sector; while at least six different proteins a₁ c₅ c''₁ d₁ e₁ and Ac45₁ form the transmembrane V₀-sector (Orlov, 2019; Kitagawa *et al.*, 2008; Drory, Frolow and Nelson, 2004). In the V-ATPaseSE-2xFKBP-GFP expressing cell line, a strong signal at the food vacuole was observed. This is consistent with the most studied function of this complex in mammal cells which is in the acidification of organelles by pumping protons into the compartment (Nelson *et al.*, 2000). Nevertheless, the V-ATPase complex has been implicated in a bewildering variety of additional roles that seem independent of its ability to translocate H⁺, including facilitating fusion of membranes, cytoskeletal tethering and metabolic sensing (Maxson and Grinstein, 2014).

In the V-ATPaseSE-2xFKBP-GFP expressing cell line a faint signal surrounding the PPM was observed (Figure 14 C). This faint signal could indicate a possible non-canonical function of

the V-ATPase in this region as a scaffold for protein-protein interactions. The subunit E of this complex was biotinylated with the REX2-mDHFR-L-BirA-3xHA and this subunit was identified as an aldolase interactor. This interaction is required to stabilize the assembled V-ATPase on the membrane (Merkulova *et al.*, 2011; Lu *et al.*, 2007). Another explanation for why this protein complex was found in the PPM is that one of the non-canonical functions of the V-ATPase is to assist in membrane fusion. The V-ATPase dock, the V₀ domains of two adjacent membranes to form a trans-complex, thereby creating a fusion pore that aids vesicle fusion (Peters *et al.*, 2001; Bayer *et al.*, 2003). Recent studies suggest that even a single subunit of V₀ can promote fusion between two membranes (Baars *et al.*, 2007; Takeda *et al.*, 2008). This non canonical function of the V-ATPase could be an explanation of why the REX2-mDHFR-L-BirA*-3xHA was able to biotinylate proteins from the PV even when it was arrested at the PPM. If the V-ATPase could create a pore on the PPM, as it was postulate for vesicle fusion (Peters *et al.*, 2001; Bayer *et al.*, 2003) then REX2-mDHFR-L-BirA*-3xHA could also be in contact with the PV proteins.

The non-canonical functions described above, and the PPM localization of the protein were a good indication of a possible function as extractor, or facilitator of the extractor, nevertheless the IFA of the V-ATPaseSE-TGD parasites using α -REX2 antibodies showed no abnormalities based on the distribution of REX2 on the MCs. Indeed, parasites with a disrupted V-ATPaseSE showed a similar phenotype to the V-ATPaseSE-GFP cell line, with a marked fluorescence surrounding the food vacuole and the PPM (Figure 14) and with no detectable growth defects.

The subunit E of this complex is a peripheral factor (Colina-Tenorio *et al.*, 2018) that probably helps with the rotation or the assembling of the A, B and C and H subunits of the V₁ region. Some other subunits as D, A or B of the V₁ or the proteins located in the non-soluble region (V₀) could be playing a more important role on the function and assembling of the V-ATPase. This could be a reason why the disruption of the subunit E was not lethal as it might not have abolished the function of the entire complex. Other V-ATPase components, such as the H and C and D subunits, which includes V₀ parts, were also found in the mass spectrometry hits, indicating that the arrested REX2 construct is in contact with the entire V-ATPase complex, not just the E subunit. It would be necessary to disrupt other subunits to find out if this protein complex is needed for protein transport across the PPM.

Additional tested proteins were Pf3D7_1226400, Pf3D7_0104500 and Pf3D7_0704300, all of them with unknown function in *Plasmodium*. Cell lines with the disrupted genes from the 3

proteins were produced, nevertheless the export to the MCs of REX2 was not impaired, showing that these proteins were not involved in protein export.

PF3D7_0830400 is a protein that contains a CRA domain which is a protein-protein interaction domain present in crown eukaryotes (Menon, Gibson and Pastore, 2004). Previously named PF08_0004, the PF3D7_0830400 protein was described as a PNEP that showed foci in the MCs when tagged episomally with GFP, and expressed under the moderate *crt* promoter (Heiber *et al.*, 2013). This protein was tagged endogenously using the SLI system and the parasites episomally expressing CRA-2xFKBP presented a different pattern when compared to the episomally tagged protein. The CRA-2xFKBP-GFP was expressed under its native promoter and the GFP signal was detected as *puncti* all around the parasite cytosol and autofluorescence of the food vacuole as previously reported with GFP tags (Birnbaum *et al.*, 2017) or potentially representing GFP-fusion protein re-internalized from the parasite periphery by endocytosis into the food vacuole. Interestingly, the cell line expressing episomally a CRA-GFP construct, exported this construct to the MCs (Heiber *et al.*, 2013), whereas in the endogenous version containing a 2xFKBP-GFP the protein is not exported. The phenotype in the endogenously tagged version could be explained by the fact that the 2xFKBP-GFP is impeding the normal protein traffic due to its larger size than GFP alone. Alternatively, endogenous expression timing and expression levels might have resulted in a more faithful representation of the location of this protein. This protein was probably detected on the biotinylation assay because it is also an exported protein, that must pass through PTEX to reach the MCs, then it was probably in contact with the arrested construct. Attempts to disrupt the CRA protein were unsuccessful and the mislocalization of the protein was not complete, as evident by *puncti* in the cytosol that were still present 12h after induction of the knock sideways. These *puncti* were not found in the iRBC and may represent degrade protein that could not be transported to the PPM. To identify better the localization of this protein a smaller tag as 3xHA could be tested.

PTEX88, an auxiliary protein of PTEX, was also analyzed in this thesis. Previous attempts to elucidate its function through reverse genetic approaches showed that, in contrast to the core components PTEX150 and HSP101, knockdown of the murine PTEX88 did not affected protein export (Chisholm *et al.*, 2016). PTEX88-deficient *P. falciparum*-infected erythrocytes displayed reduced binding to the endothelial cell receptor, CD36 (Chisholm *et al.*, 2016), suggesting that PTEX88 likely plays a role for exported proteins mediating parasite sequestration rather than making a universal contribution to the trafficking of all exported

proteins. The impossibility to obtain a TGD for *ptex88* (Table S1) is at odds with the reports of PTEX88 being not essential in *P. falciparum* (Chisholm *et al.*, 2016). This contradictory result could be explained by the fact that with the TGD, the gene would be completely removed, whereas with the conditional knockdown used in (Chisholm *et al.*, 2016), some of the protein population might still have been present.

4.2 Jamming PTEX and its implications in PfEMP1 export.

Plasmodium falciparum parasites older than approximately 18 hpi are sequestered in the post-capillary venules and various organs such as the brain and placenta, causing severe malaria (Bignami and Bastianelli, 1889; Clark, 1915). Only young parasites are found circulating in the peripheral blood (Marchiafava and Bignami, 1895). In 1988 it was revealed that the tissue-specific sequestration involves high molecular weight protein (>200 kDa), expressed on the iRBC surface in structures termed “knobs”. This protein was called *P. falciparum* erythrocyte membrane protein 1 (PfEMP1) and it has several properties shared by the SICA (schizont infected cell agglutination) or variant antigen of *P. knowlesi* (Howard *et al.*, 1988). Eight years later it was demonstrated that PfEMP1 was in fact a family of proteins encoded by the *var* multigene family (Su *et al.*, 1995; Smith *et al.*, 1995; Baruch *et al.*, 1995). Each individual of *P. falciparum* parasite expresses only a single of its PfEMP1 from its repertoire of *var* genes in a mutually exclusive fashion (Scherf *et al.*, 1998). This great variation makes the identification of the actual expressing PfEMP1 a challenging process, however the PfEMP1-3xHA cell line used in this work, and to my knowledge the first cell line where PfEMP1 is endogenously tagged, helps to overcome obstacles such as antigenic variation and ensures that the expressed PfEMP1 protein is always the same.

PfEMP1 is a TM PNEP and its delivery to the iRBC surface is dependent on different proteins along the export pathway (Boddey *et al.*, 2013; Maier *et al.*, 2008; McMillan *et al.*, 2013). For this reason, it is not possible to identify whether the reduction in the export of PfEMP1 is a direct effect of the inactivation of PTEX or if the inactivation of PTEX prevents the export of proteins that are necessary for the correct trafficking of PfEMP1

It might be assumed that PfEMP1 is translocated as described for any other TM PNEPs (Heiber *et al.*, 2013; McMillan *et al.*, 2013; Riglar *et al.*, 2013). Nevertheless, there is so far no direct evidence for this assumption. The translocation of PfEMP1 across the PVM has to date not been characterized, since most *var* genes average 8-10 kb in length, making it technically challenging to express the full-length sequences as mDHFR fusions from episomal expression

plasmids (Melcher *et al.*, 2010). In our lab a cell line was produced where PfEMP1 was successfully fused to an mDHFR domain, but its export was not blocked upon WR addition (Mesén-Ramirez, unpublished).

Since the discovery of PfEMP1 in 1988 many studies have been done to identify how this protein is transcribed, transported, and expressed. The transcription of *var* genes is initiated in early ring stages (Kyes, Pinches and Newbold, 2000) and PfEMP1 appears on iRBC surface ~16 hpi (Gardner *et al.*, 1996; Kriek *et al.*, 2003), showing that the export of PfEMP1 across the RBC cytoplasm is a slow process. Yet, the transport process across the PV region is less clear. Previous efforts to track the traffic of PfEMP1 have used transfectants expressing knobs proteins as KAHRP and PfEMP3-GFP hybrid chimeras (Knuepfer *et al.*, 2005) and truncated versions of PfEMP1 tagged with GFP (Melcher *et al.*, 2010; McMillan *et al.*, 2013). To the best of my knowledge there are no cell lines available where the complete PfEMP1 is endogenously tagged, likely due to the large size and the clonal antigenic variation of PfEMP1 (Kraemer and Smith, 2006). Also, the fact that the parasite can switch rapidly the expressed *var* gene, the exposed PfEMP1 is always different, making it a challenge to tag this protein. With the SLI methodology it was possible to endogenously tag a native PfEMP1 with a 3xHA tag (performed by Paolo Mesén-Ramirez). This protein is encoded by the gene with the PlasmoDB identification Pf3D7_0809100 and it is assured that the expressed PfEMP1 is always the same as the culture is continuously under G418 pressure. This construct is also correctly exported to the MCs where it accumulates, presumably before being transported to the knobs. With this cell line and modifying the original SLI vector (pSLI2 to pSLI2a), it was possible to obtain a double integrant cell line where it was analyzed the expression of PfEMP1 when PTP1 was disrupted or when SBP1 was arrested in the PTEX translocon.

According to the co-localization IFAs with the two MCs resident proteins PTP1 and SBP1, the signal of PfEMP1 was also mainly on the MCs. Although the final location of PfEMP1 is in the knobs, the formation of the virulence complex composed by PfEMP1 and KAHRP occurs in the MCs, hence a large amount of proteins are more detectable in this region, compared with the 2 to 3 molecules of PfEMP1 reported to be displayed in each knob of knobby cell lines (Sanchez *et al.*, 2019). Cell lines such as 3D7 were adapted to grow in vitro, and when cultured with AlbuMAX instead of human serum, they produce fewer knobs. (Tilly *et al.*, 2015). Both factors: the assembly of the PfEMP1-KAHRP complex in the knobs, and the low number of knobs expressed by 3D7, explain why the PfEMP1 signal was more intense in the MCs than in the knobs.

4.2.1 The effect of arresting SBP1 in PTEX on PfEMP1 export

SBP1 is a MCs resident integral membrane protein that is oriented so that its C-terminal domain is present in the RBC cytoplasm (Blisnick *et al.*, 2000). Similar to PfEMP1 and SBP1 is not cleaved by Plasmeprin V (Boddey *et al.*, 2013). SBP1 is not an essential structural protein of the MCs, as its absence does not affect MCs' morphology or its number markedly. Its disruption also does not affect the formation of knobs (Cooke *et al.*, 2006; Maier *et al.*, 2007), or the expression of MCs proteins as MAHRP1, REX1 or Pf332 or the knob protein KAHRP (Cooke *et al.*, 2006; Maier *et al.*, 2007) but is necessary for trafficking and translocation of PfEMP1 onto the RBC surface (Cooke *et al.*, 2006; Maier *et al.*, 2007). Therefore, even if knobs are produced on the surface of iRBCs that lack SBP1, these cells are not capable of cytoadhering due to the non-exposure of PfEMP1 (Cooke *et al.*, 2006; Maier *et al.*, 2007).

Previous work provided explanations for the effect that the disruption of SBP1 has on the exposure of PfEMP1 on the iRBC surface. In one study, when SBP1 is knocked out, PfEMP1 is inhibited in transport into the host cell (Maier *et al.*, 2007). In a different study PfEMP1 is still exported but does not reach the host cell surface (Cooke *et al.*, 2006). Cooke *et al* in 2006 postulated that the removal of SBP1 caused subtle changes in the structure of MCs, making them narrower and with a reduced intermembrane space. These alterations and the distance to the IRBC surface leads to changes that make the final translocation step of PfEMP1 markedly inefficient, thus SBP1 has an indirect effect on the PfEMP1 transport and its precise function is to mediate the final step in the translocation of PfEMP1 onto the surface of the iRBC (Cooke *et al.*, 2006). Maier *et al* in 2007 used different solubility assays to show that SBP1 is required for the transfer of PfEMP1 from the PVM to MCs, suggesting that the protein is most likely loaded directly into MCs rather than being released into the erythrocyte cytosol (Maier *et al.*, 2007). They also speculate that SBP1 has a chaperone-like function allowing interaction with PfEMP1, which is required for trafficking out of the parasitophorous vacuole and association with Maurer clefts (Maier *et al.*, 2007). However, the SBP1 protein sequence does not reveal any domains with homology to known chaperones, or to proteins known to be involved in protein trafficking or vesicular transport and such a function remains to be experimentally demonstrated. In addition, immunoprecipitation of SBP1 from iRBC lysates does not lead to the co-precipitation of PfEMP1 and experiments in which PfEMP1 and SBP1 were labelled with FRET-compatible fluorophores did not lead to the detectable transfer of energy from one molecule to the other (Cooke *et al.*, 2006). Both authors agree in the necessity of the expression

of SBP1 for PfEMP1 exposure on the host cell surface, however the moment when SBP1 acts in this role, is still unclear.

Our approach consisted of expressing a tagged SBP1 either episomally or endogenously with mDHFR-GFP in the PfEMP1-3xHA cell line. It was reported that blocking PTEX with exported proteins containing a mDHFR domain clogs the translocon and as a result that other exported proteins remain blocked in the PV region. This phenomenon was named co-blocking (Mesén-Ramírez *et al.*, 2016). Thus, blocking PTEX with SBP1-mDHFR-GFP should also block the export of PfEMP1 in the case that PfEMP1 is also transported through PTEX.

SBP1 is expressed shortly after merozoites invasion. In order to detect SBP1 starting from the beginning of the cycle, the protein was episomally expressed under the early promoter Mal7 (Gruring *et al.*, 2011). In the Mal7-SBP1-mDHFR-GFP cell line it was possible to detect live-fluorescent parasites from 4 hpi. In the cell line with the endogenously tagged SBP1, the protein was expressed under its native promoter and it was possible to observe live-fluorescent parasites at 6 hpi. These expression timing is consistent with the previously described for SBP1 (Gruring *et al.*, 2011). The detection of SBP1 via IFA showed in both cell lines that the protein was already expressed at the first time point (6hpi) (Figure 25 D and Figure 26 D) also consistent with the previously reported timing expression of SBP1 (Gruring *et al.*, 2011).

Mesén-Ramírez *et al* in 2012, demonstrated that all types of exported proteins are affected by the obstruction of the PTEX with the construct SBP1-mDHFR-GFP. The effect caused by this blocking caused that all the exported proteins remained also blocked in the PV region. In order to identify if PfEMP1 was also transported via PTEX we blocked the constructs Mal7-SBP1-mDHFR-GFP^{epi} and SBP1-mDHFR-GFP^{endo} in the PTEX translocon.

Initially the parasites were incubated with WR from the moment of the invasion (0 hpi) in order to arrest SBP1, thus blocking passage through PTEX before PfEMP1 begins to be exported. In both cell lines where SBP1 was tagged episomally or endogenous, a clear arrest of the SBP1-mDHFR-GFP construct in the PVM was observed. This producing also an accumulation of PfEMP1 in the parasite periphery. Interesting, the signal of PfEMP1 did not completely overlap with the SBP1 signal. This finding is consistent with what Riglar *et al* reported in 2013 suggesting that PfEMP1 is trafficking in a PTEX-independent fashion, also the impossibility to arrest PfEMP1-mDHFR constructs (Mesén-Ramírez, data not shown) on its way to the MCs stands for this assumption.

As previously described, SBP1 is necessary for the correct exposure of PfEMP1 on the iRBC surface, thus it is expected that the export of SBP1 starts earlier than the PfEMP1 export. SBP1 is detectable as early as 4 to 6 hpi (Gruring *et al.*, 2011) whereas PfEMP1 is first observed at the parasite surface around 8 to 11 hpi (McMillan *et al.*, 2013). In order to identify if the retention of PfEMP1 in the PV region was caused by the arrested SBP1-mDHFR-GFP construct in PTEX as a co-block effect, WR was added at the moment of the invasion (Figure 25 D middle and Figure 26 D middle). In this case, SBP1 and PfEMP1 were both retained in the PV region. This phenotype could be explained (i) if PfEMP1 is crossing the PVM trough PTEX, then the arrest of the SBP1-mDHFR-GFP construct in the translocon would lead to a co-block. (ii) if the insertion of PfEMP1 into the MCs takes place in the PV region (McMillan *et al.*, 2013), then the arrest of SBP1 would lead to a failure to insert PfEMP1 into the MCs and it would accumulate in the PV or (iii) if PTEX is blocked, not only will SBP1 not be transported, but other proteins needed for PfEMP1 trafficking, such as MAHRP, REX1 and PTPs, will also not be transported, which will cause an export defect for PfEMP1.

As all the exported proteins are co-blocked by blocking of PTEX (Mesén-Ramírez *et al.*, 2016) it was necessary to identify if the failure of export MCs resident proteins was also causing the arresting of PfEMP1. For this propose, a different blocking time was tested. WR was added to the culture 18 hpi. This time is sufficiently late in the cycle for all the other exported proteins needed for PfEMP1 trafficking to be exported to avoid this to independently affect PfEMP1 transport. In this case, a clear detection of PfEMP1 in the MCs was observed, whereas SBP1-mDHFR-GFP was detected as a mixed phenotype with signal in both MCs and the parasite periphery. The amount of SBP1 increases from 6 to 24 hpi and it is maintained until the rupture of the iRBC and merozoite release (Blisnick *et al.*, 2000) and the observed signal at the MCs corresponds to the protein exported within the first 18 hpi whereas the signal at the parasite periphery shows the arrested construct exported after this time point. Overall these results indicate that most likely PfEMP1 is transported independent of PTEX. However, due the multiple confounders in this analysis (role of SBP1 in transport and unknown site of PfEMP1 block as well as the fact that SBP1-induced co-blocking will affect several other molecules needed for PfEMP1 trafficking) a definitive conclusion can not be drawn from these experiments. In the future it could be tried to block PTEX with a different exported protein, thus eliminating the duality in the results with SBP1 (as a PTEX plugging agent and as an assistant in the export of PfEMP1). However, this would not solve the problem that these other co-blocked proteins would be absent in the host cell and so cause a transport defect of PfEMP1.

4.2.1.1 The impossibility to disrupt SBP1 in a PfEMP1 expressing cell line

After several trials it was evident that it was not possible to disrupt SBP1 in the cell line that already contained an endogenously tagged PfEMP1. These phenotypes included the integration in a different locus of the genome. Two phenotypes were observed, when parasites appeared in culture after the selection with both G418 and DSM1 drugs. These phenotypes were: (i) integration of the plasmid containing the sequence for SBP1-TGD in a different region of the genome. (ii) the disappearance from culture of integrated parasites expressing PfEMP1-3xHA. Those results suggest that the disruption of SBP1 interfered with the transport and correct exposure of PfEMP1 on the surface of the infected RBC as was demonstrated before (Maier *et al.*, 2007; Maier *et al.*, 2008). The impossibility of disrupt SBP1 and correctly express SBP1 could be explained because the pSLI and pSLI2 vectors have similar backbones. This could lead to a recombination of both plasmid within the genome, causing that pSLI2 integrates into the already integrant pSLI, thus not expressing both proteins but just one of them. However, the disruption of PTP1 (section 3.2.1.1) and others (Jan Stacker, unpublished) in a PfEMP1-3xHA cell line were successful, showing that the double integration in the same parasite using pSLI and pSLI2 is possible. Apparently, the reversion of the PfEMP1 integration is due to the SBP1 disruption and not due to technical problems, showing that the PfEMP1 trafficking defect could have a dominant negative effect that does not allow the survival of parasites with a HA-tagged PfEMP1-3xHA together with a disrupted SBP1.

4.2.2 *The effect of disrupting PTP1 on PfEMP1 export*

One of the proteins necessary for the correct formation of the MCs is the PfEMP1 trafficking protein 1 (PTP1). PTP1 together with a large complex of proteins was described as necessary for linking MCs to the host actin cytoskeleton and this is needed for the export of PfEMP1 and STEVOR proteins, directly reducing cytoadherence (Rug *et al.*, 2014).

Using the SLI system it was possible to disrupt PTP1 in a cell line that expressed PfEMP1-3xHA^{endo}. The PTP1-TGD cell line showed a cytosolic fluorescence without foci at the MCs. When the PfEMP1 was analyzed, we found no difference between the parental cell line (PfEMP1-3xHA) and the PTP1-TGD cell line regarding PfEMP1 export or MCs architecture. This contrasts with Rug *et al* which reports that the ablation of PTP1 leads to severe alterations in the architecture of MCs, and that PfEMP1 and STEVOR are no longer displayed on the iRBC surface (Rug *et al.*, 2014). Although cytoadhesion tests were not performed in this work due to the poor suitability of 3D7 for such assays, the trypsin assay (Figure 22 D) demonstrates

that PfEMP1 was exposed to the surface. However, as we did not test the adherence phenotype, and as our cell line was less adherent than the one used in Rug *et al* 2014 (*P. falciparum* strain CS2), our data cannot be compared with the data from Rug *et al* where PfEMP1 was not exported in PTP1 disrupted parasites (Rug *et al.*, 2014). However, at least the location of PfEMP1 and the architecture of the MC was unchanged in our PTP1-TGD. Our integration diagnostic PCR showed that clearly both plasmids were correctly integrated into the genome and according to the cytosolic fluorescence of PTP1-TGD-GFP, the protein was indeed disrupted, excluding technical problems as an explanation. The IFA using α -HA antibodies to detect the PfEMP1-3xHA protein showed an apparently normal distribution of the MCs with a normal morphology. However, a more in-depth examination of the MCs using electron microscopy would be needed to determine if there are indeed morphological changes of these structures. Also, it would be interesting to probe this cell line with α -SBP1, α -MAHRP and α -KAHRP antibodies to find out if these proteins are expressed in MCs and knobs. As a conclusion our data suggest that the disruption of PTP1 does not affect the export of PfEMP1 and the morphology of the MCs was not impaired judging to the limits of the IFA allow us to observe.

5 Conclusions

Conditionally foldable and direct biotinylation are methodologies that can be used mutually to identify factors involved in protein export. The stable translocation constructs obtained in this work validated unifying principles in the protein export pathway. The biotinylation of proteins belonging to the ERAD pathway indicated that the parasite displays mechanism of quality control to remove the “misfolded” protein in transit to the translocon, presumably in the PPM

The present study analyzed (using the SLI methodology) 11 proteins that potentially served as an extractor of TM-proteins out of the PPM. Although none of these proteins turned out to be necessary for the PPM extraction step, they reliably reflect the interactors of the designed constructs on its way to the MCs. This work revealed the location and function of previously unknown proteins in *P. falciparum*. Also, the obtained results corroborate what was reported regarding SBP1 being arrested on the PVM (Mesén-Ramírez *et al.*, 2016) and REX2 being arrested on PPM (Gruring *et al.*, 2012) when the mDHFR domain is folded. In the case of the SBP1 construct, mostly proteins belonging to the PTEX were biotinylated, indicating that the construct is deeply buried in the translocon. Whereas, the identification of proteins located in the parasite periphery, including the ERAD component (e.g. EMC2 and UDF1) suggested that also the interactome approach was successful and that the C-terminal region of the REX2-mDHFR-BirA*-3xHA construct was exposed to the cytosol. This might indicate that either PPM components are not involved (e.g. if simply PTEX extracts the protein from the PPM without contribution from other proteins in the PPM or PPM cytosolic face) or they were not reachable by BirA*.

The differences in interactomes of a reporter construct presumed to predominantly arrested in the PPM (REX2-based) compared to a co-blocking one likely stuck in PTEX (SBP1-based), indicates that in principle this approach was successful. Nevertheless, unfortunately, none of the candidates analyzed appeared to be involved in the extraction step out of the PPM. It must be considered that maybe our tactic is not suitable to find the extractor, possibly because its nature or the mechanism of action are not amenable to this approach. However, having obtained such a large list of proteins in MS, it cannot be excluded that one or several of these proteins, which so far remain anonymous, may be the key to the extraction and this work took the first steps towards their identification.

In this work, and thanks to the methodology of SLI, it was possible for the first time to create cell lines where two proteins were endogenously tagged in the *P. falciparum* genome,

something that to my knowledge, has not done before. It is also the first work reporting full length tagged PfEMP1 in the parasite. In addition, it also is a physiologically expressed PfEMP1 and SLI also overcomes the problem of having a mix of parasites each expressing a different PfEMP1, a problem that has plagued research into PfEMP1 since the discovery of this major virulence factor. The advantage to have a PfEMP1 endogenously tagged allowed us to study the effect of jamming PTEX on the PfEMP1 export. However many confounders complicate the study of determining if PfEMP1 needs PTEX for export such as (i) the use of SBP1 as the PTEX blocker which itself and other co-blocked proteins is necessary for PfEMP1 trafficking, and (ii) the fact that blocking PTEX does not avoid PfEMP1 export but all the exported proteins necessary for correct morphology of the MC. Using careful stage specific assays these problems were here attempted to be avoided and while it is still unsure whether PfEMP1 uses PTEX or not in order to cross the PPM, the data of this thesis overall supports the previously raised idea that PfEMP1 does not use PTEX. Future work could use a different protein to induce a co-block, however this would also co-block endogenous SBP1 and all other proteins needed for PfEMP1 transport and correct MC morphology and hence, this work here likely presents the best possible analysis using this approach based on the currently available methodology.

The analysis of how TM proteins, such as the major virulence factor PfEMP1, are extracted out of the membranes during export is an interesting field in parasite biology and additional analysis of the PV area resident proteins are needed in order to resolve the intricate series of mechanism necessary for the TM-protein extraction.

Bibliography

Abu Bakar, N., Klonis, N., Hanssen, E., Chan, C. and Tilley, L. (2010) 'Digestive-vacuole genesis and endocytic processes in the early intraerythrocytic stages of *Plasmodium falciparum*', *J Cell Sci*, 123(Pt 3), pp. 441-50.

Achan, J., Talisuna, A. O., Erhart, A., Yeka, A., Tibenderana, J. K., Baliraine, F. N., Rosenthal, P. J. and D'Alessandro, U. (2011) 'Quinine, an old anti-malarial drug in a modern world: role in the treatment of malaria', *Malar J*, 10, pp. 144.

Ajioka, J. W. (1997) *The protozoan phylum Apicomplexa. Methods* United States.

Amino, R., Thiberge, S., Blazquez, S., Baldacci, P., Renaud, O., Shorte, S. and Menard, R. (2007) 'Imaging malaria sporozoites in the dermis of the mammalian host', *Nat Protoc*, 2(7), pp. 1705-12.

Amino, R., Thiberge, S., Martin, B., Celli, S., Shorte, S., Frischknecht, F. and Menard, R. (2006a) 'Quantitative imaging of Plasmodium transmission from mosquito to mammal', *Nat Med*, 12(2), pp. 220-4.

Amino, R., Thiberge, S., Shorte, S., Frischknecht, F. and Menard, R. (2006b) 'Quantitative imaging of Plasmodium sporozoites in the mammalian host', *C R Biol*, 329(11), pp. 858-62.

Ariey, F., Witkowski, B., Amaratunga, C., Beghain, J., Langlois, A. C., Khim, N., Kim, S., Duru, V., Bouchier, C., Ma, L., Lim, P., Leang, R., Duong, S., Sreng, S., Suon, S., Chuor, C. M., Bout, D. M., Menard, S., Rogers, W. O., Genton, B., Fandeur, T., Miotto, O., Ringwald, P., Le Bras, J., Berry, A., Barale, J. C., Fairhurst, R. M., Benoit-Vical, F., Mercereau-Puijalon, O. and Menard, D. (2014) 'A molecular marker of artemisinin-resistant *Plasmodium falciparum* malaria', *Nature*, 505(7481), pp. 50-5.

Armstrong, C. M. and Goldberg, D. E. (2007) 'An FKBP destabilization domain modulates protein levels in *Plasmodium falciparum*', *Nat Methods*, 4(12), pp. 1007-9.

Baars, T. L., Petri, S., Peters, C. and Mayer, A. (2007) 'Role of the V-ATPase in regulation of the vacuolar fission-fusion equilibrium', *Mol Biol Cell*, 18(10), pp. 3873-82.

Babst, M. (2014) 'Quality control: quality control at the plasma membrane: one mechanism does not fit all', *J Cell Biol*, 205(1), pp. 11-20.

Backhaus, R., Zehe, C., Wegehingel, S., Kehlenbach, A., Schwappach, B. and Nickel, W. (2004) 'Unconventional protein secretion: membrane translocation of FGF-2 does not require protein unfolding', *J Cell Sci*, 117(Pt 9), pp. 1727-36.

Banaszynski, L. A., Chen, L. C., Maynard-Smith, L. A., Ooi, A. G. and Wandless, T. J. (2006) 'A rapid, reversible, and tunable method to regulate protein function in living cells using synthetic small molecules', *Cell*, 126(5), pp. 995-1004.

Barber, B. E., Rajahram, G. S., Grigg, M. J., William, T. and Anstey, N. M. (2017) 'World Malaria Report: time to acknowledge *Plasmodium knowlesi* malaria', *Malar J*, 16(1), pp. 135.

Baruch, D. I., Pasloske, B. L., Singh, H. B., Bi, X., Ma, X. C., Feldman, M., Taraschi, T. F. and Howard, R. J. (1995) 'Cloning the *P. falciparum* gene encoding PfEMP1, a malarial variant antigen and adherence receptor on the surface of parasitized human erythrocytes', *Cell*, 82(1), pp. 77-87.

Batinovic, S., McHugh, E., Chisholm, S. A., Matthews, K., Liu, B., Dumont, L., Charnaud, S. C., Schneider, M. P., Gilson, P. R., de Koning-Ward, T. F., Dixon, M. W. A. and Tilley, L. (2017) 'An exported protein-interacting complex involved in the trafficking of virulence determinants in *Plasmodium*-infected erythrocytes', *Nat Commun*, 8, pp. 16044.

Battle, K. E., Guerra, C. A., Golding, N., Duda, K. A., Cameron, E., Howes, R. E., Elyazar, I. R., Baird, J. K., Reiner, R. C., Jr., Gething, P. W., Smith, D. L. and Hay, S. I. (2015) 'Global database of matched *Plasmodium falciparum* and *P. vivax* incidence and prevalence records from 1985-2013', *Sci Data*, 2, pp. 150012.

Bayer, M. J., Reese, C., Buhler, S., Peters, C. and Mayer, A. (2003) 'Vacuole membrane fusion: V0 functions after trans-SNARE pairing and is coupled to the Ca²⁺-releasing channel', *J Cell Biol*, 162(2), pp. 211-22.

Bayle, J. H., Grimley, J. S., Stankunas, K., Gestwicki, J. E., Wandless, T. J. and Crabtree, G. R. (2006) 'Rapamycin analogs with differential binding specificity permit orthogonal control of protein activity', *Chem Biol*, 13(1), pp. 99-107.

Beck, J. R., Muralidharan, V., Oksman, A. and Goldberg, D. E. (2014) 'PTEX component HSP101 mediates export of diverse malaria effectors into host erythrocytes', *Nature*, 511(7511), pp. 592-5.

Belshaw, P. J., Ho, S. N., Crabtree, G. R. and Schreiber, S. L. (1996) 'Controlling protein association and subcellular localization with a synthetic ligand that induces heterodimerization of proteins', *Proc Natl Acad Sci U S A*, 93(10), pp. 4604-7.

Bignami, A. and Bastianelli, G. (1889) 'Observations of estivo-autumnal malaria', *Riforma Medica*, 6, pp. 1334-1335.

Birnbaum, J., Flemming, S., Reichard, N., Soares, A. B., Mesen-Ramirez, P., Jonscher, E., Bergmann, B. and Spielmann, T. (2017) 'A genetic system to study *Plasmodium falciparum* protein function', *Nat Methods*, 14(4), pp. 450-456.

Blisnick, T., Morales Betoulle, M. E., Barale, J. C., Uzureau, P., Berry, L., Desroses, S., Fujioka, H., Mattei, D. and Braun Breton, C. (2000) 'Pfsbp1, a Maurer's cleft *Plasmodium falciparum* protein, is associated with the erythrocyte skeleton', *Mol Biochem Parasitol*, 111(1), pp. 107-21.

Boddey, J. A., Carvalho, T. G., Hodder, A. N., Sargeant, T. J., Sleebbs, B. E., Marapana, D., Lopaticki, S., Nebl, T. and Cowman, A. F. (2013) 'Role of plasmepsin V in export of diverse protein families from the *Plasmodium falciparum* exportome', *Traffic*, 14(5), pp. 532-50.

Boddey, J. A. and Cowman, A. F. (2013) 'Plasmodium nesting: remaking the erythrocyte from the inside out', *Annu Rev Microbiol*, 67, pp. 243-69.

Boddey, J. A., Hodder, A. N., Gunther, S., Gilson, P. R., Patsiouras, H., Kapp, E. A., Pearce, J. A., de Koning-Ward, T. F., Simpson, R. J., Crabb, B. S. and Cowman, A. F. (2010) 'An aspartyl protease directs malaria effector proteins to the host cell', *Nature*, 463(7281), pp. 627-31.

Boddey, J. A., Moritz, R. L., Simpson, R. J. and Cowman, A. F. (2009) 'Role of the Plasmodium export element in trafficking parasite proteins to the infected erythrocyte', *Traffic*, 10(3), pp. 285-99.

Boersema, P. J., Raijmakers, R., Lemeer, S., Mohammed, S. and Heck, A. J. (2009) 'Multiplex peptide stable isotope dimethyl labeling for quantitative proteomics', *Nat Protoc*, 4(4), pp. 484-94.

Boucher, M. J., Ghosh, S., Zhang, L., Lal, A., Jang, S. W., Ju, A., Zhang, S., Wang, X., Ralph, S. A., Zou, J., Elias, J. E. and Yeh, E. (2018) 'Integrative proteomics and bioinformatic

prediction enable a high-confidence apicoplast proteome in malaria parasites', *PLoS Biol*, 16(9), pp. e2005895.

Boucher, M. J. and Yeh, E. (2019) 'Disruption of Apicoplast Biogenesis by Chemical Stabilization of an Imported Protein Evades the Delayed-Death Phenotype in Malaria Parasites', *mSphere*, 4(1).

Boundenga, L., Perkins, S. L., Ollomo, B., Rougeron, V., Leroy, E. M., Renaud, F. and Prugnolle, F. (2017) 'Haemosporidian Parasites of Reptiles and Birds from Gabon, Central Africa', *J Parasitol*, 103(4), pp. 330-337.

Bradley, P. J., Rayatpisheh, S., Wohlschlegel, J. A. and Nadipuram, S. M. (2020) 'Using BioID for the Identification of Interacting and Proximal Proteins in Subcellular Compartments in *Toxoplasma gondii*', *Methods Mol Biol*, 2071, pp. 323-346.

Bullen, H. E., Charnaud, S. C., Kalanon, M., Riglar, D. T., Dekiwadia, C., Kangwanrangsan, N., Torii, M., Tsuboi, T., Baum, J., Ralph, S. A., Cowman, A. F., de Koning-Ward, T. F., Crabb, B. S. and Gilson, P. R. (2012) 'Biosynthesis, localization, and macromolecular arrangement of the *Plasmodium falciparum* translocon of exported proteins (PTEX)', *J Biol Chem*, 287(11), pp. 7871-84.

Bushell, E., Gomes, A. R., Sanderson, T., Anar, B., Girling, G., Herd, C., Metcalf, T., Modrzynska, K., Schwach, F., Martin, R. E., Mather, M. W., McFadden, G. I., Parts, L., Rutledge, G. G., Vaidya, A. B., Wengelnik, K., Rayner, J. C. and Billker, O. (2017) 'Functional Profiling of a Plasmodium Genome Reveals an Abundance of Essential Genes', *Cell: Vol. 2*, pp. 260-272 e8.

Chen, J., Zheng, X. F., Brown, E. J. and Schreiber, S. L. (1995) 'Identification of an 11-kDa FKBP12-rapamycin-binding domain within the 289-kDa FKBP12-rapamycin-associated protein and characterization of a critical serine residue', *Proc Natl Acad Sci U S A*, 92(11), pp. 4947-51.

Chen, M., Shimada, T., Moulton, A., Cline, A., Humphries, R., Maizel, J. and Nienhuis, A. (1984) 'The Functional Human Dihydrofolate Reductase Gene', *The Journal of biological chemistry*, 259(6).

- Chen, Q., Fernandez, V., Sundstrom, A., Schlichtherle, M., Datta, S., Hagblom, P. and Wahlgren, M. (1998) 'Developmental selection of var gene expression in *Plasmodium falciparum*', *Nature*, 394(6691), pp. 392-5.
- Chisholm, S. A., McHugh, E., Lundie, R., Dixon, M. W., Ghosh, S., O'Keefe, M., Tilley, L., Kalanon, M. and de Koning-Ward, T. F. (2016) 'Contrasting Inducible Knockdown of the Auxiliary PTEX Component PTEX88 in *P. falciparum* and *P. berghei* Unmasks a Role in Parasite Virulence', *PLoS One*, 11(2), pp. e0149296.
- Chitwood, P. J., Juskiewicz, S., Guna, A., Shao, S. and Hegde, R. S. (2018) 'EMC Is Required to Initiate Accurate Membrane Protein Topogenesis', *Cell*, 175(6), pp. 1507-1519 e16.
- Choi, J., Chen, J., Schreiber, S. L. and Clardy, J. (1996) 'Structure of the FKBP12-rapamycin complex interacting with the binding domain of human FRAP', *Science*, 273(5272), pp. 239-42.
- Christianson, J. C., Olzmann, J. A., Shaler, T. A., Sowa, M. E., Bennett, E. J., Richter, C. M., Tyler, R. E., Greenblatt, E. J., Harper, J. W. and Kopito, R. R. (2011) 'Defining human ERAD networks through an integrative mapping strategy', *Nat Cell Biol*, 14(1), pp. 93-105.
- Chung, D. W. D., Ponts, N., Prudhomme, J., Rodrigues, E. M. and Le Roch, K. G. (2012) 'Characterization of the Ubiquitylating Components of the Human Malaria Parasite's Protein Degradation Pathway', *PLoS One*, 7(8).
- Claessen, J. H., Kundrat, L. and Ploegh, H. L. (2012) 'Protein quality control in the ER: balancing the ubiquitin checkbook', *Trends Cell Biol*, 22(1), pp. 22-32.
- Clark, H. C. (1915) 'The diagnostic value of the placental blood film in aestivo-autumnal malaria.', *J Exp Med*, 22(4), pp. 427-44.
- Clyde, D. F., Most, H., McCarthy, V. C. and Vanderberg, J. P. (1973) 'Immunization of man against sporozite-induced falciparum malaria', *Am J Med Sci*, 266(3), pp. 169-77.
- Colina-Tenorio, L., Dautant, A., Miranda-Astudillo, H., Giraud, M. F. and González-Halphen, D. (2018) 'The Peripheral Stalk of Rotary ATPases', *Front Physiol*, 9.
- Collins, W. E. and Jeffery, G. M. (2005) 'Plasmodium ovale: parasite and disease', *Clin Microbiol Rev*, 18(3), pp. 570-81.

- Collins, W. E. and Jeffery, G. M. (2007) 'Plasmodium malariae: parasite and disease', *Clin Microbiol Rev*, 20(4), pp. 579-92.
- Cooke, B. M., Buckingham, D. W., Glenister, F. K., Fernandez, K. M., Bannister, L. H., Marti, M., Mohandas, N. and Coppel, R. L. (2006) 'A Maurer's cleft-associated protein is essential for expression of the major malaria virulence antigen on the surface of infected red blood cells', *J Cell Biol*, 172(6), pp. 899-908.
- Coppi, A., Tewari, R., Bishop, J. R., Bennett, B. L., Lawrence, R., Esko, J. D., Billker, O. and Sinnis, P. (2007) 'Heparan sulfate proteoglycans provide a signal to Plasmodium sporozoites to stop migrating and productively invade host cells', *Cell Host Microbe*, 2(5), pp. 316-27.
- Coquelin, F., Boulard, Y., Mora-Silvera, E., Richard, F., Chabaud, A. G. and Landau, I. (1999) 'Final stage of maturation of the erythrocytic schizonts of rodent Plasmodium in the lungs', *C R Acad Sci III*, 322(1), pp. 55-62.
- Cowman, A. F., Coppel, R. L., Saint, R. B., Favaloro, J., Crewther, P. E., Stahl, H. D., Bianco, A. E., Brown, G. V., Anders, R. F. and Kemp, D. J. (1984) 'The ring-infected erythrocyte surface antigen (RESA) polypeptide of *Plasmodium falciparum* contains two separate blocks of tandem repeats encoding antigenic epitopes that are naturally immunogenic in man', *Mol Biol Med*, 2(3), pp. 207-21.
- Crabb, B. S., Rug, M., Gilberger, T. W., Thompson, J. K., Triglia, T., Maier, A. G. and Cowman, A. F. (2004) 'Transfection of the human malaria parasite *Plasmodium falciparum*', *Methods Mol Biol*, 270, pp. 263-76.
- Crutcher, J. M. and Hoffman, S. L. (1996) 'Malaria', in Baron S, e. (ed.). Galveston (TX): University of Texas Medical Branch at Galveston.
- Das, A. K., Cohen, P. W. and Barford, D. (1998) 'The structure of the tetratricopeptide repeats of protein phosphatase 5: implications for TPR-mediated protein-protein interactions', *Embo j*, 17(5), pp. 1192-9.
- Dave, K., Gelman, H., Thu, C. T., Guin, D. and Gruebele, M. (2016) 'The Effect of Fluorescent Protein Tags on Phosphoglycerate Kinase Stability Is Nonadditive', *J Phys Chem B*, 120(11), pp. 2878-85.

David, P. H., Hommel, M., Miller, L. H., Udeinya, I. J. and Oligino, L. D. (1983) 'Parasite sequestration in *Plasmodium falciparum* malaria: spleen and antibody modulation of cytoadherence of infected erythrocytes', *Proc Natl Acad Sci U S A*, 80(16), pp. 5075-9.

de Koning-Ward, T. F., Gilson, P. R., Boddey, J. A., Rug, M., Smith, B. J., Papenfuss, A. T., Sanders, P. R., Lundie, R. J., Maier, A. G., Cowman, A. F. and Crabb, B. S. (2009) 'A newly discovered protein export machine in malaria parasites', *Nature*, 459(7249), pp. 945-9.

De Niz, M., Burda, P. C., Kaiser, G., Del Portillo, H. A., Spielmann, T., Frischknecht, F. and Heussler, V. T. (2017) 'Progress in imaging methods: insights gained into Plasmodium biology', *Nat Rev Microbiol*, 15(1), pp. 37-54.

De Niz, M., Ullrich, A. K., Heiber, A., Blancke Soares, A., Pick, C., Lyck, R., Keller, D., Kaiser, G., Prado, M., Flemming, S., Del Portillo, H., Janse, C. J., Heussler, V. and Spielmann, T. (2016) 'The machinery underlying malaria parasite virulence is conserved between rodent and human malaria parasites', *Nat Commun*, 7, pp. 11659.

Deponte, M., Hoppe, H. C., Lee, M. C., Maier, A. G., Richard, D., Rug, M., Spielmann, T. and Przyborski, J. M. (2012) 'Wherever I may roam: protein and membrane trafficking in *P. falciparum*-infected red blood cells', *Mol Biochem Parasitol*, 186(2), pp. 95-116.

Dondorp, A. M., Nosten, F., Yi, P., Das, D., Phyto, A. P., Tarning, J., Lwin, K. M., Ariey, F., Hanpithakpong, W., Lee, S. J., Ringwald, P., Silamut, K., Imwong, M., Chotivanich, K., Lim, P., Herdman, T., An, S. S., Yeung, S., Singhasivanon, P., Day, N. P., Lindegardh, N., Socheat, D. and White, N. J. (2009) 'Artemisinin resistance in *Plasmodium falciparum* malaria', *N Engl J Med*, 361(5), pp. 455-67.

Drory, O., Frolow, F. and Nelson, N. (2004) 'Crystal structure of yeast V-ATPase subunit C reveals its stator function', *EMBO Rep*, 5(12), pp. 1148-52.

Duraisingh, M. T., Triglia, T. and Cowman, A. F. (2002) 'Negative selection of *Plasmodium falciparum* reveals targeted gene deletion by double crossover recombination', *Int J Parasitol*, 32(1), pp. 81-9.

Duval, L., Robert, V., Csorba, G., Hassanin, A., Randrianarivelojosia, M., Walston, J., Nhim, T., Goodman, S. M. and Ariey, F. (2007) 'Multiple host-switching of Haemosporidia parasites in bats', *Malar J*, pp. 157.

Eilers, M., Hwang, S. and Schatz, G. (1988) 'Unfolding and refolding of a purified precursor protein during import into isolated mitochondria', *Embo j*, 7(4), pp. 1139-45.

Eilers, M. and Schatz, G. (1986) 'Binding of a specific ligand inhibits import of a purified precursor protein into mitochondria', *Nature*, 322(6076), pp. 228-32.

Elsworth, B., Matthews, K., Nie, C. Q., Kalanon, M., Charnaud, S. C., Sanders, P. R., Chisholm, S. A., Counihan, N. A., Shaw, P. J., Pino, P., Chan, J. A., Azevedo, M. F., Rogerson, S. J., Beeson, J. G., Crabb, B. S., Gilson, P. R. and de Koning-Ward, T. F. (2014) 'PTEX is an essential nexus for protein export in malaria parasites', *Nature*, 511(7511), pp. 587-91.

Elsworth, B., Sanders, P. R., Nebl, T., Batinovic, S., Kalanon, M., Nie, C. Q., Charnaud, S. C., Bullen, H. E., de Koning Ward, T. F., Tilley, L., Crabb, B. S. and Gilson, P. R. (2016) 'Proteomic analysis reveals novel proteins associated with the Plasmodium protein exporter PTEX and a loss of complex stability upon truncation of the core PTEX component, PTEX150', *Cell Microbiol*, 18(11), pp. 1551-1569.

Epp, C., Raskolnikov, D. and Deitsch, K. W. (2008) 'A regulatable transgene expression system for cultured *Plasmodium falciparum* parasites', *Malar J*, 7, pp. 86.

Fidock, D. A., Nomura, T., Talley, A. K., Cooper, R. A., Dzekunov, S. M., Ferdig, M. T., Ursos, L. M., Sidhu, A. B., Naude, B., Deitsch, K. W., Su, X. Z., Wootton, J. C., Roepe, P. D. and Wellems, T. E. (2000) 'Mutations in the *P. falciparum* digestive vacuole transmembrane protein PfCRT and evidence for their role in chloroquine resistance', *Mol Cell*, 6(4), pp. 861-71.

Fidock, D. A. and Wellems, T. E. (1997) 'Transformation with human dihydrofolate reductase renders malaria parasites insensitive to WR99210 but does not affect the intrinsic activity of proguanil', *Proc Natl Acad Sci U S A*, 94(20), pp. 10931-6.

Flick, K. and Chen, Q. (2004) 'var genes, PfEMP1 and the human host', *Mol Biochem Parasitol*, 134(1), pp. 3-9.

Francia, M. E. and Striepen, B. (2014) 'Cell division in apicomplexan parasites', *Nat Rev Microbiol*, 12(2), pp. 125-36.

Francis, S. E. (1997) 'Biosynthesis and Maturation of the Malaria Aspartic Hemoglobinases Plasmepsins I and II', *Journal of Biological Chemistry*, 272(23), pp. 14961-14968.

Frankland, S., Adisa, A., Horrocks, P., Taraschi, T. F., Schneider, T., Elliott, S. R., Rogerson, S. J., Knuepfer, E., Cowman, A. F., Newbold, C. I. and Tilley, L. (2006) 'Delivery of the malaria virulence protein PfEMP1 to the erythrocyte surface requires cholesterol-rich domains', *Eukaryot Cell*, 5(5), pp. 849-60.

Fried, M. and Duffy, P. E. (1996) 'Adherence of *Plasmodium falciparum* to chondroitin sulfate A in the human placenta', *Science*, 272(5267), pp. 1502-4.

Galaway, F., Drought, L. G., Fala, M., Cross, N., Kemp, A. C., Rayner, J. C. and Wright, G. J. (2017) 'P113 is a merozoite surface protein that binds the N terminus of *Plasmodium falciparum* RH5', *Nat Commun*, 8, pp. 14333.

Ganesan, S. M., Morrisey, J. M., Ke, H., Painter, H. J., Laroiya, K., Phillips, M. A., Rathod, P. K., Mather, M. W. and Vaidya, A. B. (2011) 'Yeast Dihydroorotate Dehydrogenase as a New Selectable Marker for *Plasmodium falciparum* Transfection', *Mol Biochem Parasitol*, 177(1), pp. 29-34.

Gardner, J. P., Pinches, R. A., Roberts, D. J. and Newbold, C. I. (1996) 'Variant antigens and endothelial receptor adhesion in *Plasmodium falciparum*', *Proc Natl Acad Sci U S A*, 93(8), pp. 3503-8.

Garten, M., Nasamu, A. S., Niles, J. C., Zimmerberg, J., Goldberg, D. E. and Beck, J. R. (2018) 'EXP2 is a nutrient-permeable channel in the vacuolar membrane of *Plasmodium* and is essential for protein export via PTEX', *Nat Microbiol*, 3(10), pp. 1090-8.

Gehde, N., Hinrichs, C., Montilla, I., Charpian, S., Lingelbach, K. and Przyborski, J. M. (2009) 'Protein unfolding is an essential requirement for transport across the parasitophorous vacuolar membrane of *Plasmodium falciparum*', *Mol Microbiol*, 71(3), pp. 613-28.

Ghorbal, M., Gorman, M., Macpherson, C. R., Martins, R. M., Scherf, A. and Lopez-Rubio, J. J. (2014) 'Genome editing in the human malaria parasite *Plasmodium falciparum* using the CRISPR-Cas9 system', *Nat Biotechnol*, 32(8), pp. 819-21.

Gilles, H. and Warrell, D. (2019) *Essential malariology*. 4th edn. Boca Raton, FL. USA: Taylor & Francis Group, p. 352.

Goebel, M. and Yanagida, M. (1991) 'The TPR snap helix: a novel protein repeat motif from mitosis to transcription', *Trends Biochem Sci*, 16(5), pp. 173-7.

Gold, D. A., Kaplan, A. D., Lis, A., Bett, G. C., Rosowski, E. E., Cirelli, K. M., Bougdour, A., Sidik, S. M., Beck, J. R., Lourido, S., Egea, P. F., Bradley, P. J., Hakimi, M. A., Rasmusson, R. L. and Saeij, J. P. (2015) 'The Toxoplasma Dense Granule Proteins GRA17 and GRA23 Mediate the Movement of Small Molecules between the Host and the Parasitophorous Vacuole', *Cell Host Microbe*, 17(5), pp. 642-52.

Goldberg, D. E. (2012) 'Plasmodium protein export at higher PEXEL resolution', *Cell Host Microbe*, 12(5), pp. 609-10.

Goldberg, D. E., Slater, A. F., Beavis, R., Chait, B., Cerami, A. and Henderson, G. B. (1991) 'Hemoglobin degradation in the human malaria pathogen *Plasmodium falciparum*: a catabolic pathway initiated by a specific aspartic protease', *J Exp Med*, 173(4), pp. 961-9.

Goldberg, D. E., Slater, A. F., Cerami, A. and Henderson, G. B. (1990) 'Hemoglobin degradation in the malaria parasite *Plasmodium falciparum*: an ordered process in a unique organelle', *Proc Natl Acad Sci U S A*, 87(8), pp. 2931-5.

Gomes, A. R., Bushell, E., Schwach, F., Girling, G., Anar, B., Quail, M. A., Herd, C., Pfander, C., Modrzynska, K., Rayner, J. C. and Billker, O. (2015) 'A genome-scale vector resource enables high-throughput reverse genetic screening in a malaria parasite', *Cell Host Microbe*, 17(3), pp. 404-413.

Greenwood, B. M., Fidock, D. A., Kyle, D. E., Kappe, S. H., Alonso, P. L., Collins, F. H. and Duffy, P. E. (2008) 'Malaria: progress, perils, and prospects for eradication', *J Clin Invest*, 118(4), pp. 1266-76.

Gruring, C., Heiber, A., Kruse, F., Flemming, S., Franci, G., Colombo, S. F., Fasana, E., Schoeler, H., Borgese, N., Stunnenberg, H. G., Przyborski, J. M., Gilberger, T. W. and Spielmann, T. (2012) 'Uncovering common principles in protein export of malaria parasites', *Cell Host Microbe*, 12(5), pp. 717-29.

Gruring, C., Heiber, A., Kruse, F., Ungefehr, J., Gilberger, T. W. and Spielmann, T. (2011) 'Development and host cell modifications of *Plasmodium falciparum* blood stages in four dimensions', *Nat Commun*, 2, pp. 165.

Gueirard, P., Tavares, J., Thiberge, S., Bernex, F., Ishino, T., Milon, G., Franke-Fayard, B., Janse, C. J., Menard, R. and Amino, R. (2010) 'Development of the malaria parasite in the skin of the mammalian host', *Proc Natl Acad Sci U S A*, 107(43), pp. 18640-5.

Guna, A., Volkmar, N., Christianson, J. C. and Hegde, R. S. (2018) 'The ER membrane protein complex is a transmembrane domain insertase', *Science*, 359(6374), pp. 470-473.

Haase, S. and de Koning-Ward, T. F. (2010) 'New insights into protein export in malaria parasites', *Cell Microbiol*, 12(5), pp. 580-7.

Haruki, H., Nishikawa, J. and Laemmli, U. K. (2008) 'The anchor-away technique: rapid, conditional establishment of yeast mutant phenotypes', *Mol Cell*, 31(6), pp. 925-32.

Hawthorne, P. L., Trenholme, K. R., Skinner-Adams, T. S., Spielmann, T., Fischer, K., Dixon, M. W., Ortega, M. R., Anderson, K. L., Kemp, D. J. and Gardiner, D. L. (2004) 'A novel *Plasmodium falciparum* ring stage protein, REX, is located in Maurer's clefts', *Mol Biochem Parasitol*, 136(2), pp. 181-9.

Heiber, A., Kruse, F., Pick, C., Gruring, C., Flemming, S., Oberli, A., Schoeler, H., Retzlaff, S., Mesen-Ramirez, P., Hiss, J. A., Kadekoppala, M., Hecht, L., Holder, A. A., Gilberger, T. W. and Spielmann, T. (2013) 'Identification of new PNEPs indicates a substantial non-PEXEL exportome and underpins common features in *Plasmodium falciparum* protein export', *PLoS Pathog*, 9(8), pp. e1003546.

Heiny, S. R., Pautz, S., Recker, M. and Przyborski, J. M. (2014) 'Protein Traffic to the *Plasmodium falciparum* apicoplast: evidence for a sorting branch point at the Golgi', *Traffic*, 15(12), pp. 1290-304.

Hiller, N. L., Bhattacharjee, S., van Ooij, C., Liolios, K., Harrison, T., Lopez-Estrano, C. and Haldar, K. (2004) 'A host-targeting signal in virulence proteins reveals a secretome in malarial infection', *Science*, 306(5703), pp. 1934-7.

Ho, C. M., Beck, J. R., Lai, M., Cui, Y., Goldberg, D. E., Egea, P. F. and Zhou, Z. H. (2018) 'Malaria parasite translocon structure and mechanism of effector export', *Nature*, 561(7721), pp. 70-75.

Howard, R. J., Barnwell, J. W., Rock, E. P., Neequaye, J., Ofori-Adjei, D., Maloy, W. L., Lyon, J. A. and Saul, A. (1988) 'Two approximately 300 kilodalton *Plasmodium falciparum* proteins at the surface membrane of infected erythrocytes', *Mol Biochem Parasitol*, 27(2-3), pp. 207-23.

Howell, D. P., Levin, E. A., Springer, A. L., Kraemer, S. M., Phippard, D. J., Schief, W. R. and Smith, J. D. (2008) 'Mapping a common interaction site used by *Plasmodium falciparum* Duffy binding-like domains to bind diverse host receptors', *Mol Microbiol*, 67(1), pp. 78-87.

Howes, R. E., Battle, K. E., Mendis, K. N., Smith, D. L., Cibulskis, R. E., Baird, J. K. and Hay, S. I. (2016) 'Global Epidemiology of *Plasmodium vivax*', *Am J Trop Med Hyg*, 95(6 Suppl), pp. 15-34.

Hyde, J. E. (2007) 'Drug-resistant malaria - an insight', *FEBS J*, 274(18), pp. 4688-98.

Johnson, E. S., Ma, P. C., Ota, I. M. and Varshavsky, A. (1995) 'A proteolytic pathway that recognizes ubiquitin as a degradation signal', *J Biol Chem*, 270(29), pp. 17442-56.

Jonikas, M. C., Collins, S. R., Denic, V., Oh, E., Quan, E. M., Schmid, V., Weibezahn, J., Schwappach, B., Walter, P., Weissman, J. S. and Schuldiner, M. (2009) 'Comprehensive characterization of genes required for protein folding in the endoplasmic reticulum', *Science*, 323(5922), pp. 1693-7.

Kaiser, K., Matuschewski, K., Camargo, N., Ross, J. and Kappe, S. H. (2004) 'Differential transcriptome profiling identifies *Plasmodium* genes encoding pre-erythrocytic stage-specific proteins', *Mol Microbiol*, 51(5), pp. 1221-32.

Kalanon, M., Bargieri, D., Sturm, A., Matthews, K., Ghosh, S., Goodman, C. D., Thiberge, S., Mollard, V., McFadden, G. I., Menard, R. and de Koning-Ward, T. F. (2015) 'The PTEX component EXP2 is critical for establishing a patent malaria infection in mice', *Cell Microbiol*.

Kalanon, M., Bargieri, D., Sturm, A., Matthews, K., Ghosh, S., Goodman, C. D., Thiberge, S., Mollard, V., McFadden, G. I., Menard, R. and de Koning-Ward, T. F. (2016) 'The *Plasmodium* translocon of exported proteins component EXP2 is critical for establishing a patent malaria infection in mice', *Cell Microbiol*, 18(3), pp. 399-412.

Kehrer, J., Frischknecht, F. and Mair, G. R. (2016) 'Proteomic Analysis of the *Plasmodium berghei* Gametocyte Egressome and Vesicular bioID of Osmiophilic Body Proteins Identifies Merozoite TRAP-like Protein (MTRAP) as an Essential Factor for Parasite Transmission', *Mol Cell Proteomics*, 15(9), pp. 2852-62.

Khosh-Naucke, M. (2018) *Identification of novel parasitophorous vacuole proteins in P. falciparum parasites using BioID*. doctoral degree, Hamburg univeristy, Hamburg.

- Khosh-Naucke, M., Becker, J., Mesen-Ramirez, P., Kiani, P., Birnbaum, J., Frohlike, U., Jonscher, E., Schluter, H. and Spielmann, T. (2018) 'Identification of novel parasitophorous vacuole proteins in *P. falciparum* parasites using BioID', *Int J Med Microbiol*, 308(1), pp. 13-24.
- Kitagawa, N., Mazon, H., Heck, A. J. and Wilkens, S. (2008) 'Stoichiometry of the peripheral stalk subunits E and G of yeast V1-ATPase determined by mass spectrometry', *J Biol Chem*, 283(6), pp. 3329-37.
- Knuepfer, E., Rug, M., Klonis, N., Tilley, L. and Cowman, A. F. (2005) 'Trafficking determinants for PfEMP3 export and assembly under the *Plasmodium falciparum*-infected red blood cell membrane', *Mol Microbiol*, 58(4), pp. 1039-53.
- Kono, M., Herrmann, S., Loughran, N. B., Cabrera, A., Engelberg, K., Lehmann, C., Sinha, D., Prinz, B., Ruch, U., Heussler, V., Spielmann, T., Parkinson, J. and Gilberger, T. W. (2012) 'Evolution and architecture of the inner membrane complex in asexual and sexual stages of the malaria parasite', *Mol Biol Evol*, 29(9), pp. 2113-32.
- Kraemer, S. M. and Smith, J. D. (2006) 'A family affair: var genes, PfEMP1 binding, and malaria disease', *Curr Opin Microbiol*, 9(4), pp. 374-80.
- Kremer, K., Kamin, D., Rittweger, E., Wilkes, J., Flammer, H., Mahler, S., Heng, J., Tonkin, C. J., Langsley, G., Hell, S. W., Carruthers, V. B., Ferguson, D. J. and Meissner, M. (2013) 'An overexpression screen of *Toxoplasma gondii* Rab-GTPases reveals distinct transport routes to the micronemes', *PLoS Pathog*, 9(3), pp. e1003213.
- Kriek, N., Tilley, L., Horrocks, P., Pinches, R., Elford, B. C., Ferguson, D. J., Lingelbach, K. and Newbold, C. I. (2003) 'Characterization of the pathway for transport of the cytoadherence-mediating protein, PfEMP1, to the host cell surface in malaria parasite-infected erythrocytes', *Mol Microbiol*, 50(4), pp. 1215-27.
- Kuamsab, N., Putaporntip, C., Pattanawong, U. and Jongwutiwes, S. (2012) 'Simultaneous detection of *Plasmodium vivax* and *Plasmodium falciparum* gametocytes in clinical isolates by multiplex-nested RT-PCR', *Malaria Journal*, 11(1), pp. 1-8.
- Kyes, S., Horrocks, P. and Newbold, C. (2001) 'Antigenic variation at the infected red cell surface in malaria', *Annu Rev Microbiol*, 55, pp. 673-707.

- Kyes, S., Pinches, R. and Newbold, C. (2000) 'A simple RNA analysis method shows var and rif multigene family expression patterns in *Plasmodium falciparum*', *Mol Biochem Parasitol*, 105(2), pp. 311-5.
- Lamarque, M., Tastet, C., Poncet, J., Demette, E., Jouin, P., Vial, H. and Dubremetz, J. F. (2008) 'Food vacuole proteome of the malarial parasite *Plasmodium falciparum*', *Proteomics Clin Appl*, 2(9), pp. 1361-74.
- Lamb, J. R., Tugendreich, S. and Hieter, P. (1995) 'Tetratricopeptide repeat interactions: to TPR or not to TPR?', *Trends Biochem Sci*, 20(7), pp. 257-9.
- Langreth, S. G., Jensen, J. B., Reese, R. T. and Trager, W. (1978) 'Fine structure of human malaria in vitro', *J Protozool*, 25(4), pp. 443-52.
- Langreth, S. G., Reese, R. T., Motyl, M. R. and Trager, W. (1979) '*Plasmodium falciparum*: loss of knobs on the infected erythrocyte surface after long-term cultivation', *Exp Parasitol*, 48(2), pp. 213-9.
- Lazarus, M. D., Schneider, T. G. and Taraschi, T. F. (2008) 'A new model for hemoglobin ingestion and transport by the human malaria parasite *Plasmodium falciparum*', *J Cell Sci*, 121(Pt 11), pp. 1937-49.
- Leder, K., Black, J., O'Brien, D., Greenwood, Z., Kain, K. C., Schwartz, E., Brown, G. and Torresi, J. (2004) 'Malaria in travelers: a review of the GeoSentinel surveillance network', *Clin Infect Dis*, 39(8), pp. 1104-12.
- Leech, J. H., Barnwell, J. W., Aikawa, M., Miller, L. H. and Howard, R. J. (1984) '*Plasmodium falciparum* malaria: association of knobs on the surface of infected erythrocytes with a histidine-rich protein and the erythrocyte skeleton', *J Cell Biol*, 98(4), pp. 1256-64.
- Liang, J., Choi, J. and Clardy, J. (1999) 'Refined structure of the FKBP12-rapamycin-FRB ternary complex at 2.2 Å resolution', *Acta Crystallogr D Biol Crystallogr*, 55(Pt 4), pp. 736-44.
- Lim, L. and McFadden, G. I. (2010) 'The evolution, metabolism and functions of the apicoplast', *Philos Trans R Soc Lond B Biol Sci: Vol. 1541*, pp. 749-63.

Lu, M., Ammar, D., Ives, H., Albrecht, F. and Gluck, S. L. (2007) 'Physical interaction between aldolase and vacuolar H⁺-ATPase is essential for the assembly and activity of the proton pump', *J Biol Chem*, 282(34), pp. 24495-503.

Maier, A. G., Cooke, B. M., Cowman, A. F. and Tilley, L. (2009) 'Malaria parasite proteins that remodel the host erythrocyte', *Nat Rev Microbiol*, 7(5), pp. 341-54.

Maier, A. G., Rug, M., O'Neill, M. T., Beeson, J. G., Marti, M., Reeder, J. and Cowman, A. F. (2007) 'Skeleton-binding protein 1 functions at the parasitophorous vacuole membrane to traffic PfEMP1 to the *Plasmodium falciparum*-infected erythrocyte surface', *Blood*, 109(3), pp. 1289-97.

Maier, A. G., Rug, M., O'Neill, M. T., Brown, M., Chakravorty, S., Szestak, T., Chesson, J., Wu, Y., Hughes, K., Coppel, R. L., Newbold, C., Beeson, J. G., Craig, A., Crabb, B. S. and Cowman, A. F. (2008) 'Exported proteins required for virulence and rigidity of *Plasmodium falciparum*-infected human erythrocytes', *Cell*, 134(1), pp. 48-61.

Marchiafava, E. and Bignami, A. (1895) 'Two Monographs on Malaria and the Parasites of Malarial Fever: I. Marchiafava and Bignami; II. Mannaberg', *Edinb Med J*, 40(10), pp. 911-5.

Marti, M., Good, R. T., Rug, M., Knuepfer, E. and Cowman, A. F. (2004) 'Targeting malaria virulence and remodeling proteins to the host erythrocyte', *Science*, 306(5703), pp. 1930-3.

Marti, M. and Spielmann, T. (2013) 'Protein export in malaria parasites: many membranes to cross', *Curr Opin Microbiol*, 16(4), pp. 445-51.

Matthews, K., Kalanon, M., Chisholm, S. A., Sturm, A., Goodman, C. D., Dixon, M. W., Sanders, P. R., Nebl, T., Fraser, F., Haase, S., McFadden, G. I., Gilson, P. R., Crabb, B. S. and de Koning-Ward, T. F. (2013) 'The Plasmodium translocon of exported proteins (PTEX) component thioredoxin-2 is important for maintaining normal blood-stage growth', *Mol Microbiol*, 89(6), pp. 1167-86.

Matuschewski, K. (2006) 'Getting infectious: formation and maturation of Plasmodium sporozoites in the Anopheles vector', *Cell Microbiol*, 8(10), pp. 1547-56.

Matuschewski, K., Ross, J., Brown, S. M., Kaiser, K., Nussenzweig, V. and Kappe, S. H. (2002) 'Infectivity-associated changes in the transcriptional repertoire of the malaria parasite sporozoite stage', *J Biol Chem*, 277(44), pp. 41948-53.

Matz, J. M., Goosmann, C., Brinkmann, V., Grutzke, J., Ingmundson, A., Matuschewski, K. and Kooij, T. W. (2015a) 'The Plasmodium berghei translocon of exported proteins reveals spatiotemporal dynamics of tubular extensions', *Sci Rep*, 5, pp. 12532.

Matz, J. M., Ingmundson, A., Costa Nunes, J., Stenzel, W., Matuschewski, K. and Kooij, T. W. (2015b) 'In Vivo Function of PTEX88 in Malaria Parasite Sequestration and Virulence', *Eukaryot Cell*.

Matz, J. M., Matuschewski, K. and Kooij, T. W. (2013) 'Two putative protein export regulators promote Plasmodium blood stage development in vivo', *Mol Biochem Parasitol*, 191(1), pp. 44-52.

Maxson, M. E. and Grinstein, S. (2014) 'The vacuolar-type H(+)-ATPase at a glance - more than a proton pump', *J Cell Sci*, 127(Pt 23), pp. 4987-93.

Mayer, C., Slater, L., Erat, M. C., Konrat, R. and Vakonakis, I. (2012) 'Structural Analysis of the *Plasmodium falciparum* Erythrocyte Membrane Protein 1 (PfEMP1) Intracellular Domain Reveals a Conserved Interaction Epitope*', *J Biol Chem: Vol. 10*, pp. 7182-9.

Mbengue, A., Bhattacharjee, S., Pandharkar, T., Liu, H., Estiu, G., Stahelin, R. V., Rizk, S. S., Njimoh, D. L., Ryan, Y., Chotivanich, K., Nguon, C., Ghorbal, M., Lopez-Rubio, J. J., Pfrender, M., Emrich, S., Mohandas, N., Dondorp, A. M., Wiest, O. and Haldar, K. (2015) 'A molecular mechanism of artemisinin resistance in *Plasmodium falciparum* malaria', *Nature*, 520(7549), pp. 683-7.

McFadden, G. (2019) 'Apicoplast', *Current Biology*, 24(262), Available: Cell.

McKenzie, F. E., Jeffery, G. M. and Collins, W. E. (2001) 'Plasmodium malariae blood-stage dynamics', *J Parasitol*, 87(3), pp. 626-37.

McKenzie, F. E., Jeffery, G. M. and Collins, W. E. (2002) 'Plasmodium vivax blood-stage dynamics', *J Parasitol*, 88(3), pp. 521-35.

McMillan, P. J., Millet, C., Batinovic, S., Maiorca, M., Hanssen, E., Kenny, S., Muhle, R. A., Melcher, M., Fidock, D. A., Smith, J. D., Dixon, M. W. and Tilley, L. (2013) 'Spatial and temporal mapping of the PfEMP1 export pathway in *Plasmodium falciparum*', *Cell Microbiol*, 15(8), pp. 1401-18.

Melcher, M., Muhle, R. A., Henrich, P. P., Kraemer, S. M., Avril, M., Vigan-Womas, I., Mercereau-Puijalon, O., Smith, J. D. and Fidock, D. A. (2010) 'Identification of a Role for the PfEMP1 Semi-Conserved Head Structure in Protein Trafficking to the Surface of *Plasmodium falciparum* Infected Red Blood Cells', *Cell Microbiol*, 12(10), pp. 1446-62.

Menon, R. P., Gibson, T. J. and Pastore, A. (2004) 'The C terminus of fragile X mental retardation protein interacts with the multi-domain Ran-binding protein in the microtubule-organising centre', *J Mol Biol*, 343(1), pp. 43-53.

Merkulova, M., Hurtado-Lorenzo, A., Hosokawa, H., Zhuang, Z., Brown, D., Ausiello, D. A. and Marshansky, V. (2011) 'Aldolase directly interacts with ARNO and modulates cell morphology and acidic vesicle distribution', *Am J Physiol Cell Physiol*, 300(6), pp. C1442-55.

Mesen-Ramirez, P., Reinsch, F., Blancke Soares, A., Bergmann, B., Ullrich, A. K., Tenzer, S. and Spielmann, T. (2016) 'Stable Translocation Intermediates Jam Global Protein Export in *Plasmodium falciparum* Parasites and Link the PTEX Component EXP2 with Translocation Activity', *PLoS Pathog*, 12(5), pp. e1005618.

Mesén-Ramírez, P., Reinsch, F., Blancke Soares, A., Bergmann, B., Ullrich, A. K., Tenzer, S. and Spielmann, T. (2016) 'Stable Translocation Intermediates Jam Global Protein Export in *Plasmodium falciparum* Parasites and Link the PTEX Component EXP2 with Translocation Activity', *PLoS Pathog*, 12(5), pp. e1005618.

Meyer, H. H., Shorter, J. G., Seemann, J., Pappin, D. and Warren, G. (2000) 'A complex of mammalian Ufd1 and Npl4 links the AAA-ATPase, p97, to ubiquitin and nuclear transport pathways', *EMBO J*, 19(10), pp. 2181-92.

Miller, L. H., Baruch, D. I., Marsh, K. and Doumbo, O. K. (2002) 'The pathogenic basis of malaria', *Nature*, 415(6872), pp. 673-9.

Miller, L. H., Mason, S. J., Clyde, D. F. and McGinniss, M. H. (1976) 'The resistance factor to *Plasmodium vivax* in blacks. The Duffy-blood-group genotype, FyFy', *N Engl J Med*, 295(6), pp. 302-4.

Moore, L. R., Fujioka, H., Williams, P. S., Chalmers, J. J., Grimberg, B., Zimmerman, P. and Zborowski, M. (2006) 'Hemoglobin degradation in malaria-infected erythrocytes determined from live cell magnetophoresis', *FASEB J*, 20(6), pp. 747-9.

Morita, M., Nagaoka, H., Ntege, E. H., Kanoi, B. N., Ito, D., Nakata, T., Lee, J. W., Tokunaga, K., Iimura, T., Torii, M., Tsuboi, T. and Takashima, E. (2018) 'PV1, a novel *Plasmodium falciparum* merozoite dense granule protein, interacts with exported protein in infected erythrocytes', *Sci Rep*, 8(1), pp. 3696.

Morita, M., Takashima, E., Ito, D., Miura, K., Thongkukiatkul, A., Diouf, A., Fairhurst, R. M., Diakite, M., Long, C. A., Torii, M. and Tsuboi, T. (2017) 'Immunoscreening of *Plasmodium falciparum* proteins expressed in a wheat germ cell-free system reveals a novel malaria vaccine candidate', *Sci Rep*.

Mota, M. M. and Rodriguez, A. (2002) 'Invasion of mammalian host cells by *Plasmodium* sporozoites', *Bioessays*, 24(2), pp. 149-56.

Mueller, A. K., Labaied, M., Kappe, S. H. and Matuschewski, K. (2005) 'Genetically modified *Plasmodium* parasites as a protective experimental malaria vaccine', *Nature*, 433(7022), pp. 164-7.

Muller, I. B. and Hyde, J. E. (2010) 'Antimalarial drugs: modes of action and mechanisms of parasite resistance', *Future Microbiol*, 5(12), pp. 1857-73.

Ménard, R. (2013) *Malaria - Methods and Protocols. Methods in Molecular Biology (Book 923)*: Humana; 2nd ed. 2013 edition (September 19, 2012).

Nations, U. (2015) *Millennium Development Goals (Goal 6, malaria and other diseases)*: United Nations. Available at: <https://www.un.org/millenniumgoals/aids.shtml>.

Nelson, N., Perzov, N., Cohen, A., Hagai, K., Padler, V. and Nelson, H. (2000) 'The cellular biology of proton-motive force generation by V-ATPases', *J Exp Biol*, 203(Pt 1), pp. 89-95.

Newbold, C., Craig, A., Kyes, S., Rowe, A., Fernandez-Reyes, D. and Fagan, T. (1999) 'Cytoadherence, pathogenesis and the infected red cell surface in *Plasmodium falciparum*', *Int J Parasitol*, 29(6), pp. 927-37.

Newbold, C., Warn, P., Black, G., Berendt, A., Craig, A., Snow, B., Msobo, M., Peshu, N. and Marsh, K. (1997) 'Receptor-specific adhesion and clinical disease in *Plasmodium falciparum*', *Am J Trop Med Hyg*, 57(4), pp. 389-98.

Nowis, D., McConnell, E. and Wojcik, C. (2006) 'Destabilization of the VCP-Ufd1-Npl4 complex is associated with decreased levels of ERAD substrates', *Exp Cell Res*, 312(15), pp. 2921-32.

Nussenzweig, R. S., Vanderberg, J., Most, H. and Orton, C. (1967) 'Protective immunity produced by the injection of x-irradiated sporozoites of plasmodium berghei', *Nature*, 216(5111), pp. 160-2.

Oakley, M. S., Gerald, N., McCutchan, T. F., Aravind, L. and Kumar, S. (2011) 'Clinical and molecular aspects of malaria fever', *Trends Parasitol*, 27(10), pp. 442-9.

Okamoto, N., Spurck, T. P., Goodman, C. D. and McFadden, G. I. (2009) 'Apicoplast and mitochondrion in gametocytogenesis of *Plasmodium falciparum*', *Eukaryot Cell*, 8(1), pp. 128-32.

Orito, Y., Ishino, T., Iwanaga, S., Kaneko, I., Kato, T., Menard, R., Chinzei, Y. and Yuda, M. (2013) 'Liver-specific protein 2: a Plasmodium protein exported to the hepatocyte cytoplasm and required for merozoite formation', *Mol Microbiol*, 87(1), pp. 66-79.

Orlov, S. (2019) *Membrane Transporters in the Pathogenesis of Cardiovascular and Lung Disorders*. Moscow: Academic Press, ELSEVIER.

Osier, F. H., Mackinnon, M. J., Crosnier, C., Fegan, G., Kamuyu, G., Wanaguru, M., Ogada, E., McDade, B., Rayner, J. C., Wright, G. J. and Marsh, K. (2014) 'New antigens for a multicomponent blood-stage malaria vaccine', *Sci Transl Med*, 6(247), pp. 247ra102.

Pachlatko, E., Rusch, S., Muller, A., Hemphill, A., Tilley, L., Hanssen, E. and Beck, H. P. (2010) 'MAHRP2, an exported protein of *Plasmodium falciparum*, is an essential component of Maurer's cleft tethers', *Mol Microbiol*, 77(5), pp. 1136-52.

Pamarthy, S., Kulshrestha, A., Katara, G. K. and Beaman, K. D. (2018) 'The curious case of vacuolar ATPase: regulation of signaling pathways', *Mol Cancer*, 17(1), pp. 41.

Papakrivos, J., Newbold, C. I. and Lingelbach, K. (2005) 'A potential novel mechanism for the insertion of a membrane protein revealed by a biochemical analysis of the *Plasmodium falciparum* cytoadherence molecule PfEMP-1', *Mol Microbiol*, 55(4), pp. 1272-84.

Park, S., Isaacson, R., Kim, H. T., Silver, P. A. and Wagner, G. (2005) 'Ufd1 exhibits the AAA-ATPase fold with two distinct ubiquitin interaction sites', *Structure*, 13(7), pp. 995-1005.

- Pasternak, N. D. and Dzikowski, R. (2009) 'PfEMP1: an antigen that plays a key role in the pathogenicity and immune evasion of the malaria parasite *Plasmodium falciparum*', *Int J Biochem Cell Biol*, 41(7), pp. 1463-6.
- Peters, C., Bayer, M. J., Buhler, S., Andersen, J. S., Mann, M. and Mayer, A. (2001) 'Trans-complex formation by proteolipid channels in the terminal phase of membrane fusion', *Nature*, 409(6820), pp. 581-8.
- Phillips, M. A., Gujjar, R., Malmquist, N. A., White, J., El Mazouni, F., Baldwin, J. and Rathod, P. K. (2008) 'Triazolopyrimidine-based dihydroorotate dehydrogenase inhibitors with potent and selective activity against the malaria parasite *Plasmodium falciparum*', *J Med Chem*, 51(12), pp. 3649-53.
- Pieperhoff, M. S., Schmitt, M., Ferguson, D. J. and Meissner, M. (2013) 'The role of clathrin in post-Golgi trafficking in *Toxoplasma gondii*', *PLoS One*, 8(10), pp. e77620.
- Price, R. N., Tjitra, E., Guerra, C. A., Yeung, S., White, N. J. and Anstey, N. M. (2007) 'Vivax malaria: neglected and not benign', *Am J Trop Med Hyg*, 77(6 Suppl), pp. 79-87.
- Prudencio, M. and Mota, M. M. (2007) 'To migrate or to invade: those are the options', *Cell Host Microbe*, 2(5), pp. 286-8.
- Putyrski, M. and Schultz, C. (2012) 'Protein translocation as a tool: The current rapamycin story', *FEBS Lett*, 586(15), pp. 2097-105.
- Rajahram, G. S., Cooper, D. J., William, T., Grigg, M. J., Anstey, N. M. and Barber, B. E. (2019) 'Deaths from *Plasmodium knowlesi* malaria: case series and systematic review', *Clin Infect Dis*.
- Rathore, D., Hrstka, S. C., Sacci, J. B., Jr., De la Vega, P., Linhardt, R. J., Kumar, S. and McCutchan, T. F. (2003) 'Molecular mechanism of host specificity in *Plasmodium falciparum* infection: role of circumsporozoite protein', *J Biol Chem*, 278(42), pp. 40905-10.
- Richie, T. L., Billingsley, P. F., Sim, B. K., James, E. R., Chakravarty, S., Epstein, J. E., Lyke, K. E., Mordmuller, B., Alonso, P., Duffy, P. E., Doumbo, O. K., Sauerwein, R. W., Tanner, M., Abdulla, S., Kremsner, P. G., Seder, R. A. and Hoffman, S. L. (2015) 'Progress with *Plasmodium falciparum* sporozoite (PfSPZ)-based malaria vaccines', *Vaccine*, 33(52), pp. 7452-61.

Riglar, D. T., Rogers, K. L., Hanssen, E., Turnbull, L., Bullen, H. E., Charnaud, S. C., Przyborski, J., Gilson, P. R., Whitchurch, C. B., Crabb, B. S., Baum, J. and Cowman, A. F. (2013) 'Spatial association with PTEX complexes defines regions for effector export into *Plasmodium falciparum*-infected erythrocytes', *Nat Commun*, 4, pp. 1415.

Risco-Castillo, V., Son, O., Franetich, J. F., Rubinstein, E., Mazier, D. and Silvie, O. (2013) '[*Plasmodium* sporozoite entry pathways during malaria liver infection]', *Biol Aujourd'hui*, 207(4), pp. 219-29.

Risco-Castillo, V., Topcu, S., Marinach, C., Manzoni, G., Bigorgne, A. E., Briquet, S., Baudin, X., Lebrun, M., Dubremetz, J. F. and Silvie, O. (2015) 'Malaria Sporozoites Traverse Host Cells within Transient Vacuoles', *Cell Host Microbe*, 18(5), pp. 593-603.

Robinson, M. S., Sahlender, D. A. and Foster, S. D. (2010) 'Rapid inactivation of proteins by rapamycin-induced rerouting to mitochondria', *Dev Cell*, 18(2), pp. 324-31.

Roux, K. J., Kim, D. I., Raida, M. and Burke, B. (2012) 'A promiscuous biotin ligase fusion protein identifies proximal and interacting proteins in mammalian cells', *J Cell Biol*, 196(6), pp. 801-10.

Rug, M., Cyrklaff, M., Mikkonen, A., Lemgruber, L., Kuelzer, S., Sanchez, C. P., Thompson, J., Hanssen, E., O'Neill, M., Langer, C., Lanzer, M., Frischknecht, F., Maier, A. G. and Cowman, A. F. (2014) 'Export of virulence proteins by malaria-infected erythrocytes involves remodeling of host actin cytoskeleton', *Blood*, 124(23), pp. 3459-68.

Russo, G., Faggioni, G., Paganotti, G. M., Djeunang Dongho, G. B., Pomponi, A., De Santis, R., Tebano, G., Mbida, M., Sanou Sobze, M., Vullo, V., Rezza, G. and Lista, F. R. (2017) 'Molecular evidence of *Plasmodium vivax* infection in Duffy negative symptomatic individuals from Dschang, West Cameroon', *Malar J*, 16(1), pp. 74.

Russo, I., Babbitt, S., Muralidharan, V., Butler, T., Oksman, A. and Goldberg, D. E. (2010) 'Plasmeprin V licenses *Plasmodium* proteins for export into the host erythrocyte', *Nature*, 463(7281), pp. 632-6.

Salvador, N., Aguado, C., Horst, M. and Knecht, E. (2000) 'Import of a cytosolic protein into lysosomes by chaperone-mediated autophagy depends on its folding state', *J Biol Chem*, 275(35), pp. 27447-56.

SanariaInc (2019) *Safety and Protective Efficacy of Genetically Attenuated PfSPZ-GAI Vaccine in Healthy Dutch Volunteers - Full Text View - ClinicalTrials.gov*. Available at: <https://clinicaltrials.gov/ct2/show/NCT03163121>.

Sanchez, C. P., Karathanasis, C., Sanchez, R., Cyrklaff, M., Jäger, J., Buchholz, B., Schwarz, U. S., Heilemann, M. and Lanzer, M. (2019) 'Single-molecule imaging and quantification of the immune-variant adhesin VAR2CSA on knobs of *Plasmodium falciparum*-infected erythrocytes', *Commun Biol*, 2.

Sanders, P. R., Cantin, G. T., Greenbaum, D. C., Gilson, P. R., Nebl, T., Moritz, R. L., Yates, J. R., 3rd, Hodder, A. N. and Crabb, B. S. (2007) 'Identification of protein complexes in detergent-resistant membranes of *Plasmodium falciparum* schizonts', *Mol Biochem Parasitol*, 154(2), pp. 148-57.

Sanders, P. R., Gilson, P. R., Cantin, G. T., Greenbaum, D. C., Nebl, T., Carucci, D. J., McConville, M. J., Schofield, L., Hodder, A. N., Yates, J. R., 3rd and Crabb, B. S. (2005) 'Distinct protein classes including novel merozoite surface antigens in Raft-like membranes of *Plasmodium falciparum*', *J Biol Chem*, 280(48), pp. 40169-76.

Sargeant, T. J., Marti, M., Caler, E., Carlton, J. M., Simpson, K., Speed, T. P. and Cowman, A. F. (2006) 'Lineage-specific expansion of proteins exported to erythrocytes in malaria parasites', *Genome Biol*, 7(2), pp. R12.

Satoh, T., Ohba, A., Liu, Z., Inagaki, T. and Satoh, A. K. (2015) 'dPob/EMC is essential for biosynthesis of rhodopsin and other multi-pass membrane proteins in *Drosophila* photoreceptors', *Elife*, 4.

Scherf, A., Hernandez-Rivas, R., Buffet, P., Bottius, E., Benatar, C., Pouvelle, B., Gysin, J. and Lanzer, M. (1998) 'Antigenic variation in malaria: in situ switching, relaxed and mutually exclusive transcription of var genes during intra-erythrocytic development in *Plasmodium falciparum*', *Embo j*, 17(18), pp. 5418-26.

Schnell, J., Dyson, H. and Wright, P. (2004) 'Structure, Dynamics, and Catalytic Function of Dihydrofolate Reductase', *Annual review of biophysics and biomolecular structure*, 33.

Schnider, C. B., Bausch-Fluck, D., Bruhlmann, F., Heussler, V. T. and Burda, P. C. (2018) 'BioID Reveals Novel Proteins of the Plasmodium Parasitophorous Vacuole Membrane', *mSphere*, 3(1).

Schofield, L., Hewitt, M. C., Evans, K., Siomos, M. A. and Seeberger, P. H. (2002) 'Synthetic GPI as a candidate anti-toxic vaccine in a model of malaria', *Nature*, 418(6899), pp. 785-9.

Schulze, J., Kwiatkowski, M., Borner, J., Schluter, H., Bruchhaus, I., Burmester, T., Spielmann, T. and Pick, C. (2015) 'The *Plasmodium falciparum* exportome contains non-canonical PEXEL/HT proteins', *Mol Microbiol*.

Seder, R. A., Chang, L. J., Enama, M. E., Zephir, K. L., Sarwar, U. N., Gordon, I. J., Holman, L. A., James, E. R., Billingsley, P. F., Gunasekera, A., Richman, A., Chakravarty, S., Manoj, A., Velmurugan, S., Li, M., Ruben, A. J., Li, T., Eappen, A. G., Stafford, R. E., Plummer, S. H., Hendel, C. S., Novik, L., Costner, P. J., Mendoza, F. H., Saunders, J. G., Nason, M. C., Richardson, J. H., Murphy, J., Davidson, S. A., Richie, T. L., Sedegah, M., Sutamihardja, A., Fahle, G. A., Lyke, K. E., Laurens, M. B., Roederer, M., Tewari, K., Epstein, J. E., Sim, B. K., Ledgerwood, J. E., Graham, B. S. and Hoffman, S. L. (2013) 'Protection against malaria by intravenous immunization with a nonreplicating sporozoite vaccine', *Science*, 341(6152), pp. 1359-65.

Shurtleff, M. J., Itzhak, D. N., Hussmann, J. A., Oakdale, N. T. S., Costa, E. A., Jonikas, M., Weibezahn, J., Popova, K. D., Jan, C. H., Sinitcyn, P., Vembar, S. S., Hernandez, H., Cox, J., Burlingame, A. L., Brodsky, J. L., Frost, A., Borner, G. H. and Weissman, J. S. (2018) 'The ER membrane protein complex interacts cotranslationally to enable biogenesis of multipass membrane proteins'.

Singh, A. P., Buscaglia, C. A., Wang, Q., Levay, A., Nussenzweig, D. R., Walker, J. R., Winzeler, E. A., Fujii, H., Fontoura, B. M. and Nussenzweig, V. (2007) 'Plasmodium circumsporozoite protein promotes the development of the liver stages of the parasite', *Cell*, 131(3), pp. 492-504.

Sinha, S., Medhi, B. and Sehgal, R. (2014) 'Challenges of drug-resistant malaria', *Parasite*, 21, pp. 61.

Sleebs, B. E., Lopaticki, S., Marapana, D. S., O'Neill, M. T., Rajasekaran, P., Gazdik, M., Gunther, S., Whitehead, L. W., Lowes, K. N., Barfod, L., Hviid, L., Shaw, P. J., Hodder, A. N., Smith, B. J., Cowman, A. F. and Boddey, J. A. (2014) 'Inhibition of Plasmeprin V activity demonstrates its essential role in protein export, PfEMP1 display, and survival of malaria parasites', *PLoS Biol*, 12(7), pp. e1001897.

Smith, J. D., Chitnis, C. E., Craig, A. G., Roberts, D. J., Hudson-Taylor, D. E., Peterson, D. S., Pinches, R., Newbold, C. I. and Miller, L. H. (1995) 'Switches in expression of *Plasmodium falciparum* var genes correlate with changes in antigenic and cytoadherent phenotypes of infected erythrocytes', *Cell*, 82(1), pp. 101-10.

Smith, J. D., Craig, A. G., Kriek, N., Hudson-Taylor, D., Kyes, S., Fagen, T., Pinches, R., Baruch, D. I., Newbold, C. I. and Miller, L. H. (2000) 'Identification of a *Plasmodium falciparum* intercellular adhesion molecule-1 binding domain: A parasite adhesion trait implicated in cerebral malaria', *Proc Natl Acad Sci U S A: Vol. 4*, pp. 1766-71.

Smith, M. H., Ploegh, H. L. and Weissman, J. S. (2011) 'Road to ruin: targeting proteins for degradation in the endoplasmic reticulum', *Science*, 334(6059), pp. 1086-90.

Spielmann, T. and Gilberger, T. W. (2010) 'Protein export in malaria parasites: do multiple export motifs add up to multiple export pathways?', *Trends Parasitol*, 26(1), pp. 6-10.

Spielmann, T. and Gilberger, T. W. (2015) 'Critical Steps in Protein Export of *Plasmodium falciparum* Blood Stages', *Trends Parasitol*, 31(10), pp. 514-525.

Spielmann, T., Hawthorne, P. L., Dixon, M. W., Hannemann, M., Klotz, K., Kemp, D. J., Klonis, N., Tilley, L., Trenholme, K. R. and Gardiner, D. L. (2006) 'A cluster of ring stage-specific genes linked to a locus implicated in cytoadherence in *Plasmodium falciparum* codes for PEXEL-negative and PEXEL-positive proteins exported into the host cell', *Mol Biol Cell*, 17(8), pp. 3613-24.

Spillman, N. J., Beck, J. R. and Goldberg, D. E. (2015) 'Protein export into malaria parasite-infected erythrocytes: mechanisms and functional consequences', *Annu Rev Biochem*, 84, pp. 813-41.

Spork, S., Hiss, J. A., Mandel, K., Sommer, M., Kooij, T. W. A., Chu, T., Schneider, G., Maier, U. G. and Przyborski, J. M. (2009) 'An Unusual ERAD-Like Complex Is Targeted to the Apicoplast of *Plasmodium falciparum* ▽ ◆◆', *Eukaryot Cell*, 8(8), pp. 1134-45.

Spring, M., Murphy, J., Nielsen, R., Dowler, M., Bennett, J. W., Zarling, S., Williams, J., de la Vega, P., Ware, L., Komisar, J., Polhemus, M., Richie, T. L., Epstein, J., Tamminga, C., Chuang, I., Richie, N., O'Neil, M., Heppner, D. G., Healer, J., O'Neill, M., Smithers, H., Finney, O. C., Mikolajczak, S. A., Wang, R., Cowman, A., Ockenhouse, C., Krzych, U. and Kappe, S. H. (2013) 'First-in-human evaluation of genetically attenuated *Plasmodium*

falciparum sporozoites administered by bite of Anopheles mosquitoes to adult volunteers', *Vaccine*, 31(43), pp. 4975-83.

Spycher, C., Rug, M., Pachlatko, E., Hanssen, E., Ferguson, D., Cowman, A. F., Tilley, L. and Beck, H. P. (2008) 'The Maurer's cleft protein MAHRP1 is essential for trafficking of PfEMP1 to the surface of *Plasmodium falciparum*-infected erythrocytes', *Mol Microbiol*, 68(5), pp. 1300-14.

Stankunas, K., Bayle, J. H., Gestwicki, J. E., Lin, Y. M., Wandless, T. J. and Crabtree, G. R. (2003) 'Conditional protein alleles using knockin mice and a chemical inducer of dimerization', *Mol Cell*, 12(6), pp. 1615-24.

Stanway, R. R., Graewe, S., Rennenberg, A., Helm, S. and Heussler, V. T. (2009) 'Highly efficient subcloning of rodent malaria parasites by injection of single merosomes or detached cells', *Nat Protoc*, 4(10), pp. 1433-9.

Straimer, J., Gnadig, N. F., Witkowski, B., Amaratunga, C., Duru, V., Ramadani, A. P., Dacheux, M., Khim, N., Zhang, L., Lam, S., Gregory, P. D., Urnov, F. D., Mercereau-Puijalon, O., Benoit-Vical, F., Fairhurst, R. M., Menard, D. and Fidock, D. A. (2015) 'Drug resistance. K13-propeller mutations confer artemisinin resistance in *Plasmodium falciparum* clinical isolates', *Science*, 347(6220), pp. 428-31.

Straimer, J., Lee, M. C., Lee, A. H., Zeitler, B., Williams, A. E., Pearl, J. R., Zhang, L., Rebar, E. J., Gregory, P. D., Llinas, M., Urnov, F. D. and Fidock, D. A. (2012) 'Site-specific genome editing in *Plasmodium falciparum* using engineered zinc-finger nucleases', *Nat Methods*, 9(10), pp. 993-8.

Sturm, A., Amino, R., van de Sand, C., Regen, T., Retzlaff, S., Rennenberg, A., Krueger, A., Pollok, J. M., Menard, R. and Heussler, V. T. (2006) 'Manipulation of host hepatocytes by the malaria parasite for delivery into liver sinusoids', *Science*, 313(5791), pp. 1287-90.

Su, X. Z., Heatwole, V. M., Wertheimer, S. P., Guinet, F., Herrfeldt, J. A., Peterson, D. S., Ravetch, J. A. and Wellems, T. E. (1995) 'The large diverse gene family var encodes proteins involved in cytoadherence and antigenic variation of *Plasmodium falciparum*-infected erythrocytes', *Cell*, 82(1), pp. 89-100.

Szymczak, A. L., Workman, C. J., Wang, Y., Vignali, K. M., Dilioglou, S., Vanin, E. F. and Vignali, D. A. (2004) 'Correction of multi-gene deficiency in vivo using a single 'self-cleaving' 2A peptide-based retroviral vector', *Nat Biotechnol*, 22(5), pp. 589-94.

Takeda, K., Cabrera, M., Rohde, J., Bausch, D., Jensen, O. N. and Ungermann, C. (2008) 'The vacuolar V1/V0-ATPase is involved in the release of the HOPS subunit Vps41 from vacuoles, vacuole fragmentation and fusion', *FEBS Lett*, 582(10), pp. 1558-63.

Taraschi, T. F., O'Donnell, M., Martinez, S., Schneider, T., Trelka, D., Fowler, V. M., Tilley, L. and Moriyama, Y. (2003) 'Generation of an erythrocyte vesicle transport system by *Plasmodium falciparum* malaria parasites', *Blood*, 102(9), pp. 3420-6.

Taraschi, T. F., Trelka, D., Martinez, S., Schneider, T. and O'Donnell, M. E. (2001) 'Vesicle-mediated trafficking of parasite proteins to the host cell cytosol and erythrocyte surface membrane in *Plasmodium falciparum* infected erythrocytes', *Int J Parasitol*, 31(12), pp. 1381-91.

Tarr, S. J., Cryar, A., Thalassinou, K., Haldar, K. and Osborne, A. R. (2013) 'The C-terminal portion of the cleaved HT motif is necessary and sufficient to mediate export of proteins from the malaria parasite into its host cell', *Mol Microbiol*, 87(4), pp. 835-50.

The RTS, S. C. T. P. (2012) 'A Phase 3 Trial of RTS,S/AS01 Malaria Vaccine in African Infants', <http://dx.doi.org/10.1056/NEJMoa1208394>.

Tilly, A. K., Thiede, J., Metwally, N., Lubiana, P., Bachmann, A., Roeder, T., Rockliffe, N., Lorenzen, S., Tannich, E., Gutschmann, T. and Bruchhaus, I. (2015) 'Type of in vitro cultivation influences cytoadhesion, knob structure, protein localization and transcriptome profile of *Plasmodium falciparum*', *Sci Rep*.

Toh, S. Q., Glanfield, A., Gobert, G. N. and Jones, M. K. (2010) 'Heme and blood-feeding parasites: friends or foes?', *Parasit Vectors*, pp. 108.

Tomavo, S., Slomianny, C., Meissner, M. and Carruthers, V. B. (2013) 'Protein trafficking through the endosomal system prepares intracellular parasites for a home invasion', *PLoS Pathog*, 9(10), pp. e1003629.

Turner, G. D., Morrison, H., Jones, M., Davis, T. M., Looareesuwan, S., Buley, I. D., Gatter, K. C., Newbold, C. I., Pukritayakamee, S., Nagachinta, B. and et al. (1994) 'An

immunohistochemical study of the pathology of fatal malaria. Evidence for widespread endothelial activation and a potential role for intercellular adhesion molecule-1 in cerebral sequestration', *Am J Pathol*, 145(5), pp. 1057-69.

van Dooren, G. G., Marti, M., Tonkin, C. J., Stimmler, L. M., Cowman, A. F. and McFadden, G. I. (2005) 'Development of the endoplasmic reticulum, mitochondrion and apicoplast during the asexual life cycle of *Plasmodium falciparum*', *Mol Microbiol*, 57(2), pp. 405-19.

van Ooij, C., Tamez, P., Bhattacharjee, S., Hiller, N. L., Harrison, T., Liolios, K., Kooij, T., Ramesar, J., Balu, B., Adams, J., Waters, A. P., Janse, C. J. and Haldar, K. (2008) 'The malaria secretome: from algorithms to essential function in blood stage infection', *PLoS Pathog*, 4(6), pp. e1000084.

van Schaijk, B. C. L., Ploemen, I. H. J., Annoura, T., Vos, M. W., Foquet, L., van Gemert, G. J., Chevalley-Maurel, S., van de Vegte-Bolmer, M., Sajid, M., Franetich, J. F., Lorthiois, A., Leroux-Roels, G., Meuleman, P., Hermsen, C. C., Mazier, D., Hoffman, S. L., Janse, C. J., Khan, S. M. and Sauerwein, R. W. (2014) 'A genetically attenuated malaria vaccine candidate based on *P. falciparum* b9/slarp gene-deficient sporozoites', *eLife*.

VanBuskirk, K. M., O'Neill, M. T., De La Vega, P., Maier, A. G., Krzych, U., Williams, J., Dowler, M. G., Sacci, J. B., Jr., Kangwanrangan, N., Tsuboi, T., Kneteman, N. M., Heppner, D. G., Jr., Murdock, B. A., Mikolajczak, S. A., Aly, A. S., Cowman, A. F. and Kappe, S. H. (2009) 'Preerythrocytic, live-attenuated *Plasmodium falciparum* vaccine candidates by design', *Proc Natl Acad Sci U S A*, 106(31), pp. 13004-9.

Vaughan, A. M., Mikolajczak, S. A., Wilson, E. M., Grompe, M., Kaushansky, A., Camargo, N., Bial, J., Ploss, A. and Kappe, S. H. (2012) 'Complete *Plasmodium falciparum* liver-stage development in liver-chimeric mice', *J Clin Invest*, 122(10), pp. 3618-28.

Volkmar, N., Thezenas, M. L., Louie, S. M., Juszkievicz, S., Nomura, D. K., Hegde, R. S., Kessler, B. M. and Christianson, J. C. (2019) 'The ER membrane protein complex promotes biogenesis of sterol-related enzymes maintaining cholesterol homeostasis', *J Cell Sci*, 132(2).

Wang, J., Zhang, C. J., Chia, W. N., Loh, C. C., Li, Z., Lee, Y. M., He, Y., Yuan, L. X., Lim, T. K., Liu, M., Liew, C. X., Lee, Y. Q., Zhang, J., Lu, N., Lim, C. T., Hua, Z. C., Liu, B., Shen, H. M., Tan, K. S. and Lin, Q. (2015) 'Haem-activated promiscuous targeting of artemisinin in *Plasmodium falciparum*', *Nat Commun*, 6, pp. 10111.

Warncke, J. D., Vakonakis, I. and Beck, H. P. (2016) 'Plasmodium Helical Interspersed Subtelomeric (PHIST) Proteins, at the Center of Host Cell Remodeling', *Microbiol Mol Biol Rev*, 80(4), pp. 905-27.

Waterkeyn, J. G., Wickham, M. E., Davern, K. M., Cooke, B. M., Coppel, R. L., Reeder, J. C., Culvenor, J. G., Waller, R. F. and Cowman, A. F. (2000) 'Targeted mutagenesis of *Plasmodium falciparum* erythrocyte membrane protein 3 (PfEMP3) disrupts cytoadherence of malaria-infected red blood cells', *Embo j*, 19(12), pp. 2813-23.

Weill, U., Krieger, G., Avihou, Z., Milo, R., Schuldiner, M. and Davidi, D. (2019) 'Assessment of GFP Tag Position on Protein Localization and Growth Fitness in Yeast', *J Mol Biol*, 431(3), pp. 636-641.

Weisz, O. A. (2003) 'Acidification and protein traffic', *Int Rev Cytol*, 226, pp. 259-319.

White, N. J. (2017) 'Malaria parasite clearance', *Malar J*.

WHO (2017) *WHO | Global Technical Strategy for Malaria 2016–2030*: World Health Organization. Available at: <https://www.who.int/malaria/publications/atoz/9789241564991/en/>.

WHO (2018) 'World Health Organization | World malaria report 2018', *WHO*.

Malaria Vaccine Technology.

Wideman, J. G. (2015) 'The ubiquitous and ancient ER membrane protein complex (EMC): tether or not?', *F1000Res*, 4.

Wienhues, U., Becker, K., Schleyer, M., Guiard, B., Tropschug, M., Horwich, A. L., Pfanner, N. and Neupert, W. (1991) 'Protein folding causes an arrest of preprotein translocation into mitochondria in vivo', *J Cell Biol*, 115(6), pp. 1601-9.

Witsenburg, F., Salamin, N. and Christe, P. (2012) 'The evolutionary host switches of *Polychromophilus* : a multi-gene phylogeny of the bat malaria genus suggests a second invasion of mammals by a haemosporidian parasite', *Malaria Journal*, 11(1), pp. 1-10.

Wongsrichanalai, C., Pickard, A., Wernsdorfer, W. and Meshnick, S. (2002) 'Epidemiology of drug-resistant malaria', *The Lancet Infectious Diseases*, 2(4), pp. 209-218.

Wu, Y., Kirkman, L. A. and Wellems, T. E. (1996) 'Transformation of *Plasmodium falciparum* malaria parasites by homologous integration of plasmids that confer resistance to pyrimethamine', *Proc Natl Acad Sci U S A*, 93(3), pp. 1130-4.

Xu, T., Johnson, C. A., Gestwicki, J. E. and Kumar, A. (2010) 'Conditionally controlling nuclear trafficking in yeast by chemical-induced protein dimerization', *Nat Protoc*, 5(11), pp. 1831-43.

Yeh, E., Joseph L. DeRisi (2019) 'Chemical Rescue of Malaria Parasites Lacking an Apicoplast Defines Organelle Function in Blood-Stage *Plasmodium falciparum*'.

Zhang, M., Wang, C., Otto, T. D., Oberstaller, J., Liao, X., Adapa, S. R., Udenze, K., Bronner, I. F., Casandra, D., Mayho, M., Brown, J., Li, S., Swanson, J., Rayner, J. C., Jiang, R. H. Y. and Adams, J. H. (2018) 'Uncovering the essential genes of the human malaria parasite *Plasmodium falciparum* by saturation mutagenesis', *Science*, 360(6388).

Acknowledgements

Initially I would like to thank Dr. Tobias Spielmann for the great support he gave me during my PhD years, infinite thanks for the mentoring, patience, and the enormous willingness he has for teaching his students. The passion he feels for science is contagious and I feel very fortunate to graduate under his mentorship. I take this short space to emphasize the good work he does as a scientist and as a mentor.

I also thank Dr. Paolo Mesén Ramirez for teaching me the techniques of the laboratory and for share with me his experience. Special thanks to Dr. Wieteke Hoeijmakers (Radboud Institute, Nijmegen, Netherlands) for performing the mass spectrometry with my samples, from which I obtained the list of proteins to start cloning my candidates. I also thank to Samantha Gonzales for reading and correcting the language of this thesis.

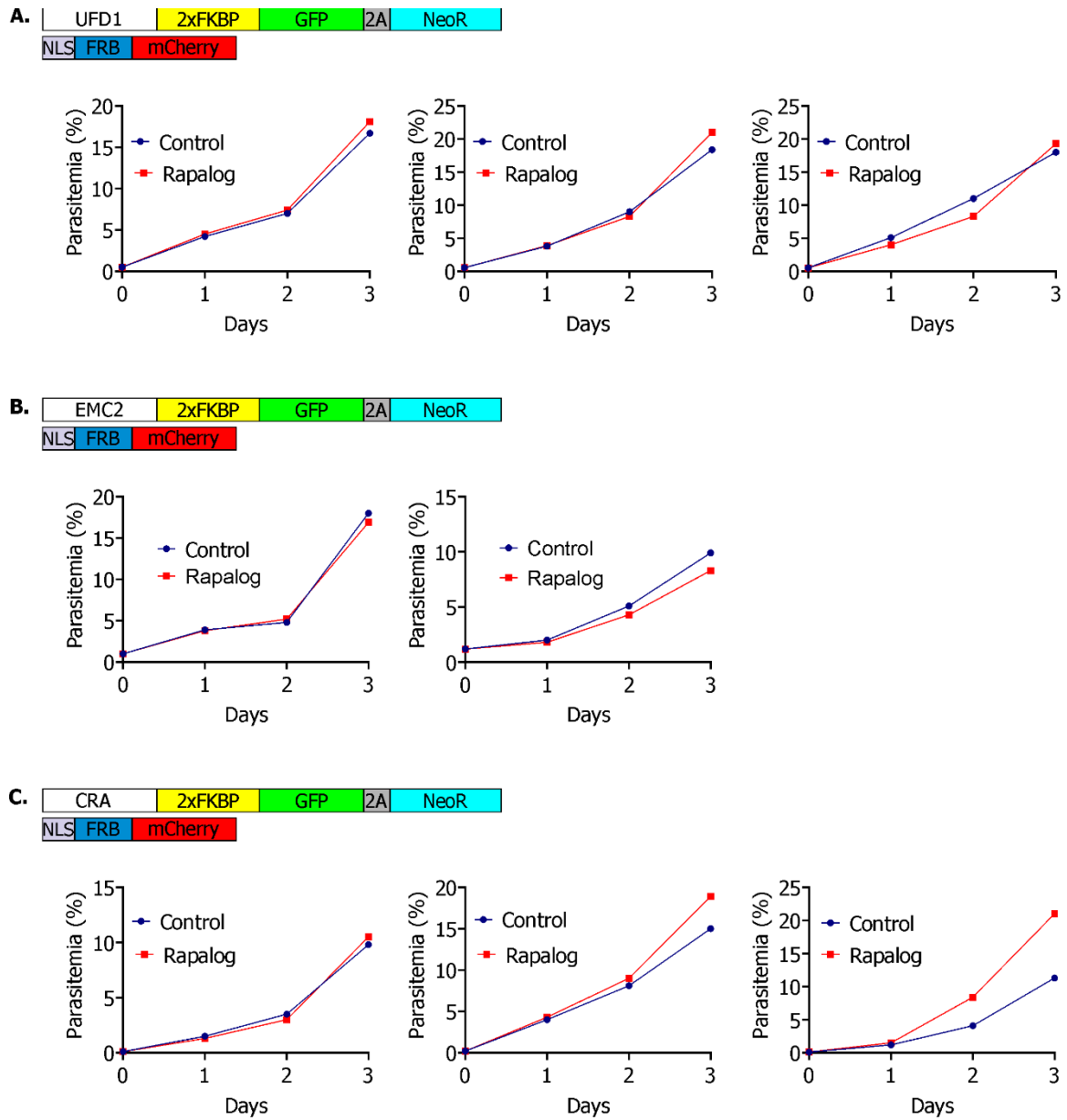
I thank the government of Colombia (Colciencias), the MINGS of the University of Hamburg and the Bernhard Nocht Institut für Tropenmedizin for financing my doctorate. I thank Germany for opening its doors to me, accepting me as a scientist, as they have accepted so many foreigners in difficult times.

I am immensely grateful to my friends and colleagues Ricarda Sabitzki, Sabine Schmidt, Sarah Scharf, Marius Schmitt and Jan Stäcker, Ulrike Fröhlke and Bärbel Bergmann for the scientific discussions and for the coffees that were always so necessary in the moments when I thought nothing would work. You are an extraordinary group and I feel honored to have worked with you.

Estoy infinitamente agradecida con mis padres Mario y Aide, y con mi hermana Lina pues, aunque no entendieran bien lo que llevo haciendo estos años, siempre me dieron su amor y apoyo incondicional. Danke an meinen Freund David für die Unterstützung in den letzten Monaten des Schreibens, to my friends Max, Ricarda, Ricardo, Gabi, Adri, Marce, Dayse, Samantha and to so many others that although I do not name them here, in my heart they will always be present.

Appendix A: Supplementary figures

Figure S1. Growth curves of mislocalization assays.



Appendix B: supplementary tables

Table S1. Attempts to integrate cell lines using G418 or DSM1

Cell line	Attempt #	Time on selection (weeks)	Result
UFD1 TGD GFP	1	8	No parasites
UFD1 TGD GFP	2	10	Wrong integrated
UFD1 TGD GFP	3	8	No parasites
UFD1 TGD GFP	4	8	No parasites
UFD1 TGD GFP	5	10	Wrong integrated
UFD1 TGD GFP	6	8	No parasites
0704300-2xFKBP-GFP	1	3	No parasites
0704300-2xFKBP-GFP	2	3	No parasites
0704300-2xFKBP-GFP	3	3	No parasites
0704300-2xFKBP-GFP	4	3	No parasites
0704300-2xFKBP-GFP	5	3	No parasites
0704300-2xFKBP-GFP	6	3	No parasites
0928600-2xFKBP-GFP	1	3	Wrong integrated
0928600-2xFKBP-GFP	2	3	Wrong integrated
0928600-2xFKBP-GFP	3	2	Wrong integrated
0928600-2xFKBP-GFP	4	3	Wrong integrated
0928600-2xFKBP-GFP	5	3	Wrong integrated
0928600-2xFKBP-GFP	6	2	Wrong integrated
0928600-TGD-GFP	1	2	Wrong integrated
0928600-TGD-GFP	2	2	Wrong integrated
0928600-TGD-GFP	3	2	Wrong integrated
0928600-TGD-GFP	4	2	Wrong integrated
0928600-TGD-GFP	5	2	Wrong integrated
0928600-TGD-GFP	6	2	Wrong integrated
YIP1-2xFKBP-GFP	1	3	Wrong integrated
YIP1-2xFKBP-GFP	2	3	Wrong integrated
YIP1-2xFKBP-GFP	3	3	Wrong integrated
YIP1-2xFKBP-GFP	4	3	Wrong integrated
YIP1-2xFKBP-GFP	5	3	Wrong integrated
YIP1-2xFKBP-GFP	6	3	Wrong integrated
YIP1-2xFKBP-GFP	7	3	Wrong integrated
YIP1-2xFKBP-GFP	8	3	Wrong integrated
YIP1-2xFKBP-GFP	9	3	Wrong integrated
YIP1-TGD-GFP	1	3	Wrong integrated
YIP1-TGD-GFP	2	3	Wrong integrated
YIP1-TGD-GFP	3	3	Wrong integrated
YIP1-TGD-GFP	4	3	Wrong integrated
YIP1-TGD-GFP	5	3	Wrong integrated
YIP1-TGD-GFP	6	3	Wrong integrated
PTEX88-TGD-GFP	1	9	Lysate culture
PTEX88-TGD-GFP	2	9	Discarded
PTEX88-TGD-GFP	3	9	Wrong integrated

PTEX88-TGD-GFP	4	9	Wrong integrated
PTEX88-TGD-GFP	5	9	Discarded
PTEX88-TGD-GFP	6	9	Discarded
PTEX88-TGD-GFP	7	8	Wrong integrated
PTEX88-TGD-GFP	8	8	Wrong integrated
PTEX88-TGD-GFP	9	8	Wrong integrated
PTEX88-TGD-GFP	10	8	Discarded
PTEX88-TGD-GFP	11	8	Discarded
PTEX88-TGD-GFP	12	8	Discarded
CRA-TGD-GFP	1	1	Contaminated
CRA-TGD-GFP	2	8	Discarded
CRA-TGD-GFP	3	8	Discarded
CRA-TGD-GFP	4	8	Discarded
CRA-TGD-GFP	5	8	Discarded
CRA-TGD-GFP	6	8	Wrong integrated
CRA-TGD-GFP	7	8	Discarded
ECM2-TGD-GFP	1	1	Contaminated
ECM2-TGD-GFP	2	8	Discarded
ECM2-TGD-GFP	3	8	Discarded
ECM2-TGD-GFP	4	8	Discarded
ECM2-TGD-GFP	5	8	Discarded
ECM2-TGD-GFP	6	8	Discarded
ECM2-TGD-GFP	7	8	Discarded
PfEMP1-3XHA ^{endo} +SBP1-TGD-GFP ^{endo}	1	11	Discarded
PfEMP1-3XHA ^{endo} +SBP1-TGD-GFP ^{endo}	2	11	Discarded
PfEMP1-3XHA ^{endo} +SBP1-TGD-GFP ^{endo}	3	11	Discarded
PfEMP1-3XHA ^{endo} +SBP1-TGD-GFP ^{endo}	4	10	PfEMP1 reverted
PfEMP1-3XHA ^{endo} +SBP1-TGD-GFP ^{endo}	5	12	PfEMP1 reverted
PfEMP1-3XHA ^{endo} +SBP1-TGD-GFP ^{endo}	6	12	Discarded
PfEMP1-3XHA ^{endo} +SBP1-TGD-GFP ^{endo}	7	12	Discarded
PfEMP1-3XHA ^{endo} +SBP1-TGD-GFP ^{endo}	8	8	Lysate culture
PfEMP1-3XHA ^{endo} +SBP1-TGD-GFP ^{endo}	9	12	SBP1 wrong integrated
PfEMP1-3XHA ^{endo} +SBP1-TGD-GFP ^{endo}	10	9	PfEMP1 reverted
PfEMP1-3XHA ^{endo} +SBP1-TGD-GFP ^{endo}	11	9	PfEMP1 reverted
PfEMP1-3XHA ^{endo} +SBP1-TGD-GFP ^{endo}	12	12	Discarded

Table S2. Mass spectrometry results.

the first 10 proteins on the list were cloned, and the highest hits are in bold

Majority protein IDs	Protein product	log ₂ Ratio H/L normalized Rex2F	log ₂ Ratio L/H normalized Rex2R	log ₂ Ratio H/L normalized SBP1F	log ₂ Ratio L/H normalized SBP1R	Ratio H/L normalized Rex2F B significant	Ratio H/L normalized Rex2R B significant	Ratio H/L normalized SBP1F B significant	Ratio H/L normalized SBP1R B significant	Number of proteins	Peptides	Unique peptides
PF3D7_0704300	conserved Plasmodium membrane protein, unknown function	0,36	0,08	0,39	-0,10		+			1	5	5
PF3D7_1472100	protein transport protein YIP1, putative	1,77	1,26	NaN	NaN					1	1	1
PF3D7_0104500	conserved protein, unknown function	0,70	1,50	NaN	NaN					1	162	162
PF3D7_0928600	conserved Plasmodium protein, unknown function	2,01	1,80	NaN	NaN					1	4	4
PF3D7_1418000	ubiquitin fusion degradation protein UFD1, putative	1,67	1,86	NaN	0,21					1	2	2
PF3D7_0830400	conserved Plasmodium protein, unknown function	1,01	2,38	-0,81	0,34					2	2	2
PF3D7_1226400	conserved Plasmodium protein, unknown function	1,13	0,70	0,84	0,35					1	30	30
PF3D7_1105600	translocon component PTEX88	1,45	0,89	0,40	0,41					1	45	45
PF3D7_0934500	V-type proton ATPase subunit E, putative	1,33	0,91	0,50	0,63					1	2	2
PF3D7_1410000	ER membrane protein complex subunit 2, putative	-1,71	1,48	NaN	2,23					1	1	1
PF3D7_0809700	RuvB-like helicase 1	-5,26	4,22	0,73	-4,10					1	5	5
PF3D7_0904400	signal peptidase complex subunit 3, putative	2,43	-5,66	NaN	-2,47					1	3	3
PF3D7_0419800	60S ribosomal protein L7ae/L30e, putative	3,68	0,45	0,95	-2,20			+		1	9	9
PF3D7_1013300	conserved Plasmodium protein, unknown function	0,64	-0,15	2,76	-1,78					1	3	3
PF3D7_1212500	glycerol-3-phosphate 1-O-acyltransferase	0,77	-0,70	-0,18	-1,46	+	+			1	41	41
PF3D7_1228600	merozoite surface protein 9	1,07	0,92	NaN	-1,40					1	38	38
PF3D7_1401600	Plasmodium exported protein (PHISTb), unknown function	1,33	0,18	NaN	-1,23					1	2	2
PF3D7_1412600	deoxyhypusine synthase	1,13	-0,88	NaN	-1,20					1	5	5
PF3D7_0934800	cAMP-dependent protein kinase catalytic subunit	0,70	-0,35	0,20	-0,94					1	2	2
PF3D7_1363400	polyubiquitin binding protein, putative	1,41	-1,56	NaN	-0,84	+			+	1	5	5
PF3D7_0813600	translation initiation factor SUI1, putative	1,06	0,24	NaN	-0,79					1	1	1
PF3D7_0207600	serine repeat antigen 5	1,87	0,66	NaN	-0,77					9	14	14
PF3D7_1444800	fructose-bisphosphate aldolase	0,78	0,76	-0,35	-0,67					1	4	4
PF3D7_0410800	conserved Plasmodium protein, unknown function	0,30	0,12	0,71	-0,66					1	30	30
PF3D7_0515000	pre-mRNA-splicing factor CWC2, putative	0,73	-1,14	0,12	-0,60					1	11	11
PF3D7_1408100	plasmepsin III	0,73	0,58	NaN	-0,56					1	5	5
PF3D7_1410400	rhostry-associated protein 1	0,69	-0,39	NaN	-0,55	+	+			1	1	1
PF3D7_1204300	eukaryotic translation initiation factor 5A	-1,10	-0,48	1,28	-0,54					3	111	110

PF3D7_1251500	ATP-dependent RNA helicase DRS1, putative	0,24	2,80	1,46	-0,52				1	15	15
PF3D7_0103200	nucleoside transporter 4	-0,13	0,58	0,54	-0,51				1	8	8
PF3D7_0935800	cytoadherence linked asexual protein 9	0,15	0,32	0,54	-0,51				1	2	2
PF3D7_0110700	chromatin assembly factor 1 protein WD40 domain, putative	1,40	0,20	0,05	-0,41	+			1	45	45
PF3D7_0704200	tRNA m5C-methyltransferase, putative	0,70	-0,60	0,23	-0,34	+	+		1	2	2
PF3D7_0709700	prodrug activation and resistance esterase	0,84	-1,76	-2,33	-0,34				1	7	7
PF3D7_0912400	alkaline phosphatase, putative	-1,22	1,90	1,50	-0,33				1	2	2
PF3D7_0112000	TatD-like deoxyribonuclease	0,72	0,05	NaN	-0,33				1	23	23
PF3D7_0918900	gamma-glutamylcysteine synthetase	0,13	-0,07	0,71	-0,32				1	2	2
PF3D7_1252100	rhoptry neck protein 3	0,56	0,11	0,55	-0,31	+	+		1	2	2
PF3D7_1216300	signal recognition particle subunit SRP19	0,15	-0,03	0,50	-0,30				1	2	2
PF3D7_1014900	conserved Plasmodium protein, unknown function	0,12	0,34	1,44	-0,30				1	2	2
PF3D7_1010700	dolichyl-phosphate-mannose protein mannosyltransferase, putative	0,14	-0,41	0,55	-0,29				1	4	4
PF3D7_1149400	Plasmodium exported protein, unknown function	0,54	-0,64	0,54	-0,27	+	+		1	93	93
PF3D7_1336000	conserved Plasmodium protein, unknown function	0,11	-0,16	0,52	-0,26				1	2	2
PF3D7_1442300	tRNA import protein tRIP	0,29	-0,18	0,80	-0,24				1	4	4
PF3D7_1435700	ataxin-2 like protein, putative	-0,06	-0,22	1,04	-0,23				1	2	2
PF3D7_0526900	transmembrane emp24 domain-containing protein, putative	0,69	-0,85	NaN	-0,23	+			1	1	1
PF3D7_1405600	ribonucleoside-diphosphate reductase small chain, putative	0,81	-0,32	NaN	-0,19				1	7	7
PF3D7_0926100	protein kinase, putative	0,34	0,09	0,61	-0,17			+	2	7	7
PF3D7_1105100	histone H2B	0,24	-0,46	0,79	-0,17				1	162	162
PF3D7_1022000	RNA-binding protein, putative	-0,34	0,43	0,54	-0,17				1	1	1
PF3D7_0524400	ribosome-interacting GTPase 1, putative	0,15	-0,06	0,56	-0,16				1	4	4
PF3D7_1454200	conserved Plasmodium protein, unknown function	-0,19	NaN	0,51	-0,16				1	6	6
PF3D7_0219400	ribosome associated membrane protein RAMP4	1,64	0,31	-0,42	-0,15				1	32	32
PF3D7_1464900	ATP-dependent zinc metalloprotease FTSH, putative	0,82	0,23	-0,48	-0,15			+	1	2	2
PF3D7_1416900	prefoldin subunit 2, putative	1,05	-3,77	NaN	-0,15				1	2	2
PF3D7_1330800	RNA-binding protein, putative	0,30	0,33	0,76	-0,14				1	6	6
PF3D7_1330600	elongation factor Tu, putative	0,76	-0,04	2,23	-0,14			+	1	3	3
PF3D7_1010100	conserved Plasmodium protein, unknown function	0,26	-0,15	0,52	-0,14				1	3	3
PF3D7_1028300	rRNA-processing protein EBP2, putative	-0,23	0,39	0,52	-0,14				1	4	4
PF3D7_1459000	ATP-dependent RNA helicase DBP5	0,86	-0,97	NaN	-0,13				1	3	3
PF3D7_1236100	clustered-asparagine-rich protein	0,02	-0,27	1,59	-0,13				1	9	9
PF3D7_0307100	40S ribosomal protein S12, putative	0,03	0,30	0,95	-0,13				1	18	18
PF3D7_0930300	merozoite surface protein 1	0,83	0,28	NaN	-0,11				1	10	10

PF3D7_1203700	nucleosome assembly protein	0,10	0,12	0,55	-0,11			1	15	15
PF3D7_0201900	erythrocyte membrane protein 3	0,02	NaN	0,51	-0,10			1	7	7
PF3D7_1302800	40S ribosomal protein S7, putative	NaN	-0,48	0,78	-0,09			1	11	11
PF3D7_1466800	conserved Plasmodium protein, unknown function	0,02	0,14	0,50	-0,09			1	3	3
PF3D7_1353300	conserved Plasmodium protein, unknown function	0,25	0,21	0,61	-0,09			1	8	8
PF3D7_0925900	conserved Plasmodium protein, unknown function	0,45	0,51	1,30	-0,09	+		1	5	5
PF3D7_0731600	acyl-CoA synthetase	NaN	-0,12	0,86	-0,08			1	2	2
PF3D7_1460300	60S ribosomal protein L29, putative	-0,18	-0,12	0,66	-0,08			1	4	4
PF3D7_1466400	AP2 domain transcription factor AP2-SP	0,32	-0,05	0,59	-0,08		+	1	3	3
PF3D7_1208900	protein phosphatase, putative	0,04	NaN	0,86	-0,07			1	18	18
PF3D7_1312700	conserved Plasmodium protein, unknown function	1,34	0,77	1,14	-0,06			1	2	2
PF3D7_1119400	ubiquitin-protein ligase, putative	0,53	-0,33	2,33	-0,06	+	+	1	23	23
PF3D7_0532100	early transcribed membrane protein 5	2,68	1,67	0,49	-0,04			1	2	2
PF3D7_0717700	serine--tRNA ligase, putative	0,04	0,22	1,12	-0,03			1	6	6
PF3D7_1402700	U2 snRNP-associated SURP motif-containing protein, putative	0,69	0,14	0,61	-0,02		+	1	1	1
PF3D7_0415500	nuclear cap-binding protein subunit 2, putative	-0,15	0,01	1,38	-0,01			1	38	38
PF3D7_0803000	peptidyl-prolyl cis-trans isomerase	0,16	0,05	1,16	-0,01			1	8	8
PF3D7_1244100	N-alpha-acetyltransferase 15, NatA auxiliary subunit, putative	1,76	-0,29	NaN	NaN			1	5	5
PF3D7_0217300	AP-2 complex subunit sigma, putative	2,57	-1,77	NaN	NaN			1	41	41
PF3D7_1324700	SNARE protein, putative	1,63	-0,65	NaN	NaN			1	1	1
PF3D7_0501500	rhoptry-associated protein 3	1,14	-0,51	NaN	NaN		+	1	15	15
PF3D7_0613700	syntaxin binding protein, putative	1,11	-0,20	NaN	NaN			3	11	11
PF3D7_0908000	P1 nuclease, putative	0,69	-0,17	NaN	NaN		+	1	5	5
PF3D7_0528800	nucleolar preribosomal GTPase, putative	1,50	NaN	NaN	NaN			1	3	3
PF3D7_0508800	single-stranded DNA-binding protein	1,43	NaN	NaN	NaN			1	4	4
PF3D7_1218200	conserved Plasmodium protein, unknown function	0,86	NaN	NaN	NaN			1	8	8
PF3D7_0907600	translation initiation factor SUI1, putative	0,80	NaN	NaN	NaN			1	1	1
PF3D7_1332800	eukaryotic translation initiation factor 6, putative	0,79	NaN	NaN	NaN			1	16	16
PF3D7_1252700	Plasmodium exported protein (PHISTb), unknown function	1,35	0,50	NaN	NaN	+		1	4	4
PF3D7_1431300	large subunit GTPase 1, putative	0,84	0,61	NaN	NaN			1	10	10
PF3D7_0316300	inorganic pyrophosphatase, putative	1,58	0,72	NaN	NaN			1	2	2
PF3D7_0820000	Snf2-related CBP activator, putative	0,82	0,74	NaN	NaN		+	1	1	1
PF3D7_1131800	oxysterol-binding protein, putative	2,11	0,83	NaN	NaN			9	14	14
PF3D7_0317500	kinesin-5	1,46	0,98	NaN	NaN			1	12	12
PF3D7_1017400	phosphomannomutase, putative	1,81	1,26	NaN	NaN			1	6	6

PF3D7_0902800	serine repeat antigen 9	0,92	1,40	NaN	NaN				1	5	5
PF3D7_0705300	origin recognition complex subunit 2, putative	1,70	1,66	NaN	NaN				1	1	1
PF3D7_0220000	liver stage antigen 3 LSA3	4,55	3,60	NaN	NaN	+	+		1	93	93
PF3D7_1139900	conserved protein, unknown function	1,05	-0,43	0,04	NaN				1	41	41
PF3D7_0924400	conserved Plasmodium protein, unknown function	NaN	NaN	0,52	NaN				1	1	1
PF3D7_0206500	conserved Plasmodium protein, unknown function	-0,02	0,07	0,53	NaN				1	19	19
PF3D7_0931100	nucleolar protein Nop52, putative	0,08	0,54	0,60	NaN				1	2	2
PF3D7_1021400	endomembrane protein 70, putative	0,47	0,32	0,62	NaN	+			14	46	44
PF3D7_1320900	RNA-binding protein, putative	0,04	0,02	0,63	NaN				1	2	2
PF3D7_0505600	conserved Plasmodium protein, unknown function	NaN	NaN	0,68	NaN				1	10	10
PF3D7_0420700	erythrocyte membrane protein 1, PfEMP1	-0,15	0,02	0,72	NaN				1	6	6
PF3D7_1475600	bromodomain protein, putative	-0,31	0,12	1,16	NaN				1	4	4
PF3D7_0501600	rhoptry-associated protein 2	0,12	-0,26	1,87	NaN				1	2	2
PF3D7_1012700	NLI interacting factor-like phosphatase, putative	0,07	-0,05	1,14	NaN				1	3	3
PF3D7_0526500	conserved Plasmodium protein, unknown function	0,01	-0,04	0,64	0,01				1	2	2
PF3D7_0936800	Plasmodium exported protein (PHISTc), unknown function	-1,51	-0,12	0,65	0,03				1	4	4
PF3D7_1306600	V-type proton ATPase subunit H, putative	2,26	0,83	-0,37	0,03				1	4	4
PF3D7_1241200	conserved Plasmodium protein, unknown function	0,70	0,09	-0,71	0,03				1	15	15
PF3D7_1008900	adenylate kinase	1,30	1,42	0,29	0,05	+	+	+	1	6	6
PF3D7_1438700	DNA primase small subunit	0,74	-2,14	-0,33	0,08			+	1	2	2
PF3D7_1421200	40S ribosomal protein S25	-0,14	0,01	0,59	0,08				1	4	4
PF3D7_1407900	plasmepsin I	2,17	-0,17	NaN	0,10				2	2	2
PF3D7_0514900	conserved Plasmodium protein, unknown function	0,34	-0,20	0,56	0,10			+	1	5	5
PF3D7_1207000	conserved Plasmodium protein, unknown function	0,04	0,56	0,62	0,11				1	11	11
PF3D7_1108500	succinyl-CoA synthetase alpha subunit, putative	3,02	-2,85	NaN	0,11				1	27	27
PF3D7_0213100	protein SIS1	0,02	-0,70	0,61	0,12				1	25	25
PF3D7_0410300	protein phosphatase PPM1, putative	0,74	-0,08	NaN	0,12				1	8	8
PF3D7_1446200	M17 leucyl aminopeptidase	1,01	0,64	1,28	0,12				1	2	2
PF3D7_1253400	#N/A	0,83	0,42	0,40	0,13				1	5	5
PF3D7_0731300	Plasmodium exported protein (PHISTb), unknown function	0,24	NaN	0,99	0,13				1	16	16
PF3D7_0202500	early transcribed membrane protein 2	0,79	NaN	NaN	0,14				1	11	11
PF3D7_1252500	Plasmodium exported protein, unknown function	0,55	0,18	1,04	0,14	+	+		1	10	10
PF3D7_1149100	Plasmodium exported protein, unknown function	-0,30	-0,06	0,52	0,15				1	32	32
PF3D7_0220200	Plasmodium exported protein, unknown function	0,81	0,34	NaN	0,16			+	1	2	2
PF3D7_1008800	nucleolar protein 5, putative	0,07	-0,16	0,63	0,16				1	2	2

PF3D7_1006700	conserved Plasmodium protein, unknown function	0,26	-0,15	0,50	0,19			1	2	2
PF3D7_1432100	voltage-dependent anion-selective channel protein, putative	0,72	-0,16	NaN	0,20			1	2	2
PF3D7_1317800	40S ribosomal protein S19	0,36	0,07	0,58	0,20		+	1	8	8
PF3D7_0303200	HAD superfamily protein, putative	0,07	0,32	0,68	0,21			1	11	11
PF3D7_1139300	AP2 domain transcription factor, putative	0,13	-0,37	0,97	0,21			1	16	16
PF3D7_0701600	Pfmc-2TM Maurer's cleft two transmembrane protein	0,15	0,09	0,51	0,23			1	8	8
PF3D7_1128000	conserved Plasmodium protein, unknown function	1,36	-0,27	NaN	0,26			1	7	7
PF3D7_0412000	conserved Plasmodium protein, unknown function	1,10	-0,06	NaN	0,27			1	17	17
PF3D7_1002000	Plasmodium exported protein (hyp2), unknown function	-0,48	0,07	3,68	0,27			1	4	4
PF3D7_1238500	conserved Plasmodium protein, unknown function	0,72	0,71	-0,29	0,28			1	6	6
PF3D7_1409600	conserved Plasmodium protein, unknown function	0,28	-0,10	1,16	0,28			1	3	3
PF3D7_1473500	conserved Plasmodium protein, unknown function	NaN	NaN	0,95	0,29			1	2	2
PF3D7_0811600	conserved Plasmodium protein, unknown function	0,72	-0,50	0,05	0,31			1	2	2
PF3D7_1237200	conserved Plasmodium protein, unknown function	2,83	-0,12	NaN	0,31			1	46	46
PF3D7_1016300	glycophorin binding protein	0,67	0,76	0,94	0,32			1	3	3
PF3D7_1467600	conserved Plasmodium protein, unknown function	1,16	0,30	-0,12	0,32		+	1	1	1
PF3D7_0821700	60S ribosomal protein L22, putative	0,16	-1,67	0,87	0,35			1	7	7
PF3D7_1324900	L-lactate dehydrogenase	0,21	0,17	1,38	0,35			1	7	7
PF3D7_0419600	ran-specific GTPase-activating protein 1, putative	0,14	-0,09	0,66	0,35			1	50	50
PF3D7_1473700	nucleoporin NUP116/NSP116, putative	0,98	0,19	0,17	0,36			1	2	2
PF3D7_1128200	multiprotein-bridging factor 1, putative	0,20	-0,25	0,87	0,36			1	11	11
PF3D7_0215500	conserved Plasmodium protein, unknown function	0,72	0,07	NaN	0,37			1	16	16
PF3D7_1129100	parasitophorous vacuolar protein 1	1,11	1,11	-0,34	0,37			1	19	19
PF3D7_0301400	Plasmodium exported protein, unknown function	2,83	0,60	0,30	0,39			1	15	15
PF3D7_1016400	serine/threonine protein kinase, FIKK family	0,91	1,01	0,52	0,43			1	3	3
PF3D7_0308600	pre-mRNA-processing factor 19, putative	0,76	-0,02	-0,44	0,44		+	1	41	41
PF3D7_1124100	beige/BEACH domain protein, putative	NaN	-0,22	0,71	0,45			1	21	21
PF3D7_1464600	serine/threonine protein phosphatase UIS2, putative	1,86	1,55	0,72	0,45			1	3	3
PF3D7_1039000	serine/threonine protein kinase, FIKK family	0,57	0,36	0,95	0,48		+	1	1	1
PF3D7_0412700	erythrocyte membrane protein 1, PfEMP1	NaN	NaN	0,59	0,49			1	25	25
PF3D7_1236000	vesicle transport v-SNARE protein VTII, putative	0,24	-0,02	1,36	0,51			1	50	50
PF3D7_0201800	knob associated heat shock protein 40	1,61	0,19	-0,12	0,51			1	21	21
PF3D7_1353000	tryptophan-rich protein, pseudogene	1,91	0,98	0,47	0,53			1	3	3
PF3D7_1420200	tetratricopeptide repeat protein, putative	2,28	-0,60	-0,50	0,53			1	1	1
PF3D7_1201000	Plasmodium exported protein (PHISTb), unknown function	0,66	1,48	0,59	0,58		+	1	2	2

PF3D7_0721100	conserved Plasmodium protein, unknown function	0,73	1,23	0,08	0,58				1	3	3		
PF3D7_0501200	parasite-infected erythrocyte surface protein	0,93	0,82	0,05	0,60				1	15	15		
PF3D7_0111800	eukaryotic translation initiation factor 4E, putative	0,04	0,06	0,58	0,61				1	27	27		
PF3D7_1216900	DNA-binding chaperone, putative	1,44	NaN	NaN	0,66				1	12	12		
PF3D7_1309500	H/ACA ribonucleoprotein complex subunit 1, putative	1,19	1,41	NaN	0,66		+	+	+	1	3	3	
PF3D7_1100200	erythrocyte membrane protein 1, PfEMP1	NaN	NaN	0,64	0,67				1	8	8		
PF3D7_1308800	tyrosine recombinase	0,89	0,42	2,02	0,72				1	2	2		
PF3D7_0729500	mRNA (N6-adenosine)-methyltransferase, putative	0,25	-0,43	0,54	0,76				1	3	3		
PF3D7_0731100	EMP1-trafficking protein	0,74	0,50	0,18	0,77		+		1	6	6		
PF3D7_1135400	conserved Plasmodium protein, unknown function	1,05	0,78	-0,10	0,88				1	25	25		
PF3D7_0301700	Plasmodium exported protein, unknown function	0,31	0,06	0,52	0,89					3	111	110	
PF3D7_0801000	Plasmodium exported protein (PHISTc), unknown function	0,57	0,59	0,60	0,94		+	+	+	+	1	3	3
PF3D7_0501300	skeleton-binding protein 1	-0,56	-0,46	0,83	0,96					1	5	5	
PF3D7_1024800	exported protein 3	1,63	1,03	0,07	1,08					1	2	2	
PF3D7_1226900	parasitophorous vacuolar protein 2	1,42	1,03	NaN	1,17					1	25	25	
PF3D7_1420700	surface protein P113	1,70	1,57	1,41	1,19					1	5	5	
PF3D7_1330300	DnaJ protein, putative	1,17	NaN	NaN	1,23			+		1	6	6	
PF3D7_1471100	exported protein 2	2,09	1,42	3,21	1,99					1	6	6	
PF3D7_1026000	conserved Plasmodium protein, unknown function	-1,52	0,10	1,01	2,28				1	2	2		
PF3D7_1436300	translocon component PTEX150	2,20	1,72	3,66	3,32				1	1	1		

